



ieaghg

FAULT PERMEABILITY

**Report: 2016/13
OCTOBER 2016**

INTERNATIONAL ENERGY AGENCY

The International Energy Agency (IEA) was established in 1974 within the framework of the Organisation for Economic Co-operation and Development (OECD) to implement an international energy programme. The IEA fosters co-operation amongst its 28 member countries and the European Commission, and with the other countries, in order to increase energy security by improved efficiency of energy use, development of alternative energy sources and research, development and demonstration on matters of energy supply and use. This is achieved through a series of collaborative activities, organised under more than 40 Implementing Agreements. These agreements cover more than 200 individual items of research, development and demonstration. IEAGHG is one of these Implementing Agreements.

DISCLAIMER

This report was prepared as an account of the work sponsored by IEAGHG. The views and opinions of the authors expressed herein do not necessarily reflect those of the IEAGHG, its members, the International Energy Agency, the organisations listed below, nor any employee or persons acting on behalf of any of them. In addition, none of these make any warranty, express or implied, assumes any liability or responsibility for the accuracy, completeness or usefulness of any information, apparatus, product or process disclosed or represents that its use would not infringe privately owned rights, including any parties intellectual property rights. Reference herein to any commercial product, process, service or trade name, trade mark or manufacturer does not necessarily constitute or imply any endorsement, recommendation or any favouring of such products.

COPYRIGHT

Copyright © IEA Environmental Projects Ltd. (IEAGHG) 2016.

All rights reserved.

ACKNOWLEDGEMENTS AND CITATIONS

This report describes research sponsored by IEAGHG. This report was prepared by:

GNS Science Consultancy

The principal researchers were:

- Andy Nicol
- Hannu Seeback
- David McNamara
- Brad Field

To ensure the quality and technical integrity of the research undertaken by IEAGHG each study is managed by an appointed IEAGHG manager. The report is also reviewed by a panel of independent technical experts before its release.

The IEAGHG manager for this report was:

James Craig and Alex Rolland

The expert reviewers for this report were:

- Quentin Fisher, University of Leeds
- John Williams, British Geological Survey
- Dominique Copin, Total
- Sylvain Thibeau, Total
- Owain Tucker, Shell (contributed to the Overview)

The report should be cited in literature as follows:

‘IEAGHG, “Fault Permeability” 2016/13, October, 2016’

Other information or copies of the report can be obtained by contacting IEAGHG at:

IEAGHG, Cheltenham Office Park, Pure Offices,
Hatherley Lane, Cheltenham,
GLOS., GL51 6SH, UK

Tel: +44(O) 1242 802911

E-mail: mail@ieaghg.org

Internet: www.ieaghg.org



FAULT PERMEABILITY

Key Messages

- CCS requires the secure retention of CO₂ in geological formations over 1000's of years. To achieve this, characterisation of target injection formations, and their structural features including faults, is essential to ensure leakage does not occur.
- Faults can either act as barriers to fluids, or as conduits for migration. Consequently, the properties of faults that dissect or form a boundary with potential CO₂ reservoirs, need to be determined.
- The significance of faults has long been recognised in the petroleum, mining and geothermal industries, but CO₂ storage is less mature and more experience and research related to faults would be beneficial.
- The objective of this study was to review recent research on the permeability (a measure of the ability of rocks to transmit fluids) of faults in CO₂ storage, particularly how different geological processes can either cause faults to help retain fluids within a reservoir, or lead to migration along or across faults. It builds upon an earlier study which looked at the role of geomechanical stress on faults¹.
- There is widespread experience of working with faults and fractures and provided there is sufficient characterisation of their properties they should not restrict storage development.
- If fault zones are present they need to be carefully characterised to ensure the development of an effective containment assessment and to inform the development of operational constraints and monitoring plans.
- A number of mitigation measures have been proposed to counter potential leakage. These include hydraulic barriers, biofilms, reactive cement grout and CO₂ back-production. Changing subsurface pressure has been seen to be effective: there is strong evidence of the reduction in flow of a natural hydrocarbon seep caused by depletion of an offshore oil reservoir hydraulically linked to the seeps.
- This work takes this research area as far as it can be taken without access to more fault-seal calibration datasets. IEAGHG will maintain a watching brief for any new information that comes into the public domain in the future.

Background to the Study

Fault zones are widely recognised as being important to the secure long term storage of CO₂ as they could provide a leakage pathway out of the target reservoir. Fault characterisation within reservoirs, especially where they extend into caprock and other overlying formations, needs to be thoroughly understood as part of any risk assessment for CO₂ storage. The aim of

¹ Criteria of Fault Geomechanical Stability During a Pressure Build-up 2015-04



this study is to review what is known about the permeability of fault zones in order to highlight under what circumstances faults may impact overall storage integrity.

The behaviour of fault zones in relation to sub-surface fluid migration is important to many industries and consequently has been comprehensively documented in the literature. CO₂ operations involve the injection and pressurization of reservoirs usually resulting in changes to the state of in-situ stresses which may alter fault properties. Instability can lead to slippage along pre-existing faults or fracture systems, which may be associated with seismicity. In addition, the movement of faults, and the generation of fractures within the damage zone adjacent to the core, may create conduits that lead to the leakage of fluids to the surrounding overburden or even to the surface.

In 2015 IEAGHG published a study reviewing the geomechanical stability of faults during pressure build up which provided a helpful background to the behaviour of faults in stress regimes relevant to CO₂ storage. This study is designed to build upon the previous work and provide a significantly broader review of the current state of fault zone permeability and also to investigate what mitigation options may be available to CO₂ storage operations if leakage was to occur.

Scope of Work

This report, produced by GNS Science, provides a succinct and relevant overview of the complexities that control fault permeability in the context of CO₂ storage. It provides a background guide on recent research on fault permeability in formations that are good candidates for CO₂ storage. In addition it draws from a number of examples of natural fluid/gas leakage along fault zones and highlights what conclusions can be drawn from these observations. The project examines the variables that control fault permeability and reviews the methods that may be available to control leakage should it occur. It also provides a summary of recent and ongoing research at CO₂ storage demonstration sites across the world which relate to fault zone permeability.

Findings of the Study

Fault zone structure & Permeability

There is widespread evidence that faults can act as seals and as potential fluid migration routes. Hydraulic conductivity and permeability are positively related to fracture aperture although high pore fluid pressures and/or preferential stress alignments are not a prerequisite for enhanced hydraulic conductivity. Open fractures are most likely to modify bulk conductivity in low permeability caprock and can increase permeability by as much as three orders of magnitude. Fracture permeability decreases with an increase in effective stress which generally increases with depth. Pore pressure is still important, especially in aquifers where it can be increased by fluid injection or decreased in depleted reservoirs by production.



Evidence for the low permeability of fault zones is provided by across-fault pressure changes, compartmentalisation of reservoirs by faults, low measured flow rates in fault zones, the differential subsidence caused by water production, and by the accumulation of large volumes of hydrocarbons against fault planes. Snøhvit CO₂ re-injection is an example where a rapid rise in reservoir pressures due to fault compartmentalisation and impermeability resulted in an operational switch to a stratigraphically higher injection interval.

Fault-zone conductivity and transmissivity are controlled by many interdependent factors including among others; fault architecture and the types of fault rocks present in a given location, mechanical strength and permeability of the host lithology, fracture aperture size and connectivity, fluid composition, pressure and gradients, extent of pre-existing mineralisation and the orientation and magnitude of normal and shear stresses.

The key factor that controls vertical conductivity is orientation of effective stress acting on a fault. There is a risk of leakage where fault zones have no tensile strength and the effective normal stress acting on a fault is near zero. These parameters can be measured and used to predict whether a fault acts a seal or a conduit.

Lateral migration across fault zones is related to the level of impermeable material that gets entrained into faults during deformation and motion. The petroleum industry uses the clay smear potential and shale gauge ratios (SGRs) to estimate this effect. The higher the clay content the lower the permeability and the higher the capillary pressure. However, these factors control flow into a fault and do not influence vertical migration which is influenced by the adjacent stress field.

Parameters influencing fault permeability

Fault zones are four-dimensional volumes of deformed rock with highly anisotropic and heterogeneous properties that evolve through time. These fault-zone complexities produce variations in structure along strike and down dip, and even over relatively short distances show at least three orders of magnitude (1×10^{-18} to $3 \times 10^{-15} \text{ m}^2$) variation in permeability across a 4 m wide fault zone where both the highest and lowest permeabilities measured are in proximity to the primary slip surface (Figure 1).

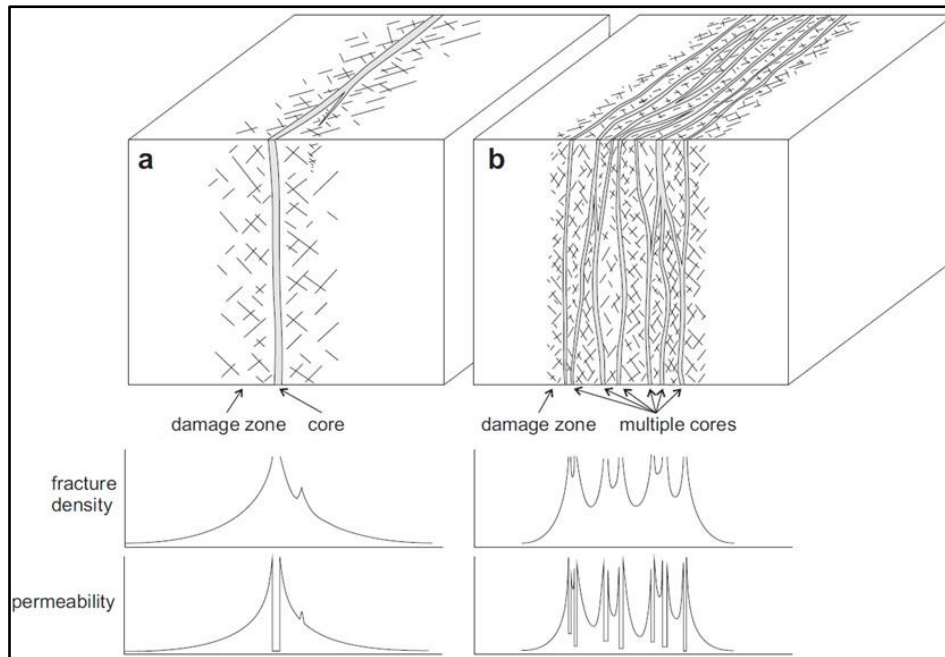


Figure 1 Structure of single core and multiple cores fault and the associated hydro-mechanical properties of fault zones (after Faulkner et al., 2010)

Fault permeability can be highly sensitive to any change in the effective stress acting normal to the fracture plane (i.e., stress dependent permeability) and, in some cases, may be increased by rising reservoir pressures during CO₂ injection.

Fault-zone structure, mechanics and fluid-flow properties are inextricably coupled and should not be considered in isolation. When the conductivity of a system is considered, the fluid type must be accounted for. However, a distinction needs to be made between lateral migration within pores in a reservoir, or lateral movement into a fault zone, and vertical migration via fractures in a fault zone.

Host rock lithology and fault displacement

The host rock lithology, depth of burial, as well as fault displacement governs the type of fault deformation and influences permeability. Quartz and feldspathic rich rocks such as sandstones will form cataclastic (a rock formed by progressive fracturing and comminution of mineral grains) textures within fault cores. At relatively low confining pressures (e.g. near surface depths < 1 km), these lithologies are characterized by grain reorganization without grain fracturing and tend to have comparable hydraulic properties to their protolith sandstones. At higher confining pressures (e.g. burial depths >1 km) cataclastic processes dominate deformation, resulting in higher capillary threshold pressures and lower fault rock permeabilities (typically 2–3 orders of magnitude below host rock) through grain fragmentation and associated infilling of pore-space. At >3 km and temperatures >90 °C disaggregation zones and cataclasites are prone to post-deformation quartz cementation and clay alteration.

Permeabilities measured in phyllosilicate-framework fault rocks (i.e. impure sandstones with clay content between 15% and 40%) typically range from < 10⁻¹⁹ to 10⁻¹⁶ m². Phyllosilicates



are silicate minerals that have a sheet like structure and include clay minerals which are hydrated alumino-silicates often formed through weathering or mechanical deformation including faulting. As the clay content of a rock increases above 40% it will form clay smears. Natural fault gouges measured under laboratory conditions simulating burial depths of ~4 km (100 MPa) show ultra-fine gouge permeabilities ranging down to 10^{-21} m^2 . For comparison caprock permeabilities are 10^{-18} m^2 or lower (Figure 2).

Although fractures in the damage zone are a focus of present research, internal fault zones also display high permeabilities (2-4 orders of magnitude higher than the host rock).

- High fluid pressures at depth can be transient resulting in episodic fluid flow.
- Pre-existing mineralisation of faults and fractures can have a greater control on bulk permeability than compressive stresses.
- Supercritical or water saturated CO_2 may increase or decrease permeabilities within fault and fracture networks through dissolution depending on the minerals present. Mineral precipitation caused by CO_2 fluids may enhance sealing properties.
- Shale and other mudrocks are well known for their tendency toward plastic deformation or creep while under stress that may close or seal fractures. Under certain conditions, such as overconsolidation, shales can become brittle and form vertical fractures.

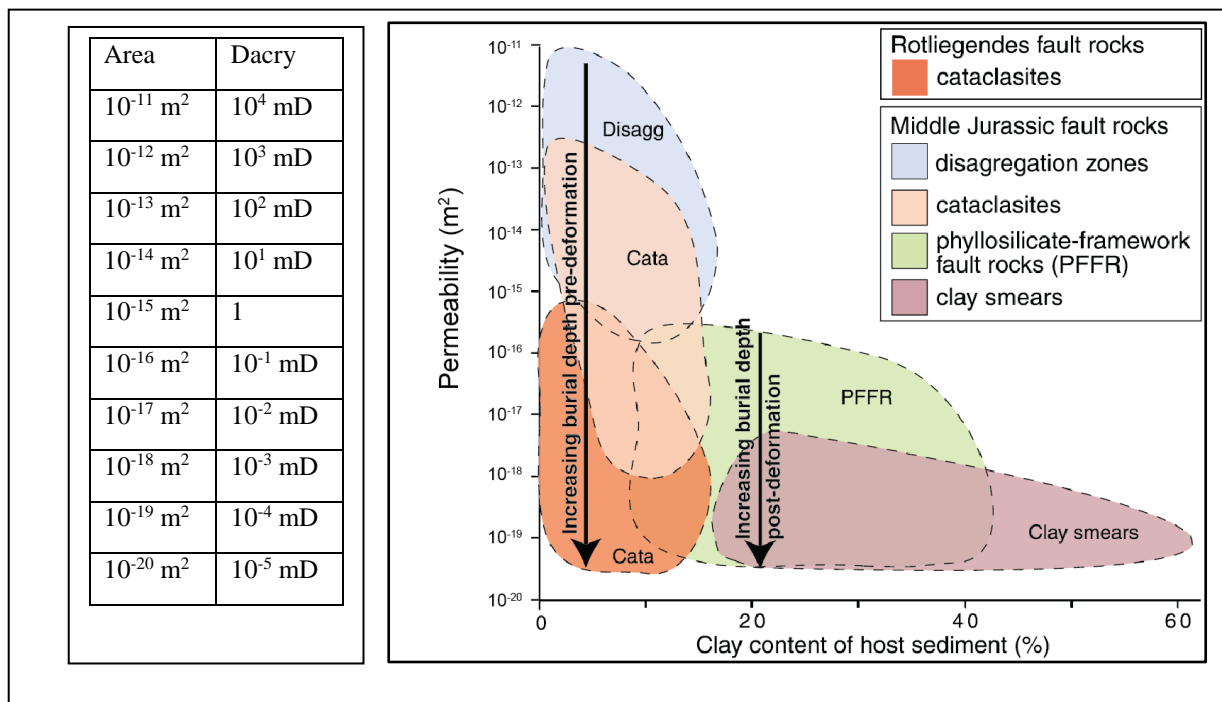


Figure 2. Summary of fault rock permeability data from the North Sea and Norwegian Continental shelf. Permeability is plotted against clay content for the various fault rock types. Also shown are the two main controls on the permeability of the faults in clean sandstones and impure sandstones (PFFR) (i.e. burial depth at the time of faulting and post-deformation burial depth, respectively).

The permeability of faults within siliciclastic petroleum reservoirs of the North Sea and Norwegian Continental shelf show variations of 2–3 orders of magnitude in permeability of



clay-rich and cataclastic faults for a given depth (Figure 2). Understanding the variability of fault permeability for a given fault or system of faults therefore requires multiple samples of fault rock from a variety of locations along fault-zones, a condition that is rarely achieved in individual studies.

An understanding of the burial and/or exhumation history of a fault is also important when considering its hydrogeological properties (see Figure 3). A range of fault and fracture properties, both hydraulically conductive and sealing, can be present in a single region for example the West Sole gas fields of the southern North Sea. In this area, core samples indicate all early formed faults and fractures were likely to be sealing, particularly those at maximum burial depth and reservoir temperature. Breached or conductive faults formed later during inversion, when brittle.

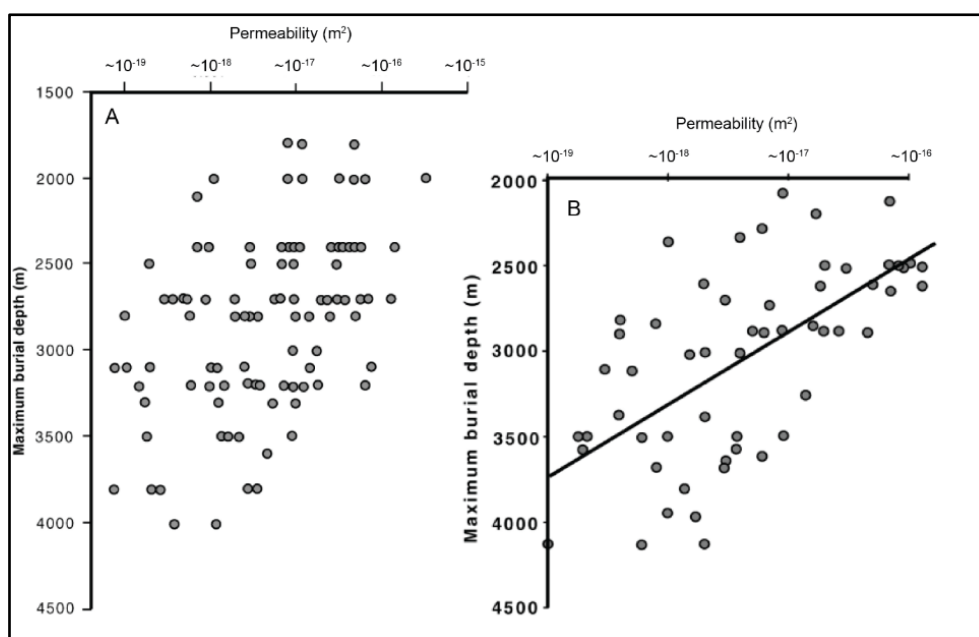


Figure 3. Permeability of phyllosilicate-framework and cataclastic fault rocks from the North Sea. A) Permeability of cataclastic fault rock against their maximum burial depth from Rotliegendes of the Southern North Sea. B) Permeability of phyllosilicate-framework fault rock against their maximum burial depth from the northern North Sea.

In summary, the primary factors controlling the hydrogeological properties of a fault include:

- the composition and rheology of the host rock and its phyllosilicate clay mineral content
- the maximum temperature and depth of burial during faulting which can affect diagenesis of fault zone rocks by inducing mineralisation.
- the stress regime at the time(s) of faulting, during any subsequent deformation event as well as the present day.
- composition of syn- and post-kinematic fluids and their reaction products

This combination of factors make site specific observations of *in situ* fault properties critical to understanding the response of faults and their associated fracture networks to elevated pressures induced during CO₂ injection.



Geomechanical properties

Mechanical stratigraphy – ie. response to mechanical failure of different lithologies (rock types, summarised in Figure 4) can create fault dip variations causing additional fault zone complexities such as splaying and the development of antithetic faults. Dilation of normal faults at lithological boundaries can significantly enhance vertical fluid flow at the surface, and create pathways for along-strike fluid migration in the subsurface. Recognition of the influence of mechanical stratigraphy on fault geometry is an important component of the characterisation of faulted aquifers, hydrocarbon reservoirs, and mineral provinces.

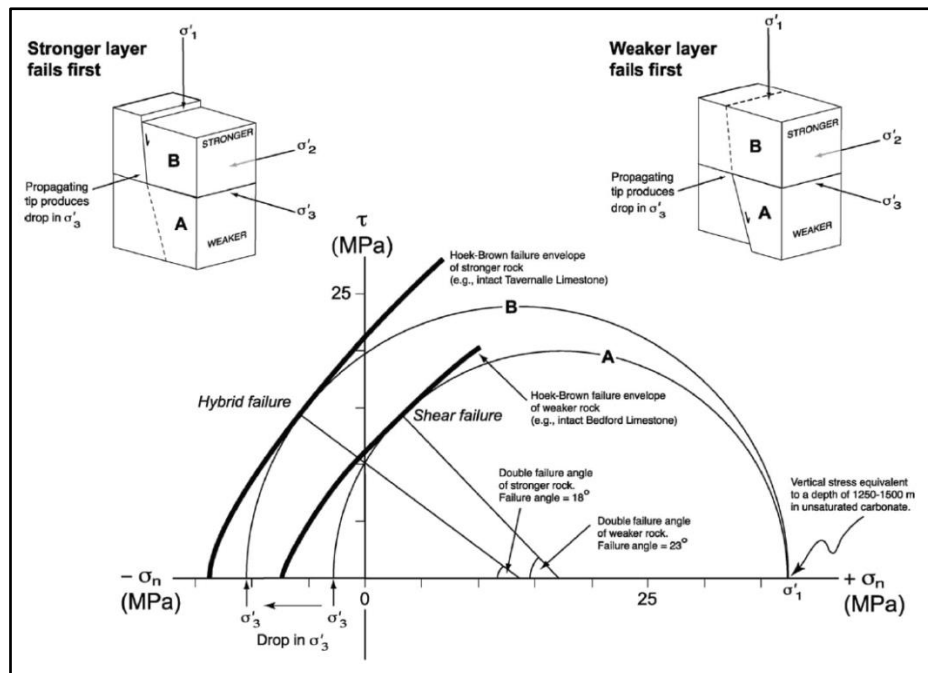


Figure 4. Mohr-space diagram illustrating how contrasting mechanical stratigraphy leads to different failure mode and failure angles in different layers. A more competent rock is more likely to fail in hybrid mode than a less competent rock under the same stress regime (in this case normal faulting).

The mechanical properties of sedimentary sequences influence failure angles and fault dip, whereas layer thickness influences the height of dip segments.

A number of algorithms have been developed to assess lateral migration of fluid across fault zones according to the clay smear and mixing conceptual models (SGR most widely used). In a number of cases these have been positively correlated to oil and gas column heights and capillary threshold pressures although these are rare and more research is needed to reduce uncertainties associated with these models.

This study concludes that understanding the effect of host rock mechanical properties on fault deformation processes, in combination with burial history, is key to the development of realistic fault structure and permeability models.

- Few studies have focused on the geometries and flow properties of faults in caprock sequences and this is a weakness in the literature.



- Polygonal faults overlie many commercial scale hydrocarbon reservoirs, indicating these faults often do not compromise caprock integrity and/or that the faulted mudstones are not the primary seal.
- Estimating damage zone thickness from the displacement or length of faults (e.g. IEAGHG, 2015a) will result in significant uncertainty in estimates of fault zone hydraulic properties.
- Many *in situ* studies highlight the highly localised and convoluted nature of fluid flow through a faulted rock volume.

In general, application of shear stress induces a dilation of the fracture, sometimes preceded by a closure phase, which causes a very large increase in global transmissivity associated with the reorientation of flow sub-perpendicular to the shear direction. Prediction of hydraulically conductive faults and fractures preferentially oriented with respect to the stress field is complicated by fracture healing whereby mineralisation of void space results in the stress independence of the fracture.

Fault cementation and dissolution

Within some reservoirs, fracture permeability is shown to be often created by dissolution or partial cementation within fractures. As a result fractures can remain ‘locked open’ and possess apertures of several millimetres resulting in high hydraulic conductivities, even *in situ* under high stress conditions at depth.

Fractures at depths of 4–6 km or more form in environments where hot ($>100^{\circ}\text{C}$), mineral-laden water promotes the precipitation of partial quartz coatings and spatially isolated, pillar-like precipitate (cement) bridges.

The healing of fractures and faults may also have two significant and competing effects on the porosity and permeability of a sedimentary sequence which may be important for CO_2 storage. Firstly, mineralisation of faults and fractures can strengthen the aggregate by increasing cementation and cohesion, which directly causes a reduction in permeability. At the same time, this lowering of permeability may weaken the rock by elevating fluid pressure, resulting in a reduction of effective stress, which in turn can cause further brittle failure. Any re-fracturing of mineralised zones could increase permeability if fractures, closed by mineralisation, become connected again.

Confining pressure and stress orientation

As differential stresses decrease and reservoir pressure increases, suitably oriented fractures will tend to dilate perpendicular to the fracture walls and fracture shearing will be a less significant process in aperture enhancement. The permeability of the dilated and connected fractures will be enhanced. This type of permeability is also referred to as pressure-sensitive permeability. If pore pressure diminishes, or minimum principal stress magnitude increases, the fracture apertures will tend to diminish or close resulting in a reduction in permeability and productivity. The stress regime that defines these conditions is presented in Figure 5. A shift



towards increasing shear stress (τ), caused by increasing pore pressure, will eventually lead to shear failure.

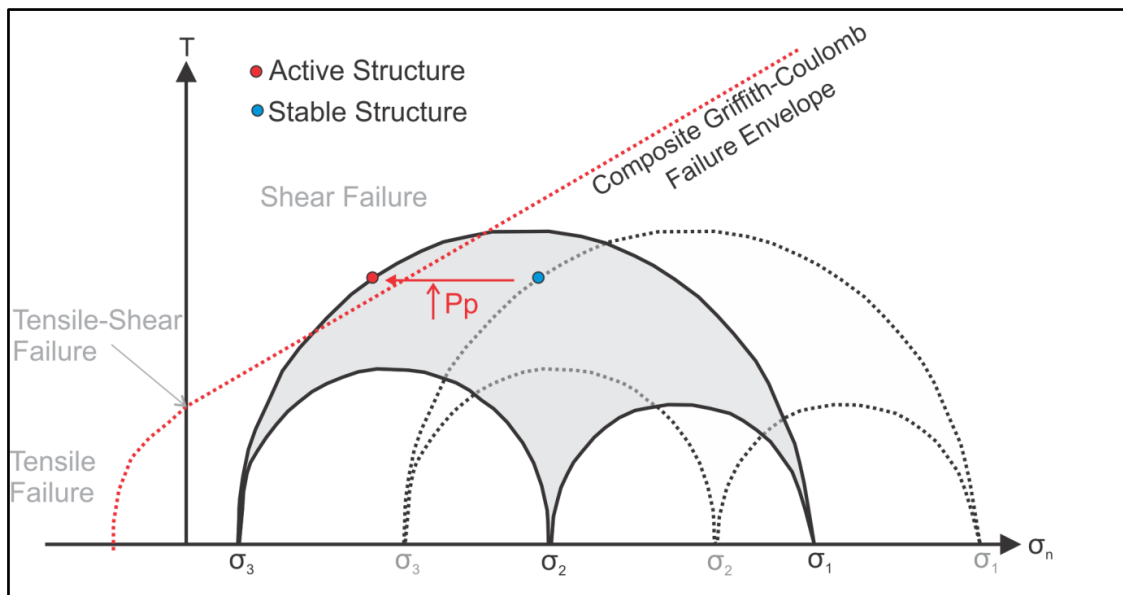


Figure 5 Mohr diagram showing influence of pore pressure increase. The Mohr diagram shows the potential effect that increasing pore pressure (P_p) has on a structures shear to normal stress ratio and where it falls relative to the composite Griffith-Coulomb Failure Envelope.

Field, well, and laboratory observations also highlight that understanding the stress history of a fractured rock mass is essential, and understanding of the present-day stress field alone is insufficient to model the hydromechanical response of *in situ* faults and fractures to stress changes.

Few studies have been conducted under *in situ* conditions with simultaneous fracture and permeability measurements at reservoir conditions. Contrary to expectations, results from this study indicate that supercritical CO_2 will not flow through the tight natural caprock fractures sampled, even with pressure differentials in excess of 51 MPa.

Fault Seal Prediction

Hydrocarbon (and CO_2) migration is generally accepted to occur in localized stringers (elongated streams of migratory fluid especially where there are bands of more permeable features such as palaeo-channels) or driven principally by buoyancy forces and opposed by the capillary properties of the rock through which the migration occurs. A seal will remain intact until the capillary pressure (that is the difference in pressure between the oil and water) at the interface between the reservoir and the seal, due to the buoyancy force of the trapped hydrocarbon column, exceeds the capillary threshold pressure of the water-wet seal. The threshold pressure is the capillary pressure at which the non-wetting (hydrocarbon) phase forms a continuous filament or stringer through the seal.



The most important fault parameter therefore in fault seal analysis is the capillary threshold pressure of the fault-rock which is controlled by the pore throat size. The smaller the pore throat size, the higher the capillary threshold pressure required before migration into a fault zone will occur and the greater the fluid column that can potentially be supported before leakage.

Fault seal analysis and geomechanical modelling are widely used to predict the potential hydraulic properties of fault zones. The Shale Gouge Ratio (SGR) analysis is most widely adopted in the petroleum and CO₂ industries and in a number of cases has been positively correlated to oil/gas column heights using capillary threshold pressures, and this correlation has been shown to vary with depth of burial.

Of particular relevance to CO₂ storage are faults cutting through low permeability strata (i.e. caprocks) that can provide pathways for fluids generated in deep, pressurized rocks to migrate into shallow levels. One consequence of this variability in permeability is that CO₂ flow along faults will often be channelized. In addition, given the complexity of fault zones predicting where, and on what faults, cross- and along-fault migration of CO₂ is likely to occur will be challenging. Temporal increases in fault permeability arising from increasing pressures due to CO₂ injection may be less challenging to predict using geomechanical considerations. However, it will be important to understand the different fluid–fluid and fluid–rock reactions associated with CO₂ migration. It is possible that such reactions will be accelerated within fault zones by grain crushing and an associated increase in grain surface area, although further work is required to confirm this in a CO₂ storage context. The presence of static fluid will result in diffusive movement of reaction products and exceptionally slow alteration.

In the majority of fault seal studies fault rock, that is the crushed rock material that is created by dislocation, is formed by smear along the fault or mixing into the fault zone of clay-rich beds in the host rock.

Further work is required to understand better the processes and quantify the heterogeneity of low permeability fault rock, to test the effectiveness of current fault-seal methods and to improve the predictive power of fault seal analysis. Access to more fault-seal calibration datasets will facilitate future advances in understanding.

Natural seeps and fault-related flow rates

CO₂ flux along faults has been widely reported from many areas around the world. One of the most studied is the Paradox Basin on the Colorado Plateau, East-Central Utah, USA. Data analysis here supports a model in which faults promote upward flow of CO₂ with flux rates greatest where small scale faults and fracture densities are highest. Flow simulation also suggests compartmentalisation by low permeability fault rock may increase pressure and promote upward flow of CO₂.

Reported fault zone permeabilities range from 10⁻⁹ to 10⁻¹⁹ m² (100 D – 10⁻⁴ mD) with cross fault permeabilities ranging from 10⁻¹⁴ to 10⁻¹⁹ m² (10 mD – 10⁻⁴ mD) and along-fault permeabilities typically between 10⁻¹² and 10⁻¹⁵ m² (1 D – 1 mD).



Maximum CO₂ flow rates for natural analogues of CO₂ seeps associated with faults are generally >0.1 t/m²/yr. For these flow rates volumes of CO₂ leakage could reach 15,000 t/yr, which is similar to the 25,000 t/yr estimated for a submarine seep (Panarea, Greece).

The migration rates of CO₂ are likely to be site- and fault-specific and could vary by at least four orders of magnitude within a given fault system. The rates of CO₂ migration along faults are likely to vary significantly on individual faults, within fault systems and between different sedimentary basins.

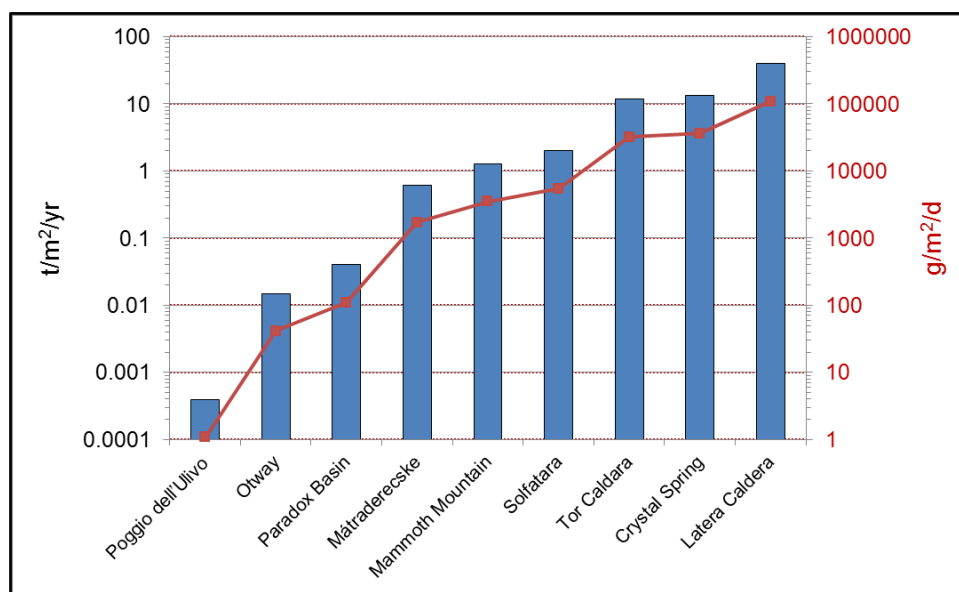


Figure 6. Maximum rates of CO₂ emissions from the analogue studies

These examples (Figure 6) are biased and represent, at best, the upper bounds of natural migration rates in faults. They do, however, demonstrate to varying degrees, the surface expression of CO₂ seeps and provide a useful natural reference. These rates are not comparable to fluid migration rates at CO₂ storage sites. However they do provide useful opportunities to study the natural occurrence of CO₂ migration along faults and the surface expression of CO₂ on a surrounding environment.

Industry Practices for Mitigation of Fault Leakage

Petroleum and geothermal experiences are most pertinent to CO₂ storage. 4D seismic, gravity, microseismic monitoring, borehole image logs and core and geochemical sampling are most common methods used to map fluid migration. Geophysical techniques offer the best opportunity to identify a 3D location of an injected fluid but resolution is too low to document fault-flow relationships. Well-based sampling offers an opportunity to provide detailed information but lacks a 3D perspective.

Fluid-flow simulation studies performed in petroleum, CO₂ storage, water extraction and radioactive waste industries can be highly sophisticated and include faults of various geometries, thicknesses and permeabilities which can be history matched. Outputs are non-unique though and uncertainty of geologic parameters is a universal weakness especially where



drilling has not been completed. Rising computer power and adequate time/resources can provide a range of scenarios.

Different fluid management solutions could be employed to temporarily or permanently arrest the pressure increase or decrease the pressure in the storage aquifer. Intervention measures could be used to create a pressure barrier in the overlying geological strata to prevent or minimize CO₂ leakage. Back-production of injected CO₂ might also be considered as an option.

In a case where an overrun increase in pressure has created a new leakage pathway through fault reactivation and/or hydraulic fracturing, for example, newly created fractures and reactivated faults may not totally close with pressure relief, particularly if they have undergone shear displacements.

Other proposed solutions include hydraulic barriers, biofilms, microbially induced calcite precipitation, reactive grout and CO₂ back-production.

Few mitigation options from oil and gas are published in public literature, specifically ones that combat along-fault flow. Pressure relief, hydraulic barrier and chemical/biological sealants are noted as possible solutions but with few trials at storage sites their effectiveness is unknown.

There is a documented case of a decrease in natural hydrocarbon seepage in the Santa Barbara Channel off the coast of southern California. The decline in seepage from structural features beneath the sea floor including faults can be attributed to the production of hydrocarbons from an offshore platform over a period of more than 20 years. This example demonstrates the impact of an increase in effective stress via reservoir depletion and could be employed as a potential mitigation measure.

The innumerable intricacies and complexities of different faults at different sites means that there are limited risk assessment guidelines concerning how faults should be treated in CO₂ storage operations.

Expert Review Comments

Six experts were invited to review the study, four of whom returned comments. There was a general consensus that the study had been well-written and sensibly compiled. All agreed that the study had considered and condensed an impressive volume of literature and therefore provided a comprehensive and valuable review of what is known (and unknown) about fault permeability in relation to CO₂ storage. It was noted, however, that the study overall had been overly influenced by research based on hard rock and outcrop analysis, not paying enough attention to rheological controls on fault permeability relevant to soft rock environments. The authors agreed and rectified this by adding a number of additional paragraphs detailing the influence of rheology on fault permeability and this enhanced the report overall making it more complete and more relevant to CO₂ storage. Reviewers also highlighted some additional



references which had not been included in the study and these have since been incorporated into the final report.

Conclusions

- Fault-zone conductivity and permeability are controlled by many interdependent factors including among others; fault architecture and the types of fault rocks present in a given location, mechanical strength and permeability of the host lithology, fracture aperture size and connectivity, fluid composition, pressure and gradients, extent of pre-existing mineralisation and the orientation and magnitude of normal and shear stresses.
- The key factor that controls vertical conductivity is the orientation of effective stress acting on a fault. There is a risk of leakage where fault zones have no tensile strength and the effective normal stress acting on a fault is near zero. These parameters can be measured and used to predict whether a fault acts a seal or a conduit.
- Properties that are pertinent to the sealing potential and conductivity including the stress regime acting on the fault, the shale gouge ratio, mechanical strength of adjacent rock formations, and fracture formation can be measured and assessed. Provided there is supporting evidence that faults can form effective seals their presence should not prevent the development of CO₂ storage sites.
- A range of fault and fracture properties, both hydraulically conductive and sealing, can be present in a single region. Understanding the burial history of a fault is also important when considering its hydrogeological properties.
- The results of detailed fault studies and *in situ* permeability measurements are supported by numerical models which show highly non-linear behaviour and flow localization for a wide range of natural well-connected critically stressed fracture networks.
- Pre-existing mineralisation of faults and fractures can have a greater control on bulk permeability than compressive stresses.
- Supercritical or water saturated CO₂ may increase or decrease permeabilities within fault and fracture networks through dissolution depending on the minerals present.
- A number of leakage mitigation measures have been proposed including hydraulic barriers created by injection above the caprock, biofilms, microbially induced calcite precipitation, reactive grout and CO₂ back-production. The decrease in natural hydrocarbon seepage in the Santa Barbara Channel off the coast of southern California has been directly attributed to the production of hydrocarbons from an offshore platform over a period of more than 20 years. This example demonstrates the impact of an increase in effective stress via reservoir depletion and could be employed as a potential mitigation measure.

Knowledge Gaps

- More *in situ* fluid-flow data and numerical flow modelling are required to quantify the effects of fault zone architecture.



- Further work is required to understand better the processes and quantify the heterogeneity of low permeability fault rock, to test the effectiveness of current fault-seal methods and to improve the predictive power of fault seal analysis. Access to more fault-seal calibration datasets will facilitate future advances in understanding.

Recommendations

The following recommendations are proposed to enhance the existing knowledge related to faults and their significance for CO₂ storage:

- Improved definition and quantification of fault hydraulic properties.
- Developing and sensitivity testing flow simulator models and geomechanical flow predictions.
- Testing and validating models with in-situ data.
- This work takes this research area as far as it can be taken without access to more fault-seal calibration datasets. IEAGHG will maintain a watching brief for any new information that comes into the public domain in the future.

Fault Permeability Study IEA/CON/15/230

A. Nicol
B. Field

H. Seebeck
D. McNamara

**GNS Science Consultancy Report 2015/206
February 2016**

DISCLAIMER

This report has been prepared by the Institute of Geological and Nuclear Sciences Limited (GNS Science) exclusively for and under contract to IEAGHG. Unless otherwise agreed in writing by GNS Science, GNS Science accepts no responsibility for any use of or reliance on any contents of this report by any person other than IEAGHG and shall not be liable to any person other than IEAGHG, on any ground, for any loss, damage or expense arising from such use or reliance.

Use of Data:

Client consent required to use data.

BIBLIOGRAPHIC REFERENCE

Nicol A.; Seebeck H.; Field B.; McNamara D. 2016. Fault Permeability Study IEA/CON/15/230, *GNS Science Consultancy Report 2015/206*. 135 p.

CONTENTS

EXECUTIVE SUMMARY	V
1.0 INTRODUCTION	1
1.1 BACKGROUND	1
1.2 PURPOSE AND AIMS OF REPORT	3
1.3 REPORT STRUCTURE	4
2.0 FAULT ZONE STRUCTURE AND PERMEABILITY	7
2.1 INTRODUCTION.....	7
2.2 FAULT ZONE STRUCTURE	8
2.3 CROSS-FAULT MIGRATION.....	11
2.4 ALONG-FAULT MIGRATION	12
3.0 PARAMETERS INFLUENCING FAULT PERMEABILITY	15
3.1 FAULT ROCK PROPERTIES	16
3.1.1 Host rock lithology and fault displacement.....	16
3.1.2 Depth	20
3.2 FAULT ZONE PROPERTIES	22
3.2.1 Mechanical stratigraphy	22
3.2.2 Fault scaling properties	27
3.2.3 Aperture.....	28
3.2.4 Connectivity of fault systems.....	30
3.3 FLUID COMPOSITION	30
3.4 FAULT CEMENTATION AND DISSOLUTION.....	32
3.4.1 Diagenetically Modified Fractures	33
3.5 CONFINING PRESSURE AND STRESS ORIENTATION.....	35
3.5.1 Fracture hydromechanical behaviour under normal stress	38
3.5.2 Fracture hydromechanical behaviour in shear	38
3.6 PORE PRESSURE	40
4.0 FAULT SEAL PREDICTION	42
4.1 METHODS	42
4.2 CALIBRATION OF RESULTS	45
4.3 UNCERTAINTIES	46
5.0 GEOMECHANICAL MODELING AND FAULT LEAKAGE	48
5.1 CRITICALLY STRESSED FAULTS	49
5.2 FRACTURE STABILITY	50
5.3 DILATION TENDENCY	52
5.4 MODEL INPUT DATA AND UNCERTAINTIES	52
5.5 CASE STUDY: KRECHBA GAS FIELD, IN SALAH, ALGERIA	55
6.0 NATURAL CO₂ SEEPS ALONG FAULTS	59
6.1 PARADOX BASIN, UTAH, USA.....	61
6.2 LATERA CALDERA, ITALY.....	65

6.3	MAMMOTH MOUNTAIN, CALIFORNIA, U.S.A.	66
6.4	MÁTRADERECSKE, HUNGARY	68
6.5	ALBANI HILLS, POGGIO DELL'ULIVO, SOLFATARA SECCA, TORRE ALFINA, ITALY	68
6.6	PANAREA, GREECE	71
7.0	CO₂ FLOW RATES ALONG FAULTS	73
7.1	FAULT PERMEABILITIES	73
7.2	CO ₂ FLOW RATES IN NATURAL ANALOGUES	75
7.3	CO ₂ FLOW MECHANISMS.....	77
8.0	INDUSTRY PRACTICES FOR MEASURING AND MITIGATING UNWANTED FLUID FLOW ALONG FAULTS	79
8.1	FAULT AND FLUID FLOW CHARACTERISATION	79
8.1.1	Seismic reflection techniques.....	79
8.1.2	Borehole Image Logs and Core	81
8.1.3	Geochemical Sampling	82
8.1.4	Microseismicity	83
8.2	FLUID FLOW SIMULATIONS.....	85
8.3	FLUID FLOW MIGRATION AND REMEDIATION	86
8.3.1	Pressure relief in the storage formation	86
8.3.2	Hydraulic barrier	87
8.3.3	CO ₂ plume dissolution and residual trapping	88
8.3.4	Chemical or biological sealants.....	88
8.3.5	CO ₂ back-production	90
9.0	APPLICATION OF FAULT PERMEABILITY REVIEW TO CO₂ STORAGE ...	92
9.1	FAULT ZONE STRUCTURE AND PERMEABILITY	92
9.2	FAULT SEAL AND GEOMECHANICAL PREDICTIONS.....	92
9.3	CO ₂ NATURAL SEEPS AND FAULT-RELATED FLOW RATES	93
9.4	INDUSTRY PRACTICES FOR MITIGATING UNWANTED FLUID FLOW ALONG FAULTS	93
10.0	KNOWLEDGE GAPS AND CHALLENGES FOR UNDERSTANDING CO₂ MIGRATION ALONG FAULTS.....	95
10.1	FAULT GEOMETRY, SCALING AND PERMEABILITY	95
10.2	CROSS-FAULT PERMEABILITY PREDICTION.....	96
10.3	ALONG-FAULT PERMEABILITY PREDICTION	97
10.3.1	Geomechanical modelling.....	98
10.4	FLOW SIMULATION MODELS.....	99
10.5	IN SITU FAULT PERMEABILITY AND FLOW RATES	99
10.6	CO ₂ CONTAINMENT MANAGEMENT	100
11.0	RECOMMENDATIONS FOR FUTURE RESEARCH	101
11.1	FAULT ZONE GEOMETRIES AND PERMEABILITY	101
11.2	FAULT STRUCTURE IN CAPROCKS	102
11.3	FLUID FLOW MODELLING AND PREDICTION	103

11.3.1	Geomechanical modelling	103
11.4	IN SITU FAULT PERMEABILITIES AND FLOW RATES.....	104
11.5	RISK ASSESSMENT FOR ALONG-FAULT FLOW	104
12.0	REFERENCES	105

FIGURES

Figure 1	Schematic diagrams illustrating fault zone models and terminology.	vi
Figure 2	Schematic diagram illustrating three of the main fault seal conceptual models.....	vii
Figure 3	Maximum rates of CO ₂ emissions from the analogue studies	viii
Figure 4	Schematic of near-surface and surface expression of fault/fracture gas seepage from depth.	x
Figure 1.1	Geomechanical processes and key technical issues associated with GCS in deep sedimentary formations	1
Figure 1.2	Flow diagram showing inter-relationships among the three main topics of structure, mechanics and fluid flow.	3
Figure 2.1	Schematic diagrams illustrating fault zone models and terminology.	9
Figure 2.2	Global compilations of fault zone data showing thickness vs displacement for fault rock	10
Figure 2.3	Photographs showing examples of outcrop scale normal faults.....	11
Figure 2.4	Schematic block model showing the spatial variation in fault elements.....	13
Figure 3.1	Schematic plot illustrating the main fault rock types generated in siliciclastic sequences.....	18
Figure 3.2	Summary of fault rock permeability data from the North Sea and Norwegian Continental shelf.....	19
Figure 3.3	Schematic summary of the main elements of permeability structure across the Median Tectonic Line.	20
Figure 3.4	Permeability of phyllosilicate-framework and cataclastic fault rocks from the North Sea.	21
Figure 3.5	Mohr-space diagram illustrating how contrasting mechanical stratigraphy leads to different failure mode and failure angles in different layers	23
Figure 3.6	Mohr-space diagrams with Hoek-Brown failure envelope.....	24
Figure 3.7	Schematic diagram illustrating the effects of confining pressure and strength contrast on fault dip variations within a multilayer sequence.....	26
Figure 3.8	Fault zone thickness and ground water inflow rate populations	28
Figure 3.9	Diagram illustrating geological carbon storage.....	31
Figure 3.10	Permeability versus effective stress	40
Figure 4.1	Schematic diagram illustrating three of the main fault seal conceptual models.....	43
Figure 4.2	Cartoon illustrating the method for using Shale Gouge Ratio (SGR) as a column height predictor	45
Figure 4.3	Shale Gouge Ratio (SGR) fault seal calibrations.....	46
Figure 5.1	Mohr diagram of critical stress criteria.	50
Figure 5.2	Mohr diagram showing influence of pore pressure increase.	51
Figure 5.3	Dilation tendency mapped on fault surfaces in the Kupe Field (New Zealand), with gas chimney locations.....	52

Figure 5.4	Schematic of a stress polygon.....	54
Figure 5.5	Transient evolution of vertical ground displacement at KB-502 well.....	56
Figure 5.6	Geomechanical model results from In Salah CO ₂ storage demonstration project.....	57
Figure 6.1	Analysis of soil gas CO ₂ measurements in the LGW fault zone	62
Figure 6.2	A conceptual diagram of CO ₂ origins and migration within the LGW and SW fault zones.....	63
Figure 6.3	Schematic model showing different structural assemblages and their influence on CO ₂ leakage from Lateral Caldera	66
Figure 6.4	Vegetation loss from CO ₂ emissions at Mammoth Mountain and Horseshoe Lake.....	67
Figure 6.5	CO ₂ flux in the Mammoth Mountain area.....	67
Figure 6.6	Map and cross section of the Mammoth Mountain area.....	68
Figure 6.7	Albani Locality map for the Albani Hills area	69
Figure 6.8	CO ₂ gas emissions in the Ardea area.....	70
Figure 6.9	CO ₂ gas emissions from the Pogglio dell'Ulivo area.....	71
Figure 6.10	Panarea Island and associated submarine gas plume	72
Figure 7.1	Bulk crustal and fault zone permeability.	75
Figure 7.2	Maximum rates of CO ₂ emissions from the analogue studies	76
Figure 7.3	Comparison of calculated migration velocities for proposed mechanisms and observed seepage velocities.....	78
Figure 8.1	Comparison of horizon time slices.....	81
Figure 8.2	Schematic of near-surface and surface expression of fault/fracture gas seepage from depth.	83
Figure 8.3	Induced seismicity	84

TABLES

Table 4.1	Summary of fault seal algorithms developed to predict the permeability of fault rock	44
Table 5.1	Summary of parameters and sources of data that are required for geomechanical modelling.....	53
Table 6.1	Terrestrial CO ₂ seeps with measured rates of CO ₂ release.....	60
Table 6.2	Documented marine seeps.....	61

EXECUTIVE SUMMARY

Mitigating the risk of CO₂ migration via faults to the atmosphere or into economically valuable resources (e.g. water aquifers or hydrocarbon reservoirs), requires an understanding of the conditions under which they promote fluid flow from the reservoir. Knowledge gaps in our understanding of CO₂ migration along faults are widely accepted. The present review adds to an earlier report (IEAGHG, 2015a) by using the published literature to examine how fault permeability is modified by fault zone and host rock properties and *in situ* stresses of anthropogenic or geological origins. The primary goal of the report is to use publically available literature to examine when, where and how faults may negatively or positively impact the storage and migration of injected CO₂. In particular, four key tasks have been undertaken and are outlined below.

TASK 1 - Provide a brief summary of the key parameters that influence the mechanical and hydraulic properties of fault zones including a summary of CO₂ flow data along faults at natural seeps.

TASK 2 - Review current oil industry practices that are used to assess and control the unwanted migration of hydrocarbons along faults. Use the experience of different industry/academic teams to assess and model fault leakage from potential CO₂ storage sites.

TASK 3 - Review the approaches used by other industries (e.g. waste disposal, hydrocarbons, civil engineering) to assess the properties, permeabilities, and leakage thresholds of faults and examine how these approaches might be useful for CO₂ storage sites.

TASK 4 - Identify the knowledge gaps in current understanding of fluid migration along faults. Identify the challenges in modelling fault permeability, and monitoring fluid migration (including CO₂), along and across faults. Recommend the direction of future research and development that is directly related to a better understanding of fault permeability.

The principal objective of this report is to provide a review and synthesis of international research and current understanding of fault permeability, with emphasis on how it could influence (positively or negatively) CO₂ storage. To address this principal aim and the four key tasks outlined above, the report contains 10 main sections. These main sections are summarized below.

Fault zone structure and permeability

It has long been known that faults can strongly influence the sub-surface movement of fluids (i.e. liquid and gas). Bulk fluid-flow rates through or along fault zones are important for many practical applications, including geothermal and hydrocarbon production and CO₂ storage. Whilst it is generally acknowledged that the structure of fault zones can be complex and spatially variable, a relatively simple fault damage zone model has been widely adopted (Fig. 1a). At outcrop scale the damage model is rarely correct in detail as fault zones form highly heterogeneous bodies. Fault surfaces are generally anastomosing, producing fault rock and fault zone thicknesses that range in excess of an order of magnitude over fault surfaces. Low permeability (clay-rich) fault rock retards cross-fault flow and, in many cases, associated jointing and small-scale faulting which may locally elevate along-fault permeabilities (Fig. 1b). Therefore, faults may simultaneously impede cross-fault flow and enhance along-fault flow to form a dual conduit-barrier system. Understanding of the bulk flow properties of fault zones has been hindered by a general lack of *in situ* flow data which can be unambiguously related to the structure of fault zones and the lithologies of the surrounding rock-volume.

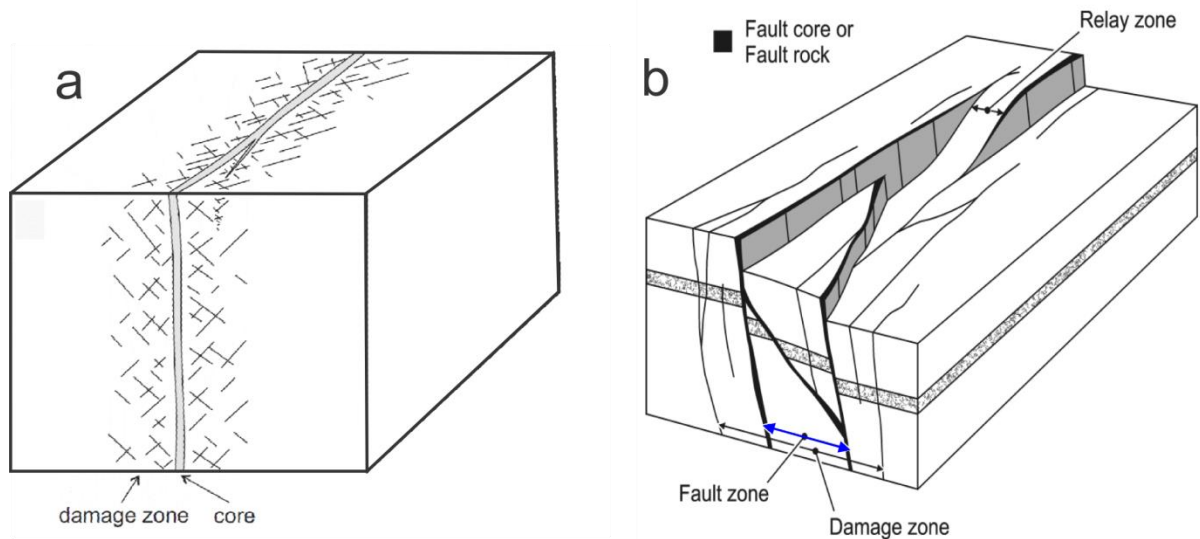


Figure 1 Schematic diagrams illustrating fault zone models and terminology. (a) Fault damage zone – fault core model where a zone of fracturing encloses a clay-rich core comprising low permeability fault rock (Chester and Logan, 1986). (b) Fault zone model in which the thicknesses of clay-rich fault rock and fault zones dominated by small faults vary over the fault surface (Childs *et al.*, 2009).

Fault-zone conductivity and transmissivity are controlled by many interdependent factors including among others; fault architecture and the types of fault rocks present in a given location, mechanical strength and permeability of the host lithology, fracture aperture size and connectivity, fluid composition, pressure and gradients, extent of pre-existing mineralisation and the orientation and magnitude of normal and shear stresses. Connectivity is critical for fluid flow in fractured media where networks of fractures above a critical density determine the flow properties of the system. For, example, fault zones in a region may have the same general fault architecture, however only those having sufficiently connected high-permeability pathways will be hydraulically conductive. In such cases the hydraulic conductivity and permeability are positively related to fracture aperture. Fracture permeability generally decreases with depth (in the absence of mineralisation), however, once formed in stronger rocks fractures are rarely completely closed due to the misalignment of rough fracture surfaces. Open fractures are most likely to modify bulk conductivity in low permeability caprocks, where their permeabilities can be at least three orders of magnitude higher than the intrinsic permeability of the host lithology. Transient high permeabilities may develop through episodic fluid flow within fault zones in response to high fluid pressures at depth. High pore fluid pressures and/or preferential alignment within a regional stress field are not necessarily prerequisites for enhanced hydraulic conductivity within a fault zone. Pre-existing mineralisation of faults and fractures can have a greater control on bulk permeability than compressive stresses. Supercritical or water-saturated CO₂ may either increase or decrease permeabilities within fault and fracture networks through dissolution or precipitation reactions. Dissolution of pre-existing mineral precipitates, such as calcite for example, may result in the bulk permeability of a seal formation increasing, resulting in leakage.

Fault seal and geomechanical predictions

Fault seal analysis and geomechanical modelling are widely used to predict the potential hydraulic properties of fault zones. In the majority of fault seal studies fault rock is inferred to primarily form due to smear along the fault or mixing into the fault zone of clay-rich beds in the host rock (Figure 2). Based on conceptual clay smear and mixing models a number of algorithms have been developed for estimating the flow properties of faults and their impact

on lateral migration of fluids in reservoir rocks. Shale Gouge Ratio (SGR) analysis is most widely adopted in the petroleum and CO₂ industries and in a number of cases has been positively correlated to oil/gas column heights using capillary threshold pressures, and this correlation has been shown to vary with depth of burial. Fault seal analysis supports the widely held view that clay-rich fault rock can compartmentalise reservoirs on production timescales, while observations from the petroleum industry suggest that fault seal on geological timescales may be less common. Tests of the SGR-based predictions of column heights are relatively rare in the published literature and further research is required to reduce uncertainties and assess the predictive power of the methodology over a range of timescales.

Geomechanical modelling methods are applied to predict the probability that structural permeability can, or has, developed and whether it can be maintained within the contemporary stress field (for further details see IEAGHG, 2015a). Three main geomechanical modelling methods are in common use for predicting the locations of along-fault flow: i) slip tendency, ii) fracture stability and iii) dilation tendency. Each method uses estimates of the stress tensor, fault orientation and fault coefficient of friction to determine the faults, or parts of faults, closest to failure, and which are assumed to have the highest permeabilities. Numerous studies of borehole data support the use of the techniques for predicting which fractures will flow, however, few publications provide independent evidence in support of the predictions at reservoir or regional scales. In addition, a number of publications suggest that non-optimally oriented fracture/faults have unpredicted high permeabilities. Further research may therefore be required to understand better the conditions in which geomechanical predictions of fluid flow along faults are likely to be of value. Research that explicitly targets the mechanical response of caprocks to injection-induced pressure increases may also be beneficial to help guide CO₂ site selection and injection strategies.

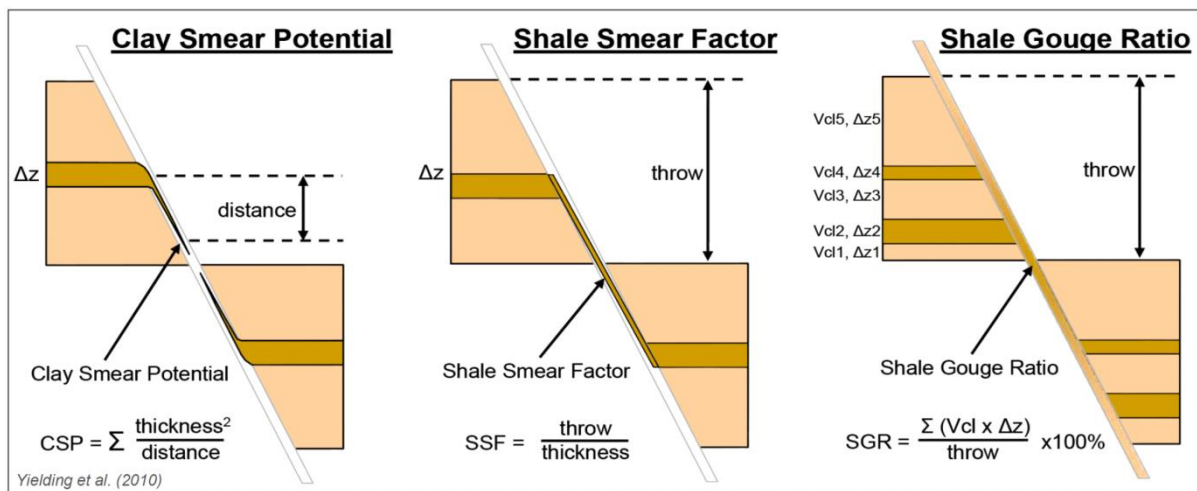


Figure 2 Schematic diagram illustrating three of the main fault seal conceptual models and associated algorithms used to predict the likelihood of low permeability clay within fault zones (from Yielding *et al.*, 2010).

CO₂ natural seeps and fault-related flow rates

Natural CO₂ seeps with fluxes at the ground surface interpreted to be facilitated by faults are widely documented in the literature. In the majority of the case studies presented in Section 6 the CO₂ fluxes are associated with volcanic or geothermal activity and the role of faults is inferred based on spatial elongation of the CO₂ anomalies and their parallelism to mapped faults. Perhaps the most complete analyses of the spatial relations between faults and CO₂ flux rates have been conducted in the Paradox Basin, where fault mapping, measurements of surface flux and flow simulation modelling have been conducted. Collectively these data and

analyses support a model in which faults can promote the upward flow of CO₂, with the flux rates being greatest where the highest densities of small-scale faults and fractures occur. Flow simulation modelling suggests that low-permeability fault rock may also compartmentalise rocks, giving rise to increased pressures and promoting upward flow of CO₂. A reservoir compartmentalisation and overpressure model may be supported by the Crystal Geyser in the Paradox Basin, which formed along an uncased abandoned petroleum exploration well drilled in the immediate footwall of the Little Grand Wash Fault. Independent of where and how faults influence the upward flow of CO₂, the present case studies are likely to be biased towards examples where the flux rates are high and, at best, might provide an indication of the upper-bound of potential rates. These high rates also indicate that self-sealing by mineral formation cannot necessarily be expected to occur in storage operations where CO₂-rich fluids migrate along faults (Heath *et al.*, 2009), particularly on sub-geological timescales (for longer timescales, see discussion in Frery *et al.*, 2015).

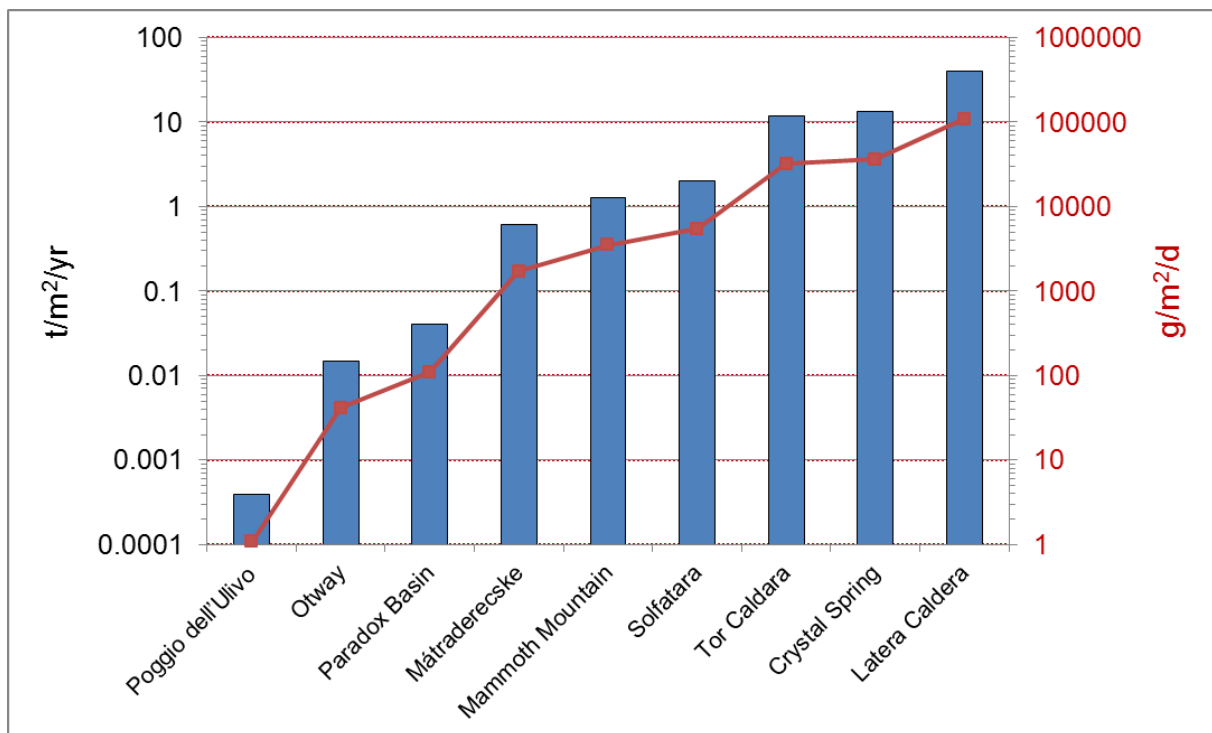


Figure 3 Maximum rates of CO₂ emissions from the analogue studies documented in Section 6. The rates plotted do not provide information on total volumes, or take into account temporal variations of rates, such as the spikes in rate that might occur during seismic pumping associated with proximal or distal earthquakes (e.g. Bonini, 2009; Todaka *et al.*, 2009; Han *et al.*, 2013, p.294).

The rates of fluid flow along faults can vary spatially and temporally. Flow rates and fault permeabilities are controlled by a range of factors including, fault-zone architecture and orientations, pore pressures, pressure gradients and fluid supply rates. Reported fault zone permeabilities range from 10⁻⁹ to 10⁻¹⁹ m², with clay-rich fault rock typically having cross-fault permeabilities of 10⁻¹⁴ to 10⁻¹⁹ m² with along-fault values more often between 10⁻¹² and 10⁻¹⁵ m². Maximum CO₂ flow rates for natural analogues of CO₂ seeps associated with faults are generally >0.1 t/m²/yr (Figure 3). For these flow rates volumes of CO₂ leakage could reach 15000 t/yr, which is similar to the 25000 t/yr estimated for a submarine seep (Panarea, Greece). These surface leakage rates and volumes are charged by sub-surface migration ranging between 100 and 1000 m/yr. Given the problems identifying and recording slow rates of migration (e.g. < 10m/yr) these values likely define the upper bound of what is possible at CO₂ storage sites rather than providing an unbiased sample of the population of flow rates. The migration rates of CO₂ are likely to be site- and fault-specific and could vary by at least

four orders of magnitude within a given fault system. A relatively small number of faults/fractures (e.g. <2%) can accommodate much of the recorded flow (e.g. 20–80%), with critically stressed faults and/or larger more connected faults potentially having the highest flow rates.

Industry practices for mitigating unwanted fluid flow along faults

Fluid extraction and injection industries, including petroleum, geothermal, waste water, CO₂ storage, can be affected by faults which locally promote and/or retard fluid flow. The experience of the petroleum and geothermal industries, in particular, has application at CO₂ storage sites for understanding and mitigating fluid-flow along faults. The techniques used to monitor, model and mitigate CO₂ flow are largely adapted/adopted from these industries. Techniques commonly used for mapping fluid migration include, 4D reflection seismic, gravity, microseismic monitoring, borehole image logs and core, and borehole geochemical sampling. While the geophysical techniques offer the best opportunity to determine the 3D location of injected fluid, they generally do not provide the resolution necessary to document the detailed spatial relationships between faults and flow. By contrast, well-based sampling techniques offer the opportunity to provide detailed information at points within a fault zone, but lack a 3D perspective on fluid flow and may miss or poorly sample the migrating fluids.

Fluid-flow simulation studies have been employed by many industries over the last 40 years (e.g., petroleum extraction, CO₂ storage, water extraction and radioactive waste management), as a tool for analysing reservoir performance during extraction/injection operations. These models can include faults and it is generally possible to vary fault geometries, thicknesses, and permeabilities. The models have reached a high level of sophistication and are validated in history-matching exercises. However, the outputs of the models are non-unique and uncertainty of the geologic input parameters (e.g. fault permeabilities) represents a universal weakness of the models. These issues are particularly severe for models constructed to predict reservoir performance before production wells are drilled; however, with the rise in computer power and the flexibility of fault modelling methods a range of possible faulting scenarios can usually be tested (given sufficient time and resources).

Potential corrective measures for undesirable CO₂ migration mainly stem from past efforts in the activities of oil and gas industry. Few measures have been outlined in the published literature to specifically combat along-fault flow, although techniques such as pressure relief, hydraulic barriers and chemical or biological sealants have received some attention as possible solutions. At the present time few of these proposed techniques have been trialled at CO₂ storage sites, and it is not known how effective they will be for remediating unwanted migration of CO₂ along faults.

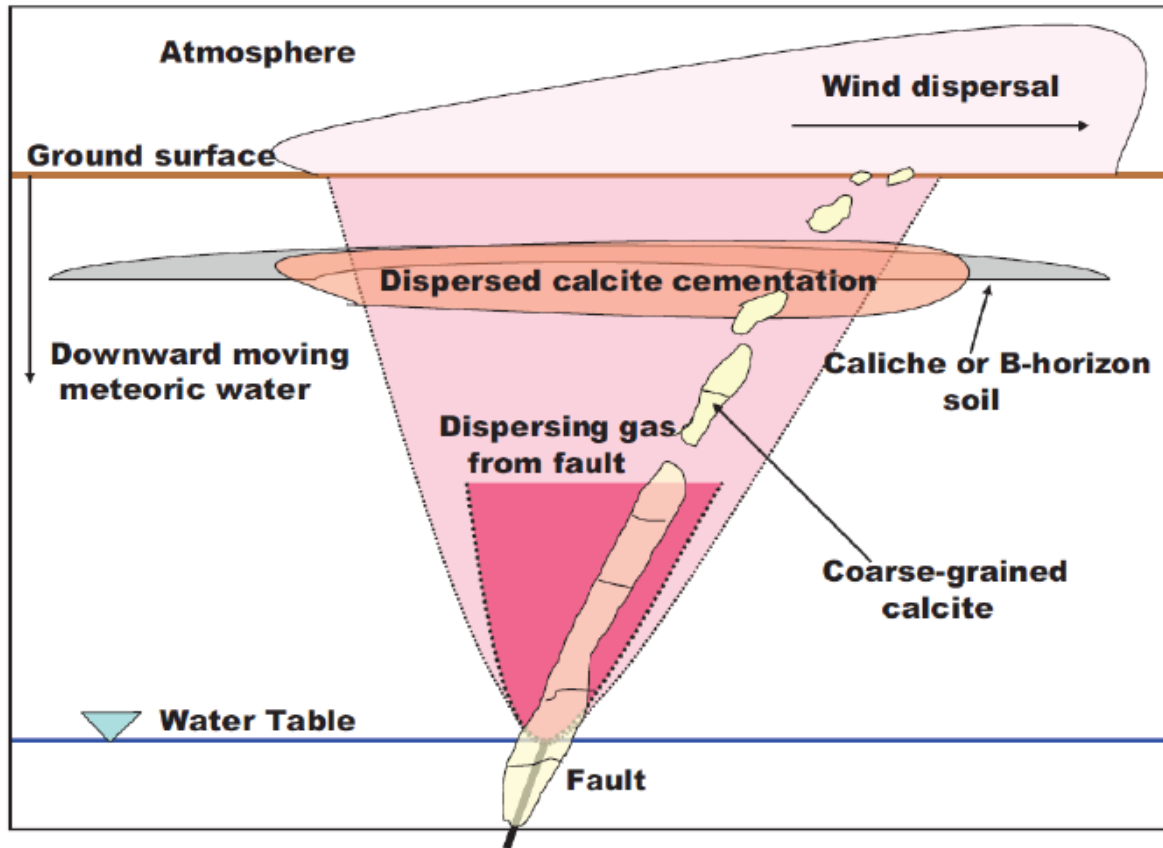


Figure 4 Schematic of near-surface and surface expression of fault/fracture gas seepage from depth. The oxidation of carbon-containing gases frequently produces secondary calcite and other near-surface alteration. Gases may, or may not be transported into the atmosphere (Klusman, 2011). Note in some cases the fault may extend to the ground surface.

Leakage identification, intervention and remediation requires a balance of engineering efficacy, geomechanical assessment and cost-benefit analysis (Zahasky and Benson, 2014). Injection shutoff or passive remediation is the fastest, easiest, and likely the cheapest method to quickly reduce leakage from the storage reservoir. Usually injection shutoff alone is not able to completely stop leakage. If passive remediation is not sufficient, various hydraulic controls such as water injection or reservoir fluid production can be employed to further reduce leakage rates and trap mobile CO₂. Water injection is usually an effective remediation technique because it: (1) increases the pressure in the overlying aquifer relative to the base of the fault and can quickly stop leakage, (2) is able to push some amount of leaked CO₂ back down the fault, (3) is able to dissolve large quantities of CO₂ in the vicinity of the water injection and finally, (4) does not require injection directly into the fracture, which is likely to be required if a chemical or biological sealant is used. In some cases, water injection alone may be sufficient to stop current and future CO₂ leakage, especially when the leak is detected early, before a large amount of CO₂ has accumulated below and above the fault. Additional hydraulic controls such as reservoir fluid production and water injection below the caprock increase rates of dissolution, thus trapping of CO₂ in the storage reservoir (Zahasky and Benson, 2014).

Knowledge gaps and recommended future research

Present understanding of fault hydraulic properties is generally not sufficiently complete to predict when and where faults are likely to influence CO₂ migration, either positively or negatively. Knowledge and data gaps include limited understanding of heterogeneities in fault geometries and fault-zone permeabilities, the scaling of fault properties from outcrop to reservoir scales, and the spatial and temporal variations in stress conditions. These knowledge

gaps have implications for whether flow simulation and geomechanical models contain sufficient information to adequately describe CO₂ migration in faulted reservoirs and caprocks. Independent reservoir pressure and flow data are essential for testing the predictions of the models and for increased understanding of the main processes that modify CO₂ flow across and along faults. The collection and analysis of fault-specific flow data at CO₂ storage sites may assist in developing CO₂ migration management plans for faulted reservoirs and caprocks.

Recommendations for future research fall into three main categories; i) improved definition and quantification of fault hydraulic properties, ii) continued development and sensitivity testing of flow simulation models and geomechanical flow predictions, and iii) validation of models using empirical fluid flow data from fault zones. To improve understanding of the geometric and hydraulic properties of faults, studies of fault outcrop, analogue and numerical models are required. For example, Discrete Element Modelling could be used to determine the conditions under which high and low permeability rock volumes form in fault zones and have the potential to impact CO₂ migration. Of particular importance for CO₂ storage is faulting and its influence on caprock integrity. Future research should address the question “under what circumstances (e.g. fault properties, caprock rheology, reservoir pressures and ambient stress conditions), and how, are faults (and fractures) in mudstone caprocks likely to impact on the bulk permeability of these rocks” at potential CO₂ storage sites. Fluid flow simulations and geomechanical modelling are important tools for examining the role of faults in CO₂ migration. Testing the predictions of numerical modelling results using *in situ* flow measurements is critical for the continued development of these techniques, while increases in computer power and sensitivity testing of the input parameters will be key aims of modellers.

Although it is widely accepted that faults represent a risk for undesirable migration of injected CO₂, there are few specific guidelines for how they should be treated in a risk assessment framework. These guidelines could address key questions including: i) under what circumstances (e.g. size faults, rock types and reservoir stresses) should CO₂ contact with a fault be avoided, ii) what investigations are required to characterise the flow properties of faults, iii) under what geological and stress conditions are faults likely to constitute a leakage risk, iv) what monitoring of faults are necessary/useful to record along-fault migration, v) what constitutes acceptable levels of migration from the geological container and how do we record these migration rates, and vi) what course of action should be taken if migration exceeds pre-defined limits.

1.0 INTRODUCTION

1.1 BACKGROUND

CO₂ storage in sub-surface rock formations is an important solution for mitigating the rise of atmospheric greenhouse gases and associated climate change (e.g. Rochelle *et al.*, 2004; IPCC, 2005; Kampman *et al.*, 2014a; Birkholzer *et al.*, 2015). Effective storage of CO₂ in geological formations requires injection and long-term (e.g. >1000 years) residence in secure reservoirs. The importance of fault permeability for effective containment of CO₂ in the sub-surface is widely recognised (e.g. Streit and Hillis, 2004; Tsang *et al.*, 2007; Rutqvist, 2012) (Figure 1.1). Mitigating the risk of CO₂ migration via faults to the atmosphere or into economically valuable resources (e.g. water aquifers or hydrocarbon reservoirs), requires an understanding of the conditions under which they promote fluid flow from the reservoir. Knowledge gaps in our understanding of CO₂ migration along faults were identified at a Modelling and Risk Management Networks meeting in Trondheim during June 2013 (IEAGHG, 2013b). As a result of this Trondheim meeting the IEAGHG commissioned a study to review the geomechanical stability of faults during pressure build-up (IEAGHG, 2015a). The IEAGHG report was completed in April 2015 and highlights key factors influencing the mechanical stability of faults in response to CO₂ injection. The present study adds to the earlier report (IEAGHG, 2015a) mainly by examining the published literature on how fault architecture and changes in stresses influence their permeability.

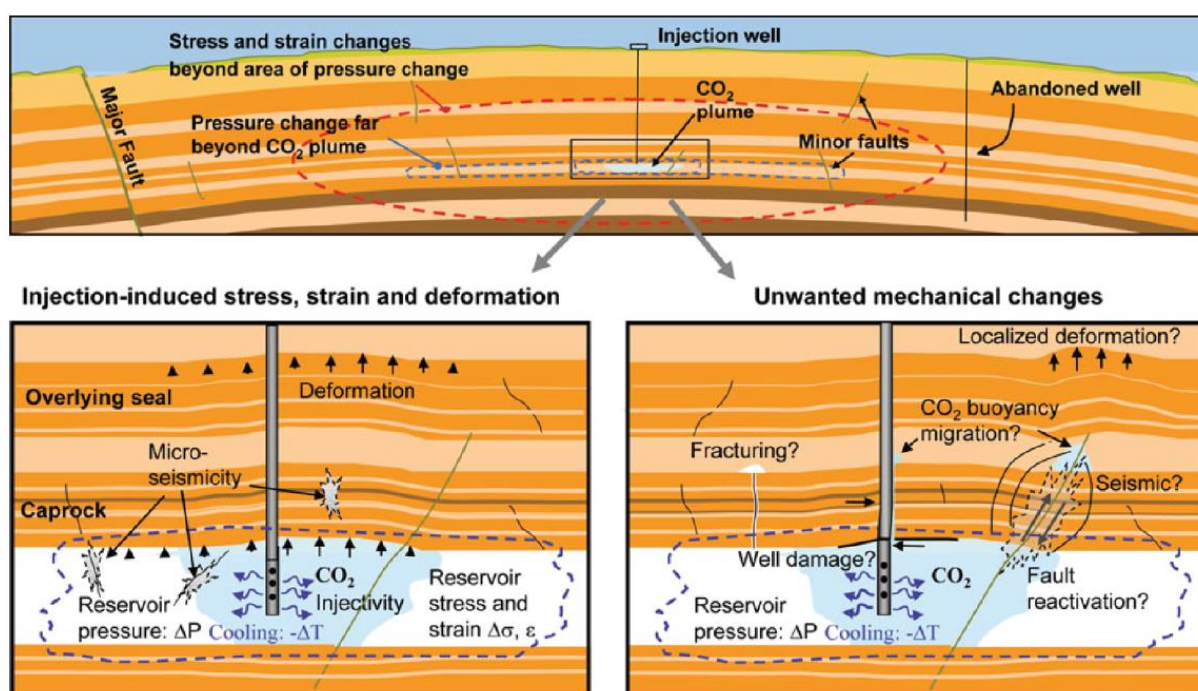


Figure 1.1 Geomechanical processes and key technical issues associated with GCS in deep sedimentary formations (Rutqvist, 2012). Top: the different regions of influence for a CO₂ plume, reservoir pressure changes, and geomechanical responses in a multi-layered system with minor and major faults. Bottom left: injection induced stress, strain, deformations and potential microseismic events as a result of changes in reservoir pressure and temperature. Bottom right: unwanted inelastic changes that might reduce storage efficiency and cause concerns in communities close to the storage site.

Faults can displace CO₂ reservoirs and caprocks. In such cases they have the potential to modify the storage capacity, maximum injection rates and reservoir pressures, and seal integrity in CO₂ storage systems (Figure 1.1). Faults may form due to a range of processes

including; far-field plate motions, folding, gravitational sliding, volcanic intrusion, crustal unloading associated with uplift and anthropogenic activities, such as fluid injection or extraction. This report focuses on faults that pre-date CO₂ injection which, in many cases, are of tectonic origin and form due to extension of the rock (i.e. normal faults). These faults can form barriers to across-fault flow and conduits to along-fault flow (Gibson, 1998; Odling *et al.*, 1999; Bense and Person, 2006; Faulkner *et al.*, 2010; Manzocchi *et al.*, 2010). Precisely how faults will impact on fluid flow is dependent on a number of factors (Figure 1.2), including the rheologies and burial depths of host rocks, permeabilities and relative permeabilities of fault rock and the rock formation hosting the fault (referred to here as host rock), the pressure and temperature conditions of the reservoir and fluids, the composition of the fluids and the fracture¹ geometries (e.g. dimensions, interconnectedness and apertures) (Caine *et al.*, 1996; Cox, 1999; Faulkner *et al.*, 2010; Manzocchi *et al.*, 2010) (Figure 1.2). The values of these parameters and the resulting fluid-flow rates may change between faults or parts of faults, and from one CO₂ storage site to another. The influence of these factors on permeability and fluid flow may also change through time at individual sites in response to changes in pressures, temperatures and injection rates. It is possible, for example, that increases in pore pressure or decrease in effective stresses arising from injection will increase fracture apertures, induce fault slip and/or generate new fractures, all of which could locally promote the flow of CO₂ and brine from the storage container (Rutqvist, 2012; Rinaldi *et al.*, 2014; IEAGHG, 2015a). Migration of CO₂ along faults also occurs at sites where pressures and temperatures were not modified by anthropogenic injection (e.g. see faults from the Paradox Basin, Utah, USA; Shipton *et al.*, 2004; Dockrill and Shipton, 2010). Analysis of natural CO₂ seeps suggests that even in well managed storage systems where ambient reservoir conditions are maintained during CO₂ injection migration along faults is possible. Therefore, if faults are present in reservoir and/or caprocks they should be considered as potential migration pathways even in circumstances where CO₂ injection is not expected to significantly increase reservoir pressures.

¹ 1The term "fracture" refers to discontinuities that accommodate shear displacement (fault), pure dilation (e.g. joint) or a hybrid structure accommodating both shear and dilation.

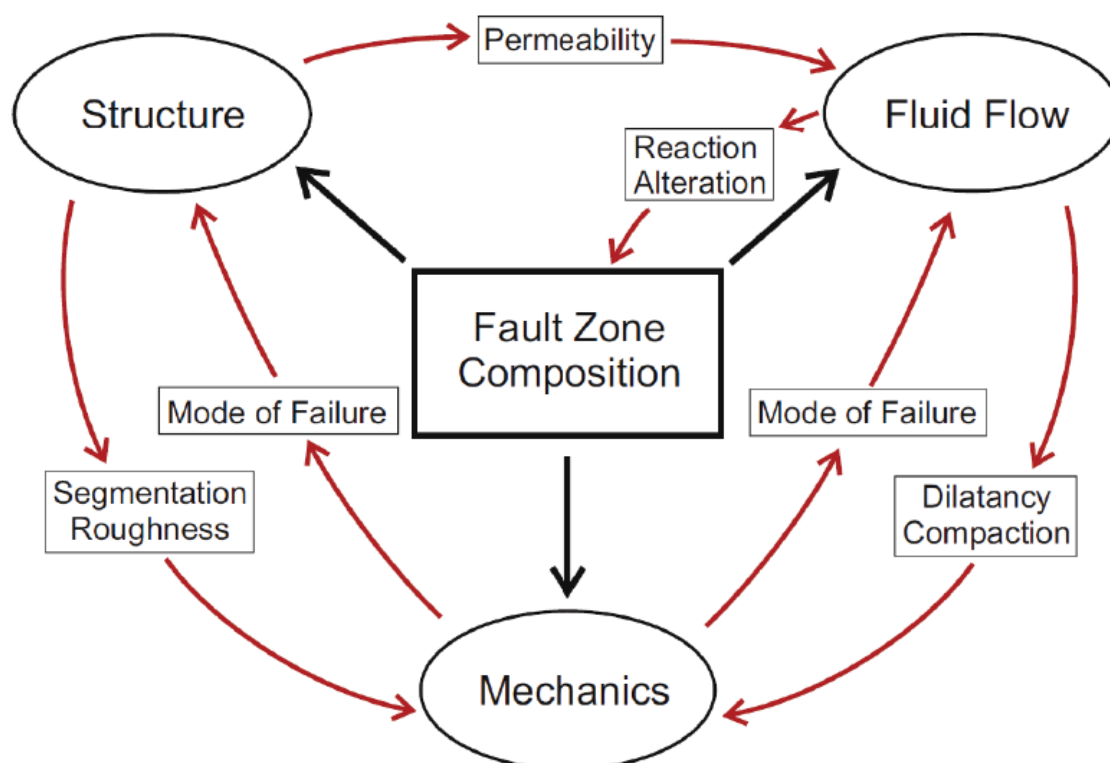


Figure 1.2 Flow diagram showing inter-relationships among the three main topics of structure, mechanics and fluid flow. Mode of failure refers to whether or not seismic slip occurs (Faulkner *et al.*, 2010).

1.2 PURPOSE AND AIMS OF REPORT

Faults have the potential to change the physical and economic performance of storage systems by compartmentalising reservoirs, increasing the effective reservoir dimensions and compromising caprock integrity (e.g. Streit and Hillis, 2004; Cartwright *et al.*, 2007; Bretan *et al.*, 2011; Rinaldi *et al.*, 2014). Consequently, the locations of faults with respect to the CO₂ storage system and their impact on fluid-flow should be appraised during site characterisation. However, key questions remain about when, where and how faults may negatively or positively impact the storage and migration of injected CO₂. Of particular interest for understanding how faults can impact fluid flow are the following questions:

- How does fault architecture (fracture pattern, width of core / damage zone, length of displacement) govern permeability?
- What are the mechanical and hydraulic properties of fault zones in sealing formations and transition zones?
- What insights can natural CO₂ seeps provide especially when compared to potential geological CO₂ storage sites in terms of flux rates, duration and fault characteristics?
- What is the potential range of CO₂ leakage rates from storage containers and how much leakage could occur before detection?
- What are the current limitations of existing geomechanical models and analytical methods?

Addressing these questions of where and how faults modify fluid flow is critical for developing risk management procedures at storage sites where faulting disrupts reservoir and/or caprocks. This study provides a summary of current research and understanding of fault

permeability that is directly relevant to CO₂ storage. In addition, the report identifies industry practices for analysing faults and modifying undesirable migration of fluids, knowledge gaps in our understanding and the future research necessary to improve management of fault-related CO₂ migration. Four key tasks have been addressed in the report and are outlined below.

Task 1

A brief summary of the mechanical and hydraulic properties of fault zones. The task contains the following elements:

- Explanation of how different parameters such as fault architecture, stress regime and fluid composition influence the sealing properties of faults and the conditions that could cause leakage (i.e. along-fault flow).
- Identification of the conditions that might lead to slip reactivation and CO₂ migration along faults.
- Indication of the potential range of leakage rates and the length of time before subsequent detection.
- Summary of current research on natural CO₂ seeps from faults to provide a context for comparison with CO₂ storage sites. This will include a summary of the rate of natural seepage along faults and the timescales of such processes.

Task 2

Review current oil industry practices that are used to assess and control the unwanted migration of hydrocarbons along faults. The experience of different industry/academic teams is used to assess and model fault leakage thresholds from potential CO₂ storage sites.

Task 3

Review the approaches used by other industries (e.g. waste disposal, hydrocarbons, civil engineering) to assess the properties and permeabilities of faults and examine how these approaches might be useful for controlling permeability and developing remediation measures for unwanted leakage at CO₂ storage sites.

Task 4

Identify the knowledge gaps in current understanding of fluid migration along faults. Outline the challenges in modelling fault permeability, and monitoring fluid migration (including CO₂), along and across faults. Recommend directions for future research and development directly related to improved definition of fault permeabilities.

1.3 REPORT STRUCTURE

The principal objective of this report is to provide a review and synthesis of international research and current understanding of fault permeability, with emphasis on how it could influence (positively or negatively) CO₂ storage. To address this principal aim and the four key tasks outlined in Section 1.2 the report has 10 main sections (including the introduction - Section 1). The contents and purpose of each of the main sections are summarised below.

Section 2 - Fault zone structure and permeability. This section provides a general overview of fault zone structure and how the different elements of fault zones influence fault permeability. It is intended to set the context for later discussions in Sections 3–5 where more detailed

consideration is given to fault permeability and its control on fluid flow. The section also provides an overview of the state of knowledge for faults as barriers and conduits to fluid flow.

Section 3 - Parameters influencing fault permeability. Reviews the influence of fault rock (Section 3.1) and fault zone (Section 3.2) properties, and their relationships to host rock lithological and mechanical stratigraphy (Sections 3.1.1 and 3.2.1), on fluid flow. It also examines the impact of fluid composition and cementation/dissolution on fluid flow (Sections 3.3 and 3.4). Given the potential for carbonate precipitation arising from CO₂ injection and long-term storage operations, these sections may have particular relevance to CO₂ storage projects. The section finishes with consideration of the role of confining pressures, stress orientation and pore pressure on fluid flow along faults (Sections 3.5 and 3.6).

Section 4 - Fault seal analysis. Fault seal analysis is widely utilised in fluid extraction and injection industries to predict the potential for low permeability fault rock to retard lateral flow of fluid. This section briefly summarises the methods and calibration data that underpins fault seal predictions, which are based on algorithms where low permeability fault rock is derived from clay-rich beds in the host rock (Figure 2.3b). Uncertainties in the predictions are also discussed.

Section 5 - Geomechanical modelling and fault leakage. Observations and theories for pressures and stresses presented in Section 3 are further considered in Section 5, where geomechanical methods for predicting the potential locations of fault-parallel fluid flow are discussed. This section also includes discussion of uncertainties associated with geomechanical modelling (Section 5.4) and a summary of the results from CO₂ injection into a low permeability reservoir at In Salah, Algeria (Section 5.6). The reader is referred to a recently published IEAGHG report on fault stability during pressure build-up for further information on geomechanical modelling (IEAGHG, 2015).

Section 6 - Natural CO₂ seeps along faults. Natural CO₂ seeps provide an indication of the volumes and rates of CO₂ emission that are possible at the ground surface in the presence of faulting. This section reviews data and observations from a dozen natural CO₂ seeps (nine terrestrial and three submarine), to inform discussion of the key spatial relationships between faults and CO₂ seeps. They provide information about how migration occurs along faults and at what rates (Section 7). Uncertainties in the interpretations for these natural analogues are also discussed.

Section 7 - CO₂ flow rates along faults. Although the rates of CO₂ migration along faults vary significantly, there is value in documenting the rates (and volumes) of migration to help constrain possible values at CO₂ storage sites where little or no flow data are available. Section 7 presents fault permeability and flow rate data from a number of studies and for the natural analogues outlined in Section 6. The implications of these values for CO₂ storage sites and flow mechanisms are considered.

Section 8 - Industry practices for measuring and mitigating unwanted fluid flow along faults. Extraction and injection industries, including petroleum, geothermal and CO₂ storage, can be affected by faults which locally promote and/or retard fluid flow. The experiences of the petroleum and geothermal industries, in particular, have application at CO₂ storage sites and are discussed in this section. The section focuses on industry practices for fault and fluid flow characterisation (Section 8.1), fluid flow simulations (Section 8.2), and remediation of migration (Section 8.3). The section is structured according to the practices rather than the industry.

Section 9 - Application of learnings from sections 2-7 for CO₂ storage. Understanding fault permeability is important for effective containment and management of injected CO₂. The learnings from this report for CO₂ storage projects are here discussed under three main headings: i) fault zone structure and permeability, ii) fault seal and mechanical predictions, iii) fluid flow along faults at natural CO₂ seeps and, iv) industry practices for mitigating unwanted flow.

Section 10 - Knowledge gaps and challenges for understanding CO₂ migration along faults. Present understanding of fault hydraulic properties is generally not sufficiently complete to predict when and where faults are likely to influence CO₂ migration, either positively or negatively. This section highlights a number of knowledge gaps in the understanding of faults and their potential controls on CO₂ migration. These gaps include limited understanding of heterogeneities in fault geometries and fault-zone permeabilities (Section 10.1), the scaling of fault properties from outcrop to reservoir scales (Section 10.1), the utility of cross and along fault permeability predictions (Sections 10.2 and 10.3), the paucity of *in situ* flow data for testing models (Sections 10.4 & 10.5) and the apparent absence of detailed guidelines to managing unwanted CO₂ migration along faults (Section 10.6).

Section 11 - Recommendations for future research. This section highlights research that could be undertaken to decrease the knowledge gaps and increase understanding of the processes that promote fluid flow along faults. Three main categories of recommendations are proposed; i) improved definition and quantification of fault hydraulic properties, ii) continued development and sensitivity testing of flow simulator models and geomechanical flow predictions, and iii) validation of models using empirical fluid flow data from fault zones.

2.0 FAULT ZONE STRUCTURE AND PERMEABILITY

2.1 INTRODUCTION

Bulk fluid-flow rates through or along fault zones are important for many practical applications, including geothermal, hydrocarbon production and CO₂ storage. In order to assess whether a proposed site will be capable of storing injected CO₂ over time-intervals of at least 100's of years it may be necessary to examine the permeability of faults and how it changes with increasing CO₂ fluid pressures. Two aspects of fault hydraulic behaviour are likely to be important in CO₂ storage. First, will a fault within a reservoir act as a sealing lateral barrier thus permitting CO₂ to accumulate and, if so, how will this influence reservoir pressures (and injectivity) and CO₂ column height? Secondly, will CO₂ migrate along a fault out of the designated storage container? Such flow may occur at ambient fault permeabilities (i.e. in the absence of fault reactivation or instability), and/or due to increasing pore-fluid pressure generated by CO₂ injection which triggers fault instability and reactivation (Section 4), leading to transient increases in permeability and potential migration of CO₂ (Bretan *et al.*, 2011).

It has long been known that faults can strongly influence the sub-surface movement of fluids and gas (e.g. Figure 1.1, and Wade, 1913; Illing, 1942; Neglia, 1979; Sibson, 1981b; Hooper, 1991; Caine *et al.*, 1996; Carruthers and Ringrose, 1998; Morretti, 1998; (Cox, 1999); Aydin, 2000; Shipton *et al.*, 2004; Wibberley *et al.*, 2008; Faulkner *et al.*, 2010). Fault zones are most likely to modify CO₂ migration pathways where their permeabilities differ from those of the surrounding host rock by at least two orders of magnitude, the faults are large or highly connected, and local stresses promote fault dilation (Wallace and Morris, 1986; Balberg *et al.*, 1991; Barton *et al.*, 1995; Bour and Davy, 1997; Evans *et al.*, 1997; Cox, 1999; Sanderson and Zhang, 1999; Seebeck *et al.*, 2014). The hydraulic behaviour of faults depends on a number of factors including; host and fault rock rheology, fault zone and host rock permeabilities, structural anisotropy, bulk stress conditions, pressure differentials across the fault and fluid viscosity (Caine *et al.*, 1996; Evans *et al.*, 1997; Cox, 1999; Wibberley *et al.*, 2008; Manzocchi *et al.*, 2010; Edlmann *et al.*, 2013) (Figures 1.1 and 1.2). For the purposes of generating static models in reservoir flow simulations these factors can be divided into two groups; i) geometrical scaling properties of the fault system (e.g. Figure 2.1) and, ii) flow properties of the faults. Fault flow properties are generally incorporated into reservoir simulations as transmissibility multipliers which modify calculated flow rates across a fault (e.g. Manzocchi *et al.*, 1999). The calculation of geologically meaningful fault transmissibility multipliers requires predictors of both fault rock thickness (Figure 2.2) and permeability. The techniques used to construct numerical reservoir simulations for petroleum fields also have application for CO₂ storage reservoirs.

Faults can act as both barriers to lateral fluid-flow and conduits for along-fault flow. Study of the mechanical process of sandstone and shale deformation indicates that fault permeabilities may be greater during deformation than after it ceases (e.g. Fossen *et al.*, 2007; Zhang and Rothfuchs, 2008; Zhang, 2011; Ballas *et al.*, 2015). Evidence for the low permeability of fault zones is provided by across-fault pressure changes, compartmentalisation of reservoirs by faults, low measured flow rates in fault zones, the differential subsidence caused by water production, and by the accumulation of large volumes of hydrocarbons against fault planes (e.g. Hooper, 1991; Yielding *et al.*, 1997; Barr, 2007; Van Hulten, 2010). These phenomena would not be possible if fault surfaces were, in their entirety, always high permeability conduits for migrating fluids. In contrast, evidence for the vertical migration of fluids via fault zones is equally strong. Mineralization of fault zones, fluid potential "drawdown", thermal anomalies, salinity anomalies, seismic anomalies, gas flux anomalies, the local mineralisation of

sandstones near fault zones, underfilled structural closures intersected by faults and high fluid flow rates all indicate that fault zones are fluid migration pathways (e.g. Hooper, 1991; Cox, 1999; Barr, 2007; Annunziatellis *et al.*, 2008; Faulkner *et al.*, 2010; Hermanrud *et al.*, 2014; Jung *et al.*, 2014b; Seebeck *et al.*, 2014). Of particular relevance to CO₂ storage, faults cutting through low permeability strata (i.e. caprocks) can provide pathways for fluids generated in deep, pressurized rocks to migrate into shallow levels (Dewhurst and Hennig, 2003; Miller *et al.*, 2004; Ilg *et al.*, 2012). Evidence for such vertical migration in petroleum systems includes; oil seeps from seafloor fault scarps, thermal anomalies co-located with faults, fluid pressure compartmentalisation, temporal variations in hydrocarbon fluid chemistry produced from the same reservoir, and geochemical anomalies seen in fault zone core samples.

A plausible model that accounts for the contradictory fault-permeability evidence is the theory of episodic or periodic flow (Hooper, 1991; Sibson, 1996; Miller *et al.*, 2004; Leclère *et al.*, 2015). This model predicts that when faults are active, permeabilities and fluid pressure gradients are increased, and the movement of fluids up faults is possible; but, when faults are inactive, permeabilities are reduced, and flow is retarded. Increases in fault permeability during slip (either during creep or discrete events, e.g., earthquakes) may be facilitated by dilation, refracturing of mineralized zones and high transient fluid pressures (Hooper, 1991; Sibson, 1996). As a result of these processes a fault may, at different times, be both a pathway and a barrier to fluid migration. Temporal variation of fault permeability may also result from the precipitation or dissolution of mineral cements (Section 3.4). Such temporal changes in fault permeability may have particular relevance to CO₂ storage where pressure management has the potential to reduce fault dilatancy and CO₂ flow rates.

2.2 FAULT ZONE STRUCTURE

Many studies of fault zones have been published over the last 30 years (e.g. Chester and Logan, 1986; Wallace and Morris, 1986; Caine *et al.*, 1996; Childs *et al.*, 1996; Shipton *et al.*, 2006; Wibberley *et al.*, 2008; Childs *et al.*, 2009; Faulkner *et al.*, 2010). Whilst it is generally acknowledged that the structure of fault zones can be complex and spatially variable, the relatively simple fault damage zone model has been widely adopted (Figure 2.1a). In this model shear displacements are accommodated by two main elements referred to as fault core and fault damage zone (Figure 2.1a). Displacements are focused in the fault core which comprises low permeability material that is generally considered to impede cross-fault flow of fluids (e.g. Caine *et al.*, 1996). The core (also referred to as “fault rock” in the literature, see Childs *et al.*, 2009) is enclosed within a damage zone that comprises joints and small-scale faults, which are often inferred to elevate permeability and to promote fluid-flow along fault zones. The damage zone model is attractive in part because it is well suited to presentation in cross section, is easily visualised and has the potential to be numerically modelled. However, few faults observed in outcrop adhere to the damage zone model (Childs *et al.*, 2009), which does not incorporate sufficient variability of fault zone structure to adequately define the flow properties of faults (e.g. Figures 2.3a–b). In particular, the damage zone model has a limited ability to describe 3D fault zone structure and hydraulic properties.

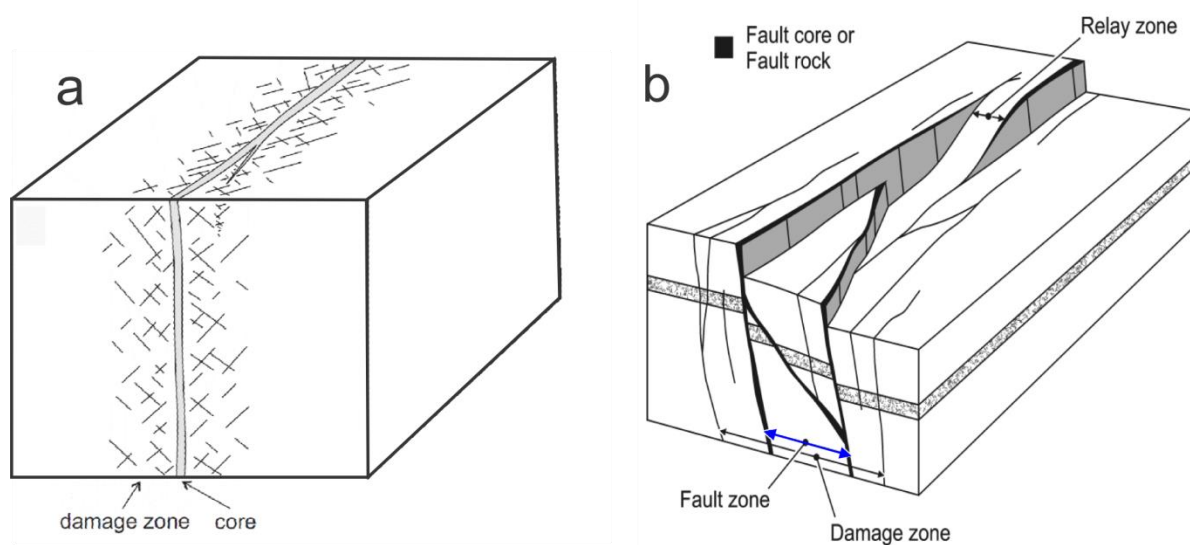


Figure 2.1 Schematic diagrams illustrating fault zone models and terminology. (a) Fault damage zone – fault core model where a zone of fracturing encloses a clay-rich core comprising low permeability fault rock (Chester and Logan, 1986). More complex versions of this model contain multiple fault cores (Faulkner *et al.*, 2010). (b) Fault zone model in which the thicknesses of clay-rich fault rock and fault zones dominated by small faults vary over the fault surface (Childs *et al.*, 2009).

Fault zones exhibit extreme internal complexity and heterogeneous displacement distribution (Wallace and Morris, 1986; Caine *et al.*, 1996; Childs *et al.*, 1996; Childs *et al.*, 2009; Faulkner *et al.*, 2010). The highest shear displacements are focused within (or bounding) fault rock that typically contains clay-rich fault gouge and breccia. Fine-grained fault rock can be produced by a number of processes including; crushing and intense fracturing of host rock, smearing of mudstone beds into the fault zone and/or injection of wall rock into the fault zone. Fault rock is generally (but not always) accompanied by small-scale faults and joints which collectively form the fault zone (Figure 2.1b). As fault zones include fault rock and associated small-scale faulting/jointing in the rock volume adjacent to the fault rock, this term is not directly comparable to the term damage zone. Relating the geometries and dimensions of fault zones and fault damage zones is further complicated by limited rigorous quantitative definitions of these terms (for further discussion of fault zone terminology, see Childs *et al.*, 2009).

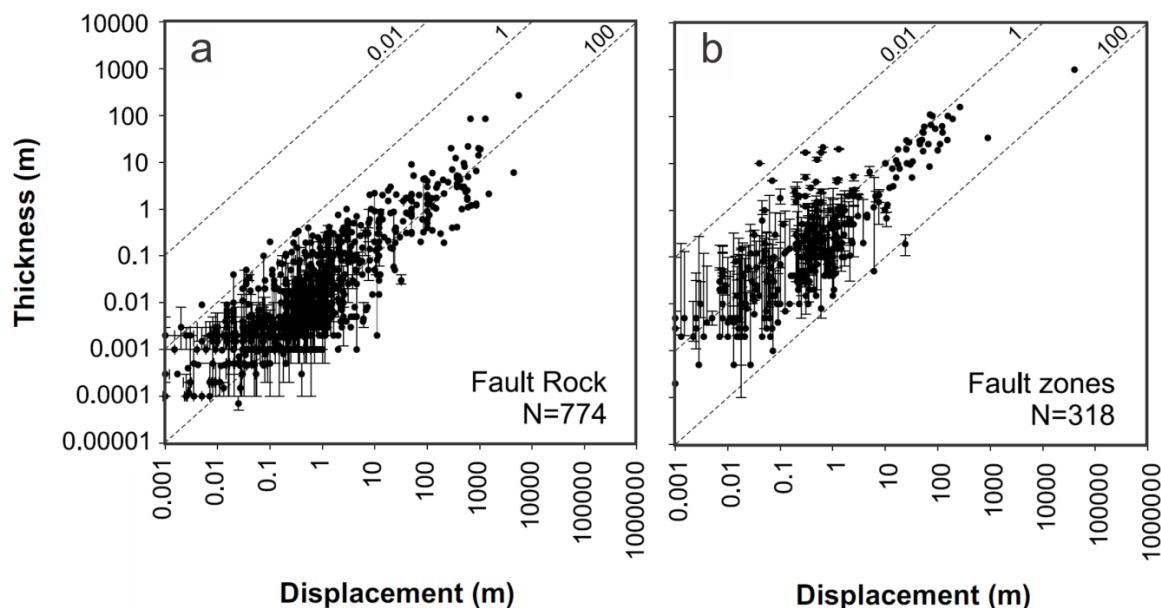


Figure 2.2 Global compilations of fault zone data showing thickness vs displacement for fault rock (a) and fault zones (b). Figure modified from Fig. 4 of Childs *et al.* (2009). Refer to Childs *et al.* (2009) for description of data sources.

Fault zones are irregular over scales from millimetres to kilometres (Wallace and Morris, 1986; Caine *et al.*, 1996; Childs *et al.*, 1996; Evans *et al.*, 1997; Wibberley *et al.*, 2008; Childs *et al.*, 2009; Faulkner *et al.*, 2010). They typically comprise an anastomosing system of intersecting fault slip surfaces and fault rock, which bound lenses of variably fractured host rock (e.g. Wallace and Morris, 1986; Wibberley *et al.*, 2008; Childs *et al.*, 2009; Faulkner *et al.*, 2010; Nicol *et al.*, 2013a). These fault lenses can be observed in cross section and map view, and produce variations in the width of fault zones and fault rock over the fault surface (Childs *et al.*, 2009; Awdal *et al.*, 2014). Although the thicknesses of fault zones show a broad positive relationship with displacement (i.e. larger faults tend to have wider fault zones and thicker fault rock), there is significant heterogeneity of fault zone thickness for a given displacement. The thicknesses of both fault zones and fault rock can change on individual structures by an order of magnitude or more over distances of metres (e.g. Childs *et al.*, 2009; Nicol *et al.*, 2013a) (Figures 2.2 & 2.3). The widest fault zones on individual faults are generally associated with fault complexities, including segmentation and segment boundaries (e.g. relays), fault bends, fault intersections, fault branch lines and fault terminations. In many cases these zones of fault complexity are sites of increased numbers of joints and small-scale faults, and are considered to be zones of likely elevated fault-zone permeability (e.g. Cox, 1999; Gartrell *et al.*, 2004; Dockrill and Shipton, 2010; Ilg *et al.*, 2012; Hermanrud *et al.*, 2014). These studies indicate that fluid flow (water, gas and supercritical CO₂) within fault zones can be highly channelized and heterogeneous. The suggestion that fault complexities may represent sites of elevated permeability (relative clay-rich fault material and/or the host rock) and channelized fluid flow has relevance for CO₂ migration studies, however, the model has not yet been extensively tested using fluid-flow data and it is not clear under what conditions (e.g. rock rheologies, fault geometries and stresses) fault-zone complexities promote fluid flow.

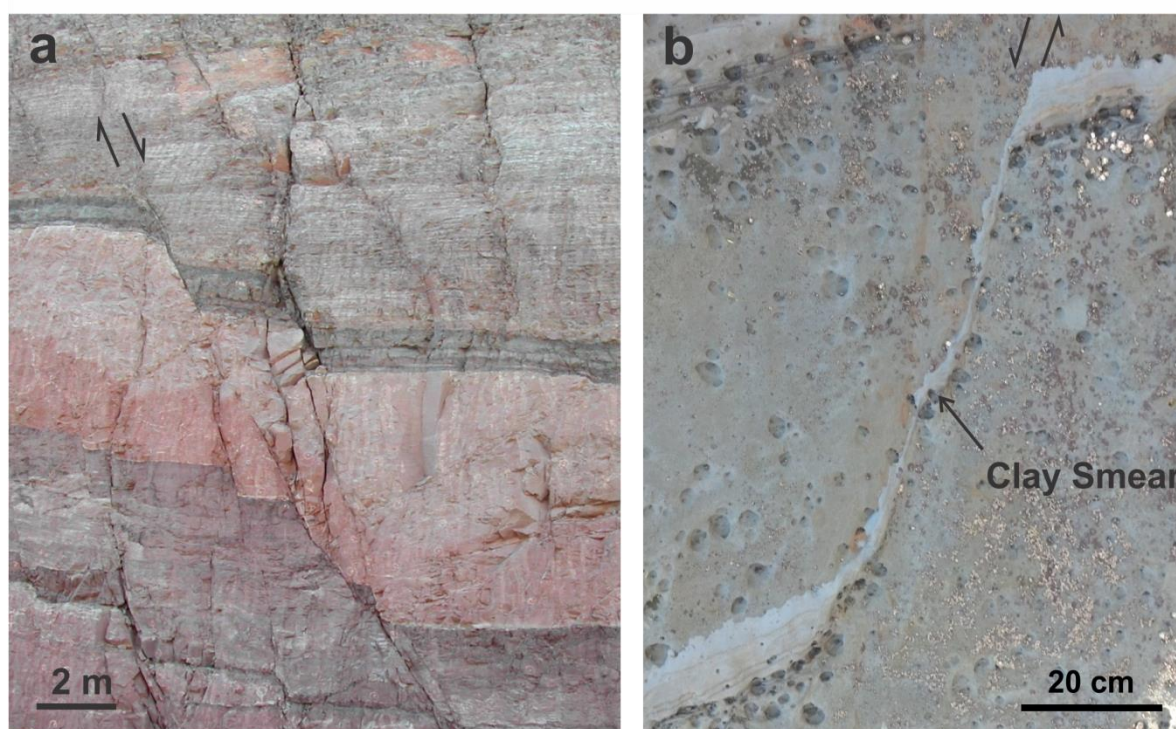


Figure 2.3 Photographs showing examples of outcrop scale normal faults. a) Normal fault within the Honaker Trail Formation from the immediate hanging wall of the Moab Fault exposed in a road cutting adjacent to the entrance to Arches National Park, Utah, USA. b) Small normal fault within the Mount Messenger Formation turbidites, Mohakatino coastline, north Taranaki, New Zealand. Note the continuous smear of the shale bed (see Section 2.3 for further discussion). Arrows show the location of the main fault surface and sense of shear in both cases.

2.3 CROSS-FAULT MIGRATION

Several studies have indicated that clay-rich fault rock has the potential to impede cross-fault fluid flow in reservoirs (e.g. Bouvier *et al.*, 1989; Jev *et al.*, 1993; Knipe, 1997; Yielding *et al.*, 1997; Manzocchi *et al.*, 1999; Sperrevik *et al.*, 2002; Yielding, 2002; Childs *et al.*, 2007; Freeman *et al.*, 2008; Eichhubl *et al.*, 2009; Manzocchi *et al.*, 2010; Yielding *et al.*, 2010; Yielding, 2012). Many of these studies have been driven by the petroleum industry and its desire to predict where hydrocarbons in sandstone reservoirs are most likely to be trapped by faults on geological timescales, and under what circumstances faults might compartmentalise reservoirs on production timescales. The ability of faults to retard or trap migrating fluids and to compartmentalise reservoirs also has relevance for CO₂ storage projects over timescales of hundreds of years. Faults that impede CO₂ flow may decrease the rate and efficiency of injection and increase reservoir pressures. Snøhvit CO₂ re-injection is an example where rapid rise in reservoir pressures due to fault compartmentalisation resulted in a switch to a stratigraphically higher injection interval (IEAGHG, 2015b). High reservoir pressures due to fault compartmentalisation can also be mitigated by decreasing injection rates and/or increasing the number of injector wells, both of which carry some cost to operations. By contrast, small faults could locally baffle CO₂ flow and promote trapping and increased stability of the injected CO₂ plume. Whether fault impedance of CO₂ is positive or negative for CO₂ storage is likely to be site-specific and will depend on a range of parameters including; injection rates and volumes, reservoir size and geometry, fault sizes and geometries, and reservoir stress conditions.

Studies of cross-fault permeability have mainly been limited to interbedded sandstone-mudstone sedimentary sequences displaced by normal faults (e.g. Yielding *et al.*, 1997;

Manzocchi *et al.*, 2010). For these sequences, where the reservoir is faulted against low permeability mudstones, the fault is generally assumed to be sealing via juxtaposition. In circumstances where sandstone units are in contact across the fault it could be sealing or leaking to cross-fault flow. At any given point in time it is possible that a fault may be sealing at one location and leaking at another. To determine what stratigraphic units are juxtaposed across a particular fault it is common to construct an Allan Diagram which displays the distribution of the main lithological units in the footwall and hanging wall of a fault over the mapped extent of the fault surface (Allan, 1989). Allan Diagrams (also referred to as juxtaposition diagrams) are routinely produced by software (e.g. TrapTester) and have been used for both petroleum industry studies and CO₂ storage assessment (e.g. Yielding *et al.*, 2010; Bretan *et al.*, 2011). Although displacement backstripping is routine and some studies have incorporated fault displacement evolution to assess changes in juxtaposition and sealing properties through time (e.g. Reilly *et al.*, 2016), these analyses can be regarded as static on production timescales. Therefore, they do not take account of changes in fault sealing that might arise from pressure transients during fluid injection.

2.4 ALONG-FAULT MIGRATION

The coincidence of faults with gas seeps at the seabed, gas chimneys in seismic reflection lines and water springs at the ground surface supports the notion that faults can in some instances promote up-sequence flow (e.g. Hooper, 1991; O'Brien *et al.*, 1999; Dewhurst and Hennig, 2003; Boles *et al.*, 2004; Sager *et al.*, 2004; Canet *et al.*, 2006; Canet *et al.*, 2010; Ilg *et al.*, 2012). Many studies infer that along-fault flow is facilitated by the presence of open fractures, but there are few independent data available to support the proposed mechanisms that lead to fracture opening or flow localisation (see Cartwright *et al.*, 2007). *In situ* measurements suggest that along-fault permeabilities can be up to nine orders of magnitude higher than those of the surrounding rocks and may be as high as 10⁻¹³ to 10⁻¹¹ m² (i.e. 0.1 to 100 D; e.g. Ingebritsen and Manning, 2010). One to two orders of magnitude difference in permeability between the fault zone and unfaulted seal will, in many cases, be sufficient to promote up-fault migration. In general terms it is believed that at many sites along-fault fluid migration will likely be governed by the three-dimensional distribution and connectivity of high permeability rock (or fractures) within fault zones (e.g. Cox, 1999; Sanderson and Zhang, 1999; Seebeck *et al.*, 2014) (Section 3), by variations in the stress tensor along faults (Section 5) (e.g. Morris *et al.*, 1996; Ferrill and Morris, 2003) and changes in reservoir pressure (e.g. Faulkner *et al.*, 2010) (Sections 3 & 5).

Many *in situ* studies highlight the highly localised and convoluted nature of fluid-flow through fractured media (e.g. Tsang and Neretnieks, 1998; Cox, 1999). For example, studies of groundwater flow indicate that most of the flow is confined to point sources within highly fractured zones of the larger faults (Seebeck *et al.*, 2014). Channelized fluid flow is inferred to reflect the heterogeneous structure of fault zones and, in particular, spatial variations in the thickness of low-permeability fault rock and in the clustering of open faults and joints (Figure 2.4). Heterogeneous fault zone hydraulic properties reflect changes in the densities, dimensions and connectivity of small-scale open fractures in fault zones (Eichhubl *et al.*, 2009). The dimensions of fault zones change with a number of variables including displacement, host rock type and fault surface geometry (e.g. Childs *et al.*, 2009). Wider zones of fault-related fracturing comprising greater numbers of fractures are commonly observed within fault relays, close to fault intersections, proximal to fault bends and surrounding fault tips (see also Childs *et al.*, 1996; Gartrell *et al.*, 2004; Childs *et al.*, 2009; Eichhubl *et al.*, 2009). Regions of high fracture densities are most likely to contain long fractures and/or interconnected fracture networks which may enhance up-sequence fluid flow (Figure 2.4) (Cox, 1999; Sanderson and Zhang, 1999; Philip *et al.*, 2005; Seebeck *et al.*, 2014) (Section 3). Steeply inclined zones of

fracturing, such as might be observed at lateral relays or adjacent to steeply inclined fault intersections, are likely to be most problematic for seal integrity. The results of detailed fault studies and *in situ* permeability measurements are supported by numerical models which show highly non-linear behaviour and flow localization for a wide range of natural well-connected critically stressed fracture networks (Zhang and Sanderson, 1998; Sanderson and Zhang, 1999; Tsang *et al.*, 2007). For such fault/fracture systems the variability in the distribution and rate of flow can be accounted for if the system is at or close to the percolation threshold (e.g. Cox, 1999; Sanderson and Zhang, 1999). A percolation threshold is reached when enough elements connect to allow fluid-flow across the entire width of the network and the reservoir or seal becomes permeable (Zhang and Sanderson, 1998).

With detailed analysis of outcrop, core and/or seismic reflection data it is possible to quantify the geometries, sizes and densities of faults (e.g. Gillespie *et al.*, 1993; Childs *et al.*, 2009; Nicol *et al.*, 2013a), however, such quantification appears to be rarely achieved in petroleum fields, geothermal reservoirs or potential CO₂ storage sites. A lack of this type of detailed fault analysis at potential CO₂ storage sites may reflect the uncertain utility of these data and the fact that they cannot as yet be routinely incorporated into flow simulators. More *in situ* fluid-flow data and numerical flow modelling are required to quantify the effects of fault zone architecture (e.g. dimensions and density of small-scale faulting) on fluid migration through seal rocks.

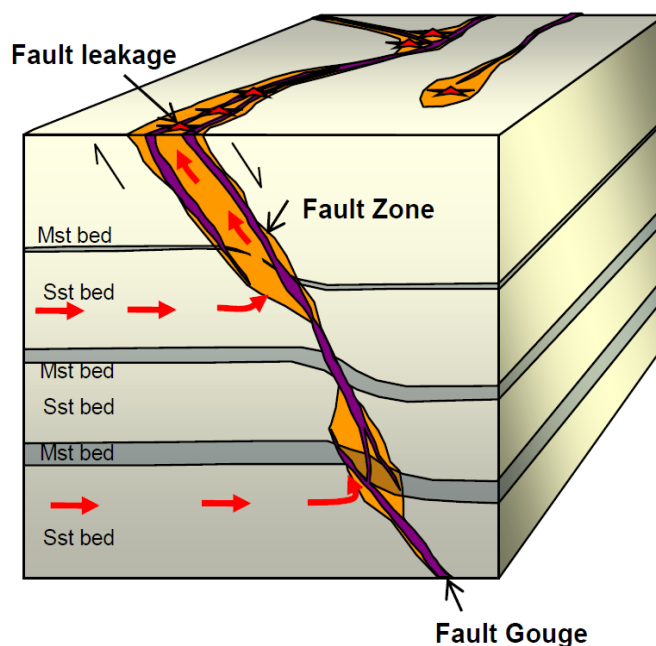


Figure 2.4 Schematic block model showing the spatial variation in fault elements (i.e. gouge shown in purple and fault zone in orange) and their potential influence on along-fault fluid flow. Stars on the top of the block show the locations of up-fault flow.

Fluid-flow pathways in the crust are also thought to be driven by elevated stresses and by fluid pressure gradients that depart from hydrostatic (e.g. Sibson, 1996; Cox, 1999; 2007; Tsang *et al.*, 2007). Several geomechanical techniques have been developed for predicting the most likely locations of along-fault migration of fluids (see Section 5). These techniques utilise the locations and geometries of faults together with estimates of the regional stress tensor to estimate the faults or parts of faults that are closest to failure and, therefore, most likely promote fluid flow (e.g. Morris *et al.*, 1996; Ferrill and Morris, 2003; Section 5). While the theory that underpins these geomechanical techniques is widely accepted, the predictions remain untested in many cases. Such testing and examination of the factors that promote along-fault

flow are in their formative stages and should be a focus of future work. Given a limited understanding of the detailed mechanisms that lead to along-fault flow it cannot be discounted that some faults passing through caprocks will reduce their ability to trap injected CO₂ rising under buoyancy forces. In such cases up-sequence flow could result in charge of shallower reservoirs and leakage at the ground surface. Therefore, understanding where and how faults are likely to enhance CO₂ flow is critical for the effective management of CO₂ storage sites.

3.0 PARAMETERS INFLUENCING FAULT PERMEABILITY

Fault zones are four-dimensional volumes of deformed rock with highly anisotropic and heterogeneous properties that evolve through time. Although occupying only a small fraction of the crust, fault zones have a strong influence on the crust's mechanical and hydraulic properties. Faults are complex zones composed of linked fault segments, one or more high strain slip surfaces contained within regions of high and low strain (often called fault core and damage zone), Riedel shears, splay faults, dilational and contractional jogs, relay ramps (Caine *et al.*, 1996; Childs *et al.*, 1996; Shipton and Cowie, 2001; Faulkner *et al.*, 2003; Childs *et al.*, 2009; Faulkner *et al.*, 2010; Michie *et al.*, 2014). These fault-zone complexities produce variations in structure along strike and down dip, even over relatively short distances (Childs *et al.*, 1996; Shipton and Cowie, 2001; Lunn *et al.*, 2008; Faulkner *et al.*, 2010; Seebeck *et al.*, 2014) (for additional discussion see Section 2). The magnitude and direction of fluid flow through a volume of rock is generally governed by the fluid pressure gradient, host rock permeability anisotropy (e.g. bedding, foliation), and the structural permeability associated with faults, folds and fractures. Combinations of these parameters have led to the localised high-volume flows required to develop ore deposits in fault zones (Sibson, 1996; Cox, 1999; Rowland and Simmons, 2012). Four main factors influence the hydraulic properties, composition, structure and mechanical behaviour of fault rocks (Yielding *et al.*, 2010). These are:

- The composition and rheology of the host rock that is displaced across a fault, in particular the content of fine-grained phyllosilicate clay minerals.
- The stress conditions at the time of faulting, which are most strongly controlled by the tectonic setting, the initial depth of burial during faulting and fluid injection or extraction.
- The maximum temperature experienced by the fault zone after faulting, controlled by the maximum post-faulting burial depth and the geothermal gradient.
- The composition of syn- and post-kinematic fluids and their reaction products.

Within the petroleum industry, fault permeability is usually most important in low to moderate matrix permeability reservoirs; as in more permeable rock, fluid flow within any fault system may be significantly less than the flow through the rock matrix. Faults could also impact the injection and storage of CO₂, where they may play an important role in controlling the migration of crustal fluids over a broad range of spatial and temporal scales. Fault-zone structure, mechanics and permeability can vary significantly on human timescales of years to tens of years (e.g. Barr, 2007; Obeahon *et al.*, 2014) and during the lifetime of CO₂ storage projects. For CO₂ storage, understanding fault permeability within low permeability caprocks is of primary importance. Fault permeability can be highly sensitive to any change in the effective stress acting normal to the fracture plane (i.e., stress dependent permeability) (Barton *et al.*, 1995; Townend and Zoback, 2000) and, in some cases, may be increased by rising reservoir pressures during CO₂ injection. The magnitude of changes in pore pressures during CO₂ injection and the associated hydraulic response of faults is likely to be site specific, as it is for hydrocarbon fields. For example, in some hydrocarbon fields low permeability fractured reservoirs do indeed show a productivity decline on pore pressure drawdown, whilst others show no productivity decline even after significant reductions in fluid pressures (Dyke, 1995). High differential pressures created between fault bounded compartments during production can also lead to changes in fault permeability. Here, fault seal breaks down when the pressure differential between isolated compartments exceeds the capillary entry pressure estimated for the fault rock (Hillier, 2003; Obeahon *et al.*, 2014).

Faults can modify fluid migration over a range of spatial length scales. At the basin scale, faults and fault-related folds control vertical deformation (uplift and subsidence) and hence can influence temperature, fluid pressure gradients and migration (e.g. Hooper, 1991). At smaller scales, fault zones control the compartmentalisation or flow pathways of fluids migrating through a volume of rock (Wallace and Morris, 1986; Yielding *et al.*, 1997; Barr, 2007; Van Hulten, 2010). The recognition of transient high permeability along faults has important implications for the storage of CO₂ under pressures higher than the original formation pressure (Leclère *et al.*, 2015). Fault-zone structure, mechanics and fluid-flow properties are inextricably coupled and should not be considered in isolation (Faulkner *et al.*, 2010) (Figure 1.2). This report focuses on fault zone structure and fluid flow properties. For example, upper crustal fault rocks are commonly altered (e.g. Evans and Chester, 1995; Cavailhes *et al.*, 2013) and are not simply a granulated product of their protolith. These fault rocks are in some cases low- to medium-grade metamorphic rocks with authigenic growth of clays and other minerals (Faulkner *et al.*, 2010; Cavailhes *et al.*, 2013). The secondary mineralization of fault zones has important implications for their permeability structure (Section 3.4). In this section we also examine the processes and factors which control the permeability of fault zones and their hydraulic properties. The section focuses on the processes that can influence the hydraulic properties of fault zones and is broken down into three main parts; i) fault properties (Sections 3.1 and 3.2), ii) fluid composition, cementation and dissolution (Sections 3.3 and 3.4), and iii) pressures and stresses (Sections 3.5 and 3.6). Four possible mechanisms have been proposed for promoting increased permeability at depth, each creating natural fracture permeability of contrasting stress dependency (Dyke, 1995); i) surface roughness asperity model (Section 3.2.3), ii) block rotation (Section 3.2.3), iii) diagenetically modified fractures (Sections 3.4), and iv) zero effective normal stress (Section 3.5). How a particular lithology responds to changes in effective stress is controlled by which of these mechanisms dominate *in situ* permeability.

3.1 FAULT ROCK PROPERTIES

3.1.1 Host rock lithology and fault displacement

The rock types present in a fault zone are highly dependent on the lithology being deformed and the pressure, temperature and strain rate during deformation (Shipton *et al.*, 2006; Faulkner *et al.*, 2010; Yielding *et al.*, 2010). Different lithologies may produce different deformation products under the same stress, strain and temperature conditions. For example, two sandstone units in close proximity (a lithic arkose to feldspathic litharenite and a quartz arenite) with common slip and thermal histories display contrasting fault-rock and damage-zone attributes (Laubach *et al.*, 2014). Characterisation of fault-zone structure, therefore, requires an understanding of the deformation processes active during fault formation in a given litho-tectonic setting (e.g. Ferrill and Morris, 2008; Childs *et al.*, 2009; Soden and Shipton, 2013; Laubach *et al.*, 2014; Michie *et al.*, 2014). The deformation processes by which faults initiate and grow depend on a variety of factors including, among others, host rock composition and strength (e.g. Wilson *et al.*, 2003; van der Zee and Urai, 2005), mechanical stratification (e.g. Ferrill and Morris, 2003; Schöpfer *et al.*, 2007; Ferrill and Morris, 2008; Ferrill *et al.*, 2011), pre-existing structures (e.g. Giba *et al.*, 2012) and magnitude of displacement (e.g. Power *et al.*, 1988; Faulkner *et al.*, 2003; Shipton *et al.*, 2006; Childs *et al.*, 2009). For recent reviews on the internal structure of fault zones the reader is referred to Wibberly *et al.* (2008) and Faulkner *et al.* (2010).

The permeability of fault zones is governed by the spatial distribution of rock deformation products (e.g. fault rock and fractures) in three dimensions and the evolution of these properties over time. The spatial distribution of rock products within a fault zone is a function

of the stress field and the mechanical properties of the rock at the time of deformation (see Figure 3.1) (Childs *et al.*, 2009).

Although fault zone structure and hydraulic properties have been examined in a range of rock types, much attention has been focused on low permeability fault rock within siliciclastic sequences that characterise many oil and gas reservoirs. Permeabilities measured in these phyllosilicate-framework fault rocks typically range from $< 10^{-19}$ to 10^{-16} m² (Figures 3.2 and 3.3) (e.g. Fisher and Knipe, 2001). Natural fault gouges measured under laboratory conditions simulating burial depths of ~4 km (100 MPa) show ultra-fine gouge permeabilities ranging down to 10^{-21} m² (Wibberley and Shimamoto, 2003). These types of low permeability fault rock also have a permeability anisotropy of 2-3 orders of magnitude between measurements oriented perpendicular (lowest relative permeability) and parallel (high relative permeability) to the primary slip surface (e.g. Faulkner and Rutter, 1998; Shipton *et al.* 2002; Farrell *et al.*, 2014). The highest relative fault rock permeability in these studies is generally parallel to the slip direction. While damage zones and their associated microfracturing are a focus of present research (e.g. Faulkner *et al.* 2010), high permeabilities (2-4 orders of magnitude higher than the host rock) have also been documented within fault zones (e.g. Wibberley and Shimamoto, 2003; Tanikawa *et al.*, 2009). Wibberley and Shimamoto (2003), for example, show the high variability of permeabilities measured across a large fault zone (Figure 3.3). Smaller displacement faults can have similar permeability variations. Tanikawa *et al.* (2009) show a two orders of magnitude (1×10^{-18} to 3×10^{-15} m²) variation in permeability across a 4 m wide fault zone where both the highest and lowest permeabilities measured are in proximity to the primary slip surface. These studies highlight that the internal components of fault zones also have the potential to be high permeability conduits for fluid flow under the right conditions.

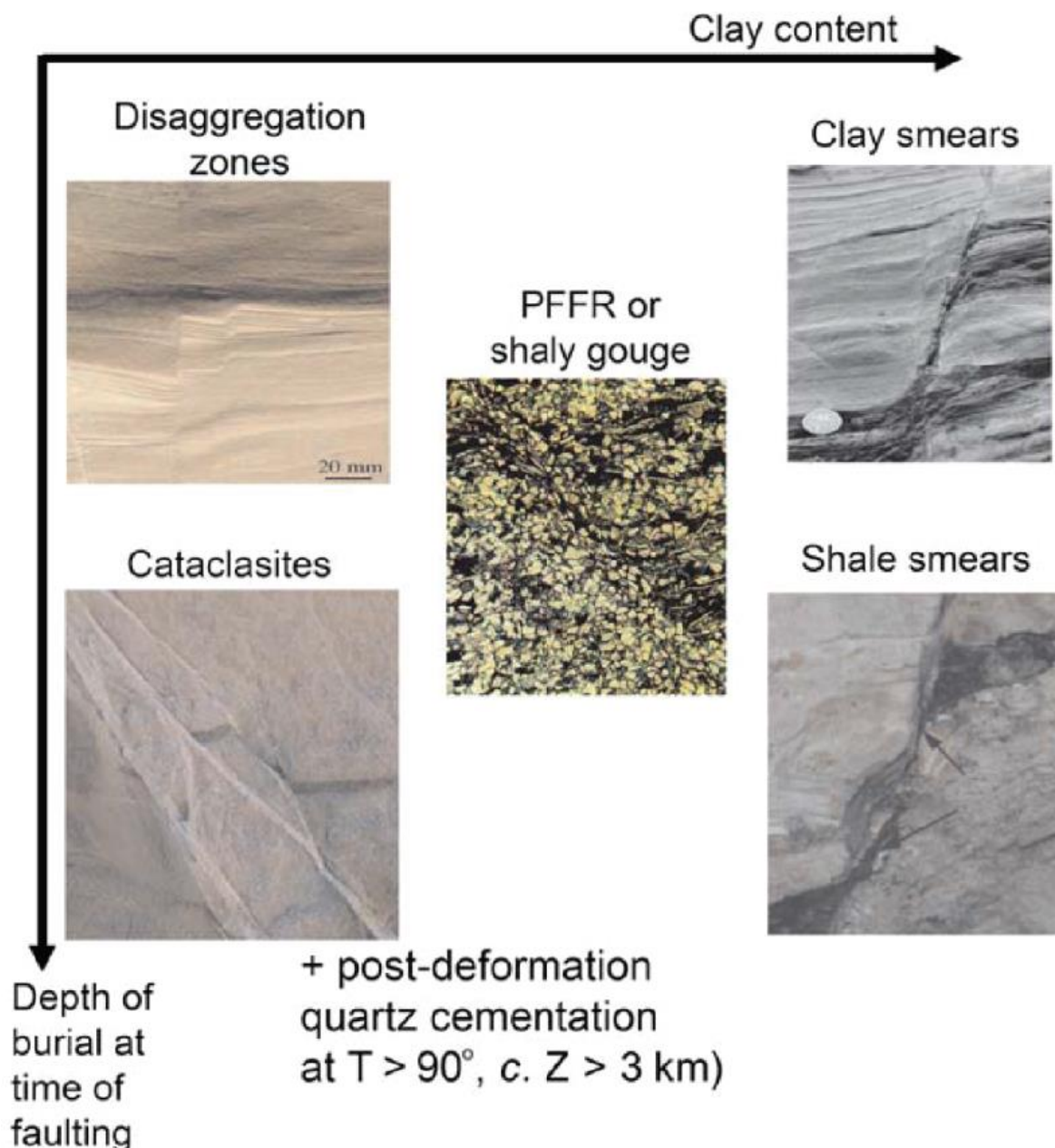


Figure 3.1 Schematic plot illustrating the main fault rock types generated in siliciclastic sequences. (from Yielding *et al.*, 2010) The axes represent two of the three main controls (clay content, and stress conditions during faulting); the third main control is post-faulting temperature history. Refer to Yielding *et al.* (2010) for data sources.

In siliciclastic sequences the types of fault rock developed depends largely on the relative proportions of sand to fine grained (clay/shale) lithologies, the degree of lithification of the host rock, the depth, and displacement. In clay-rich sequences, clay or shale smears can form over the fault plane (Figures 2.3 & 3.1). Clay smears represent ductile deformation in a fault-zone, and are often wedge-shaped with the thickest smear immediately adjacent to the source bed (e.g. Lehner and Pilaar, 1997; Aydin and Eyal, 2002; Eichhubl *et al.*, 2005; van der Zee and Urai, 2005; Yielding *et al.*, 2010). Although most often developed in poorly lithified sequences, 'clay' smears can form in more lithified sequences by abrasion rather than ductile flow. This process results in thin shale veneers of variable thickness along the fault plane (Lindsay *et al.*, 1993; Yielding *et al.*, 2010). Clay smears tend to become more discontinuous with increasing fault displacement. Discontinuities can occur at any point in the smear (often near the upthrown or downthrown source bed) (Childs *et al.*, 2007) and represent 'weak' points in the fault seal. Figure 3.2 shows an example of the general relationships between fault-rock permeabilities

relative to their clay content (Fisher and Knipe, 2001). While the permeability of fault rock decreases systematically as a function of increased clay content, there is considerable variability in permeabilities (2–3 orders of magnitude) for any given clay content (e.g. Fisher and Knipe, 2001).

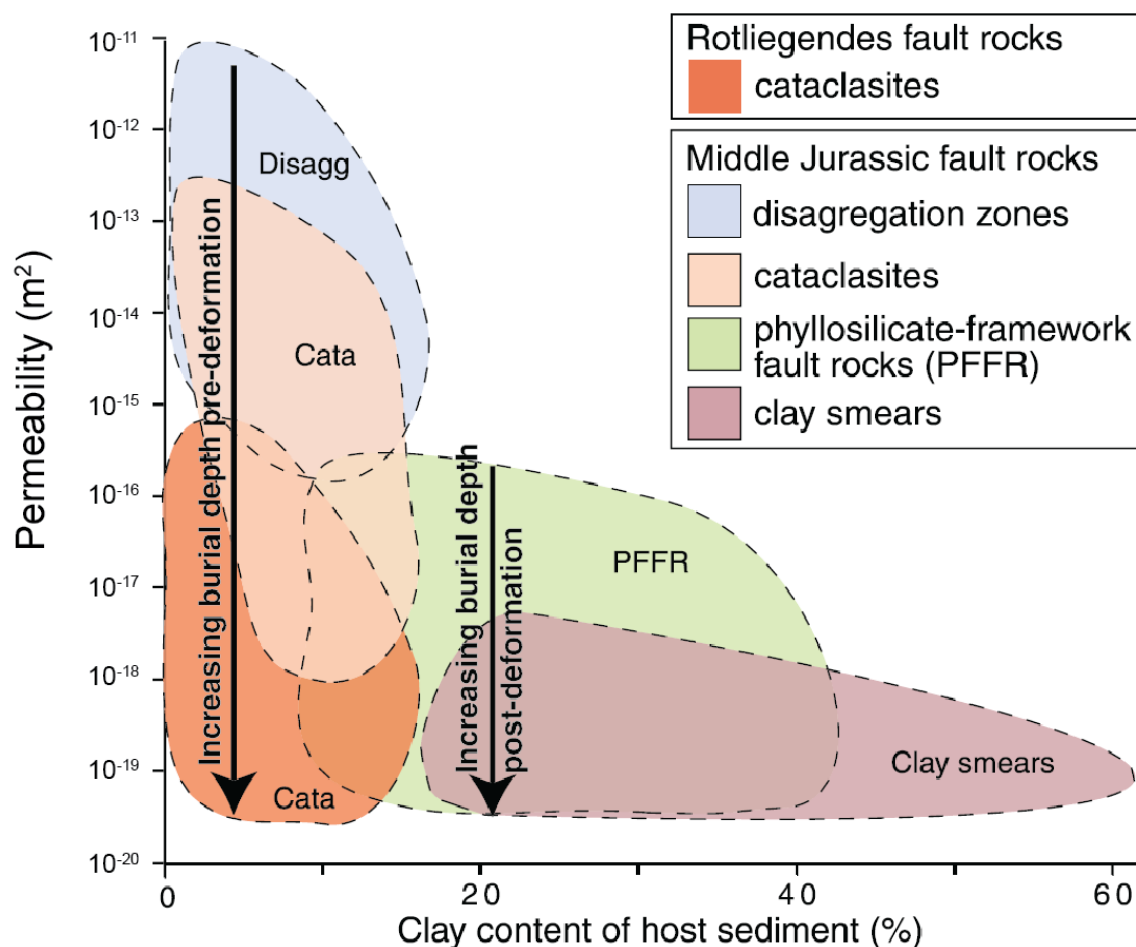


Figure 3.2 Summary of fault rock permeability data from the North Sea and Norwegian Continental shelf (from Fisher and Knipe, 2001). Permeability is plotted against clay content for the various fault rock types. Also shown are the two main controls on the permeability of the faults in clean sandstones and impure sandstones (i.e. burial depth at the time of faulting and post-deformation burial depth, respectively). Original scale in mD shown as equivalent SI units.

In sediments of intermediate composition (15–40% phyllosilicate), microfaults are characterized by a texture termed phyllosilicate-framework fault rock (PFFR) (Fisher and Knipe, 1998), or more simply clay matrix gouge or shaly gouge (e.g. Gibson, 1998). Deformation-induced mixing of quartz grains and clay matrix occurs, generally without grain fracturing (Yielding *et al.*, 2010).

In sand-dominated sequences, the principal fault rocks are disaggregation zones and cataclasites (Figure 3.2) (Fisher and Knipe, 2001; Sperrevik *et al.*, 2002; Fossen and Gabrielsen, 2005). Disaggregation zones in sandstones, for example, are formed during fault slip at relatively low confining pressures (e.g. near surface depths < 1 km), are characterized by grain reorganization without grain fracturing and tend to have comparable hydraulic properties to their protolith sandstones. At higher confining pressures (e.g. burial depths > 1 km) cataclastic processes dominate deformation, resulting in higher capillary threshold pressures and lower fault rock permeabilities (typically 2–3 orders of magnitude below host rock) through grain fragmentation and associated infilling of pore-space (e.g. Fisher and Knipe, 2001). At depths > 3 km and temperatures > 90 °C (i.e., typical geothermal gradient)

disaggregation zones and cataclasites are prone to post-deformation quartz cementation and clay alteration (e.g. Fisher *et al.*, 2003; Cavailhes *et al.*, 2013).

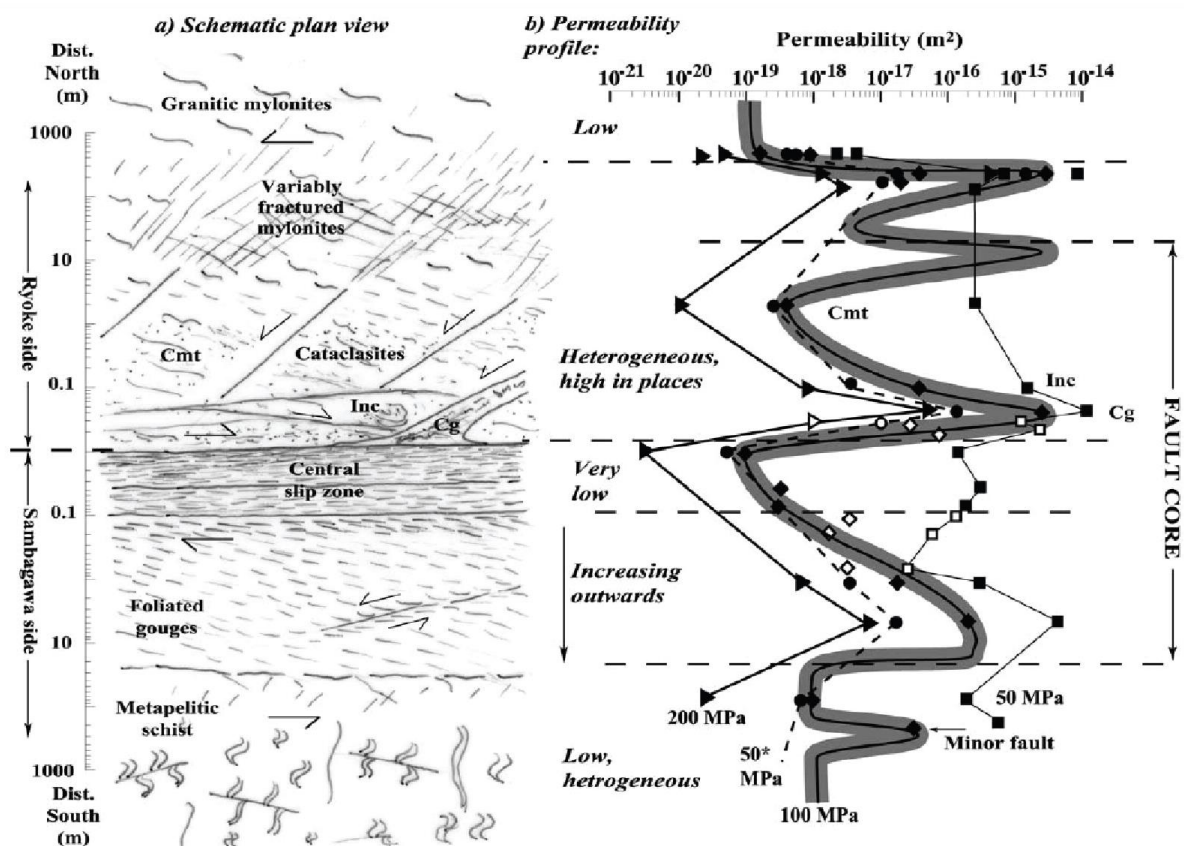


Figure 3.3 Schematic summary of the main elements of permeability structure across the Median Tectonic Line. (from Wibberley and Shimamoto, 2003). (a) Summary of the structural zones; (b) summary of permeability data distribution for different confining pressures. Abbreviations: Cmt and Inc denote cemented and incohesive foliated cataclasites, respectively, and Cg denotes crenulated gouge.

3.1.2 Depth

The general trend of decreasing bulk rock permeability with depth in the shallow crust (< 1 km) is consistent with the closure of pore and fracture apertures with increasing effective pressure (e.g. Wei *et al.*, 1995; Ohman *et al.*, 2005; Ishii *et al.*, 2010). This simple linear relationship for stress-induced fracture closure, however, changes as effective pressure increases. As the contact area between asperities of opposing fracture surfaces increases so does the fracture stiffness, resulting in fracture apertures reaching maximum closure; after this point additional increases in effective pressure results in no further decrease in permeability (Ohman *et al.*, 2005)(see section 3.5 for further discussion). The depth of fault formation is also an important consideration when considering the permeability of a fault zone. Hydraulic transmissivities in mudstones, for example, show a strong dependence on the depth of fault formation which controls the principal mode of failure (Ishii *et al.*, 2010). Here, the growth of faults, primarily by segment linkage via tensile splay cracks at depths shallower than 400 m, can result in highly permeable zones which are in contrast to deeper fault sections, where faults are primarily formed by shear failure (Ishii *et al.*, 2010).

Studies of fault rock generally show an inverse relationship between effective pressure (maximum burial depth) and permeability (e.g. Faulkner and Rutter, 2000; Faulkner, 2004; Wibberley *et al.*, 2008; Tanikawa *et al.*, 2009; Morrow *et al.*, 2014). However, like other properties of fault-zones, fault-rock permeability for a given depth shows a high degree of variability. For example, the permeability of faults within siliciclastic petroleum reservoirs of the

North Sea and Norwegian Continental shelf show variations of 2–3 orders of magnitude in permeability of clay-rich and cataclastic faults for a given depth (Figure 3.4) (Fisher and Knipe, 2001). Understanding the variability of fault permeability for a given fault or system of faults therefore requires multiple samples of fault rock from a variety of locations along fault-zones, a condition that is rarely achieved in individual studies.

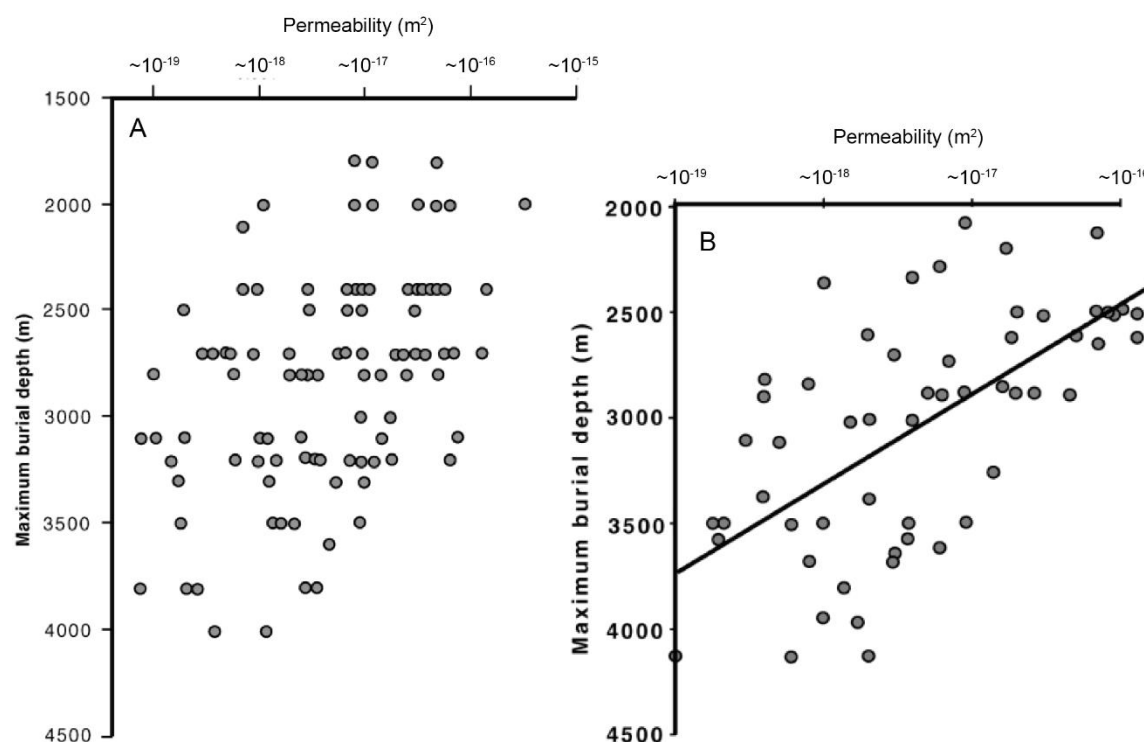


Figure 3.4 Permeability of phyllosilicate-framework and cataclastic fault rocks from the North Sea. (from Fisher and Knipe, 2001). A) Permeability of cataclastic fault rock against their maximum burial depth from Rotliegendes of the Southern North Sea. B) Permeability of phyllosilicate-framework fault rock against their maximum burial depth from the northern North Sea. Original scale in mD shown as equivalent SI units.

An understanding of the burial and/or exhumation history of a fault is also important when considering its hydrogeological properties. A range of fault and fracture properties, both hydraulically conductive and sealing, can be present in a single region. The West Sole gas fields of the southern North Sea, for example, show an inverse spatial relationship between open fractures and sealing faults at depths of ~ 3 km over spatial scales ranging from the field segment to the individual well (Barr, 2007). In this area, core samples indicate all early formed faults and fractures were likely to be sealing, particularly those at maximum burial depth and reservoir temperature. Breached or conductive faults formed later during inversion, when brittle, cemented reservoir and fault rocks deformed at lower temperatures and pressures (Barr, 2007). In a similar way, fractures associated with the Sellafield radioactive waste disposal facility show little stress-sensitivity. Here, hysteresis in shear stress associated with uplift resulted in stress relaxation with non-critically stressed faults remaining or becoming conductive (Sathar *et al.*, 2012).

As detailed in section 3.1.1, the phyllosilicate content has a primary control on the hydraulic and mechanical properties of fault zones. Cavailhes *et al.* (2013) describe normal fault zones cutting a foreland arkosic turbiditic formation suffering high-T diagenesis and formed under conditions typical of deeply buried reservoirs (i.e., 200°C , 6–7 km). Microstructural analyses

show a large proportion of phyllosilicates ($\leq 34\%$) in the fault rock, derived from near-complete feldspar alteration and disaggregation during deformation. Faults with offsets much lower than bed thickness were found to have large feldspar-to-phyllosilicate transformation ratios, implying that the origin of the phyllosilicates is purely transformational (Cavailles et al., 2013).

In summary, the primary factors controlling the hydrogeological properties of a fault include; the composition and rheology of the host rock and its phyllosilicate clay mineral content, the maximum temperature and depth of burial during faulting and the stress regime at the time(s) of faulting, during any subsequent deformation event as well as the present day. These combination of factors make site specific observations of *in situ* fault properties critical to understanding the response of faults and their associated fracture networks to elevated pressures induced during CO₂ injection.

3.2 FAULT ZONE PROPERTIES

3.2.1 Mechanical stratigraphy

In layered sedimentary sequences, small faults are commonly restricted to mechanically strong layers like limestone or sandstones (Nicol *et al.*, 1996; Gross *et al.*, 1997; Wilkins and Gross, 2002; Soliva and Benedicto, 2005). Whether faults extend into adjacent clay layers also occurs at various scales which is dependent on parameters such as the thickness of the clay layer, its rheological properties, and displacement (Roche *et al.*, 2012). Faults cross-cutting multilayer sedimentary sequences often form complex fault zones. These fault zones include several fault segments that may or may not connect (Segall and Pollard, 1980; Peacock and Sanderson, 1991; Cartwright *et al.*, 1995; Childs *et al.*, 1996; Crider and Pollard, 1998; Peacock, 2002; Walsh *et al.*, 2003), with secondary fractures formed in lower strain regions of distributed deformation that are often focused near irregularities in the main fault (Kim *et al.*, 2004). Many studies have concluded that the heterogeneity of a multilayer sedimentary sequence strongly controls fault zone architecture (e.g. Childs *et al.*, 2009). For instance, segment linkage commonly occurs within layers or at layer interfaces (e.g. Peacock and Zhang, 1994; Childs *et al.*, 1996; Roche *et al.*, 2012). Using the distinct element numerical modelling method, Schöpfer *et al.* (2007) show that faults within multilayer models are highly segmented at low confining pressure and high strength contrast with fault bound blocks progressively rotated and incorporated into the fault zone. As the confining pressure increases or the strength contrast decreases, faults become less segmented and resemble the geometries of cataclastic shear zones. Both numerical and experimental results show that the bulk ductility and the area of microfracturing increase with increasing confining pressure (Patton *et al.*, 1998; Schöpfer *et al.*, 2007).

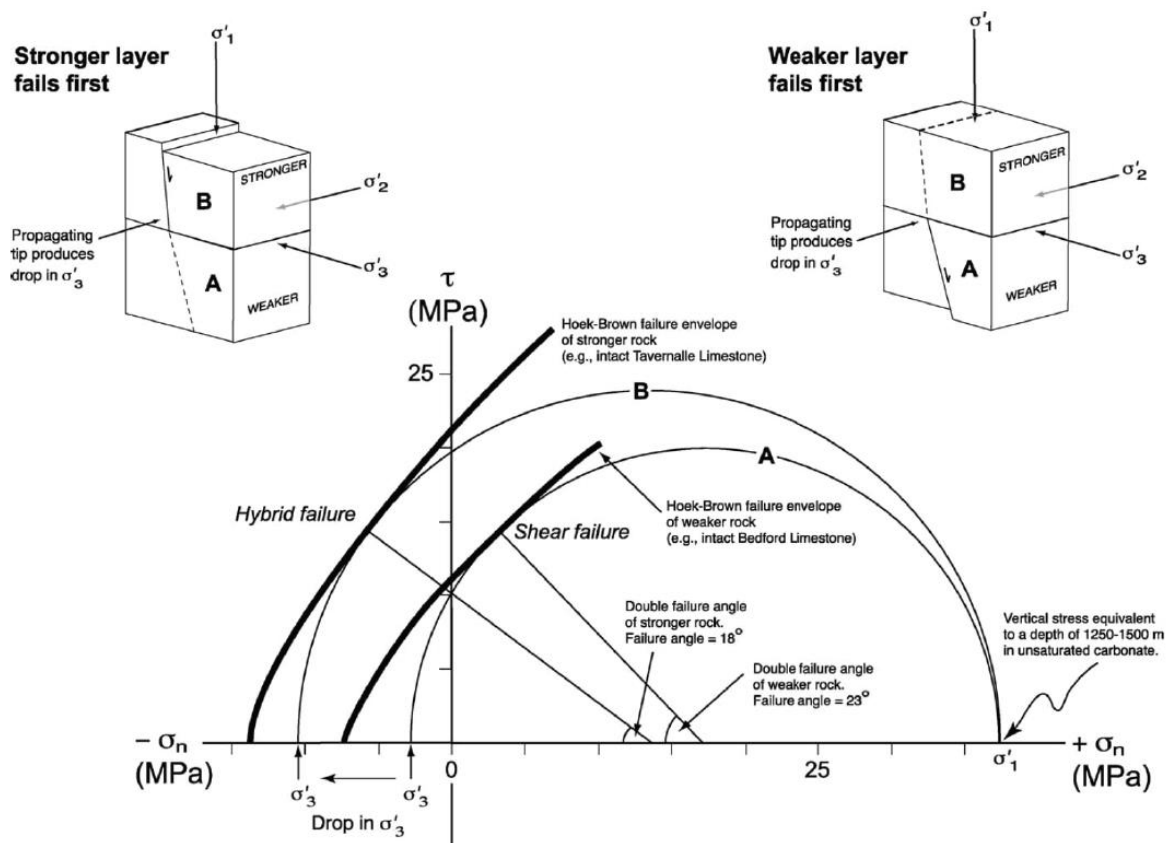


Figure 3.5 Mohr-space diagram illustrating how contrasting mechanical stratigraphy leads to different failure mode and failure angles in different layers (from Ferrill and Morris, 2003). A more competent rock is more likely to fail in hybrid mode than a less competent rock under the same stress regime (in this case normal faulting). See Ferrill and Morris (2003) for data sources.

Failure of a mechanically layered sedimentary sequence (i.e., rocks of different compositions, porosities, thicknesses and strengths) at shallow depths or high fluid pressures results in fault dips that vary with lithology (Figure 3.5) (Sibson, 1996; Ferrill and Morris, 2003). Outcrop and experimental studies suggest that the geometry of faults is strongly dependent on the strength contrast of the layers, layer stacking, and (effective) confining pressure (Peacock and Zhang, 1994; Childs *et al.*, 1996; Patton *et al.*, 1998; Schöpfer *et al.*, 2007; Michie *et al.*, 2014). Numerical modelling and outcrop studies of normal faults, for example, have shown that faults initiate as steep/vertical extension fractures in the strong layers which are linked via shallow dipping faults within the weak layers (e.g. Peacock and Zhang, 1994; Crider and Pollard, 1998; Micarelli *et al.*, 2005; Schöpfer *et al.*, 2006). These variations in fault dip are the result of differences in friction angle or failure mode from layer to layer (Figure 3.5) (Gross, 1995; Sibson, 1998; Ferrill and Morris, 2003). Faults that cut several mechanically distinct layers will commonly display dip changes between layers. The most extreme refracted fault trajectories occur in dilational normal faults associated with hybrid failure (Figure 3.6), which can develop in mechanically heterogeneous rock sequences by slip on faults cutting with different shear failure angles or different failure modes (Gross, 1995; Sibson, 1998; Ferrill and Morris, 2003). The greater the variation of fault dip along a fault zone, the greater the space problems that arise with segment linkage during fault growth. These fault dip variations cause additional fault zone complexities, such as splaying and the development of antithetic faults (Schöpfer *et al.*, 2007). Dilational normal faulting at lithological boundaries can significantly enhance vertical fluid flow at the surface, and create pathways for along-strike fluid migration in the subsurface. Recognition of the influence of mechanical stratigraphy on fault geometry is an important

component of the characterisation of faulted aquifers, hydrocarbon reservoirs, and mineral provinces (Ferrill and Morris, 2003).

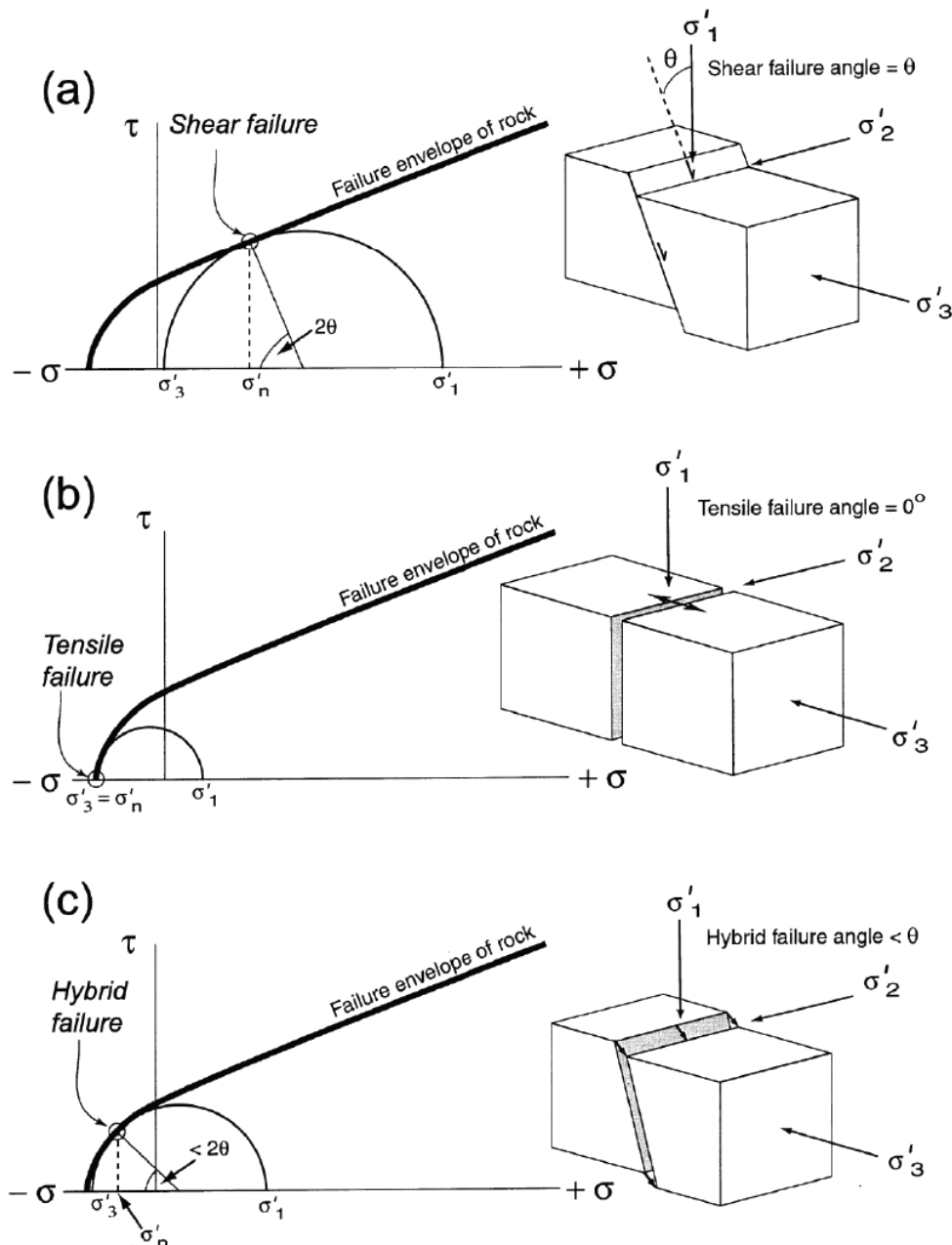


Figure 3.6 Mohr-space diagrams with Hoek-Brown failure envelope (from Ferrill and Morris, 2003) illustrating different failure modes: (a) shear failure, (b) tensile failure, (c) hybrid failure.

The anisotropy of the sedimentary sequence not only induces variations in the attitude of fault segments but also in the fracturing mode (Roche *et al.*, 2012). The distinct element numerical models of Schöpfer *et al.* (2007) show a full range of fracture modes and transitions between extension, hybrid, and shear fracturing of mechanically strong layers (e.g. Figure 3.6). Although the full range of fracture types is defined at the macroscale, i.e. on the scale of the layers, microscale fracturing within the models is either in tension or in shear with tensile failure being the predominant mechanism at all confining pressures applied in the study (Figure 3.5). These results are consistent with existing theories that suggest that hybrid and shear fractures arise from the linkage of stepped (mode I) cracks (Reches and Lockner, 1994; Engelder, 1999; Schöpfer *et al.*, 2007). Changes in fracture mode across lithological boundaries are also observed in outcrop studies. For example, fault segments can exhibit little mineralization in

clay layers and thick calcite veins in limestones, indicating preferential opening and cementation within these competent layers (Roche *et al.*, 2012). Vein fill in pull-aparts on refracted faults are a common outcrop indicator of fluid conduits developed on the steeper parts of faults. Fault zone growth in the study of Roche *et al.* (2012) is consistent with a “coherent model” (cf. Walsh and Watterson, 1991) and is strongly influenced by the sedimentary sequence. In the limestone layers for example, faults grew in several steps, including opening and frictional sliding on 80° dipping segments. Faulting in clay layers was in the form of 40° dipping faults and sub-horizontal faults. The sub-horizontal faults generally developed early under the same extensional regime as normal faults and disturbed the fault architecture. The fault zone thickness increases with the limestone layer thickness and the presence of sub-horizontal faults in clay beds (Roche *et al.*, 2012). Once a fault develops, the locus and direction of slip are controlled by the confining pressure, the resolved stresses and the frictional resistance to sliding for each fault segment (e.g. Figure 3.7). The mechanical properties of sedimentary sequences influence failure angles and fault dip, whereas layer thickness influences the height of dip segments (Ferrill and Morris, 2003).

Variation in mechanical properties within a layer can also be as influential a control on fault architecture as discrete stratigraphic horizons (Soden and Shipton, 2013). The influence of rock properties on fault deformation processes means fault structure cannot be predicted solely using displacement scaling relationships (Shipton *et al.*, 2006). For example, Soden and Shipton (2013) demonstrate that accurate characterisation of the mechanical stratigraphy, from which predictions of joint spacing can be made, would improve predictions of fault architecture. This study concludes that understanding the affect of host rock mechanical properties on fault deformation processes, in combination with burial history, is key to the development of realistic fault structure and permeability models (Soden and Shipton, 2013).

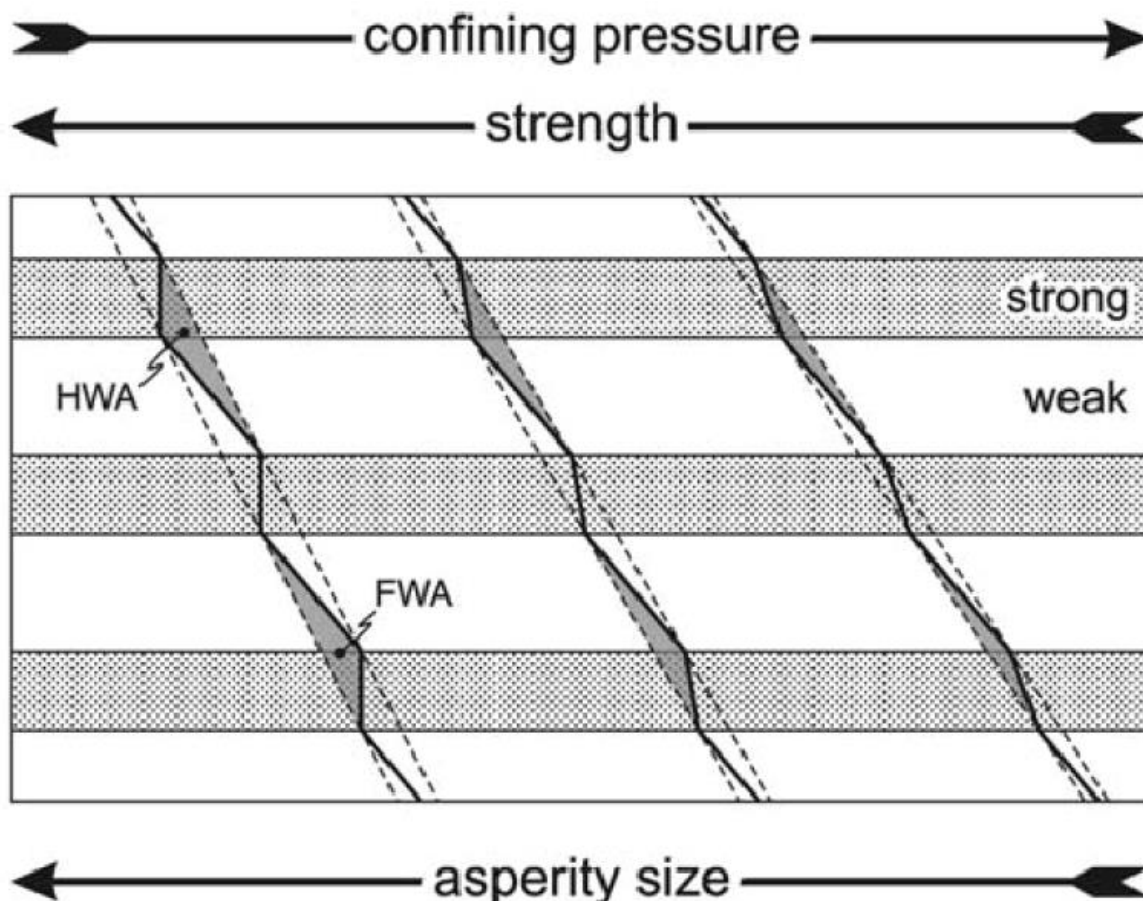


Figure 3.7 Schematic diagram illustrating the effects of confining pressure and strength contrast on fault dip variations within a multilayer sequence (from Schöpfer *et al.*, 2007), and consequently, the dimensions of fault asperities (shaded regions; HWA and FWA are hanging wall asperity and footwall asperity, respectively).

Many of the studies of fault zones presented in the literature are from reservoir sandstones or from interbedded sandstone/shale sequences. Few studies have focused on the geometries and flow properties of faults in caprock sequences and this is a weakness in the literature (see Section 11.2). Polygonal fault systems are structures largely confined to fine-grained caprocks and have been widely reported in the literature (e.g. Cartwright, 2011; Laurent *et al.*, 2012; Tewksbury *et al.*, 2014; Seebeck *et al.*, 2015). They are strata-bound non-tectonic normal faults formed in hemi-pelagic sediments, typically in a series of mechanically stratified tiers, across vast areas along the majority of continental margins (Cartwright, 2011). The mechanism by which polygonal faults form is uncertain; however, recent outcrop studies indicate that in some cases repeated episodes of fluid flow at high pressures are an important component of the process (Cartwright, 2011; Tewksbury *et al.*, 2014). Individual tiers with generally little lithological variation form mechanical boundaries which control vertical fault segmentation (Cartwright, 2011; Laurent *et al.*, 2012; Seebeck *et al.*, 2015). Outcrops indicate polygonal faults form in a hybrid mode of dilational shear failure, which in some cases creates sufficient long lived void space for calcite crystal growth (Tewksbury *et al.*, 2014). While polygonal faults have the potential to form high permeability pathways through intrinsically low permeability caprock formations (e.g. Gay *et al.*, 2004), caprock sequences in the North Sea deformed by polygonal faults overlie many commercial scale hydrocarbon reservoirs, indicating these faults often do not compromise caprock integrity and/or that the faulted mudstones are not the primary seal (Cartwright *et al.*, 2007).

3.2.2 Fault scaling properties

Power-law or self-similar distributions have been demonstrated for a range of fault attributes including; fault displacement (e.g. Walsh *et al.*, 1991; Yielding, 1992), fault length (e.g. Gillespie *et al.*, 1993; Watterson *et al.*, 1996), fault zone width (e.g. Shipton *et al.*, 2006; Seebeck *et al.*, 2014) and fault flow rates (Seebeck *et al.*, 2014) (e.g. Figure 3.8). These scaling relationships are accompanied by a broad positive correlation between fault displacement and fault-rock thickness (e.g. Hull, 1988; Marrett and Allmendinger, 1990; Childs *et al.*, 2009) (Figure 2.2). As fault rocks are generally weaker than the host rock, the cause of a continual increase in fault rock thickness with increasing displacement is uncertain and a number of models have been proposed to account for observations (e.g. Scholz, 1987; Hull, 1988; Power *et al.*, 1988; Faulkner *et al.*, 2003; Childs *et al.*, 2009). Generally, fault rock thickness within these models is strongly dependent on host and fault rock rheological properties (Section 3.2.1). Childs *et al.* (2009) propose a geometric model in which the thickness and distribution of fault architectural elements, such as low permeability fault rock (fault core) and associated high permeability fracture zones (damage zones), are largely controlled by fault geometry. Childs *et al.* (2009) argue that internal fault zone geometry and the distribution of fault rock thickness over the fault surface are strongly influenced by the locations and dimensions of steps or bends of the fault surface produced during fault propagation. In this model, the heterogeneity of fault rock thickness variations and fault rock type reflect both fault segmentation and fault surface asperities over a wide range of scales. Regardless of the model used to account for fault growth, given the high variation in the fault rock or fault zone thickness-displacement relationship (Figure 2.2) and the variations between individual data sets (Shipton *et al.*, 2006; Childs *et al.*, 2009) estimating damage zone thickness from the displacement or length of faults (e.g. IEAGHG, 2015a) will result in significant uncertainty in estimates of fault zone hydraulic properties.

Fluid flow pathways in the crust are influenced by the permeability of the rock volume over a variety of spatial and temporal scales, and by fluid pressure gradients that depart from hydrostatic (Sibson, 1996; Cox, 1999). Many *in situ* studies highlight the highly localised and convoluted nature of fluid flow through a faulted rock volume (Wallace and Morris, 1986; Paillet *et al.*, 1987; Levens *et al.*, 1994; Tsang and Neretnieks, 1998; Cox, 1999; Evans *et al.*, 2005; Seebeck *et al.*, 2014). Numerical models of rock deformation consistent with these studies show highly non-linear behaviour and flow localization are features of a wide range of natural well-connected critically stressed fracture networks (Sanderson and Zhang, 1999; Tsang *et al.*, 2007). Both *in situ* and numerical studies cited above demonstrate that a small fraction of the elements within the fault-fracture network are associated with the majority of flow.

Highly localised flow from a small number of faults and a wide range of flow rates indicate that flow along faults is non-uniform. Seebeck *et al.* (2014) demonstrate in some fault systems that flow rates from faults are power-law with low slopes (Figure 3.8). These low power-law slopes suggest that flow rate is highly heterogeneous, a feature which derives from the variability of fault zone structure and content (e.g. fault zone and fault rock thickness, fault strike and fracture densities), as well as the connectivity of the fault-fracture network. Fault zone thickness, for example, ranges over 2.5 orders of magnitude for a given throw, variations that typically arise due to increased thicknesses of fault zones at segment boundaries, fault bends and fault intersections (Section 2) (Childs *et al.*, 1996; Childs *et al.*, 2009; Seebeck *et al.*, 2014). Comparison of the power-law slopes for fault zone thickness and associated flow rates in Seebeck *et al.* (2014) suggests the fault zone thickness slope is shallower than that of flow rate. This relationship between fault zone thickness and flow rate indicates that flow may be more heterogeneous than structure. This is a property of numerical non-linear fault-fracture

flow systems (Zhang and Sanderson, 2001), in which the dimensionality of flow is more localized, and therefore lower, than that of structure. In these circumstances flow properties of fault zones, which are of primary interest for CO₂ storage, are therefore highly variable both in distribution and rate (under relatively low stress and driving pressures) (Seebeck *et al.*, 2014).

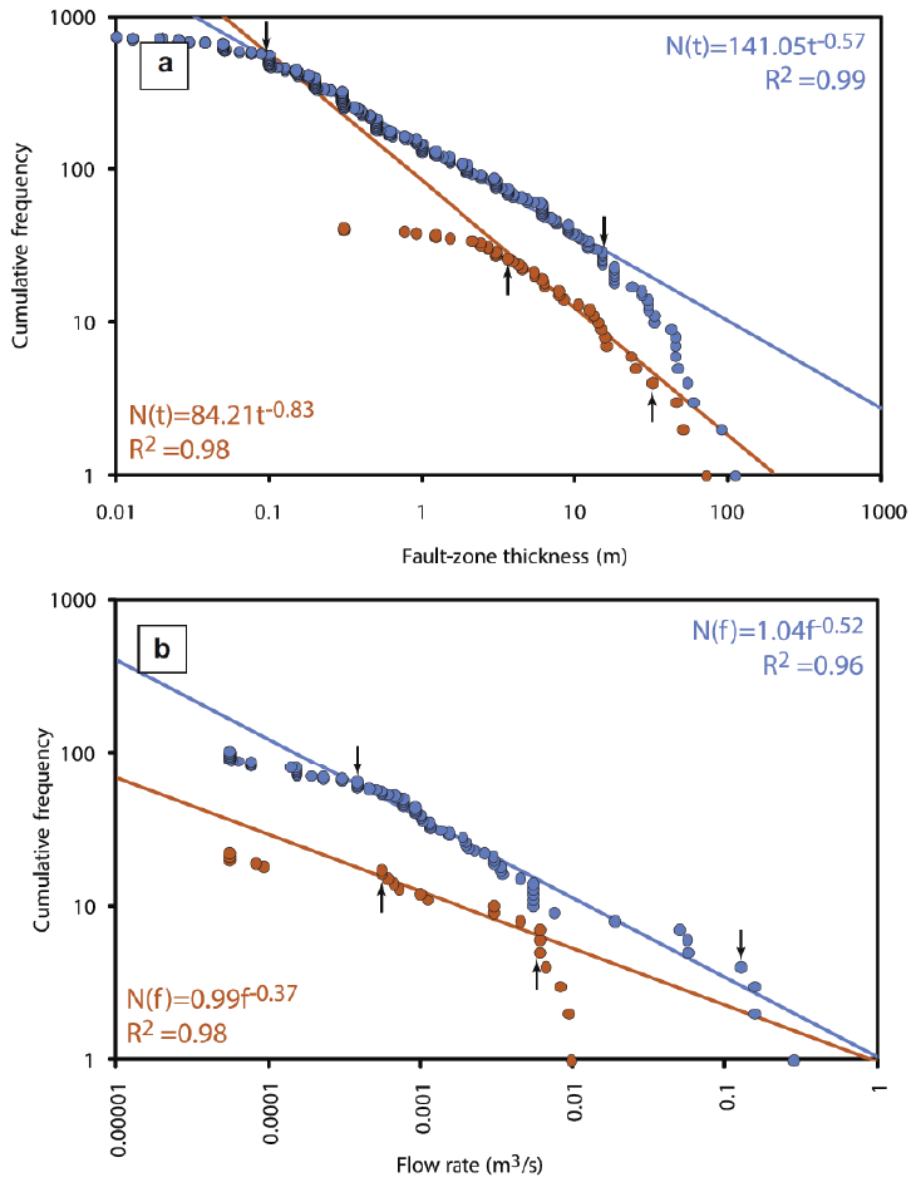


Figure 3.8 Fault zone thickness and ground water inflow rate populations (from Seebeck *et al.* 2014). (a) Fault zone thicknesses from poorly consolidated Miocene strata (orange filled circles) and indurated Mesozoic turbidite sequence (blue filled circles). (b) Flow rates from fault zones, key as in (a). Best fit power-law trends (coloured lines) derived from the central segment (defined between arrows) of each population.

3.2.3 Aperture

Fracture aperture width, in combination with connectivity (Section 3.2.4), strongly influences the bulk permeability of a rock volume. Absolute fracture apertures are generally considered pressure sensitive so that fracture permeability decreases with depth down to a certain point (Bandis *et al.*, 1983; Hillis, 1998; Manning and Ingebritsen, 1999; Gentier *et al.*, 2000; Ingebritsen and Manning, 2010; Ishii *et al.*, 2010). Fracture apertures are also dependent on rheology which increases in strength with depth (e.g. Chang *et al.*, 2006), allowing in some cases, fractures to remain open. Tracer tests show that the decrease in transmissivity that occurs with increasing normal stress is associated with increasingly distinct channelling within

fractures (Gentier *et al.*, 2000) and is discussed further in Section 3.5.1. This channelling is strongly linked to correlation lengths identified from geostatistical analysis of surface profiles and data obtained from the casts of fracture void space. Modelling results show that deformation of fracture surfaces with increasing normal stress causes substantial, non-uniform changes in void-space geometry that can change the flow regime (Gentier *et al.*, 2000). In general, application of shear stress induces an dilation of the fracture, sometimes preceded by a closure phase, which causes a very large increase in global transmissivity associated with the reorientation of flow sub-perpendicular to the shear direction (Gentier *et al.*, 2000).

Dilation can increase fault permeability because, at stresses close to failure, microcracks form parallel and sub-parallel to the fault plane. If fluid pressure gradients are also parallel to the fault plane, this will lead to fluids flowing preferentially along the zone of anisotropic permeability. The effects of dilation will be greatest closest to the fault where the deviatoric stresses are maximum. Dilation has been reported to be important as much as 100 m from a fault plane (Sibson, 1981a); however, the width of the dilated zone is variable and depends on the size of the fault (Fyfe *et al.*, 1978). If dilation increases permeabilities over a wide zone (>200 m), then even relatively small increases in permeability can lead to the fault being a significant fluid conduit (Hooper, 1991). Refracturing of mineralised zones increases fault permeability through the reconnection of previously cemented fractures. The reactivation of the fault potentially leads to the connection of highly permeable pathways. In order for this process to be effective, the rock must be moderately-to-well lithified, since, if the rock is poorly lithified, the fractures cannot remain open and permeabilities will not increase (Hooper, 1991). Favoured localities for high permeability fracture zones include short-lived irregularities along large-displacement fault zones such as dilational jogs, relay ramps, secondary transfer faults, and other forms of link structure (Sibson, 1996; Cox, 1999; Wibberley *et al.*, 2008; Faulkner *et al.*, 2010).

The conventional rock mechanics model of fracture permeability centres around mismatches between the two rough fracture surfaces creating small voids through which fluid can flow (Section 3.5). Flow occurs predominantly along open channels between asperities, which under *in situ* conditions at depth normally possess apertures on the order of tens of microns (e.g. Gentier *et al.*, 2000; Gutierrez *et al.*, 2000). Stress is transmitted across the fracture through the point contacts of the asperities. This model predicts that fracture permeability is highly sensitive to changes in the effective normal stress; as the stress increases the proportion of asperities touching each other increases, thereby reducing the aperture and span of the flow channels (Barton *et al.*, 1995; Dyke, 1995; Gentier *et al.*, 2000; Gutierrez *et al.*, 2000). Prediction of hydraulically conductive faults and fractures preferentially oriented with respect to the stress field is complicated by fracture healing (discussed below) whereby mineralisation of void space results in the stress independence of the fracture (Evans *et al.*, 2005).

Fracture apertures may also be enhanced by block rotation during deformation. During faulting, folding or high pressure injection, blocks undergo shear displacement and rotate, locally creating open fractures (Dyke, 1995; Sanderson and Zhang, 1999; Evans *et al.*, 2005; William Carey *et al.*, 2015). Stresses are transmitted through the structure at block contacts. Low stress magnitudes and friction on the fractures between the blocks, especially at the block corners, prevent the structure closing up tight. At greater depths, under high confining pressures, this type of fracture permeability is unlikely to dominate fluid flow (Dyke, 1995). However, at depths ≤ 3500 m under the conditions of fluid injection, Evans *et al.* (2005) document newly permeable fractures clustering around major pre-stimulation flowing fractures which they interpreted to represent the shear failure of pre-existing, small-scale fractures that defined the internal architecture of pre-existing shear structures.

3.2.4 Connectivity of fault systems

Fracture connectivity is an important feature controlling the bulk permeability of a faulted (and jointed) rock mass. As the number of faults and fractures increases, they form “clusters” of connected fractures, which grow in size as more fractures are added to the system. Fracture networks can be described using the well-established theory of percolation. Percolation networks can be described in terms of three types of elements: backbone elements that connect one side of the system to the other and support the majority of flow through the network, dangling or dead-end elements that branch from the flow backbone, and isolated elements which are disconnected from other system elements (Balberg *et al.*, 1991; Cox, 1999; Odling *et al.*, 1999). A ‘percolation threshold’ is reached when enough elements connect to allow fluid flow across the entire width of the network and the medium becomes permeable (Stauffer, 1987; Zhang and Sanderson, 1998; Berkowitz *et al.*, 2000). The permeability of a fractured-rock matrix system close to the threshold behaves in a typical ‘critical phenomena’ fashion, i.e. large changes in system permeability occur for small changes in fracture density (Zhang and Sanderson, 1998; Tsang *et al.*, 2007).

Connectivity in a fracture system depends on the fracture orientation and size distributions, on fracture density and on fracture spatial distribution (Odling *et al.*, 1999). With increasing fracture density, the largest (spanning) cluster contains an increasing proportion of the total fracture area. Orientation plays a role because fractures belonging to the same orientation set tend not to intersect each other until fracture density becomes high, whereas orientation sets at a high angle to each other increase intersection likelihood. Fracture size distribution plays an important role because, for the same density and orientation distribution, collections of short fractures are less well connected than collections of long fractures (Balberg *et al.*, 1991; Odling *et al.*, 1999).

Bour & Davy (1997) have shown that for random 2D fracture patterns, the exponent of the power-law distribution has an important control on the nature of connectivity. The power-law exponent describes the relative abundance of fractures of different sizes. Bour & Davy (1997) identified three basic types of behaviour. For exponents (cumulative frequency length distribution) less than -2.0 (steeper slopes than -2.0), the small fractures dominate connectivity because the largest fractures are not abundant enough to be well connected with each other. By contrast, for cases where the exponent is greater than -1.0 (shallower slopes than -1.0) the connectivity depends on the largest fractures present and small fractures play an insignificant role. Between these two exponents, both large and small fractures contribute to connectivity and therefore fluid flow (Bour and Davy, 1997; Odling *et al.*, 1999).

3.3 FLUID COMPOSITION

Permeable fault zones, laterally discontinuous seals, fractured or corroded caprock may allow the migration of buoyant supercritical CO₂ from a reservoir (Figure 3.9). Understanding the fluid–fluid and fluid–rock reactions that may inhibit or facilitate CO₂ migration from a reservoir toward the surface is key for demonstrating the sealing capacity of the geological overburden, above deep storage reservoirs (e.g. Edlmann *et al.*, 2013). Therefore, understanding the geochemical behaviour of CO₂ stored in geological reservoirs, over a range of time-scales, is important for quantifying the risk of leakage. For example, CO₂ dissolution in brine will tend to stabilize the CO₂ in a reservoir (e.g. Gilfillan *et al.*, 2009). However, reactions between CO₂-charged brines and reservoir minerals may either enhance the long-term storage security by precipitation of carbonate minerals or promote leakage through mineral dissolution and corrosion of caprock and fault seal (Bickle, 2009; Kampman *et al.*, 2014b). Alternatively, mineral dissolution may decrease rock strength and thereby the ability of a fault to support

open fractures, hence lowering the risk of leakage through compactional processes (e.g. Sleep and Blanpied, 1992; Leclère *et al.*, 2015 or mineral dissolution may increase leakage risk as deformation of cemented rocks may lead more easily to dilation and enhanced permeability through the generation of tensile fractures (e.g. Vass *et al.*, 2014).

The undesirable consequences of CO₂ migration from the target reservoir (Figure 3.9) include escape of CO₂ toward the surface and contamination of shallow potable aquifers by: (i) intrusion of CO₂, resulting in dissolution and desorption of potentially toxic metals from minerals by acidic CO₂-charged fluids and (ii) entrainment of deep formation brine with the migrating CO₂, which may contain high concentrations of metals and radionuclides (Kampman *et al.*, 2014b).

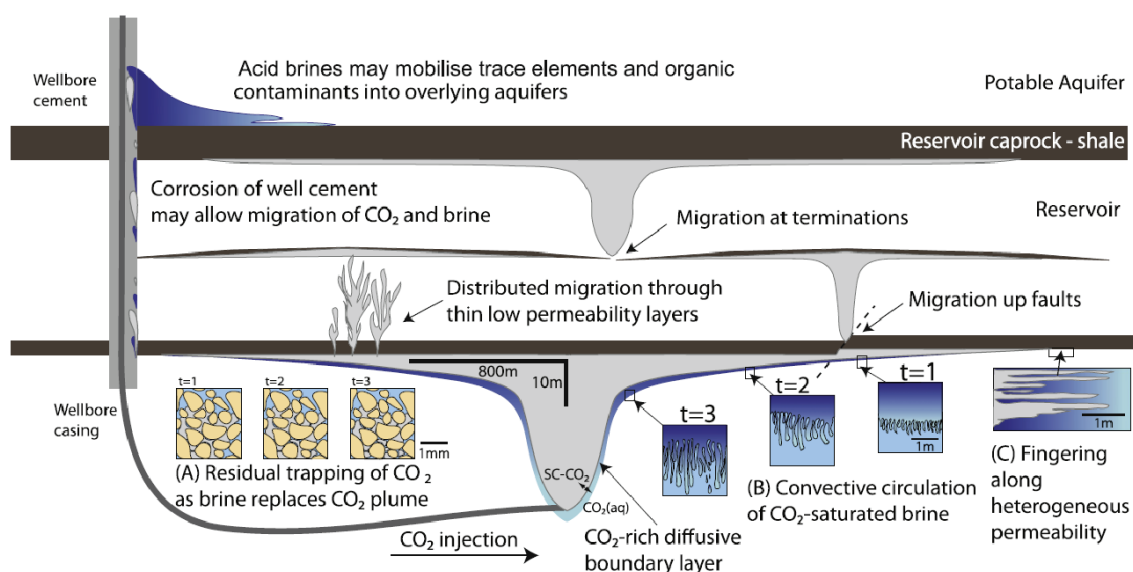


Figure 3.9 Diagram illustrating geological carbon storage (from Kampman *et al.*, 2014a). CO₂ from concentrated sources is separated from other gasses, compressed and injected into porous geological strata at depths >800 m where it is in a dense or supercritical phase (from Kampman *et al.*, 2014a). The CO₂ is lighter than formation brines, rises and is trapped by impermeable strata. The risks are that the light CO₂ will exploit faults or other permeable pathways to escape upwards and acid CO₂-charged brines might corrode the caprocks or fault zones. A variety of processes will tend to stabilise the CO₂ including 1) capillary trapping in bubbles of CO₂ after the CO₂ plume has passed (inset A), 2) dissolution in formation brines which forms a denser fluid which will sink (inset B), where fingering along bedding-related heterogeneities will enhance dissolution (inset C), and 3) precipitation of CO₂ in solid form as carbonate minerals as a result of reactions between CO₂-charged brines and silicate minerals (Kampman *et al.*, 2014a).

Analysis of rock samples from the Paradox Basin, for example, indicates that CO₂ saturated brines produce dissolution and precipitation of some common rock forming minerals. CO₂ concentrations at depth in the Paradox Basin are close to theoretical CO₂ saturation at hydrostatic pressures, and decrease upwards becoming increasingly undersaturated at shallower depths (Kampman *et al.*, 2014b). Quantitative mineralogy of representative samples from a CO₂-charged reservoir unit are depleted in hematite, calcite and feldspar and enriched in dolomite and clay, compared to a compilation of representative unaltered samples (Kampman *et al.*, 2014b). The dissolution of hematite grain coatings, assemblages of gypsum and pyrite in open fractures and presence of dissolved CH₄ in the reservoir fluids suggest the bleaching reactions may occur through a series of linked reactions involving CO₂ (Kampman *et al.*, 2014b). The distribution of dolomite in the core is highly heterogeneous with some areas containing extensive zones of pore-occluding Fe-rich dolomite cements, whilst other areas are free of cement and contain abundant secondary porosity (Kampman *et al.*, 2014b).

Recent results from Paradox Basin indicate that: (i) both free phase CO₂ and brine comigrate from deep reservoirs, (ii) brine meteoric water mixing in the vicinity of a fault zone is an effective means of dissolving this migrating CO₂ and, (iii) such fluid–fluid interactions can efficiently retard the migration of free phase CO₂ to the surface. Therefore, a significant fraction of the CO₂-migrating from deeper reservoirs is likely transported away from faults by regional groundwater flow (e.g. Bickle and Kampman, 2013; Kampman *et al.*, 2014b).

The results of Kampman *et al.* (2014b) highlight the potential retentive capacity of the geological overburden above deep CO₂ reservoirs, for retarding CO₂ migration to the surface. This capacity is site-specific and future CO₂ storage programmes should incorporate a study of caprock formations overlying the target reservoir, including the hydrodynamics, permeability and fluid geochemistry of overlying aquifers, in order to understand the likely migration pathways of leaking CO₂-charged fluids and the trapping potential of the geological overburden.

When the permeability of a system is considered, the fluid type must be accounted for. The movements of hydrocarbons and water, for example, occur at different rates because they are influenced by different forces. Sediment compaction-generated forces drive both hydrocarbons and water flow; however, hydrocarbons in a water saturated system are also affected by buoyancy and displacement potentials. Hydrocarbons tend to rise vertically due to buoyancy, while displacement pressures tend to retard flow. The displacement potential is the capillary entry pressure necessary to replace water in a pore space by hydrocarbons. This capillary entry pressure can prevent the flow of oil in a fine-grained rock, even if water is flowing through the same rock (eg. Hooper, 1991). Bretan *et al.*, 2013 consider the capillary entry pressure of CO₂ is comparable to that of hydrocarbons under some conditions.

A supercritical fluid exhibits physiochemical properties intermediate between those of liquids and gases. Mass transfer is rapid with supercritical fluids because their dynamic viscosities are nearer to those of normal gaseous states (Fenghour *et al.*, 1998; Heidaryan *et al.*, 2011). For example, hydraulic fracture propagation is different for fluids with different viscosities under the same injection conditions. Low viscosity fluids with properties of supercritical CO₂ will create relatively thin and much shorter fractures in comparison with fluids exhibiting properties of water (Zhou and Burbey, 2014). CO₂ flow along fractures in shale at reservoir conditions, for example, may be controlled by a critical fracture threshold (Edlmann *et al.*, 2013). Knowledge and experience gained from observations of field experiments and industry indicates that overall storage efficiency is low, CO₂ prefers high-permeability flow paths, low-permeability regions in the reservoir are bypassed, that CO₂ breakthrough to observation wells is usually faster than models predict and that fast-flow paths can evolve with time (Birkholzer *et al.*, 2015). Preferential flow and bypassing may occur, due to very small variations in permeability and capillary entry pressure, because of the low viscosity (10-20 times lower than that of brine) and density of CO₂ (Birkholzer *et al.*, 2015). Further discussion of the behaviour of CO₂ migration can be found in Birkholzer *et al.* (2015).

3.4 FAULT CEMENTATION AND DISSOLUTION

Precipitation or dissolution of minerals in reservoirs, caprocks and/or fault seals may impact the integrity and viability of the CO₂ storage system over injection time scales (e.g. <100 years). In recent years, the role of crustal fluids and the reactions they impart on fault zones have received much attention by those interested in the mechanics of earthquakes and faulting (Tenthorey *et al.*, 2003). Hydrothermal reactions can change the strength and behaviour of fault zones via mineral transformations, gouge densification/cementation, fault healing and

sealing and by causing changes in hydraulic properties, which in turn may alter the effective stress state of the fault zone (Tenthorey *et al.*, 2003; Evans *et al.*, 2005; Cavailhes *et al.*, 2013).

Fault healing generally strengthens faults through hydrothermal and/or compactional processes during the interseismic period. Fault healing encompasses compactional processes such as ductile creep, the fluid-assisted densification and cementation of fault rock and the healing and sealing of fractures through mineral precipitation (e.g. Dieterich, 1972; Sleep and Blanpied, 1992; Vass *et al.*, 2014). Cementation processes may lead to increases in fault contact area under dry conditions which potentially modify the frictional behaviour of faults and fractures (Gale *et al.*, 2014; Laubach *et al.*, 2014). Although crustal fluids are widely believed to play a key role in fault mechanics, the complex interplay between chemical reaction, fault strength and hydraulic properties, such as permeability, is one that remains poorly understood (Tenthorey *et al.*, 2003; Laubach *et al.*, 2014).

Geomechanics (Section 5) provides a model by which detailed fault and fracture geometry (length, spacing and aperture distributions), and the stresses these features are subject to, can be calculated. Geomechanical theory is dependent on assumptions of elastic behaviour and fractures being contained within single mechanical layers (Olson *et al.*, 2007). However, even if fracture network geometry were precisely decipherable, another aspect of the problem is the modification of the mechanically derived fractures by diagenesis (e.g. Gale *et al.*, 2014). For example, Dyke (1995) uses examples of long-term fluid depletion from several hydrocarbon reservoirs to compare their actual behaviour to those inferences drawn from conventional geomechanical theory. In the majority of cases presented by Dyke (1995), there is no dramatic decrease in fracture permeability with increasing effective stress due to the reduction in fluid pressure associated with fluid extraction. In the study of Dyke (1995), short term well tests were analysed and shown to often possess flow rate dependent production rather than stress dependent permeability. Formation damage, non-Darcy flow and changes in fluid properties can often result in flow rate sensitive effects such as those observed in the examples presented by Dyke (1995).

Within some reservoirs, fracture permeability is shown to be often created by dissolution or partial cementation within fractures. As a result fractures can remain 'locked open' and possess apertures of several millimetres resulting in high hydraulic conductivities, even *in situ* under high stress conditions at depth (Dyke, 1995; Rutqvist and Stephansson, 2003; Laubach *et al.*, 2004; Gale *et al.*, 2007; Tsang *et al.*, 2007). Dyke (1995) emphasises the importance of understanding the diagenetic history of a rock mass, together with the implications of this type of fracture permeability for reservoir behaviour and fluid flow with the sub-surface. While these observations of open fractures are derived from reservoir fracture or joint networks, these observations have important implications for fault zones, particularly those that have experienced hydrocarbon migration in the past (Section 3.3), where the partial or total dissolution of cements may have occurred. Observations from experimental studies and tunnel excavations indicate clay-rich sedimentary rocks (shale) cannot support the preservation of open fractures (Section 3.5) without the presence of cements (e.g. Bastiaens *et al.*, 2007; Zhang and Rothfuchs, 2008; William Carey *et al.*, 2015).

3.4.1 Diagenetically Modified Fractures

Circulating ground water frequently induces precipitation and dissolution processes within permeable formations at depth. Calcite, quartz, pyrite, dolomite or ankerite precipitates are commonly deposited within fractures leading to cementation and a reduction in permeability (e.g. Laubach *et al.*, 2004; Laubach *et al.*, 2014). Partially cemented fractures are created if this precipitation process is complete and does not totally mineralise the fracture void space,

or if subsequent dissolution leaches out some of the mineralisation. The partial mineralisation or secondary dissolution of fractures can therefore result in highly conductive fluid pathways that have apertures of several millimetres (Dyke, 1995; Laubach *et al.*, 2004). In carbonate rocks, for example, fracture permeability can be created by similar processes through the dissolution of the host rock on the fracture faces. This produces flow channels surrounded by partly healed fracture bridges (Dyke, 1995; Laubach *et al.*, 2004). It is these permeable fractures locked open either by partial mineralisation or by localised dissolution of the matrix rock that are responsible for the majority of fluid flow within numerous hydrocarbon reservoirs (Dyke, 1995).

Fractures at depths of 4–6 km or more form in environments where hot (>100°C), mineral-laden water promotes the precipitation of partial quartz coatings and spatially isolated, pillar-like precipitate (cement) bridges (Laubach, 2003; Laubach *et al.*, 2004). Open fractures frequently contain these bridges, which are natural by-products of mineral precipitation during fracture opening (Laubach, 2003). Modelling of cement precipitation shows that at temperatures typical of sedimentary basins, these structures are likely to be ubiquitous (Lander and Laubach, 2015). Laubach *et al.* (2004) have found mineral bridges in every suite of opening-mode fractures inspected from rocks below ~3 km (as well as in many rocks at shallower depths which may or may not have been uplifted from greater depth) in a data set that includes most of the major basins in the continental United States and many basins in other parts of the world.

Systematic studies of mineralization patterns within hydrocarbon reservoir fractures are rare (Marrett and Laubach, 1997). This partly reflects inadequate sampling of subsurface fracture populations, making trends in cement patterns challenging to recognize. In addition, many fractures in outcrop are poor analogues to those in reservoirs because they have experienced different mineralisation histories and near-surface alteration of the infilling mineral suites. Nevertheless, core studies show that diagenetic modification of fracture pore space augments rock and fracture strength such that open, conductive fractures can be sustained for long periods in some geochemical and tectonic settings, whereas fractures in other rocks are partly or completely occluded. In some sedimentary rocks, shifts in degree of fracture mineralisation from open to sealed occurs locally over vertical distances of only a few centimetres (Marrett and Laubach, 1997). These spatial heterogeneities in the extent of fracture mineralisation will add to the overall complexity of flow pathways.

Even though formation waters may have been originally in equilibrium, during movement along the fracture they may undergo sufficient temperature, pressure or pH changes to possess significant dissolution or precipitation potential. This is relevant to CO₂ storage as fluid-fluid and fluid-rock reactions show that dissolution and precipitation reactions have occurred in natural systems in the presence of supercritical CO₂ (Kampman *et al.*, 2014a) (Section 3.4). In this way, narrow intense zones of dissolution or precipitation could be associated with high permeability pathways (e.g. Dyke, 1995; Dockrill and Shipton, 2010; Kampman *et al.*, 2014a).

The healing of fractures and faults may also have two significant and competing effects on the porosity and permeability of a sedimentary sequence which may be important for CO₂ storage. Firstly, mineralisation of faults and fractures can strengthen the aggregate by increasing cementation and cohesion, which directly causes permeability decrease. At the same time, this lowering of permeability may weaken the rock by elevating fluid pressure, resulting in a reduction of effective stress, which in turn can cause further brittle failure (Tenthorey *et al.*, 2003). Any re-fracturing of mineralised zones could increase permeability if fractures, closed by mineralisation, become connected again (Evans, 2005).

The breaking strength of mineralised fractures has a greater influence on the rock strength than the elastic modulus (Vass *et al.*, 2014). It is therefore important to understand the breaking strength of mineralised faults and fractures in target locations such as reservoirs and caprocks associated with CO₂ storage. A fracture's breaking strength depends on the different mineral assemblages within the fracture but also on the fracture-wall rock contact. Calcite, especially combined with other soft minerals such as gypsum, can make the fractures weak in sandstones, for example, while quartz would strengthen fractures in mudstones (Vass *et al.*, 2014).

As partially mineralised fractures can possess *in situ* apertures of several millimetres, a small number of open fractures can dominate fluid flow. While these fractures may be relatively rare their high permeability could still contribute significantly to rock mass permeability. This suggests that the total number of conductive fractures within a rock mass may not be the major control on fracture permeability, and that the characteristics of individual fractures could be more important. In this sense, characterising statistically anomalous fractures (i.e., those with the largest apertures) could be more important in predicting flow behaviour than understanding the statistics of the majority (Dyke, 1995; Laubach *et al.*, 2004). For example, impermeable fractures can also be critically stressed, implying that critical stressing may be a necessary, but not a sufficient, condition for permeability to develop (Evans, 2005).

Under conditions of depletion (during which no local cooling of the rock mass occurs) the inference of *in situ* stress directions from preferential fluid flow is called into question by Dyke (1995). Dyke's contention is that if the distribution of fractures in a lithology was homogeneous and possessed no preferential orientation, and if fracture apertures were stress dependent, the link between preferential fluid flow and *in situ* stress could be made. However if fractures are locked open by diagenetic processes with apertures that are relatively stress independent, the link between preferential fluid flow and *in situ* stress becomes tenuous (Dyke, 1995). Dyke (1995) suggests preferential flow direction will be controlled by the orientation of any major fractures, not the present day *in situ* stresses. In many cases the two directions may coincide, simply because the palaeo-stress state under which the fractures formed is the same as the *in situ* stress state. In these cases the assertion that needs to be checked is whether paleo-stresses are an indicator of *in situ* stresses, and not whether preferential fluid flow is a direct indicator of *in situ* stress (Dyke, 1995).

3.5 CONFINING PRESSURE AND STRESS ORIENTATION

The continuity of fracture porosity is of fundamental importance for fluid migration in CO₂ storage. While some authors, as discussed in the previous section, have focused on the role of burial history and diagenesis that occurs contemporaneously with or after fracturing events to understand the factors that control permeability (Dyke, 1995; Durham, 1997; Laubach *et al.*, 2004; Barr, 2007; Sathar *et al.*, 2012), others emphasise *in situ* stress as a determinant for which fractures are likely to be hydraulically conductive and which are not (Barton *et al.*, 1995; Townend and Zoback, 2000; Ferrill and Morris, 2003; Streit and Hillis, 2004; Mildren *et al.*, 2005). In the latter model, the maximum permeability direction in fractured media is expected to align with the maximum compressive stress for opening mode fractures or with the strike orientation of critically stressed faults. Rutqvist and Stephansson (2003) provide a review of the role of hydromechanical coupling in fractured rock. While this topic is covered in depth in Section 5 we introduce some basic concepts and caveats to this conventional theory.

Additional steps are also included in the fault-seal workflow (discussed in Section 4) to assess the risk that a fault which is sealing in all other respects might leak because of fault reactivation

(Bretan *et al.*, 2011). In such models, the seal/leak behaviour of the fault is principally controlled by the stress state and fault rock mechanical properties (e.g. (Ferrill *et al.*, 1999); Mildren *et al.*, 2005). Here, a critically stressed fault close to failure may develop dilatant micro-fracturing that result in open pathways which allow buoyant fluid to migrate up the fault zone and away from the target formation. Assessing whether a fault is critically stressed should form part of CO₂ storage risk assessment (e.g. Fang and Khaksar, 2013). It requires knowledge of the *in situ* stress magnitudes and directions, pore-pressure, orientation of the fault with respect to the principal stress axes, and the geomechanical strength of the fault rock. This type of approach is often termed “geomechanical analysis” and has been used over recent years to investigate the mechanical stability of faults within CO₂ reservoirs and to estimate CO₂ column heights that specific faults could support without undergoing reactivation (Streit and Hillis, 2004; Chiamonte *et al.*, 2008; Bretan *et al.*, 2011).

The geometry (strike and dip) of a fault relative to the principal stresses, and the stress magnitudes, strongly influence the estimate of how close the fault is to failure (Section 5.1) and the maximum pore fluid pressure a fault can sustain. These estimates therefore require accurate mapping of fault geometries from available data, as well as reliable determinations of the prevailing stresses and fault rock properties. In cases where pressure depletion has occurred, stresses need to be determined after depletion to incorporate depletion induced stress changes (Streit and Hillis, 2004). Since *in situ* stresses are determined from well log data and pressure testing data, the availability of such data strongly influences how accurately stresses are constrained (Streit and Hillis, 2004). Hence, data availability, well locations, and well spacing are limiting factors in the identification of stress heterogeneities, such as local rotations of principal stress axes or changes in stress magnitudes that may occur in the vicinity of some faults (e.g. Barton and Zoback, 1994).

Fracture-related hydrocarbon production can be either stress dependent or rate dependent. The rate of development of stress-dependent fracture permeability is controlled by how fracture aperture and, in certain cases, fracture connectivity interact with the present-day *in situ* reservoir stress (Ameen *et al.*, 2012). This depends on two competing factors: the differential stresses and the minimum effective stresses in the reservoir. The latter depends on the reservoir pore pressure and the magnitude of the minimum principal stress. High reservoir pressures (high differential stresses and lower effective minimum stress) may result in incipient shear deformation of preferentially oriented, barren, open fractures (hairline fractures) creating mismatching fracture walls and channel type apertures (Section 3.5.1). This results in enhancing the permeability of connected, sheared fractures (e.g. Evans *et al.*, 2005). In addition, suitably oriented pre-existing faults may slip and become more permeable. This hypothesis is mostly based on laboratory and theoretical studies on fractured rock mass stability and the impact of fracture deformation on their hydraulic properties, especially in the process of shearing (Gentier *et al.*, 2000; Gutierrez *et al.*, 2000; Lee and Cho, 2002). A reduction in the reservoir pressure (lower differential stresses) will not reverse the shear process, and the created mismatch apertures will stay open. However, laboratory, outcrop, and seismicity studies indicate that if differential stresses increase or stay at the same level, the shearing of fractures commonly progresses and asperities on such fracture walls tend to break and pulverize, resulting in gouges and diminishing fracture apertures and local fracture permeability (Lee and Cho, 2002).

As differential stresses decrease and reservoir pressure increases, suitably oriented fractures will tend to dilate perpendicular to the fracture walls and fracture shearing will be a less significant process in aperture enhancement. The permeability of the dilated and connected fractures will be enhanced. This type of permeability is also referred to as pressure-sensitive permeability. If pore pressure diminishes or minimum principal stress magnitude increases,

the fracture apertures will tend to diminish or close, resulting in a reduction in permeability and productivity. Reservoirs with this type of fracture permeability are very sensitive to reservoir pressure, particularly in cases where pore pressure is equal to the minimum horizontal stress (i.e. zero effective normal stress, Dyke, 1995). Damage to fracture permeability can be permanent because of pressure depletion and consequent fracture closure. Such reservoirs are best developed with pressure support. Ameen *et al.* (2012) show that after repeated cycles of drawdown and build-up in well tests reservoir pressure returns to levels close to the initial preproduction magnitudes after shut-in. If fracture permeability had been stress dependant, the pressure would have declined irreparably. Dyke (1995) demonstrated in a review that many highly productive fractured reservoirs depend on partly mineralized fractures with channel-type apertures. Such apertures are stiffened by the mineralization and tend to stay open irrespective of the orientation of the fracture relative to the *in situ* stresses (Laubach *et al.*, 2004) and irrespective of production-related pressure depletion (Ameen *et al.*, 2012; Ameen, 2014). Field, well, and laboratory observations also highlight that understanding the stress history of a fractured rock mass is essential, and understanding of the present-day stress field alone is insufficient to model the hydromechanical response of *in situ* faults and fractures to stress changes (Barr, 2007; Sathar *et al.*, 2012).

Triaxial tests on different mudrocks and shales from North Sea reservoirs and adjacent areas sheared at different effective confining stresses show that during burial, mudrocks behave as normally consolidated materials and deform ductilely in response to increasing load (Nygård *et al.*, 2006). Several processes like uplift, chemical diagenesis and overpressure build-up, however, result in mudrocks becoming overconsolidated and deforming in a brittle manner during loading. Combining a relationship between normalized undrained shear strength and overconsolidation ratio for mudrocks with a correlation between compressional wave velocity and apparent pre-consolidation stress (which accounts for both mechanical and chemical diagenesis) could be used as a tool to evaluate possible leakage of sealing formations (Nygård *et al.*, 2006).

There are several lines of evidence that suggest that generating long-lasting permeability in clay-rich sedimentary rocks (shale) is difficult. During hydraulic fracturing, for example, the use of proppants is apparently required to maintain the permeability of the generated fracture system over production timescales. Shale and other mudstones are well known for their tendency toward plastic deformation or creep while under stress that may close or seal fractures (William Carey *et al.*, 2015). In laboratory friction experiments, shale samples with clay and organic content above ~30% by weight, for example, show coefficient of friction ~0.4 and consistently velocity-strengthening behaviour, while those below this threshold show increased strength and velocity-weakening behaviour (Kohli and Zoback, 2013). This transition in frictional strength and stability suggests a change in the shale grain packing framework from rigid clast supported to clay mineral and organic matter supported (Kohli and Zoback, 2013). Many studies investigate the permeability of artificial fractures (sawn or split samples) or artificially separated natural fractures in shale using triaxial or shear-box devices (e.g. Gutierrez *et al.*, 2000; Zhang and Rothfuchs, 2008; Zhang, 2011; Kohli and Zoback, 2013; Zhang, 2013). While these studies provide valuable data on fracture behaviour they are unable to evaluate the permeability and behaviour of natural, stress-induced fractures. Fracture-induced permeability has, however, been investigated for excavation damage zones associated with nuclear waste repositories (Bastiaens *et al.*, 2007; Zhang and Rothfuchs, 2008). These studies show that shale, with the application of hydrostatic or deviatoric stress over time, has a high capacity for self-healing and permeability reduction.

3.5.1 Fracture hydromechanical behaviour under normal stress

While the laboratory study of the hydromechanical behavior of fractures under normal stress bears little resemblance to *in situ* stresses at reservoir depths, it allows understanding of a fracture's response under carefully controlled conditions. From a modelling point of view, the phenomena that must be considered when studying fractures under normal stress are simpler than those for fractures in shear; the natural granite fractures that Gentier *et al.* (2000) studied, for example, generally exhibit only elastic behaviour under normal stress. In addition, the deformation that occurs for fractures under normal stress is relatively small compared to the large deformations and displacements that occur under shear stress (Gentier *et al.*, 2000).

Measurements of fracture closure show that it does not increase linearly with increased applied normal stress; closure increases rapidly at low normal stresses and then approaches a constant value (maximal closure) (Gentier *et al.*, 2000; Lee and Cho, 2002). Maximum closure is typically 10–20% (up to 30–40% in some cases) of the mean geometrical fracture aperture (measured from matched surface profiles or casts of the void space obtained before load is applied to the sample) (Gentier *et al.*, 2000).

Measurements of normal displacement show that closure is non-uniform across the fracture. Normal displacement is always accompanied by a small tangential displacement, resulting from the roughness of the fracture, which can be measured during the experiment. Tangential displacement can represent from 5–10% of normal displacement for a fracture without infill and 20–30% for fractures with hard infill (Gentier *et al.*, 2000). Fracture closure with increasing normal stress is accompanied by both a reduction in mean aperture and an increase in contact area, which reduces the volume of void area through which flow can occur (Gentier *et al.*, 2000).

As contact area is non-uniformly distributed on the fracture surface it increases non-linearly with normal stress. Contact area (the area with aperture smaller than 20 μm) does not exceed 40–60% of the nominal fracture area for normal stresses up to 65 MPa (approximately 2.5 km using density of 2700 kg/m^3 – in a sedimentary basin this is likely to be a little deeper as near surface rocks will be less dense than 2700 kg/m^3) (Gentier *et al.*, 2000).

The hydro-mechanical behaviour of an extensional fracture in shale under normal loading was investigated experimentally by Gutierrez *et al.* (2000). Representative analogues of hydraulic fractures in shaly formations were obtained by de-mineralising a cemented natural fracture in block samples of Kimmeridge shale. Gutierrez *et al.* (2000) details that the fractures, at the time they were created, had approximately nine orders of magnitude higher permeability than the intrinsic permeability of the intact shale. Shale fracture permeability decreased following an empirical exponential law when normal stress increased, however, loading the sample to an effective normal stress twice as much as the intact rock unconfined compressive strength did not completely close the fracture (Gutierrez *et al.*, 2000). Despite an order of magnitude reduction in fracture permeability after loading to an effective normal stress of 10 MPa (approximately twice the unconfined compressive strength of the intact shale), fracture permeability was still eight orders of magnitude larger than the permeability of the intact shale (Gutierrez *et al.*, 2000).

3.5.2 Fracture hydromechanical behaviour in shear

Gentier *et al.* (2000) found a global increase in intrinsic transmissivity with increasing shear displacement of typically two to three orders of magnitude for a tangential displacement of about 1 mm in granites. This increase is directly related to the dilatancy of the fracture resulting from the roughness of the fracture surfaces. Measurements indicate that dilatancy induces

normal displacements of two to three times the initial aperture, when tangential displacements are between 2 and 2.5 mm (Gentier *et al.*, 2000; Lee and Cho, 2002).

The hydro-mechanical behaviour of an extensional fracture in shale under shear loading was investigated experimentally by Gutierrez *et al.* (2000). Shearing of the fracture at a constant effective normal stress lower than the unconfined compressive strength of the shale caused dilation of the fracture and an order of magnitude increase in fracture permeability. This increase resulted in a difference of ten orders of magnitude between the permeability of the fracture and the intact shale (Gutierrez *et al.*, 2000). Shearing at a constant normal stress higher than the unconfined compressive strength of the intact shale caused closure of the fracture and resulting in an approximately six order of magnitude reduction in fracture permeability. This reduction in permeability results from shear-induced gouge formation and transported particles occluding fracture apertures. While the permeability reduction was close to six orders of magnitude, fracture permeability was still approximately three orders of magnitude higher than the permeability of the intact rock (Gutierrez *et al.*, 2000).

The ability of rough fractures to retain much of their permeability in the presence of contact stresses across the fracture plane can be attributed to the microscopic structure and roughness of the fracture surfaces. Even in the case of severe loading exceeding the strength of the sediment matrix, it appears that the microscopic asperities at the fracture surface are able to keep some space and channels along the fracture to allow for fluid flow and to maintain enhanced permeability. Based on experimental results (e.g. Gentier *et al.*, 2000; Gutierrez *et al.*, 2000; Lee and Cho, 2002), it can be concluded that the current definition of a “closed” fracture when the fracture surfaces come in contact is unrealistic. There is therefore a need to distinguish between physically or mechanically open/closed fractures and hydraulically open/closed fractures. Once fractures are created they are difficult to hydraulically close through reduction in pore pressure or increases in normal stress across the fracture. Also, for fluids to flow along fractures, it is not necessary that large overpressures, which are in the order of the stiffness of the sediment matrix, be maintained to keep the fractures hydraulically parted. Unless fractures get mineralised and cemented, they can stay open even if the fracture surfaces are in contact and fluids may still flow, provided there is a sufficient hydraulic gradient to induce flow. This implies that fluids have a longer window of opportunity to migrate, once fractures are created, than previously assumed in some models (Gutierrez *et al.*, 2000).

Few studies have been conducted under *in situ* conditions with simultaneous fracture and permeability measurements at reservoir conditions. One such study, however, documents the interaction of supercritical CO₂ with fractured caprock samples recovered from depths of up to 4 km (Edlmann *et al.*, 2013). Contrary to expectations, results from this study indicate that supercritical CO₂ will not flow through the tight natural caprock fractures sampled, even with pressure differentials in excess of 51 MPa. Below the critical point where CO₂ enters its gas phase, however, the CO₂ flows readily through the caprock fractures (Edlmann *et al.*, 2013). The contradictory experimental observations found by Edlmann *et al.* (2013) are linked to the complex interplay between the fluid conductivity response of the CO₂ phase to the fracture properties, the influence of stress on the fracture aperture, the chemical interaction between the rock minerals and the CO₂ fluid, the fluid pressure influencing the fracture permeability, the influence of CO₂ phase on the capillary entry pressure and the relationship between CO₂ phase on the wettability, interfacial tension and contact angle (Edlmann *et al.*, 2013). These data suggest the possibility of a critical threshold of fracture aperture size which controls CO₂ flow along the fracture (Edlmann *et al.*, 2013).

3.6 PORE PRESSURE

Large volumes of CO₂ may be geologically stored by injecting pressurized supercritical CO₂ into saline formations or depleted hydrocarbon reservoirs (e.g. Streit and Hillis, 2004; Tsang *et al.*, 2007; Rinaldi and Rutqvist, 2013). CO₂ Injection requires displacement or compression of existing formation fluid and therefore needs to be at pressures above that of the formation pore fluid pressure. Increased formation pressures due to CO₂ injection can potentially open fractures and cause slip on pre-existing faults (e.g. Rinaldi and Rutqvist, 2013). Many laboratory and *in situ* experiments have shown that increasing pore fluid pressure in rocks and faults increases permeability (Figure 3.10), reduces their strength and can induce brittle failure. Brittle failure results from increasing pore fluid pressure (P_f) leading to low effective stresses $\sigma' = (\sigma - P_f)$. Positive effective normal stresses ($\sigma_n - P_f$) resist sliding motion along the fault surface induced by shear stresses acting parallel to the fault. Higher pore fluid pressures decrease the resistance to sliding leading to slip (fault reactivation) (Sibson, 1996; Streit and Hillis, 2004; Leclère *et al.*, 2015). Fault reactivation would create or enhance fracture permeability while the formation of networks of interlinked open fractures and rough fault surfaces could provide conduits for the escape of CO₂-rich fluid from a reservoir or a saline formation (e.g. Sibson, 1996; Miller *et al.*, 2004; Streit and Hillis, 2004; Hermanrud *et al.*, 2014).

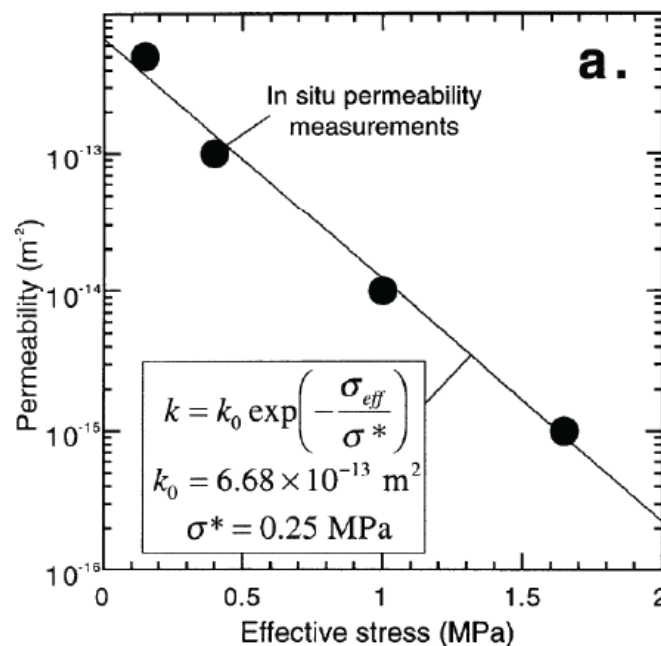


Figure 3.10 Permeability versus effective stress (from Revil and Cathles, 2002) (a) Direct *in situ* permeability measurements inside the Red Fault system. These data can be fitted by an exponential law where k_0 is the permeability at zero effective stress and σ^* is a pressure sensitivity constant for permeability.

The permeability of fault gouge is a strongly decreasing function of effective stress (Figure 3.10), and hence a strongly increasing function of the pore fluid pressure (Section 3.6). For example, *in situ* measurements within the Red Fault system are well represented by the permeability/effective stress relationship (Revil and Cathles, 2002):

$$k = k_0 \exp(-\sigma_{\text{eff}}/\sigma^*)$$

where σ_{eff} is the effective stress ($\sigma_{\text{eff}} = (\sigma - P_f)$ where σ is the confining pressure, approximated by the lithostatic stress, and P_f is the pore fluid pressure), k_0 is the permeability at zero effective stress, and σ^* is a constant, which describes the influence of the compactional response of the porous material upon the permeability (Revil and Cathles, 2002).

The early view that the high-pressure injections serve to drive extensive “mode 1” hydrofractures in crystalline rock is not supported by observation (Evans *et al.*, 2005). Rather, Evans *et al.* (2005) find that shearing of fractures and faults within the rock mass in response to the elevated pore pressure is the primary permeability creating mechanism during large scale injection. Laboratory experiments (e.g. Gentier *et al.*, 2000; Gutierrez *et al.*, 2000; Lee and Cho, 2002) and theoretical considerations (Wang *et al.*, 1988) provide a firm basis to expect that shearing of naturally rough fractures produces irreversible increases in fracture permeability. However, the essential details of the process as it occurs within reservoirs, such as the scale of coherent slip, and its relation to structure, are rarely directly measured (Evans *et al.*, 2005).

Despite the fact that fault-hosted fluid flow is still poorly understood, several studies, both theoretical and observational, have increased our understanding of the interaction of fluids and faults. One popular model maintains that fluids may intermittently propagate as shock waves along faults at geologically fast rates (from m/yr to km/yr) (Rice, 1992; Revil and Cathles, 2002). The shock waves are excited in the subsurface when the rock permeability is a strongly nonlinear function of fluid pressure — a characteristic of highly fractured zones, such as fault zones. These episodic flow events could be considered in terms of pore pressure build up followed by release when the Coulomb failure criterion is exceeded. Such behaviour is reminiscent of the fault-valve model, in which fluid flow along faults is episodic and initiated by an increase in fault zone permeability in response to fault slip (Sibson, 1990). Leclère *et al.* (2015) provide a brief review of the mechanisms of the development, maintenance, and diffusion of high fluid pressures in faults.

The direction of the fluid pressure gradient is also important. For fluid to flow along a permeable fault, the pressure gradient must be continuous and at least sub-parallel to the fault plane. Hence, if the direction of the fluid potential gradient is not continuous but reverses with depth, then long-distance migration along a sub-vertical fault is impossible. Reversals in fluid pressures commonly occur in interstratified sandstone/shale sequences. Therefore, since the details of fluid potentials around faults are often unknown, it may be very difficult to determine whether a fault plane is not “leaking” because it is of low permeability or because fluid pressure barriers exist in the section (Hooper, 1991).

4.0 FAULT SEAL PREDICTION

In circumstances where faulted sandstones are juxtaposed, seal analysis is performed to predict the potential for fault seal to lateral flow. These analyses were primarily developed for the petroleum industry and highlight the importance of fine-grained fault rock for locally reducing fault permeability in multilayer sand-shale sequences (e.g. (Bouvier *et al.*, 1989; Lindsay *et al.*, 1993; Fulljames *et al.*, 1997; Knipe, 1997; Lehner and Pilaar, 1997; Yielding *et al.*, 1997; Manzocchi *et al.*, 1999; Rivenæs and Dart, 2002; Sperrevik *et al.*, 2002; Bense and Person, 2006; Childs *et al.*, 2007; Jolley *et al.*, 2007; Freeman *et al.*, 2008; Faulkner *et al.*, 2010; Manzocchi *et al.*, 2010; Yielding *et al.*, 2010; Noorsalehi-Garakani *et al.*, 2013). Fault seal analysis is based on the premise that faults in petroleum reservoirs form capillary (or membrane) seals (Jennings, 1987; Watts, 1987; Yielding *et al.*, 1997; Brown, 2003; Manzocchi *et al.*, 2010; Bretan *et al.*, 2011). Hydrocarbon (and CO₂) migration is generally accepted to occur in localized stringers driven principally by buoyancy forces and opposed by the capillary properties of the rock through which the migration occurs (e.g. England *et al.*, 1987; Carruthers and Ringrose, 1998; Bretan *et al.*, 2011). Sealing occurs where these capillary forces prevent further migration. A seal will remain intact until the capillary pressure (that is the difference in pressure between the oil and water) at the interface between the reservoir and the seal, due to the buoyancy force of the trapped hydrocarbon column, exceeds the capillary threshold pressure of the water-wet seal. The threshold pressure is the capillary pressure at which the non-wetting (hydrocarbon) phase forms a continuous filament or stringer through the seal.

The most important fault parameter therefore in fault seal analysis is the capillary threshold pressure of the fault-rock (Yielding *et al.*, 1997; Manzocchi *et al.*, 2010; Bretan *et al.*, 2011), which is controlled by the pore throat size. The smaller the pore throat size, the higher the capillary threshold pressure required before leakage through the fault zone will occur and the greater the hydrocarbon column that can potentially be supported before leakage (Yielding *et al.*, 1997; Manzocchi *et al.*, 2010; Bretan *et al.*, 2011).

4.1 METHODS

In the majority of fault seal studies fault rock is inferred to primarily form due to smear along the fault or mixing into the fault zone of clay-rich beds in the host rock (Figure 2.3b). Based on conceptual clay smear and mixing models a number of algorithms have been developed for estimating the flow properties of faults and their impact on lateral migration of fluids. Conventional fault permeability predictors vary from those that assume fault rocks formed due to mixing of the faulted sequence (e.g. Shale Gouge Ratio or SGR method) (Yielding *et al.*, 1997; Manzocchi *et al.*, 1999; Sperrevik *et al.*, 2002), to those in which the beds become progressively more sheared (and thinned) with increasing displacement and distance from the source bed (e.g. Clay Smear Potential or CSP method; Lehner and Pilaar, 1997: Shale Smear Factor or SSF method; Lindsay *et al.*, 1993). The CSP, SSF and SGR algorithms are schematically illustrated in Figure 4.1, while further details of these algorithms and others presented in the literature are summarized in Table 4.1.

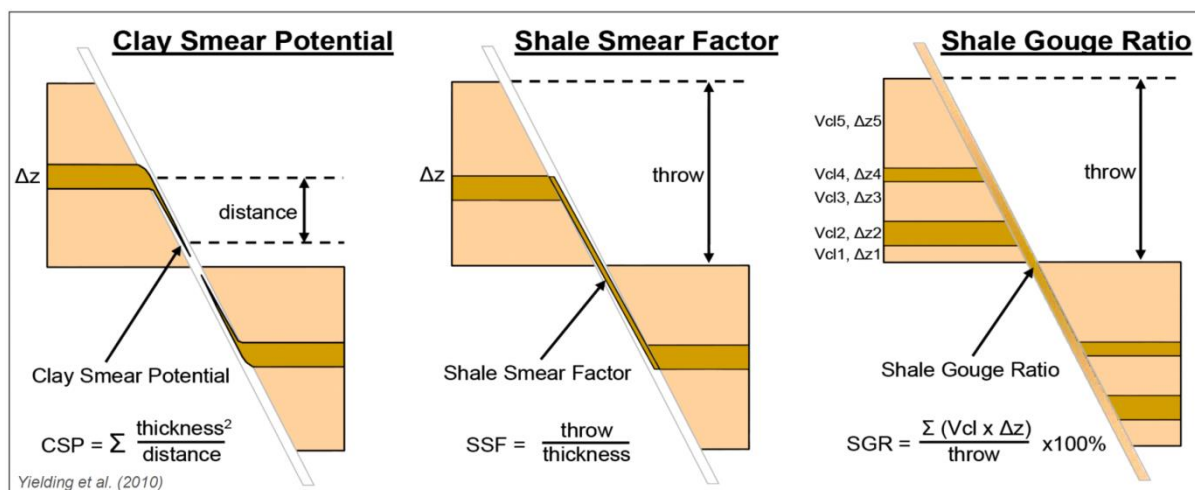


Figure 4.1 Schematic diagram illustrating three of the main fault seal conceptual models and associated algorithms used to predict the likelihood of low permeability clay within fault zones (from Yielding et al., 2010).

Shale Gouge Ratio (SGR) is the most widely utilized of the algorithms summarized in Table 4.1 (Yielding *et al.*, 1997; Manzocchi *et al.*, 1999; Childs *et al.*, 2002; Sperrevik *et al.*, 2002). For the SGR method the phyllosilicate or clay fraction in the fault rock is considered to be equal to the value of SGR, which is the proportion of clay (or shale) within a sequence that has moved past a point on a fault (Figure 4.1, Table 4.1). SGR can be calculated for each point on a fault surface using the fault displacement and the clay content of the faulted sequence that has passed that point. Clay content is typically estimated by mapping individual clay beds in outcrop or by modelling clay (V_{clay}) variations in gamma ray well logs (Yielding *et al.*, 1997). SGR can be transformed to a fault rock threshold pressure for fault seal analysis in exploration or to a permeability for production purposes. Relationships between SGR and both permeability and threshold pressure can change between studies, perhaps due to variations in the depth of burial, diagenesis and/or fault-rock generation mechanisms (Childs *et al.*, 2002; Sperrevik *et al.*, 2002; Childs *et al.*, 2007; Manzocchi *et al.*, 2010).

Table 4.1 Summary of fault seal algorithms developed to predict the permeability of fault rock generated by the entrainment of host rock clay beds into fault zones (from Giger et al., 2013).

Algorithm	Formula*	Predictive Application	Mechanisms	References
Clay smear potential (CSP)	$CSP = c \times \sum t_{sh}^n / d^m$ $c = 1, m = 1, n = 2$ Variations: Calibration factor $c \neq 1$ to account for rheology and stress dependency Smear factor (SF = CSP, but where $c = 1, m \neq 1, n \neq 2$) ¹ , also referred to as generalized smear potential (GSP) by ²	Thickness of clay smear	Injection, flow	Bouvier et al., 1989; Lehner and Pilaar, 1997 Fulljames et al., 1997 ¹ Yielding et al., 1997 ² Doughty, 2003
Shale smear factor (SSF)	$SSF_{[c]} = S_{t[c]} / t_{sh}^{**}$ Variation: Probabilistic shale smear factor (PSSF)	Continuity of clay smear, seal breakdown for $SSF = SSF_c$	Abrasion, shear/drag, injection/flow	Lindsay et al., 1993 Childs et al., 2007
Shale gouge ratio (SGR)	$SGR = \sum [V_{sh(i)} \times t_{sh(i)}] / S_t$ Variation: Effective shale gouge ratio (ESGR) with weighting factor, essentially a hybrid of CSP and SGR	Distribution of phyllosilicates along fault zone, seal strength when calibrated	Abrasion, wear, grain-scale mixing	Fristad et al., 1997; Yielding et al., 1997 Knipe et al., 2004; Freeman et al., 2010

* c = constant to calibrate for rheology and stress; d = distance between the shale/clay source layer and a point in the fault zone; m and n = scaling exponents; S_t = cumulative or total slip; t_{sh} = thickness of phyllosilicate-rich (clay/shale) layer; V_{sh} = volumetric fraction of phyllosilicates.

**The subscript $_{[c]}$ denotes the critical S_t at which clay smears become discontinuous (seal breakdown).

The SGR method is relatively straightforward to implement for faults on the scale of individual petroleum reservoirs or CO₂ storage sites using a combination of stratigraphic data from wells and seismic reflection lines that constrain fault locations and geometries. However, examination of fault rock exposed in outcrops suggests that the stratigraphic mixing inherent in the SGR method may not account for the heterogeneity of fault zone structure observed (Childs *et al.*, 2007). In particular, anastomosing and discontinuous fault rock has the potential to produce high clay content in fault zones where the clay content in the host rock is relatively low (and *vice versa*). An alternative approach to the SGR method is to consider that the fault zone structure is a perfect shear zone, with all clay and sand units being continuous between the source layer cutoffs (SSF Model Figure 4.1) until SSF exceeds a critical value (SSF_c) at which point the beds become discontinuous. For $SSF > SSF_c$ the sheared mudstone beds can be placed randomly between the source mudstone beds and stacked on top of each other within the fault zone (this approach is referred to as the Probabilistic Shale Smear Factor – PSSF, Table 4.1). In realizations where the mudstone beds are collectively unbroken along the fault between the source beds the fault is inferred to be sealing (Childs *et al.*, 2007; Yielding, 2012). Because the model is stochastic it can be run many times to test the stability of the results and their sensitivity to changes of input parameters.

CO₂ storage reservoirs are likely to contain water (brine) and supercritical CO₂ phases. In petroleum and CO₂ industries the fault seal methods outlined above require an estimate for the size of the pore throats within fault-zones and the interfacial tension of the two phases (Jennings, 1987; O'Connor, 2000; Bretan *et al.*, 2011). The value of interfacial tension for CO₂ – brine in a reservoir will depend upon pore pressure and pore-water salinity. For example, data from the Norwegian continental shelf show that CO₂-brine interfacial tension values are c. 28 mN/m, which are comparable to typical oil-brine values used in the hydrocarbon industry (default value of 30 mN/m) (Chalbaud *et al.*, 2006; Chalbaud *et al.*, 2009). Given the overall similarity between the CO₂-brine and oil-brine data, methods for analysing fault seal integrity, such as shale-gouge ratios (SGR), can be applied to a CO₂-brine system (Bretan *et al.*, 2011).

4.2 CALIBRATION OF RESULTS

The results of the SGR and PSSF methods have, in some cases, been validated by comparison of the method outputs with capillary threshold pressures and trapped column heights (Yielding *et al.*, 1997; Yielding, 2002; 2012). The correlation between capillary threshold pressure and the clay content of laboratory samples (e.g. Fisher & Knipe 1998; Gibson 1998; Sperrevik *et al.* 2002), coupled with the assumption that the Shale Gouge Ratio (SGR) provides a proxy for the clay content of fault rock, provides the basis for the most commonly applied fault seal prediction methods (e.g. Yielding *et al.* 1997; Yielding *et al.*, 2010; Bretan *et al.*, 2011). The conceptual basis of the method is summarized in Figure 4.2, for an accumulation formed on the down-thrown side of a membrane seal (Figure 4.2A) (Manzocchi *et al.*, 2010). Heterogeneity in the high permeability reservoir rocks results in a variable SGR profile over the sand-on-sand juxtaposition window (Figure 4.2B). Capillary threshold pressure is mapped onto the fault surface (Figure 4.2C) using one of the industry standard relationships (e.g. Sperrevik *et al.*, 2002; Bretan *et al.*, 2011) which link threshold pressure exponentially to SGR (Manzocchi *et al.*, 2010). Buoyancy-driven hydrocarbons or CO₂ migration is stopped by low permeability fault rock, and the accumulation forms behind it. As the accumulation column height grows, the capillary pressure at each point in the accumulation increases (dotted lines in Figure 4.2C) (Manzocchi *et al.*, 2010). Eventually, the capillary pressure at some point in the accumulation matches the capillary threshold pressure of the fault rock, allowing migration through the fault, and limiting the height of the fault-bounded accumulation. As Figure 4.2C indicates, the critical leak point controlling the column height need not be at the top of the accumulation, at the hydrocarbon–water contact, or at the position with lowest SGR (Manzocchi *et al.*, 2010).

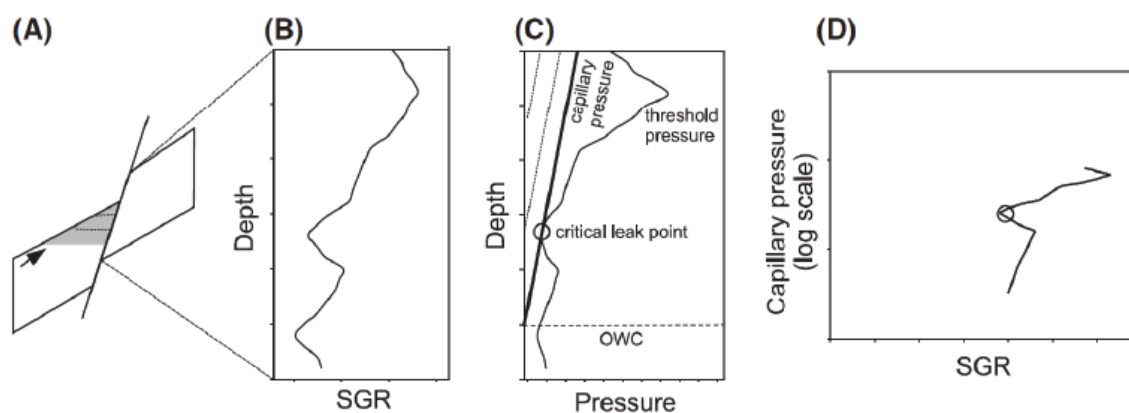


Figure 4.2 Cartoon illustrating the method for using Shale Gouge Ratio (SGR) as a column height predictor (from Manzocchi *et al.*, 2010). (A) A hydrocarbon column (grey) on the downthrown side of a fault. The arrow indicates the migration direction and the dashed lines show hydrocarbon–water contacts during the filling of the reservoir. (B) SGR versus depth profile along the length of the sand-sand juxtaposition window. (C) Capillary threshold pressure (curve) is estimated as a direct function of SGR. Also plotted is the capillary pressure in the accumulation in its final state (thick solid line) and with two earlier hydrocarbon–water contacts (dotted lines corresponding to the dotted lines in A). The open circle indicates the depth at which the capillary pressure of the reservoir equals the capillary threshold pressure of the fault rock and therefore this position defines the total seal capacity of this fault. (D) Plot of SGR against reservoir capillary pressure, with the leak point indicated by the circle.

In one approach linking SGR to capillary threshold pressure (e.g. Yielding *et al.*, 2010; Bretan *et al.*, 2011), data from fault-bounded oil and gas reservoirs with known hydrocarbon–water contacts (and resulting capillary pressure/depth data) are used to calibrate empirical fault seal envelopes (e.g. Figure 4.3). Capillary pressure versus SGR defines a spread of data associated with a particular fault and, if the hydrocarbon column height is controlled by a fault seal, one point in this distribution represents a critical leak point (e.g. Figure 4.2D). When capillary pressure/SGR data from multiple faults in a field are combined, the distribution of data

provide constraints on the capillary pressure that can be supported by a particular SGR value (Figure 4.3A). Figure 4.3 is a global compilation of normal faults (active at depths of less than 2 km), for which the across-fault pressure difference was assumed to be equal to the capillary pressure (Yielding, 2002). The maximum burial depths of these faults were found to influence the seal envelopes, in this case, deeper faults were found to be capable of sealing larger hydrocarbon columns (Figure 4.3) (Manzocchi *et al.*, 2010). Discussion and updated versions of Figure 4.3 are provided by Bretan *et al.* (2011) and Yielding *et al.* (2010).

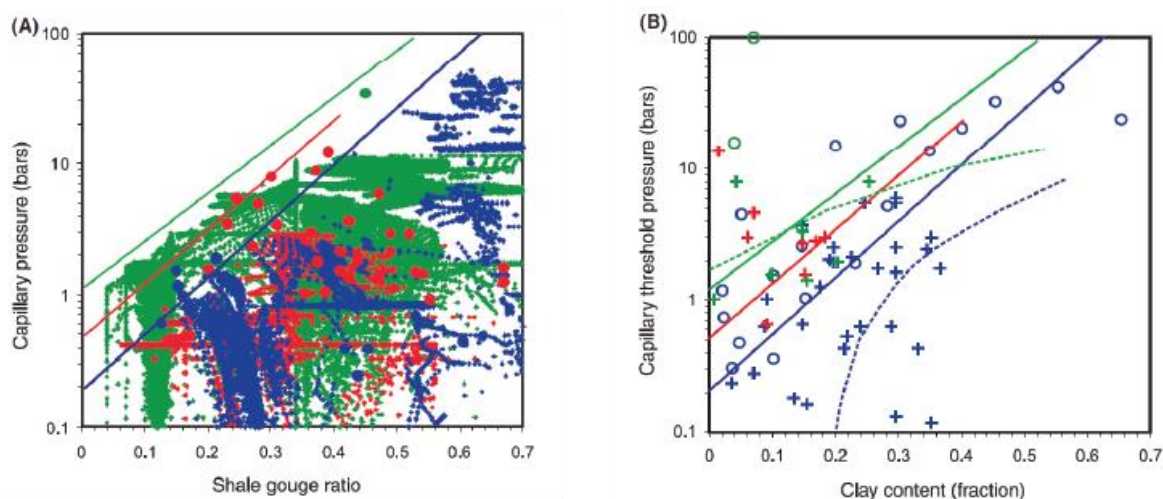


Figure 4.3 Shale Gouge Ratio (SGR) fault seal calibrations (from Manzocchi *et al.*, 2010). (A) Compilation of SGR versus capillary pressure adjacent to the fault for faults in a variety of extensional basins. Clouds of small points represent entire fault data (e.g. the line in Figure 4.2D), while large circles correspond to trap-critical points (e.g. the circle in Figure 4.2D). The data are coloured according to present day depth of burial (<math>< 3.0\text{ km}</math> in blue, 3.0–3.5 km in red and 3.5–5 km in green) and the coloured lines represent fault seal envelopes representative of these three classes of faults. Redrawn from Yielding (2002). (B) Seal-failure envelopes from (A) compared with laboratory measurements of capillary threshold pressure obtained by Gibson (1998) shown as circles, and Sperrevik *et al.* (2002) shown as crosses. Hydrocarbon–water threshold pressures for these laboratory measurements have been calculated based on a hydrocarbon–water interfacial tension of 40 mN/m and a 30° contact angle. The dashed seal-failure envelopes for the deepest and shallowest depth classes are taken from Yielding *et al.* (2010) and derive from their latest analysis of the global compilation of field data.

4.3 UNCERTAINTIES

Despite efforts to calibrate fault-seal predictions with empirical reservoir pressures, column heights and flow information (e.g. Figure 4.3), these predictions and their application to individual faults can carry significant uncertainty (James *et al.*, 2004). Possible sources of these uncertainties are listed below:

- Many poorly constrained input parameters (e.g. bed and fault geometries, fault clay content and fault displacements), are required to produce fault flow solutions which are non-unique. It has been suggested that membrane seals can usually be explained by juxtaposition seal (James *et al.*, 2004).
- Definition of fault zone structure and detailed clay smear geometries is poor to non-existent in the models and they may not capture the heterogeneous structure of the zones.
- Sub-seismic faults are difficult to account for and may locally modify juxtaposition and clay-smear geometry.
- Definition of clay content (V_{clay}) from gamma ray logs is non-unique and model-dependent. Subjective decisions about the boundary between sand-dominated and mud-dominated rock types could modify the fault seal predictions

- The smear geometries and the resulting fault seal predictions may be influenced by diagenesis and clay mineralogy which are not explicitly accounted for in the algorithms.
- Fault seal predictions are rarely validated using column height or capillary threshold pressure data for the basin that contains the fault(s) of interest. Uncertainties remain about the local applicability of seal predictions using global input parameters or calibrations.

These uncertainties highlight the fact that although fault-seal predictions are widely utilized throughout the petroleum and CO₂ storage industries, the results can be accounted for by multiple interpretations. Increasingly, unpublished data from the petroleum industry has raised doubts over whether faults are capable of sealing on geological timescales (e.g. Vrolijk *et al.*, 2012; Hermanrud *et al.*, 2014). By contrast, a growing body of evidence from the petroleum industry demonstrates that fault seal can be effective on production timescales (see Manzocchi *et al.*, 2010 and references therein). Experiences from the petroleum industry (e.g. Van Hulst, 2010) and CO₂ storage (e.g. Snøhvit, IEAGHG, 2015b) point to the key role faults can play in reservoir compartmentalisation. Further work is required to understand better the processes and quantify the heterogeneity of low permeability fault rock, to test the effectiveness of current fault-seal methods and to improve the predictive power of fault seal analysis. Access to more fault-seal calibration datasets will facilitate future advances in understanding. Presently the largest fault-seal calibration datasets are held by large petroleum companies; however, these are neither published nor publically available.

5.0 GEOMECHANICAL MODELING AND FAULT LEAKAGE

Geomechanical modelling methods permit the probability of fault permeability to be estimated (for further details see IEAGHG, 2015a). These methods are used in the petroleum, CO₂ industries and geothermal industries where constraints on the along-fault fluid flow are required. The contribution of tectonic and local stresses to the development of structural permeability within reservoir rocks is recognised as a critical component of fault seal and cap-rock integrity in migration studies in the petroleum industry (Zoback, 2010 and references therein), fluid flow studies in the geothermal industry (Barton *et al.*, 2013; Khair *et al.*, 2015), and in investigating the longevity and integrity of CO₂ storage in sedimentary reservoirs (Rutqvist, 2012; Vilarrasa *et al.*, 2013). The interactions between stress cycling, deformation, and fluids and gas flow have also been widely studied in the context of earthquakes (e.g. Byerlee, 1993; Muir-Wood and King, 1993; Sibson, 1994), at the crustal scale (e.g. Townend and Zoback, 2000) and recently in the context of petroleum and geothermal development (Deichmann and Giardini, 2009; Evans *et al.*, 2012; Ellsworth, 2013; Holland, 2013). Validation of geomechanical theory and models has occurred predominantly in hard rock environments (e.g. granites) and, as yet, there is little evidence to support the applicability of this model to rocks that have a tendency to deform ductilely (e.g. shale) under reservoir conditions (e.g. Kohli and Zoback, 2013; Zhang, 2013; William Carey *et al.*, 2015).

Faults and fractures in the brittle crust play an important role in the subsurface movement of fluids such as hydrocarbons and geothermal waters (Brace, 1980; Wiprut and Zoback, 2000; 2002; Davatzes and Hickman, 2010; Dezayes *et al.*, 2010). These structures can both enhance fluid flow within the fault zones and restrict fluid flow across fault zones (see Section 2). How a fault impacts fluid flow depends on a range of factors including; rock types enclosing the fault, fault dimensions, amount of displacement on the fault, and the magnitudes and orientations of the principal stresses acting on the fault surface. During individual slip events (i.e. earthquakes) fractures and faults within fault zones and surrounding fractured strata are thought to dilate, increasing their permeability. The magnitude and orientation of the stress field, and type of fault failure or fracture propagation may influence the spatial distribution and magnitude of this transient structural permeability.

The link between structure, stress, and permeability has resulted in the development of geomechanical modelling with the aim to understand better and explain fluid flow observations in complex structural and stress regimes, and to predict stresses acting on rocks away from points of measurement (Rutqvist and Stephansson, 2003; Hunt and Boulton, 2005). Geomechanical modelling methods are applied to predict the probability that structural permeability can, or has, developed and whether it can be maintained within the contemporary stress field. Geomechanical modelling methods used to predict up-dip fault permeabilities are of three main types based on the geological processes that increase permeability:

1. Slip Tendency/Critically Stressed — Structures that are at or close to failure/reactivation within the current stress field are most likely to be permeable due to their propensity to continually fail, maintaining asperities which operate as fluid flow pathways.
2. Fracture Stability — The critical pore pressure perturbation required to induce failure of a structure in shear, extensional shear, or extension controls the ability of said structure to act as a fluid conduit.
3. Dilation Tendency — Structures dilate under certain orientations within a given stress regime leading to enhanced up-dip permeability.

The analysis of CO₂ injection into deep geological formations requires sophisticated numerical models capable of modelling non-isothermal multiphase flow, the migration of supercritical CO₂ and brine coupled with geomechanical processes (Rutqvist, 2012). Recently, some of these numerical simulations have been used to assess long-term geochemical and geomechanical changes in reservoir and caprock when exposed to CO₂. Rutqvist (2012 and references therein) detail a number of numerical simulations that have been applied to the study of geomechanical aspects of geologic carbon storage, as well as simulations in which multiphase flow codes have been linked with geomechanical codes. Some coupled fluid flow and geomechanical simulators have also included geochemistry of various levels of sophistication (e.g. from nonreactive to fully reactive solute transport). These coupled fluid-geomechanical models require a large number of input parameters that are often not readily available, such as parameters for rock-fluid interactions or fault properties. Therefore an understanding of the interaction of model parameters and their uncertainties is required when interpreting results.

5.1 CRITICALLY STRESSED FAULTS

Critically stressed structures are faults and fractures that are optimally orientated for reactivation (more likely to experience slip) in a given stress field (Wiprut and Zoback, 2002). Ferrill *et al.* (1999) define slip tendency as the ratio of shear stress (T) to effective normal stress (σ_n) acting on a cohesionless structure, such that higher shear stresses, or lower effective normal stresses, acting on a structural plane increase the slip tendency. When this ratio equals zero the structure has a low slip tendency and when it equals one the structure has a high slip tendency. It is generally assumed that when the ratio of shear stress to normal stress on a structural plane is ≥ 0.6 that slip will occur based on Byerlee's friction law (Byerlee, 1978).

Such critically stressed structures, or even those critically stressed structures which have recently slipped (e.g. Evans *et al.*, 2005), are theorised and observed to be permeable as movement along their planes will have opened fractures (Zhang and Sanderson, 1996a) that have yet to become resealed. The time scales over which a structure will maintain this slip-generated permeability are thought to depend on the geological environment (geothermal, groundwater or gas reservoir), properties of the fluid travelling through the structure (temperature, pressure, single or multi-phase, chemistry, mineralisation and pH), and properties of the structure itself (aperture, surface roughness, wall-rock/mineralogy, etc.).

Evidence for links between critically stressed structures and permeability comes from a number of studies. Using temperature logs and borehole images from wells in Cajon Pass, Long Valley and Yucca Mountain to test the relationship between critically stressed structures within the present-day stress field and structures associated with fluid flow, Barton *et al.* (1995) determined that structures in crystalline rock optimally oriented for shear failure exhibited higher permeability. Precise temperature measurements were used to detect localised thermal anomalies, indicating fluid flow in or out of the borehole, and borehole images were used to determine which fractures and faults, if any, were associated with these thermal anomalies. Structures deemed hydraulically conductive, when represented on a 3-D Mohr diagram, dominantly (70–80%) displayed normal to shear stress ratios ≥ 0.6 (critically stressed). Most non-flowing fractures have normal to shear stress ratios ≤ 0.6 , and so are not critically stressed. The orientations of the flowing fractures were distinct within the total fracture population and different to the orientations of the non-flowing fractures. Direct flow tests and Stoneley and refracted wave amplitudes in a well at Cajon Pass were able to identify a number of main fractures that contributed more than 80% of the fluid flow in the well. These fractures plotted over or near the normal to shear stress ratio = 0.6 line providing direct evidence for flow associated with fractures optimally oriented to the stress field for frictional failure.

Similar studies involving correlation of critically stressed fractures to zones of flow in wells have been carried out in Dixie Valley (Barton *et al.*, 1998), Desert Peak (Davatzes and Hickman, 2009), Coso Geothermal Field (Davatzes and Hickman, 2010), Soultz Enhanced Geothermal Field (Evans, 2005), the Hellisheidi Geothermal Field (Batir, 2011), the Wairakei Geothermal Field (McLean and McNamara, 2011), and the Rotokawa Geothermal Field (McNamara *et al.*, 2015). At Desert Peak and Dixie Valley spinner flow meter logs were utilised in conjunction with temperature logs and borehole image logs to identify that critically stressed fractures correlated to fluid flow indicators (Barton *et al.*, 1998; Davatzes and Hickman, 2009). Interestingly, in the Coso and Soultz Geothermal Fields, indications of fluid flow did not correlate with critically stressed structures, or structures associated with stress field perturbations which indicated recent structural slip activity. This was attributed to the inability to distinguish uniquely flowing fractures from impermeable ones, as the high ratio of shear stress to effective normal stress was similar for both. In the Wairakei Geothermal Field a correlation was found between fluid flow zones and the occurrence of wide aperture fractures oriented preferably to the S_{Hmax} direction (McLean and McNamara, 2011), while at the Rotokawa Geothermal Field the fractures associated with fluid flow had the same or similar properties (orientation, density, aperture) as fractures not associated with fluid flow (McNamara *et al.*, 2015). When the approximate stress field for the Rotokawa Geothermal Field (Davidson *et al.*, 2012) was applied to the fracture population (Davidson, 2013) no correlation was found between fluid flow zones and the locations of the critically stressed fractures, though this may reflect the limited data available to fully characterise the *in situ* stress field. While optimal structure orientation within a stress field is an important consideration when considering open flow pathways in the subsurface it is useful to bear in mind that this may not always be the case (Laubach *et al.*, 2004; Sathar *et al.*, 2012; Cuss *et al.*, 2015), and that other processes, such as chemical alteration can play a significant role in the evolution and maintenance of a subsurface structurally controlled flow path.

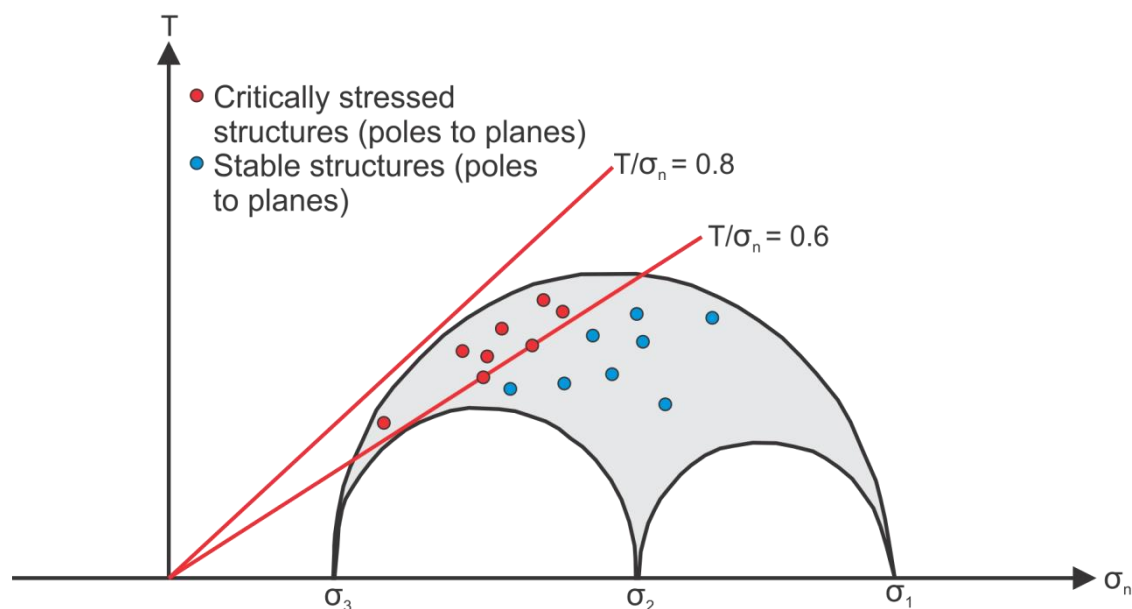


Figure 5.1 Mohr diagram of critical stress criteria. Mohr diagram showing the conditions under which a structure can be considered critically stressed within a given stress field.

5.2 FRACTURE STABILITY

Wiprut and Zoback (2002) further developed the critically stressed fault model by including pore pressure (Pp) in geomechanical modelling. They defined the risk of reactivation based upon the increase in pore pressure needed to induce failure on individual structures. It was

postulated that increases in a fluid column height or high fluid pressures within a reservoir could eventually induce slip on any structures within close proximity of these pore pressure variations. This pore pressure induced slip is then inferred to increase the permeability within that structural plane, leading to events such as leakage from reservoir traps, and increased fluid flow through a reservoir to a well.

Fracture stability developed when the cemented fault rock strength data was included in rock failure envelopes, advancing the understanding of pore pressure perturbations needed to induce slip on a structure (Mildren *et al.*, 2005). Prior to this, structural reactivation models utilised a failure envelope based on cohesionless frictional law (Byerlee, 1978). This theory does not capture the mechanical properties of structures where mineralisation may result in fault planes gaining significant cohesive strength. Cohesive strength (C) for fault rock can be included during calculations of reactivation risk using a composite Griffith-Coulomb failure envelope (Sibson, 1996) which allows prediction of shear, tensile, and hybrid tensile failure behaviour (Mildren *et al.*, 2005). Whether failure occurs as shear, extensional shear, or extension depends on the deviatoric stress ($\sigma_1 - \sigma_3$), orientation of the structure relative to the stress field, and the fault rocks tensile strength, cohesive strength, and coefficient of internal friction (Figure 5.2). The lower the structures stability the smaller the increase in P_p needed to induce failure on that structure (Mildren *et al.*, 2005).

In a study of the Kupe area in the Taranaki Basin, New Zealand, it was found that applying a fracture stability model (assuming hydrostatic pressures), meant that very little increases in pore pressure were required to induce failure in the faults in this basin (Hemmings-Sykes, 2012). When spatially correlating the occurrence of gas chimneys on these faults and fracture stability it was found that there was no distinguishable difference in the stability compared to fault areas not associated with gas chimneys. These results show that care must be taken when applying the results of geomechanical modelling of structures, and that testing against data on actual fluid flow is required.

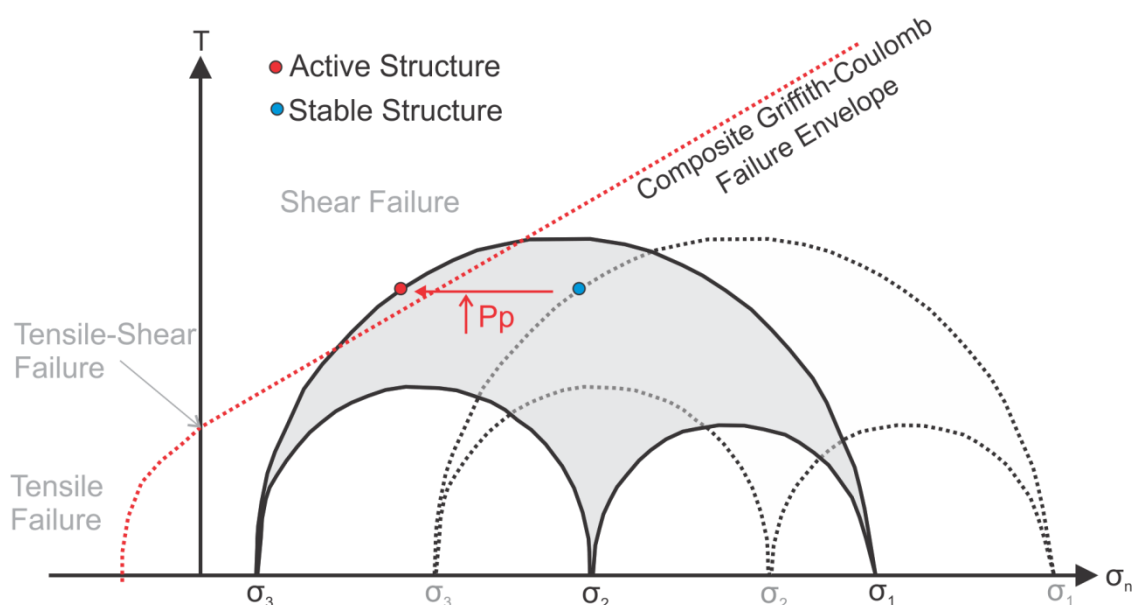


Figure 5.2 Mohr diagram showing influence of pore pressure increase. Mohr diagram showing the potential effect increasing pore pressure (P_p) has on a structures shear to normal stress ratio and where it falls relative to the composite Griffith-Coulomb Failure Envelope

5.3 DILATION TENDENCY

Dilation tendency is a measure of the extent to which structures under certain stress conditions will open through dilation or tension. This is important as dilating structures can be inferred to be open, thus locally enhancing fluid flow in the subsurface. Fracture dilation in fault zones is well established in field-based studies which demonstrate that zones of dilating structure are typically the locations of mineral deposition or enhanced fluid flow (e.g. Sibson, 1989; Nguyen *et al.*, 1998; Branquet *et al.*, 1999; Ferrill and Morris, 2003). Numerical modelling has also been able to show that dilation can be inferred to be associated with enhanced fluid flow (Matthai and Fischer, 1996; Zhang and Sanderson, 1996b; a; Zhang *et al.*, 2008). Correlation of areas of inferred enhanced fluid flow and high dilation tendency on a structure is not always positive. Hemmings-Sykes (2012) found that fault regions of high dilation tendency do not always spatially match with gas chimneys (Figure 5.3).

Dilation tendency is calculated for a structures orientation within a given stress field and is represented as a dimensionless parameter representing the probability that structure is dilated (Ferrill *et al.*, 1999). Dilation tendency is related to a structures aperture and thus is a direct function of σ_n acting on a fractures surface. By resolving the principle stresses and pore pressure on a structures surface a calculation incorporating σ_n can be obtained to determine the dilation tendency (T_d),

$$T_d = (\sigma_1 - \sigma_n) / (\sigma_1 - \sigma_3)$$

where σ_1 is the maximum principle stress magnitude, σ_n is the normal stress, and σ_3 is the minimum principle stress magnitude. The tendency of a structure to dilate increases as the σ_n acting on it decreases. The closer σ_n is to σ_1 the lower the tendency for that structure to dilate.

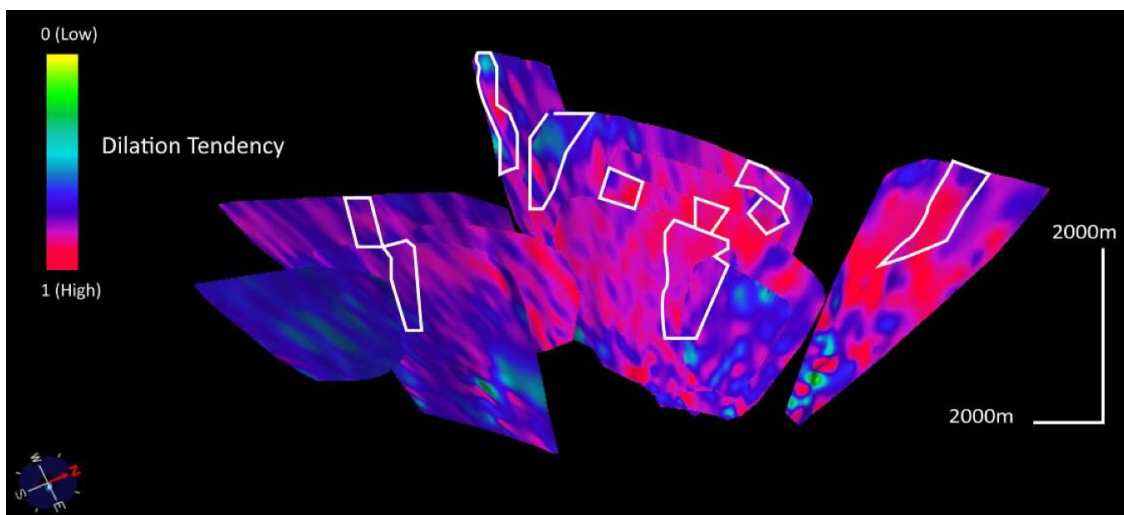


Figure 5.3 Dilation tendency mapped on fault surfaces in the Kupe Field (New Zealand), with gas chimney locations outlined in white (from Hemmings-Sykes, 2012).

5.4 MODEL INPUT DATA AND UNCERTAINTIES

Geomechanical models require a significant body of input data. The key input parameters and the techniques most often employed to quantify these parameters are outlined in Table 5.1. The parameters can be divided into three main types: i) *in situ* stresses, ii) rock physical properties and, iii) structural characterisation. *In situ* stresses include the orientations and magnitudes of the three principal axes, the strength of the host rock and frictional coefficient of fault rock, and fault geometries (including locations and dimensions).

Table 5.1 Summary of parameters and sources of data that are required for geomechanical modelling.

	Parameter	Data
<i>In situ</i> Stress	<i>In-situ</i> stress orientations	Borehole image log analyses, earthquake focal mechanisms, tectonic setting knowledge
	Vertical Stress magnitude (S_v) – determined from.	Density and/or sonic wireline logs
	Horizontal Minimum Stress magnitude (S_{hmin})	Minifrac tests and extended leak-off tests
	Horizontal Maximum Stress magnitude (S_{hmax})	Constraint based models using data on borehole breakouts and drilling induced tensile fractures obtained from borehole image logs.
	Pore pressure (P_p)	Seismic data – elastic wave velocities in a seismic velocity to pore pressure transform. Sonic logs – sonic velocity and empirically data used for vertical effective stress subtracted from total vertical stress for pore pressure. Sonic and resistivity logs – Eaton’s method for effective vertical stress with ratio of sonic log velocities and resistivity values. Repeat Formation Testers (RFT) – wireline tool measures pore pressure along borehole. Modular Formation Dynamics Tester (MDT) – wireline tool measures pore pressure in borehole. Drill Stem Test Data (DST) – drill stem tool measures pore pressure in borehole.
Rock Physical Properties	Lithology effective rock strength or unconfined strength test (UCS).	Laboratory tests & geophysical logs including P-wave velocity (V_p), Young’s Modulus (derived from V_p), and porosity or density logs.
	The strength and friction coefficient of a structure.	Fault strength (τ) = friction coefficient (μ) x ($\sigma_n - P_p$)
Structural characterisation	Fault orientations and locations	Outcrop mapping, seismic surveys, tectonic setting knowledge, borehole image logs and core.

Most geomechanical models impose a homogenous stress field orientation across a fault system. As many studies have shown stress field orientation can be spatially heterogeneous (both vertically with depth or horizontally across an area) (Blake, 2013; McNamara *et al.*, 2015), introducing the possibility of different structures and/or different parts of the same structure experiencing variable stress conditions, which have the potential to locally modify fault-parallel fluid-flow rates. Spatial variations in the magnitudes and orientations of the stress field should be considered when carrying out a geomechanical model study. However, these variations (if present) are rarely documented and this lack of detail has the potential to introduce

unquantifiable uncertainties on the results. When exact stress magnitude values cannot be determined, stress polygons can be constructed with what data are available, based on the frictional strength of faults (Figure 5.4). These diagrams can provide bounds for potential stress magnitudes for a given fault.

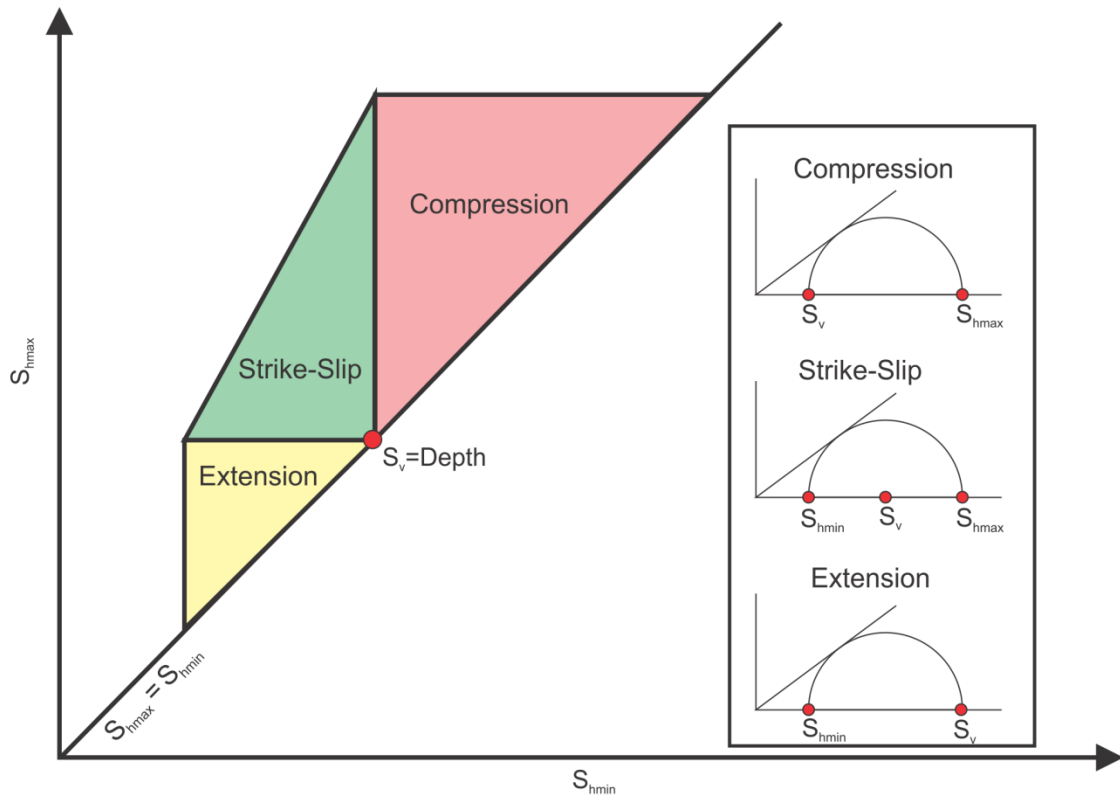


Figure 5.4 Schematic of a stress polygon. Inset shows 2D Mohr diagram representations of the three end member Andersonian stress regimes.

Geomechanical modelling may have particular relevance for CO₂ storage where injection of CO₂ has the potential to produce reservoir overpressure (excess P_p over the hydrostatic pressure). These overpressures are an important consideration in fault stability tests, as they can significantly decrease the amount of stress required on fault surfaces to induce slip.

Structures can slip/dilate and potentially flow under various stress regimes based on the strengths of the fault/fracture and rock/fill. These strength properties are often treated as homogenous within stratigraphic units which could lead to incorrect assessments of a structures stability or slip/dilatant tendency. The friction coefficient of faults generally varies between 0.6 and 0.85 though values as low as 0.2 have been found for clay materials, which should be borne in mind when considering fault gouge strength. Additionally the presence of water in cap rocks has been noted to lower the friction coefficient, the presence of carbonic acid on carbonate reservoir rocks reduces its frictional and tensile strength, and increasing temperatures can lower the fault gouge frictional coefficient (IEAGHG, 2015a). As much information on the variability of a lithology's or fault rock's UCS, friction coefficient, density, porosity, and permeability should be acquired to accurately capture the effect their heterogeneity has on the ability of a fracture to dilate or slip.

Numerous studies of borehole data support the use of the techniques for predicting which fractures will flow (e.g., Barton *et al.*, 1995), however, few publications provide independent evidence in support of the predictions at reservoir or regional scales. In addition, a number of publications suggest that non-optimally oriented fractures/faults have unpredicted high permeabilities (e.g.; Laubach *et al.*, 2004; Hemmings-Sykes, 2012; Sathar *et al.*, 2012;

Seebeck *et al.*, 2014; Cuss *et al.*, 2015). For example, based on high-quality fracture and stress data sets, Laubach *et al.* (2004) demonstrate that contrary to geomechanical theory, opening-mode fractures misaligned with respect to modern-day maximum horizontal compressive stress (SH_{max}) can remain open. In the Laubach *et al.* (2004) study, divergence between SH_{max} and open fractures that are hydraulically conductive, range from a few degrees to 90° , raising the possibility that open hydraulically conductive fractures can have any strike relative to SH_{max} and that mineralisation can cause resistance to fracture closure. Open fractures governing fluid flow are documented in extensive core collections that include horizontal well data and associated production data. These results document a fundamental discrepancy between observation and the expectation that open fractures are necessarily oriented parallel or nearly parallel to modern-day maximum horizontal compressive stress (Laubach *et al.*, 2004). Therefore, further research is required to understand better the conditions in which geomechanical predictions of fluid flow along faults is likely to be of value.

5.5 CASE STUDY: KRECHBA GAS FIELD, IN SALAH, ALGERIA

One of the most important sites for understanding the geomechanics associated with CO_2 injection is the In Salah CO_2 storage project (a joint venture between Statoil, BP, and Sonatrach) (IEAGHG, 2013c; Rinaldi and Rutqvist, 2013). Over a period of ~8 years at the Krechba gas field (In Salah, Algeria) 0.5 to 1.0 million tons of CO_2 per year have been injected into a 20 m thick water-filled Carboniferous sandstone with a relatively low permeability (<20 mD), through horizontal wells (about 1–1.5 km long at a 2 km depth). The CO_2 is co-produced with hydrocarbons, then separated and re-injected through three wells (KB-501, KB- 502, and KB-503) into the saline formation, in the water leg of the Krechba gas field.

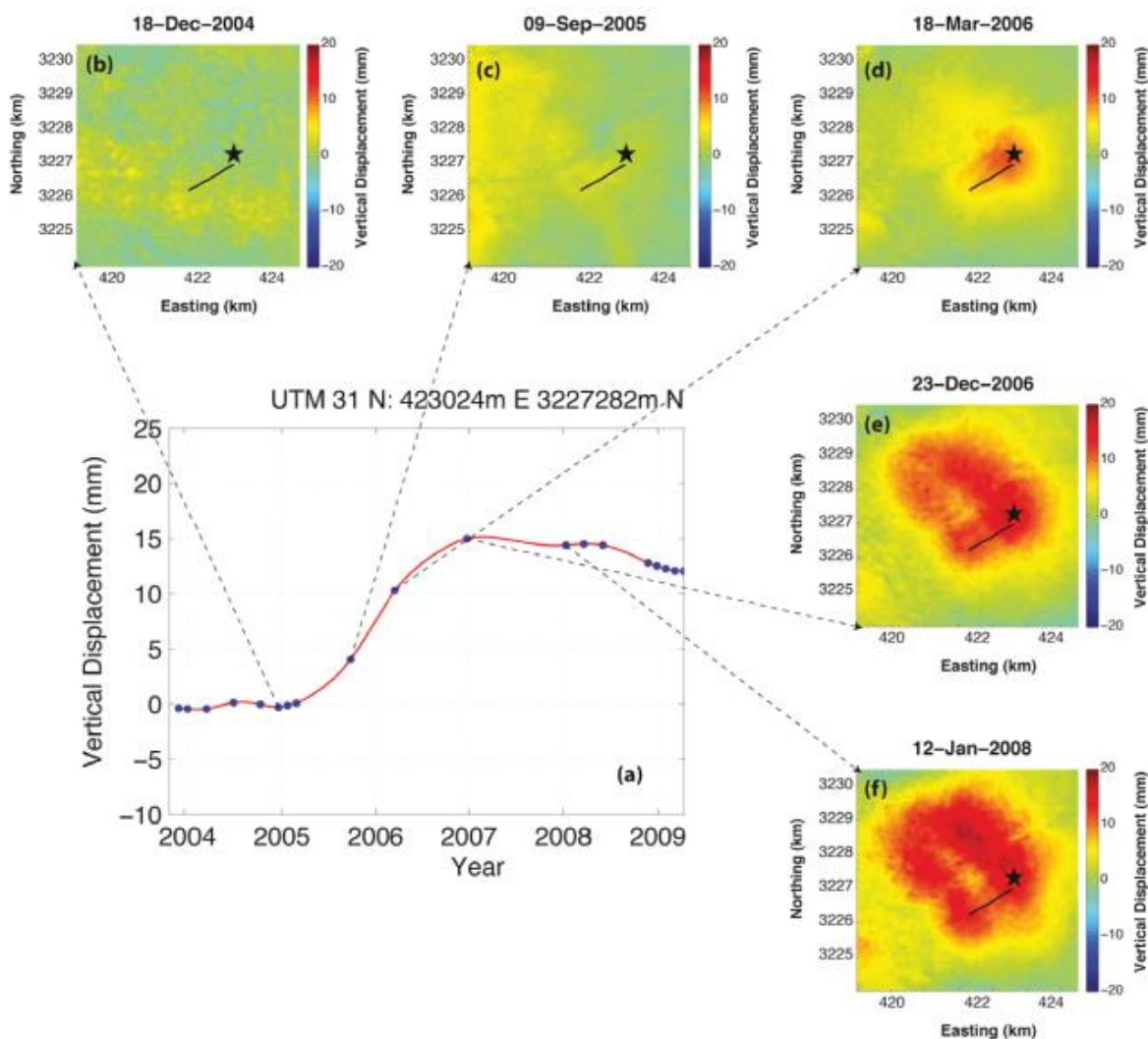


Figure 5.5 Transient evolution of vertical ground displacement at KB-502 well (from Rinaldi and Rutqvist, 2013) (a). The black star indicates the point for the transient evolution results in (b-f). First sighting of the double lobe uplift after about 8 months of CO₂ injection (January/February 2006) (d). Injection started in April 2005, and lasted for about 2 years. The shut in occurred in mid-2007. InSAR data evaluated by MDA (MacDonald, Dettwiler and Associates Ltd.) Canada and Pinnacle Technology.

CO₂ injection at KB-502 began in April 2005 (Figures 5.5 and 5.6). During the first 6 months of injection InSAR data illustrated a transient evolution of ground displacement indicating uplift of <5 mm (April–September 2005, Figure 5.5a). The injection pressure increased sharply around September 2005 with ground uplift reaching a value of 10 mm with a fracture zone possibly reactivating in January/February 2006, along with a first sighting of a double-lobe uplift pattern (Figure 5.5d). With continued injection, the ground uplift kept increasing and after 2 years of injection reached a displacement of around 15 mm (Figure 5.5e). The KB-502 well was shut in mid-2007 after almost 3 years of injection, but ~20 mm of ground uplift remained 1 year after the shut in (Figure 5.5a and f). Then a small subsidence phase occurred, but at a rate much lower than the uplift phase (Rinaldi and Rutqvist, 2013).

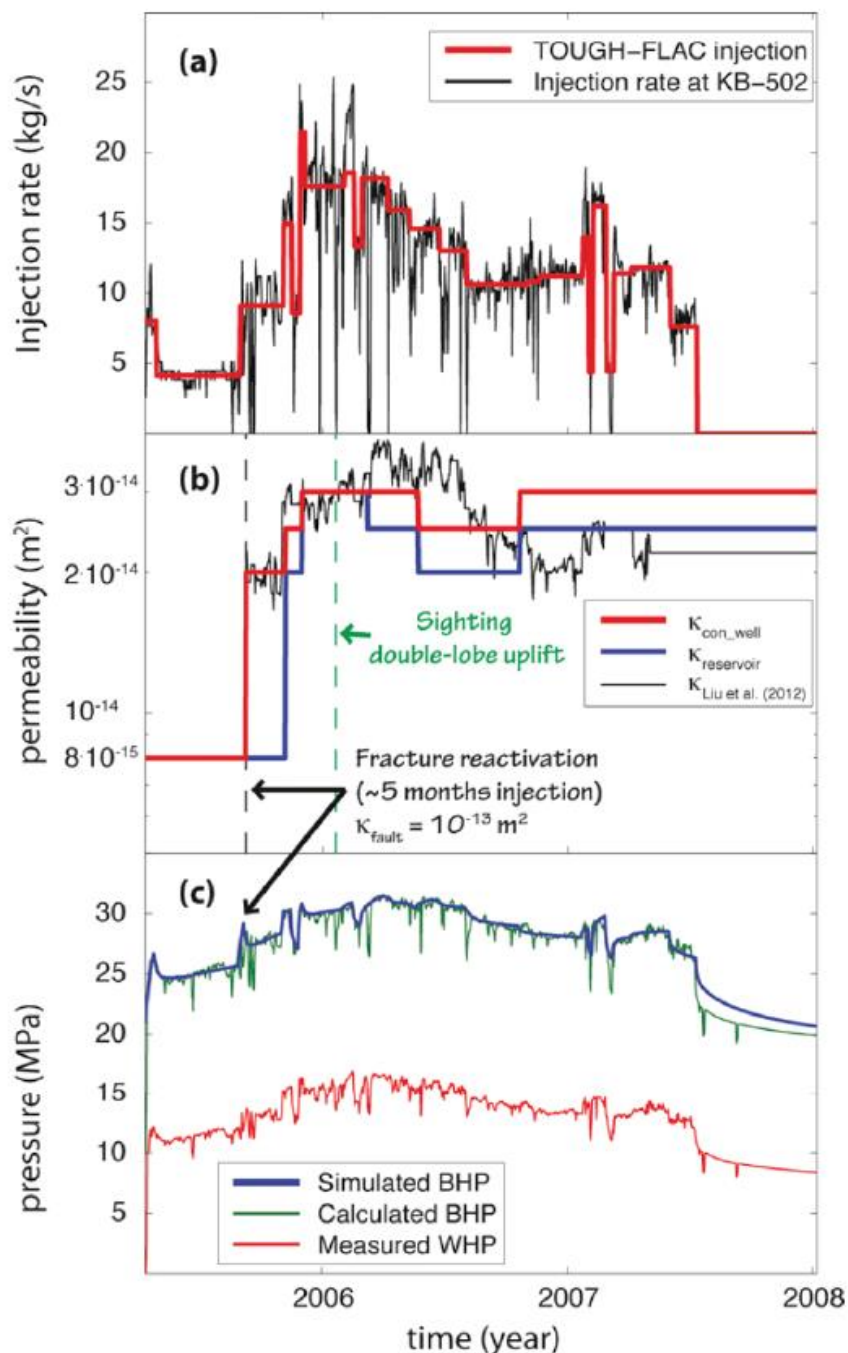


Figure 5.6 Geomechanical model results from In Salah CO₂ storage demonstration project (from Rinaldi and Rutqvist, 2013) (a) Simulated injection rate with TOUGH-FLAC (red line) and measured CO₂ injection rate at KB-502 (black line); (b) assumed changes in permeability at CO₂ injection zone level for the entire reservoir (blue line) and for the zone connected to the injection well (red line). The biggest change (2.5 times initial value) occurs when the fracture zone activates, after 5 months of injection; (c) Measured wellhead pressure (WHP, red line), calculated bottomhole pressure (BHP, green line), and simulated BHP pressure with TOUGH-FLAC (blue line) (Rinaldi and Rutqvist, 2013).

Several studies at Krechba suggest reactivation of a fracture zone due to elevated pore fluid pressure. When the estimated bottom-hole pressure exceeded 28.6 MPa an abrupt increase in the injectivity indicated the tensile opening of a pre-existing fault/fracture (Bissell et al., 2011; Shi et al., 2012). The analysis of Shi et al. (2012) indicated that the fault/fracture zone reactivated when the injection pressure peaked (at the beginning of 2006), and (using changes in the fracture transmissibility) obtained a precise match between simulated and calculated bottom hole pressure at KB-502 (Rinaldi and Rutqvist, 2013).

Rinaldi and Rutqvist (2013) developed a numerical model of the KB-502 region with the coupled geomechanical and fluid flow simulator TOUGH-FLAC. Assuming a time-dependent reservoir permeability and fracture zone, Rinaldi and Rutqvist (2013) fitted the pressure changes within the injection zone (Figure 5.6). They show such changes in permeability can be explained as the opening and/or extension of existing fractures within the injection zone, and fracturing, or fracture-zone reactivation, which increases the average permeability as a function of the injection pressure. These models simulated activation of the fracture zone by substantially increasing its permeability, enabling the fluid to propagate along the fracture zone (Rinaldi and Rutqvist, 2013).

The fracture-zone properties in the models of Rinaldi and Rutqvist (2013) were determined by model calibration with field data. The fracture zone dimensions, a fracture zone 3500 m long and extending 350 m above the reservoir, were consistent with current interpretations of a 2009 3D seismic survey. The permeability of the fracture zone is a key element, and its field initial value is unknown. Rinaldi and Rutqvist (2013) considered a spatially uniform permeability of 10^{-13}m^2 , i.e., a high value in agreement with the permeability of a highly fractured zone. The fracture zone (80 m-wide in total) was modelled as a series of three 20 m-wide zones with orthotropic mechanical properties, separated from each other by a 10 m-wide intact caprock. The total volume of this fracture zone is small when compared to the total volume of the reservoir, hence the use of a higher (or lower) permeability within the fracture zone has a low impact on the average permeability of the reservoir and produces negligible changes on the simulated displacement as long as the match with the field pressure was kept. The assumption of a spatially uniform permeability produces a trade-off between fracture-zone geometry and flow properties (Rinaldi and Rutqvist, 2013).

Overall, the analysis of Rinaldi and Rutqvist (2013) supports the notion that the fracture zone is confined to the lower caprock unit immediately above the reservoir and does not appear to penetrate the upper caprock unit or the overlying aquifer. Modelling a permeable fracture all the way through the caprock shows that CO_2 would quickly move up via buoyancy into the aquifer, whereas in the field, no anomalies have been noted from the soil gas, surface flux, shallow aquifer, or microbiology monitoring work (Mathieson *et al.*, 2011; Rinaldi and Rutqvist, 2013). Instead modelling matches all available field observations reasonably well for a fracture zone of limited height, including all time evolutions and the shape of surface deformation, time-evolution of injection pressure, and the 3D seismic indications of the CO_2 saturated fracture zone extending thousands of meters laterally (but only a few hundred meters vertically). The conclusion from Krechba is that overpressures induced by CO_2 injection can elevate fracture permeabilities which can be effectively modelled using geomechanical flow simulators.

6.0 NATURAL CO₂ SEEPS ALONG FAULTS

Natural CO₂ seeps provide an indication of the volumes and rates of CO₂ emission that are possible at the ground surface. Reviews of natural CO₂ seeps have been undertaken by many researchers as they provide analogues for leakage from CO₂ storage sites (e.g. IEAGHG, 2005; NASCENT, 2005; Lewicki *et al.*, 2007; Kirk, 2011). This report draws on these reviews and on site-specific publications to inform discussion of the key spatial relationships between faults and CO₂ seeps. Many of the analogues are interpreted to form in association with migration along faults. They provide information about how migration occurs along faults and at what rates (Section 7). The examples presented also illustrate both the benefits of CO₂ (e.g. mineralised water is used commercially or where geysers form tourist attractions - Crystal Springs), and the detrimental effects of CO₂, such as destruction of flora and fauna (ECO₂, 2015). While we draw some general conclusions from the natural analogues presented, the volumes and rates of CO₂ flow, and their environmental impact are site-specific. The rates of natural seepage are dependent on a range of factors including; subsurface geology (e.g. fault and stratal geometries and permeabilities), local topography, weather and the source of the CO₂. Such seeps can have diurnal and seasonal variations (Graziani *et al.*, 2014).

In this section we briefly present a series of case studies for natural analogues where CO₂ is seeping from the ground surface and has been documented to be related to faulting. Observations are from nine natural terrestrial CO₂ seeps, primarily from USA and Italy, and three submarine seeps (Tables 6.1 and 6.2). The smaller number of submarine seeps most likely reflects data sampling variance between terrestrial and submarine sites, rather than the greater frequency of the former. These examples provide an indication of the volumes and rates of CO₂ flow and are not intended to be an exhaustive review of natural analogues (this would require a report in its own right). It is worth noting, however, that the analogues presented are likely biased towards examples where the flow rates and volumes are high. Smaller natural analogues of CO₂ are less likely to be widely reported in the literature (and therefore to be reported here) or are too small to have the impact on fauna and flora required to draw attention to their existence. Detection limits of natural CO₂ seeps depend on a number of factors including; the methods used to measure CO₂ and dimensions of the sample array, the rates of emission, the rates of diffusion and the longevity of studies. Recognition of seeps as being fault-related requires that the faults and the seeps can be accurately located. In many cases fault traces are not clearly preserved, vents may not precisely coincide with a fault and/or CO₂ seepage may be characterised by a single vent rather than an alignment of multiple vents along a fault trace. In such circumstances the causal relationships between faults and seeps may be open to interpretation. Additional data from natural gas storage facilities may provide useful information on CO₂ migration (e.g. Chen *et al.*, 2013) and its relationships to faults or fractures. However, review of seepage at natural gas facilities has not been undertaken here as the supercritical form of CO₂ and its propensity for dissolution in formation waters are different to the properties of natural gas.

Table 6.1 Terrestrial CO₂ seeps with measured rates of CO₂ release that generally occur under normal conditions (e.g. they do not include higher rates reported during or immediately after earthquakes; e.g. Streit and Watson, 2005).

Parameter	Paradox Basin	Crystal Spring (in Paradox Basin)	Mammoth Mountain	Solfatara, Phlegraean Fields	Albani Hills, Tor Caldera	Latera Caldera	Mátraderecske	Poggio dell'Ulivo & Torre Alfina	Otway
Region	Utah	Utah	California	West of Naples	SE of Rome	Latium	Mátra mountains	Rome-Perugia	W of Melbourne
Country	USA	USA	USA	Italy	Italy	Italy	Hungary	Italy	Australia
Timing of seepage	110,000 Ka to modern; 40 Ka use of single pathway	Modern; from well intersection with fault	Modern	Modern	Modern; rapid release associated with seismic events	Modern	Modern	Modern	Modern
Surface dimensions	Springs, travertine mounds, gas seeps	Wellhead area/geyser	0.48 km ²	0.5 km ²	6000 and 55000 m ²	Diffuse soil; vents; springs; aligned along faults	—	e.g. 1.5 km ² at Poggio dell'Ulivo	Various
Fault name	Little Grand Wash; Salt Wash	Little Grand Wash	Multiple faults	Multiple faults	Two faults	Multiple	Multiple	Inferred from NW-SE trend of flux	Various
Fault length	61 & ~15 km	~15 km	—	—	—	—	—	150 m? long flux	Various
Fault throw	Up to 210 m of vertical separation	—	—	—	—	—	—	—	—
Fault type	Normal; 70-80° dips; cut seal	Normal, anastomising	Normal	Normal, caldera	Normal, caldera	Vertical, caldera	—	—	?Normal
Hanging wall lithology	Sandstone, shale?	Sandstone, shale, salt	Volcanics	Volcanics	Volcanics	Volcanics	Andesite	Flysch?	—
Foot wall lithology	Sandstone, shale?	Sandstone, shale, salt	Volcanics	Volcanics	Volcanics	Volcanics	Andesite	Flysch?	—
Permeability	Cross-fault perm << up-dip perm; fluids move up in footwall damage zone	Leakage via damage zones	—	—	—	Leakage via fractures on one side of the fault, and likely at the intersection of two faults	—	—	From surveys above faults; also from diffuse sources
Source of CO ₂	Clay-carbonate reactions; also carbonate thermal decomposition?	Clay-carbonate reactions	Magmatic	Magmatic	Magmatic and decarbonation of fractured carbonates	Meta-carbonates	Geothermal/kaarst	Geothermal/Mesozoic carbonates	Magmatic?; in sandstones, and fractured Belfast Mst
Depth of source	1500-2000 m	1000-1500 m, feeding reservoir at 300-500 m	3000 m	A few 1000 m	—	1000-1500 m	1000 m	400 m at Torre Alfina	~2000 m at Pine Lodge
Pressure at source depth	—	—	High	—	—	—	—	40 bar; releases when higher	Various
Temperature at source depth (°C)	—	?100-200; much less in reservoir	150	215 (modelled)	—	—	—	140-150	Various
Wet or dry venting?	Water-borne	Water-borne	Dry? Plus in groundwater	Wet and dry?	Dry? Plus in groundwater	—	—	Dry? Plus in groundwater	—
Impurities?	Locally, oil; S ²⁻ , Cl ⁻ etc.	96-99% CO ₂ ; also Ar, N ₂ , O ₂	He	He, Ne, Ar, N ₂ , As, Hg	N ₂ , H ₂ S, He, Rn & thermogenic CH ₄	CH ₄ , H ₂ S, N ₂ , O ₂	CH ₄ , Rn, SO ₂	Ca, NaCl, SO ₄	—
Detection method	Soils; springs	Springs	Soil, aerial gas flux	—	—	Soil; gas vents, springs	—	Springs	Soil
Rate of CO ₂ at surface (varied units)	0.0365 t/m ² /yr; in places (total unknown)	13.234 t/m ² /yr	0.19 t/m ² /yr	1.1 t/m ² /pa; average 0.41 t/m ² /yr, max 2 t/m ² /yr	0.44 t/m ² /yr; max 11.6 t/m ² /yr	39.4 t/m ² /yr	0.073-0.146 t/m ² /yr (to 0.62 t/m ² /yr)	1.76 X10 ⁻⁵ to 3.96 x 10 ⁻⁴ t/m ² /yr	<1 kg/m ² /yr, but likely rates up to 1000 t/yr after earthquakes; 3.7-7.5 x 10 ⁻³ to 1.5 x 10 ⁻² t/m ² /yr; rates from diffusion.
References	Shipton <i>et al.</i> , 2004; Shipton <i>et al.</i> , 2005; Burnside <i>et al.</i> , 2007; Lewicki <i>et al.</i> , 2007; Jung <i>et al.</i> , 2014b; Jung <i>et al.</i> , 2015	Baer and Rigby, 1978; Shipton <i>et al.</i> , 2004; Gouveia <i>et al.</i> , 2005; (Shipton <i>et al.</i> , 2005); Jung <i>et al.</i> , 2014b; Watson <i>et al.</i> , 2014	Lewicki <i>et al.</i> , 2007	Chiodini <i>et al.</i> , 2001; Lewicki <i>et al.</i> , 2007; Voltattorni <i>et al.</i> , 2009	Chiodini and Frondini, 2001; Lewicki <i>et al.</i> , 2007; Voltattorni <i>et al.</i> , 2009	Cavarretta <i>et al.</i> , 1985; Astorri <i>et al.</i> , 2002; Annunziatellis <i>et al.</i> , 2004; Pearce <i>et al.</i> , 2004; Lewicki <i>et al.</i> , 2007; Arts <i>et al.</i> , 2009; Pettinelli <i>et al.</i> , 2010; Bigi <i>et al.</i> , 2013	Pearce <i>et al.</i> , 2004; Lewicki <i>et al.</i> , 2007	Chiodini <i>et al.</i> , 1999; NASCENT, 2005; Streit and Watson, 2005	Watson <i>et al.</i> , 2004; Streit and Watson, 2005; Streit and Watson, 2007

Table 6.2 Documented marine seeps . Blank fields (dashes) indicate that no data are available.

	Panarea	Juist salt dome	Southern North Sea
Region	Tyrrhenian Sea	Southern North Sea	Southern North Sea
Country	Greece	Germany	Netherlands
Setting (water depth)	~10–20 m; up to 30 m	~30 m	<50 m
Surface dimensions	15 km ² ?	–	<2.5 km on seismic
Fault name	Several	Fractures formed during salt dome emplacement	Multiple
Fault length	–		–
Fault type	–		Normal
Seismic image	–	Yes	Yes
Hanging wall lithology	–	–	Various clastics
Foot wall lithology	–	–	Incl. salt (diapir)
Known aperture range	–	–	–
Source of CO ₂ (magmatic etc)	Volcanic/hydrothermal	Likely biogenic	Biogenic & thermogenic
Depth of source	–	–	450-800 m
Pressure at source depth	–	–	–
Temperature at source depth	–	–	–
CO ₂ concentration near seabed	–	~90±30 µmol/L; up to 318 µmol/L	–
Impurities	H ₂ S, CH ₄ , He, H, N ₂ , O ₂	–	CH ₄ , H ₂ S, C ₂ H ₆
Rate of CO ₂ pa, sea bed	Est. 25000 t/yr over 15 km ² area	–	–
Rate of fluids, sea bed	≤4.14 x 10 ⁴ m ³ /yr per vent; 1670-8500 t/m ² /yr; >>1600 t/yr CO ₂	–	Unknown
References	Italiano <i>et al.</i> , 2001; IEAGHG, 2005; Voltattorni <i>et al.</i> , 2009; Caramanna <i>et al.</i> , 2011; Kirk, 2011	ECO ₂ website; McGinnis <i>et al.</i> , 2011	Schroot and Schüttenhelm, 2003; IEAGHG, 2005

6.1 PARADOX BASIN, UTAH, USA

CO₂ flux along faults has been widely reported for the Paradox Basin (e.g. Shipton *et al.*, 2004; Burnside *et al.*, 2007; Dockrill and Shipton, 2010), and here we primarily report the recent results of Jung *et al.* (2014b, 2015), which also summarise much previous work. In order to

identify various factors that control CO₂ leakage in fault systems Jung *et al.* (2014b) investigated a natural analogue for soil CO₂ fluxes in Paradox Basin on the Colorado Plateau, East-Central Utah, USA. A total of 332 and 140 soil CO₂ flux measurements were made at 287 and 129 sites in the Little Grand Wash (LGW) and Salt Wash (SW) fault zones, respectively (Figure 6.1). Measurement sites for CO₂ flux involved conspicuous CO₂ degassing (e.g. CO₂-driven springs/geysers) and linear features (e.g. joints/fractures and areas of diffusive leakage around a fault damage zone). CO₂ flux anomalies were mostly observed along the fault traces. Specifically, CO₂ flux anomalies were focused in the northern footwall of the both LGW and SW faults (Figure 6.1d) (Jung *et al.*, 2014b). For further background information on Paradox Basin as a natural analogue for leakage of CO₂ from storage reservoirs see Lewicki *et al* (2007).

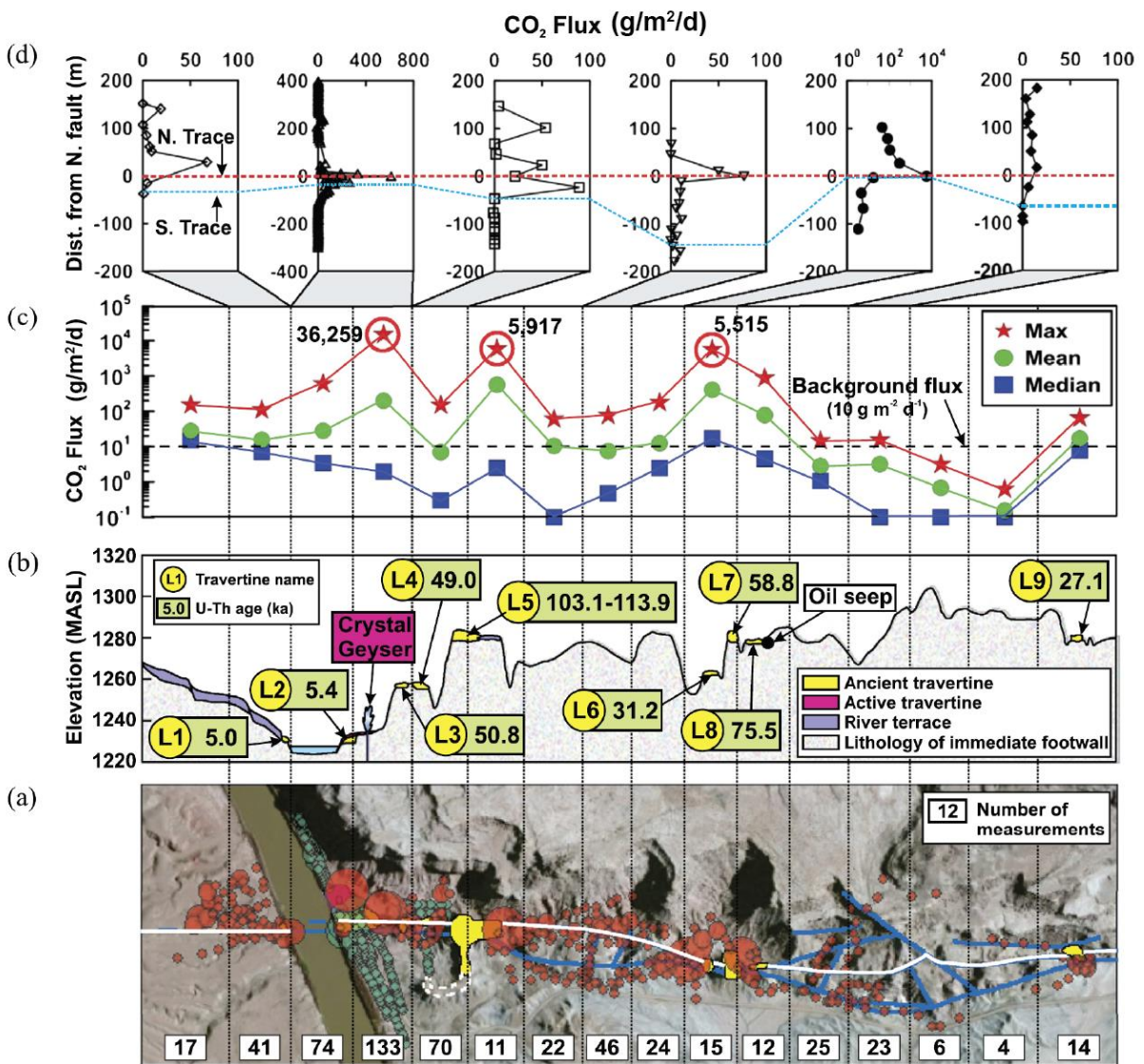


Figure 6.1 Analysis of soil gas CO₂ measurements in the LGW fault zone (from Jung *et al.*, 2014b). (a) CO₂ flux map with measurement population in each zone. (b) A topographic profile along the major north fault trace indicated by white line in (a). (c) Plots show calculated maximum, mean and median values of CO₂ fluxes in each zone. Bold numbers with red circles indicate the three most anomalous CO₂ fluxes. Dashed line represents an upper limit of background flux (<10g/m²/d). (d) CO₂ fluxes for 7 designated zones in (c) plotted against distance from the north major fault trace. Red and blue dotted lines delineate the north and south fault traces, respectively.

The east–west trending and 70–80° south dipping LGW and SW faults cut the north-plunging Green River anticline (Sipton *et al.*, 2005). The depth of faulting and permeability of the faults

are presently unknown. Nevertheless, the faults have been thought of as conduits for vertical flow of gaseous CO₂ and CO₂-rich fluids, and also as barriers for cross-fault fluid flow perhaps due to clay-rich gouges (cm to m thick) (e.g. Dockrill and Shipton, 2010).

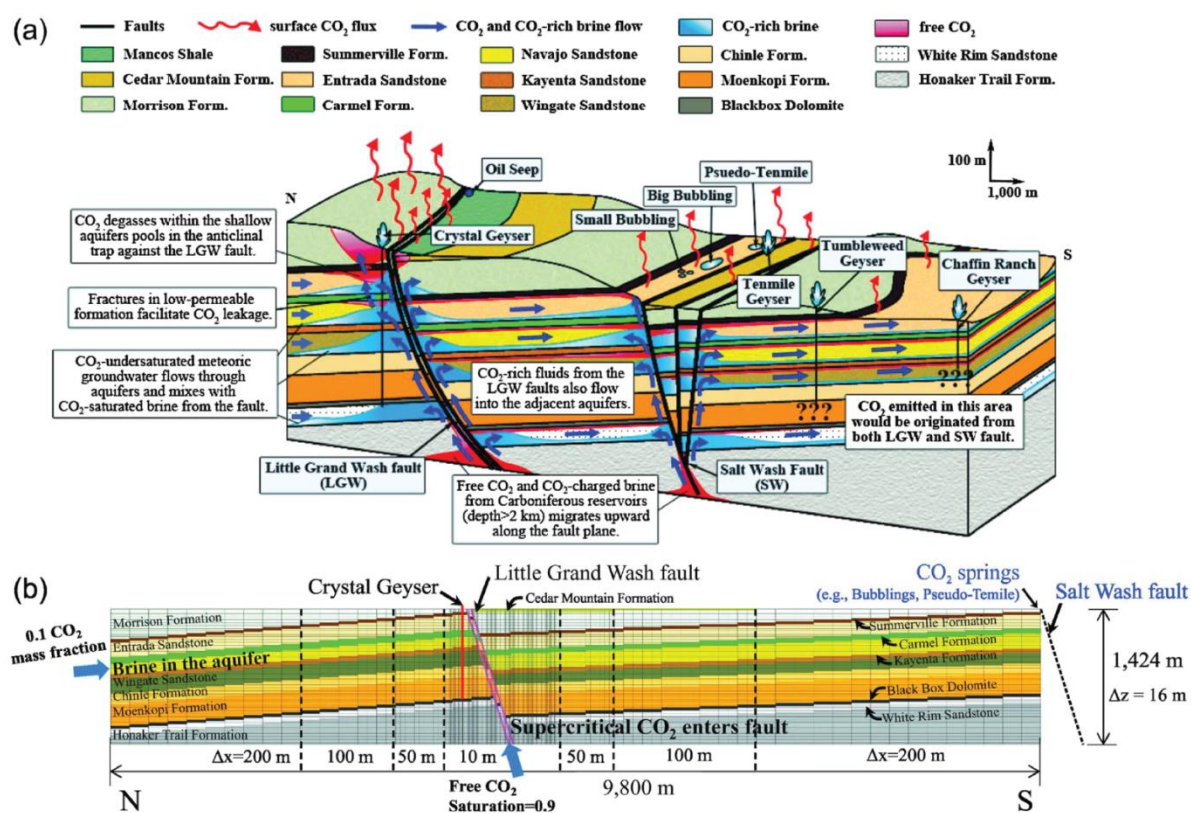


Figure 6.2 A conceptual diagram of CO₂ origins and migration within the LGW and SW fault zones (Jung *et al.*, 2014b; Jung *et al.*, 2015). Free CO₂ and CO₂-saturated brine are represented in red and blue, respectively. Meteoric groundwater recharges from the San Rafael Swell to the northwest of the area (light purple arrows) and flows through the aquifers (Entrada, Navajo, Kayenta, Wingate, and White Rim Sandstones). (b) A 2-D north-south cross-sectional flow domain in the LGW fault zone. CO₂-undersaturated brine (Navajo Sandstone) and supercritical CO₂ (the fault) were included as CO₂ sources (Jung *et al.*, 2015).

Anomalous CO₂ fluxes also appeared in active travertines adjacent to CO₂-driven cold springs and geysers (e.g. 36,259 g/m²/d at Crystal Geyser, i.e., 13.23 t/m²/yr), ancient travertines (e.g. 5,917 g/m²/d or 2.16 t/m²/yr), joint zones in sandstone (e.g. 120 g/m²/d or 0.04 t/m²/yr), and brine discharge zones (e.g. 5,515 g/m²/d or 2.01 t/m²/yr) (Jung *et al.*, 2014b). The observations of Jung *et al.* (2014) indicate that CO₂ has escaped through those pathways and that CO₂ leakage from these fault zones does not correspond to point source leakage.

CO₂ flux anomalies observed by Jung *et al.* (2014b) do not always coincide with mapped fault traces. In this case, anomalous fluxes of CO₂ ranging from 27 to 120 g/m²/d (0.001–0.044 t/m²/yr) appeared around joint zones within the bleached Entrada Sandstone exposed in the northern footwall of the SW fault zone. Extensive bleaching of the Entrada Sandstone from red to pale yellow is attributed to the reduction of hematite by reducing fluids (e.g. hydrocarbon) that migrated through fractures and joints (e.g. Dockrill and Shipton, 2010; Kampman *et al.*, 2014a). Observations of CO₂ flux anomalies therefore indicate that CO₂ is still being released through the fractures, that were pathways for ancient reducing fluids (Jung *et al.*, 2014b).

High CO₂ fluxes of 5,917 g/m²/d and 888 g/m²/d (2.16–0.32 t/m²/yr) were also observed within 30 m of large travertine deposits (69,660m³ and 10,213m³, respectively) (Jung *et al.*, 2014b). These observations indicate that the most highly-transmissive conduits conveyed the

most CO₂-rich fluids to the surface leaving larger volumes of ancient travertines, and that these conduits were not healed by mineral precipitate. Therefore, CO₂ gas still escapes through high permeability conduits even after several hundred thousand years (Burnside et al., 2013).

In areas where two strands of the LGW fault are closely spaced (e.g. <30 m) high CO₂ flux anomalies can be observed. For example, where the distances between two major fault traces are below 30 m CO₂ flux anomalies of 613 g/m²/d and 5,515 g/m²/d (0.22–2.01 t/m²/yr) were recorded (Jung *et al.*, 2014b). The negative relationship between major fault spacing and flux rates may arise because decreased fault spacing may locally promote increased densities of small-scale faults and joints which increase permeability and promote the upward transport of gaseous CO₂ to the surface.

In order to characterize CO₂ leakage along faults and wellbores, Jung *et al.* (2015) conducted numerical simulations using TOUGH2-MP/ECO2N. These numerical simulations are based on an integrated finite difference method that can demonstrate multiphase flow of a H₂O-NaCl-CO₂ system under typical reservoir conditions (T ≤ 100°C and P ≤ 60MPa) (Jung et al., 2015). A 2-D numerical model was developed corresponding approximately to local geology along a north-south cross section traversing the Crystal Geyser and the LGW fault (Figure 6.2a). The model is 1424 m high and 9800 m wide consisting of 205 (x-direction) by 89 (z-direction) grid blocks (total of 18,245 grid blocks) (Figure 6.2b). For numerical simulations, the model was discretized in space with Δz = 16 m and Δx fining from 200 m to 1 m in the vicinity of Crystal Geyser and the LGW fault (Figure 6.2b). This local mesh refinement allowed the use of a small, detailed model in the area of interest for thoroughly resolving CO₂-brine migration (Jung *et al.*, 2015). The two parallel fault traces were set to be 40 m apart at the surface and were assumed to have a constant 20 m width including the damage zone (Kampman *et al.*, 2014b); with a total vertical throw of 180 m and no geometrical complexity (Dockrill and Shipton, 2010). Due to a lack of data on regional fault permeability (*k*), various *k* values ($k_v=1\times 10^{-17}$ – 5×10^{-13} m²) were tested corresponding to a high, intermediate, and low-*k* fault. As fault hydraulic anisotropy can vary by two to three orders of magnitude when fault throw is ~200 m (Bense and Person, 2006), different fault anisotropy ratios ($v = k_v/k_h$) of 1, 10, 50, and 100 were tested in the simulations. Models with different properties of the LGW fault were evaluated by matching the computed results with field soil CO₂ flux measurements, and an approximate range of regional fault *k* were determined. From these numerical modelling results Jung et al. (2015) infer that the LGW fault has permeabilities ranging 1×10^{-17} m² ≤ $k_h < 1\times 10^{-16}$ m² and 5×10^{-16} m² ≤ $k_v < 1\times 10^{-15}$ m².

While the numerical models of Jung *et al.* (2015) were not capable of distinguishing fault rock (fault core) and fault zone permeabilities due to grid-scale limitations, the simulation results suggest that juxtaposition of aquitards and aquifers cannot account for the observed CO₂ migration without the addition of low-*k* fault rock. Such low-*k* fault rock cannot completely prevent CO₂ leakage to the surface due to the pressure build-up that accompanies the constant supply of CO₂ which eventually exceeds the critical threshold for the fluid displacement over geological time. A low-*k* fault rock also facilitates the formation of secondary CO₂ reservoirs at shallow depths above 300 m (i.e. anticlinal traps within the Navajo and Entrada Sandstones). Continuous CO₂ accumulation in shallow reservoirs could result in fluid pressures capable of opening fractures with resultant leakage. Secondary near surface CO₂ reservoirs provide a conducive environment for amplifying geyser-like eruptions with the conditions necessary to promote these eruptions as follows: (1) multiphase conditions reduce fluid mobility of each phase enabling large accumulations of CO₂, (2) consequent overpressures that cause the first release of brine along with high-rate discharge of CO₂ and brine in the later stages at the surface, and (3) sufficient heat transfer between CO₂-rich fluids and surrounding formations

that develop multiphase conditions (e.g. exsolution of aqueous CO₂ and/or boiling of liquid CO₂). The creation of secondary near-surface CO₂ reservoirs could pose a significant problem as they are generally accompanied by contamination of shallow potable groundwater resources. The possibility that a low-*k* fault rock will promote the formation of a secondary CO₂ reservoir at shallow depths, therefore, needs to be taken into account during the initial screening stage for geological storage of CO₂ (Jung *et al.*, 2015).

6.2 LATERA CALDERA, ITALY

The Latera Caldera, ~100 km northwest of Rome, provides an analogue of CO₂ migration up faults, appearing as vents, springs and soil gas. Its usefulness as an analogue for leakage from a CO₂ storage site is diminished by the high temperatures and hydrothermal geochemistry of the fluids involved, but it is included because flow rates (Table 6.1) have been recorded and their spatial relations to faults studied. The caldera is about 8 x 12 km across and includes a geothermal reservoir in metamorphosed carbonate rocks at depths of 1000 to 1500 m, with hot, migrating fluids producing a range of mineral assemblages (Cavarretta *et al.*, 1985).

Outcrop and geophysical studies support the suggestion that CO₂ is migrating upwards along faults. Geophysical (including electromagnetic techniques and ground-penetrating radar) and geochemical methods of CO₂ flux detection highlight a NNW–SSE anomaly aligned with a fault (Pettinelli *et al.* 2010). CO₂ is interpreted to migrate upwards from the geothermal reservoir along NW-SE and NE-SW trending faults and reaches the surface as springs, vents and soil emissions; soil emissions of CO₂ appear to be aligned along the mapped faults (Annunziatellis *et al.*, 2004; Pearce *et al.*, 2004). Annunziatellis *et al.* (2004) described several faults in outcrop and inferred two models of fault geometry, each with differing CO₂ flux profiles (Figure 6.3). For further background information on Latera Caldera as a natural analogue for leakage of CO₂ from storage reservoirs see Lewicki *et al.* (2007).

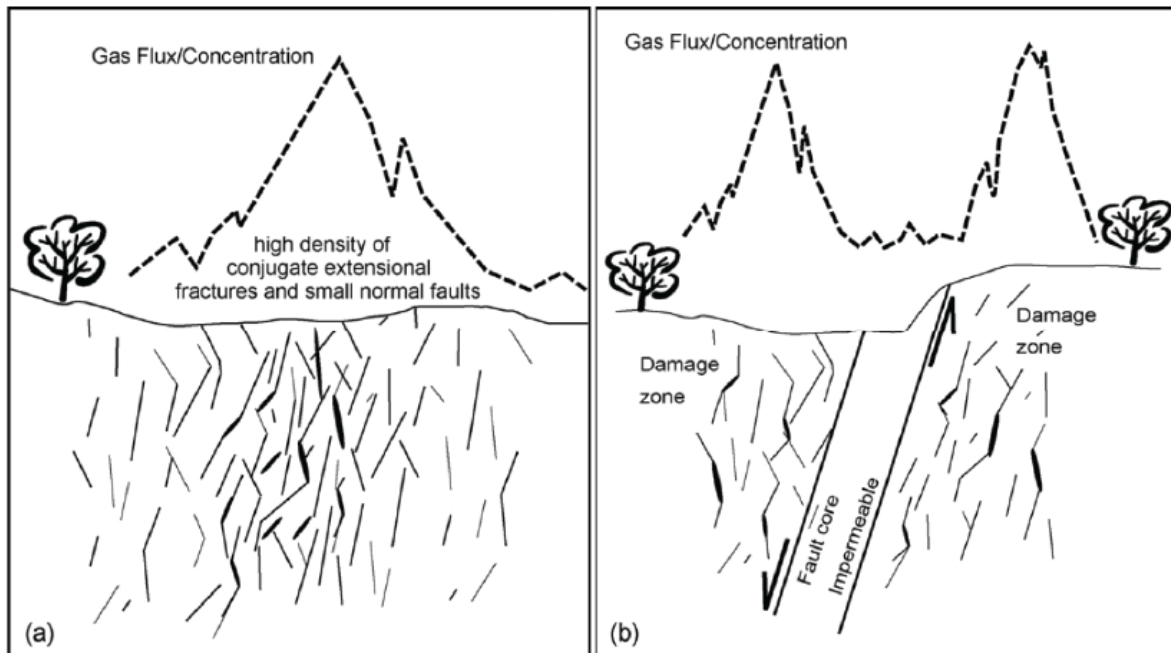


Figure 6.3 Schematic model showing different structural assemblages and their influence on CO₂ leakage from Latera Caldera (from Annunziatellis *et al.*, 2008). These two models of fault zone could represent temporal changes as the fault develops, or spatial changes along strike either due to variable displacement and/or to fault segmentation. (a) The fault network configuration results in more open interconnected gas migration pathways, resulting in higher gas flux rates. (b) The fault core/damage zone model shows the development of a very low permeability core, bounded by damage zones that maintain the high permeability fault network (Annunziatellis *et al.*, 2008).

6.3 MAMMOTH MOUNTAIN, CALIFORNIA, U.S.A.

Mammoth Mountain (California) provides an analogue for diffuse CO₂ flux above a fault at a lateral scale of hundreds of metres (Figure 6.4). The source of the gas is magmatic and the Mammoth Mountain volcano emits CO₂ from soil and steam vents, with rates possibly associated with volcanic activity (e.g. dike emplacement) and related seismicity (IEAGHG, 2005). Flux rates documented in the area, show a diffuse, NW trend that appears to be related to the Mammoth Mountain Fault (Figures 6.5 & 6.6) (Rogie *et al.*, 2001). Emissions over a six week period ranged from 218 to 3500 g/m²/d (Lewicki *et al.*, 2008; equivalent to rates of 0.08 to 1.28 t/m²/yr). For further background information on Mammoth Mountain as a natural analogue for leakage of CO₂ from storage reservoirs see Lewicki *et al.* (2007).



Figure 6.4 Vegetation loss from CO₂ emissions at Mammoth Mountain and Horseshoe Lake (after Lewicki *et al.*, 2008).

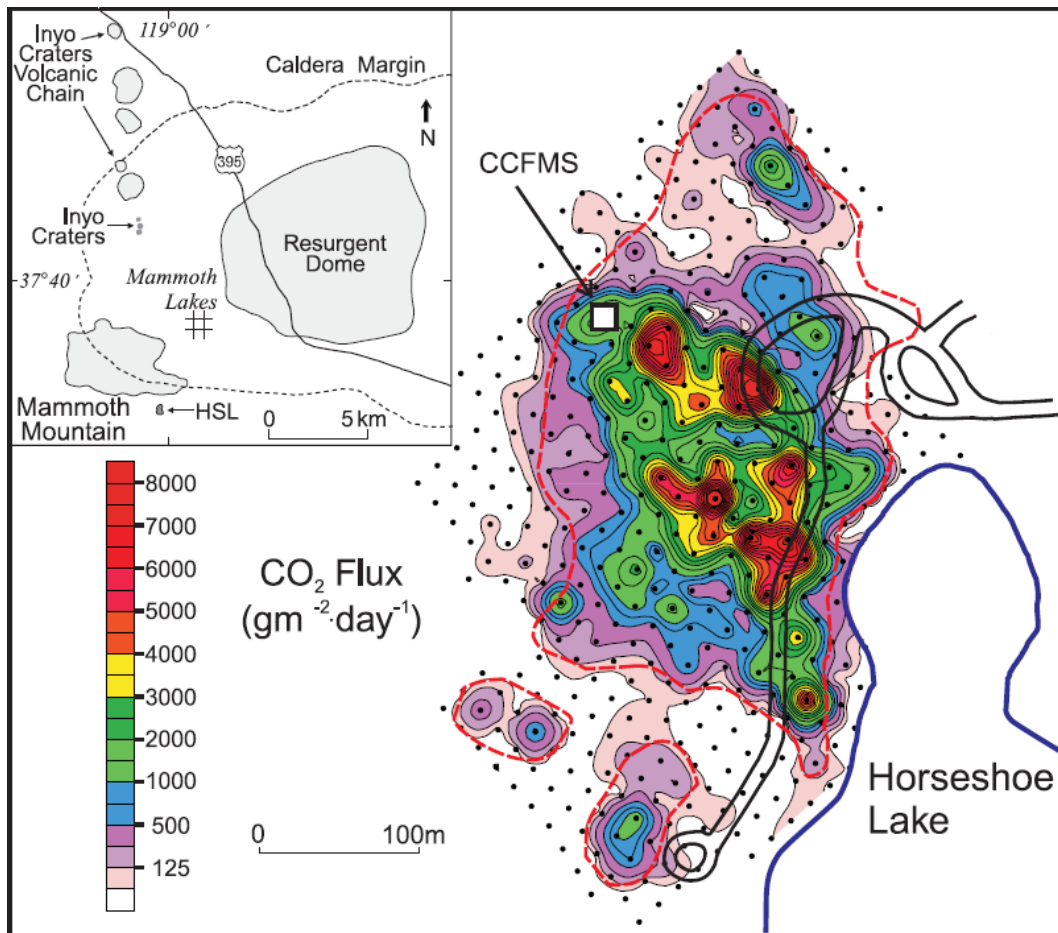


Figure 6.5 CO₂ flux in the Mammoth Mountain area (from Rogie *et al.*, 2001). Horseshoe Lake is labelled HSL in the inset diagram.

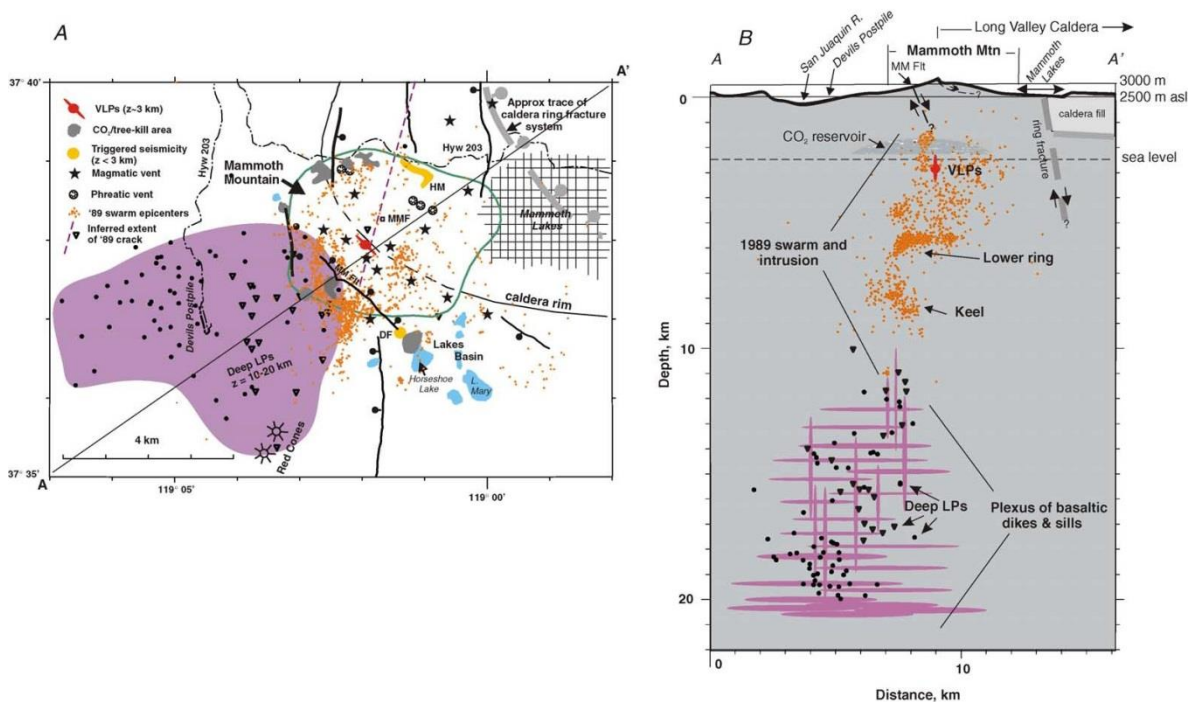


Figure 6.6 Map and cross section of the Mammoth Mountain area (after Hill and Prejean, 2005). Note the position of the Mammoth Mountain Fault in relation to the NW trend of high CO₂ flux in Figure 6.5. Orange and black dots represent hypocentres of earthquakes.

6.4 MÁTRADERECSCKE, HUNGARY

Mátraderecske, a town in Hungary, has gas vents fed by hydrothermal activity/mineralisation via a karst water reservoir at a depth of ~1000 m (Pearce *et al.*, 2004; NASCENT, 2005). The site has seismically active faults nearby. The gas reaches the surface via faults and fractures in strongly weathered Eocene andesite, which is overlain by Eocene and Oligocene sands and clays. The CO₂ seeps form gas vents and CO₂-rich springs (Pearce *et al.*, 2004; NASCENT, 2005). According to NASCENT (2005, p. 73) “the gas migrates laterally against local seals and can escape along faults opening to the surface; where the seal is missing, the gas escapes directly”. The average gas flux is about 5–10 L/hr/m² but along faults it can reach 400 L/hr/m² (Pearce *et al.*, 2004).

6.5 ALBANI HILLS, POGGIO DELL’ULIVO, SOLFATARA SECCA, TORRE ALFINA, ITALY

The Albani Hills region of Italy (Figure 6.7), about 20 km from Rome, includes the Poggio dell’Ulivo, Solfatara Secca, and Torre Alfina areas of CO₂-rich springs and emissions. Chiodini and Frondini (2001) detected shallow groundwater oversaturated in CO₂ in the Albani Hills area (Figure 6.8) and inferred this could explain episodes of fatal sudden gas release in historical times. There is common low magnitude seismic activity in the area and Chiodini and Frondini (2001) inferred fault-control on one of the anomalies detected. For further background information on Poggio dell’Ulivo, Solfatara Secca, and Torre Alfina as a natural analogues for leakage of CO₂ from storage reservoirs see Lewicki *et al.* (2007).

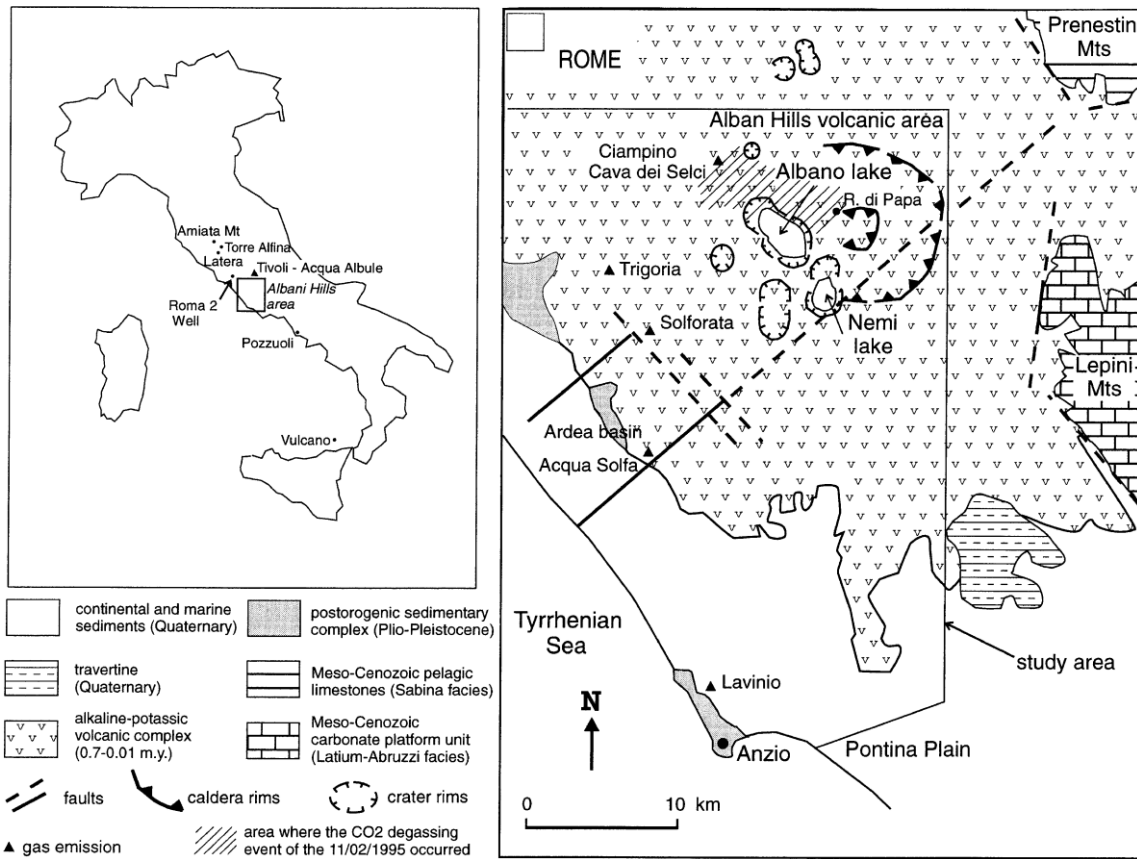


Figure 6.7 Albani Locality map for the Albani Hills area (from Chiodini and Frondini, 2001).

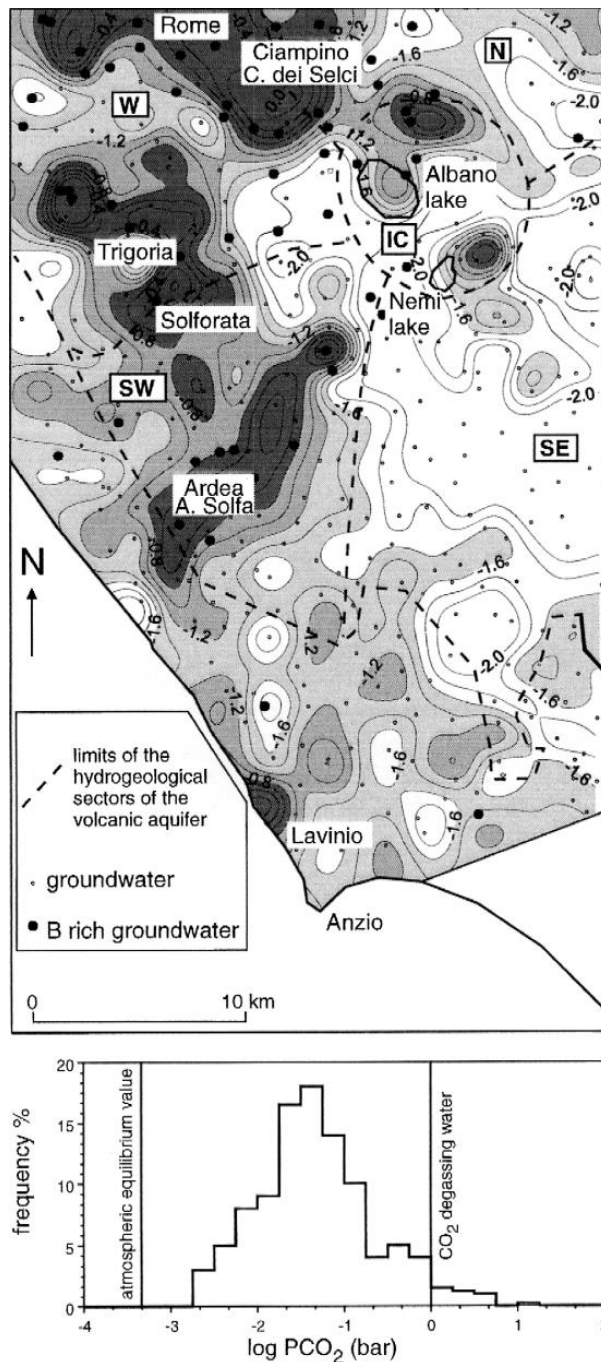


Figure 6.8 CO₂ gas emissions in the Ardea area (from Chiodini and Frondini, 2001). Log pCO₂ map contoured at 0.25 log units. The Ardea pCO₂ anomaly SW of Albano Lake is inferred to be related to a NE-trending fault (Chiodini and Frondini, 2001).

The Poggio dell'Ulivo hydrothermal area to the north of Rome exhibits diffuse degassing, with an elongate, northwest-southeast trend of highest CO₂ flux that might be due to fault control (Chiodini *et al.*, 1999; Figure 6.9a). Vents in the Solfatarata area nearby, a sub-circular depression with a diameter of 12 km, have highest recorded CO₂ vent fluxes (up to around 5 kg/m²/d \approx 1.8 t/m²/yr), which occur in an area bordered by faults and fractures (Voltattorni *et al.*, 2009). These faults and fractures may locally elevate increase permeability and promote increased fluxes.

The Tor Caldera area of Italy has been monitored for CO₂ flux using soil gas measurements. Maximum soil gas fluxes of 31746 g/m²/d (mean 1079 g/m²/d), equivalent to 11.6 t/m²/yr

(maximum, 0.4 t/m²/yr mean) were recorded in 2007 at Tor Caldera by Voltattorni *et al.* (2009), who inferred that the flux was controlled in part by underlying faults and fractures.

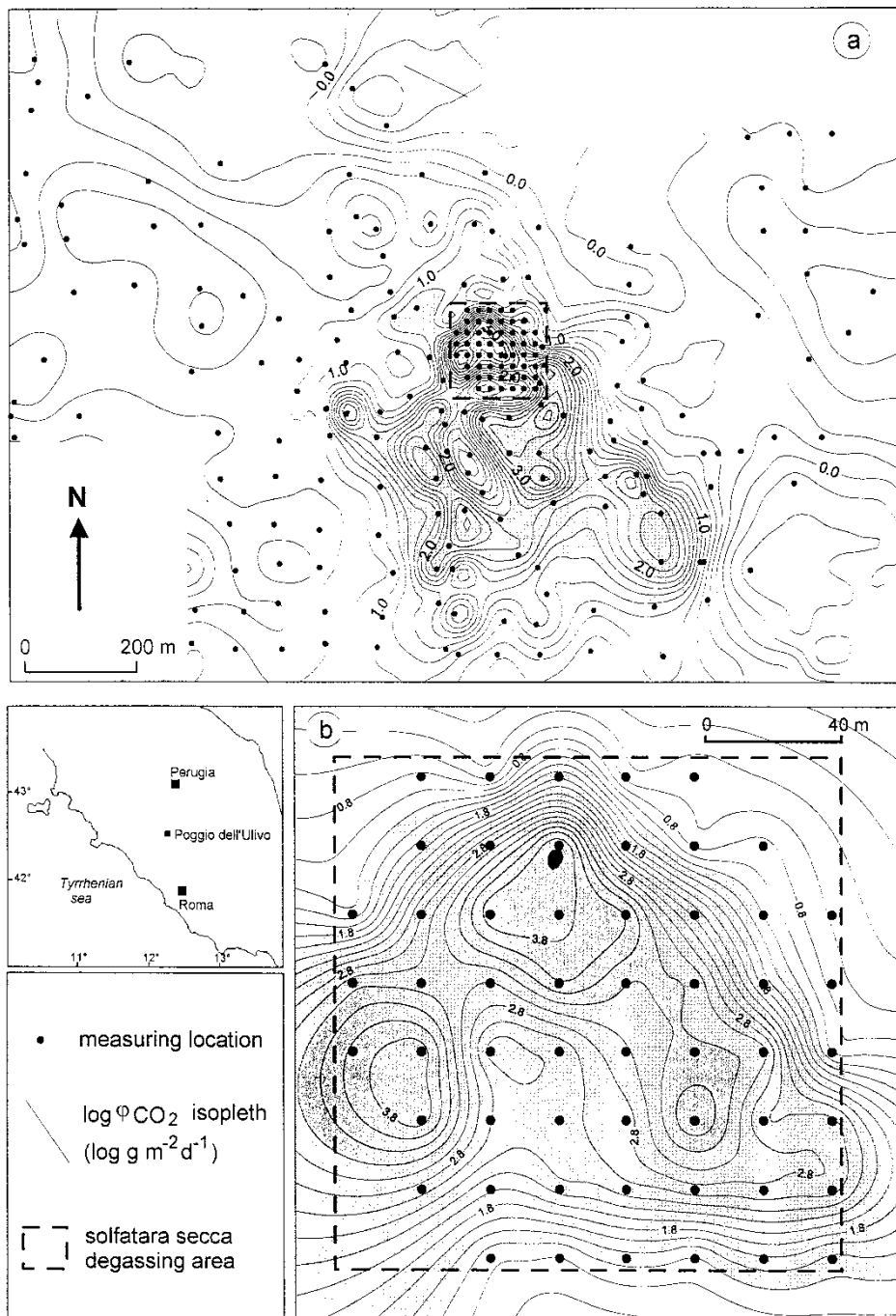


Figure 6.9 CO₂ gas emissions from the Poggio dell'Ulivo area (from Chiodini *et al.*, 1999) (a) and the Solfatara secca area within it (b).

6.6 PANAREA, GREECE

The Panarea gas seeps are near Panarea Island, one of the Aeolian Islands in the Tyrrhenian Sea, Greece, in water depths around 10–20 m (Figure 6.10). The source of the CO₂ is volcanic and the emissions followed a large gas burst in 2002, with a range of vents emitting at various temperatures (see Voltattorni *et al.*, 2009). The regional structure is controlled by active faults, though an association of vents with individual faults is not clear in the publications viewed as part of this study, and it seems likely the vents are related to small, unmapped faults or fracture

networks associated with collapse deformation, with percolation up through gravels and agglomerates (see Capaccioni *et al.*, 2007).

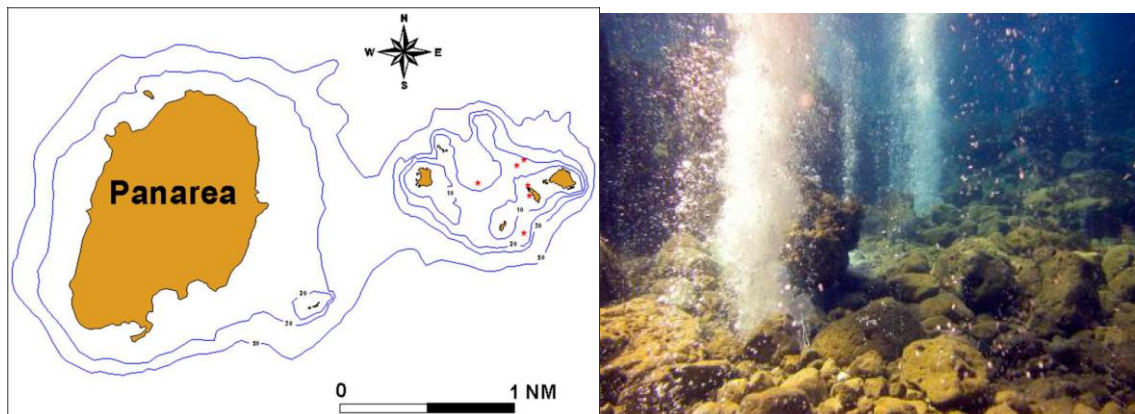


Figure 6.10 Panarea Island and associated submarine gas plume (left and right, respectively) (from Canamarra *et al.*, 2011).

Water chemistry has been studied directly underwater by scuba divers, with CO₂ flux volumes and rates determined using an inverted plastic funnel that was also used to collect gas samples (Canamarra *et al.*, 2011). This study provides proven methods for monitoring submarine gas emissions at water depths accessible by divers. The seeps are locally associated with bacterial mats (Gugliandolo *et al.*, 2006) and metal sulphosalts (Voltattorni *et al.*, 2009). Minimum emissions of CO₂ from an area of <15 km² in the Tyrrhenian Sea have been estimated as 25000 t/yr, though most of this is absorbed by sea water, with only 70–80 t/yr reaching the atmosphere (depending on the methods used to make the calculation, the seafloor depth, bubble size and gas absorption rates; Italiano *et al.*, 2001). Given that there was a major gas eruption in 2002, it is likely that discharge rates will vary considerably over timescales of years to decades. The usefulness of this as a case study stems mainly from the orders of magnitude of discharge (albeit from a hydrothermal source) and the methods of study employed in a shallow marine setting.

7.0 CO₂ FLOW RATES ALONG FAULTS

The rates of CO₂ migration along faults are likely to vary significantly on individual faults, within fault systems and between different sedimentary basins. Despite these variations there is value in documenting the rates (and volumes) of fluid migration to help constrain possible values at CO₂ storage sites where little or no flow data are available. Given the wide range of rates, the large number of factors that could influence these rates and the issues associated with measuring representative flow rates, caution should be exercised when using these values. As there will be problems identifying and recording slow rates of migration (e.g. < 10m/yr) the values presented are likely to define the upper limit of what is possible rather than providing an unbiased sample of the population of flow rates. This bias is illustrated by the absence from this report of unpublished examples from the petroleum industry where little or no evidence for fault-related flow has been noted.

Fluid-flow rates along faults could be influenced by a number of factors including; fault zone composition and architecture, pressure gradients along or across the faults (e.g. driving pressure and CO₂ flashing depths caused by pressure reduction, e.g. Watson *et al.*, 2014), depth of burial and buoyancy of the fluid, tectonic stress regime and fault orientation (see Section 5), supply of injected fluids (e.g. injection rate of CO₂ and connectivity of faults) and composition of fluids (e.g. Nadai, 1950; Yielding *et al.*, 1997; Childs *et al.*, 2007; Tsang *et al.*, 2007; Becker *et al.*, 2010; Faulkner *et al.*, 2010; Ilg *et al.*, 2012; Birkholzer *et al.*, 2015). The flow rates presented in this section are subject to measurement uncertainty and, like fault permeability, should be interpreted with care. The rates vary spatially and temporally (< 1 t/m²/yr vs >10 t/m²/yr), and could be influenced by both bedrock conditions (e.g. host rock rheology, pressure gradients and fault permeability) and non-geological factors (e.g. weather and sampling strategies, see Section 6 for further discussion). Quantification of rates on individual faults depends, for example, on how directly rates can be determined (from shallow groundwater/vadose zones, or localised, dry venting), and the method used (such as atmospheric monitoring or determining dissolved CO₂ and detection limits with respect to background levels of CO₂). An important inference from the analogue studies presented in Section 6 is recognition of the difficulty of detecting, quantifying and interpreting CO₂ flow rates for faults. The rates documented in Table 6.1 should therefore be considered in the context of their specific sites and the measurement methods. To understand the variability of flow rates it may be necessary to take many measurements over a wide area and long duration (e.g. up to years). Similar sampling strategies will be a requirement of CO₂ storage sites and should aid interpretations of the measurements.

7.1 FAULT PERMEABILITIES

Many factors will directly affect the fault zone permeability. For example, faults and fractures striking sub-parallel to the trend of the maximum stress are the most likely structures to be hydraulically conductive under the Coulomb failure criterion. Compilations of bulk crustal and fault-zone permeabilities are presented in Figure 7.1A and 7.1B, respectively. Fault zone permeabilities can be modelled to decrease with depth (see red and blue lines on Figure 7.1B). Fault zone permeabilities derived from *in situ* measurements together with values inferred from seismicity and modelled in flow simulations, range from 10⁻¹⁶ to 10⁻⁹ m², with the majority of values between 10⁻¹⁵ and 10⁻¹² m². These estimates of permeability overlap with, and in some cases are higher than, the 10⁻¹⁹ to 10⁻¹¹ m² (0.0001 – 10 000 mD) reported for fault-rock permeability from the North Sea and Norwegian Continental shelf (Manzocchi *et al.*, 2010). The higher crustal scale permeabilities may reflect the influence of critically stressed fractures which maintain near hydrostatic pore pressures over scales of 1–10 km (Ingebritsen and

Manning, 2010). Therefore, the permeability at the core plug scale may not represent the bulk permeability of a reservoir or caprock formation at larger scale (Evans *et al.*, 1997). Irrespective of whether datasets indicate differing permeability ranges they are considered to provide order of magnitude estimates only and are likely to change in space and time on individual faults. Such changes in permeability may directly reflect increases in fracture apertures induced by over-pressure and are directly applicable to CO₂ storage.

In a study of the relationship between fault zone structure and ground water flow into tunnels Seebeck *et al.* (2014) show near surface (< 500 m depth) fault zone permeabilities of 10^{-12} – 10^{-9} m² (i.e. 1 to 1000 D) (derived from borehole packer tests and application of Darcy's law) in both a highly deformed indurated turbidite sequence and poorly lithified shallow marine strata. Bulk permeabilities in this example were calculated using flow rates and tunnels areas over length scales from kilometres to centimetres for a range of estimated hydrostatic pressures and yielded very similar bulk permeabilities for both the poorly lithified and indurated rocks (Seebeck *et al.*, 2014). These bulk permeabilities are higher than those of both types of protolith sampled from core plugs (e.g. indurated turbidite 10^{-17} – 10^{-15} m² and shallow marine strata 10^{-15} – 10^{-13} m²) by up to six (shallow marine strata) and eight (indurated turbidite) orders of magnitude. This again highlights the scale dependence of permeability measurement where the greater bulk permeability of the rock (compared to that measured at the core plug scale), is most often inferred to be due to the presence of faults.

Fault zone permeabilities as little as 1–2 orders of magnitude higher than the intrinsic permeability of the host rock may be required to promote significant in-plane fault zone fluid flow (Molinero *et al.*, 2002; Wibberley and Shimamoto, 2003; Evans *et al.*, 2005; Seebeck *et al.*, 2014).

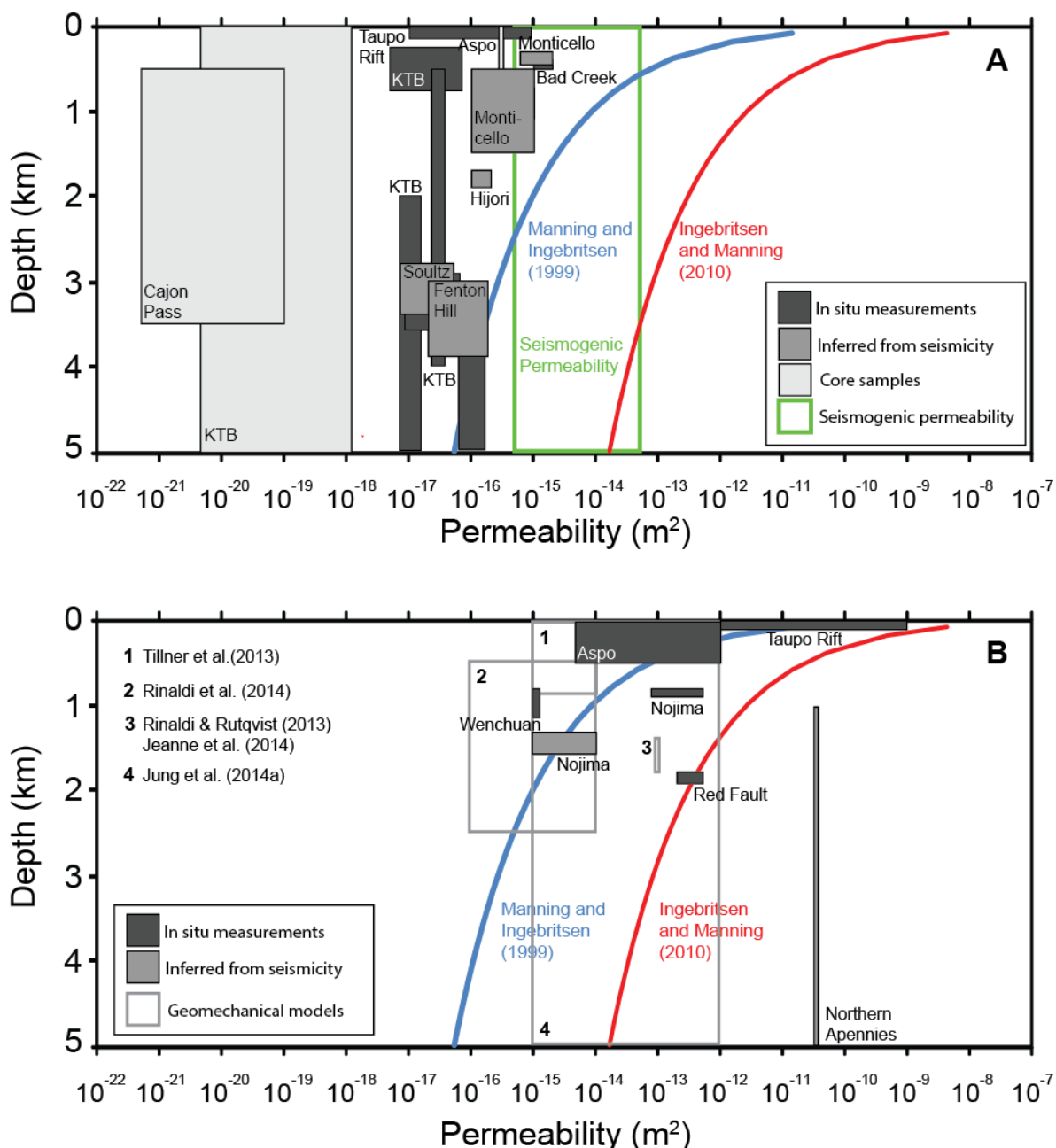


Figure 7.1 Bulk crustal and fault zone permeability. (A) Crustal permeabilities after Townend and Zoback (2000) with additional *in situ* data from Hancox (1975), Molinero *et al.* (2002) and seismogenic permeability from Talwani *et al.* (2007). Permeability with depth inferred from geothermal/metamorphic data of Manning and Ingebritsen (1999) (blue line) and from seismicity/metamorphism from Ingebritsen and Manning (2010) (red line). (B) *In situ* and model fault/fracture zone permeabilities. *In situ* data from; Kitagawa *et al.* (1999), Molinero *et al.* (2002), Revil and Cathles (2002), Xue *et al.* (2013), Seebeck *et al.* (2014), inferred from seismicity; Tadokoro *et al.* (2000), Miller *et al.* (2004). Permeabilities used in the recent geomechanical models of Tillner *et al.* (2013), Rinaldi and Rutqvist (2013), Jeanne *et al.* (2014), Jung *et al.* (2014a) and Rinaldi *et al.* (2014) (grey outline boxes) shown for reference.

7.2 CO₂ FLOW RATES IN NATURAL ANALOGUES

The CO₂ seeps presented in Section 6 provide information on CO₂ flow rates (Figure 7.2), although many sites reviewed did not provide quantitative data on the volumes, areas or longevity of the seeps. The flow rates for each analogue are maxima and range from 0.00001 to 30 t/m²/yr, with the majority of terrestrial sites >0.1 t/m²/yr (Figure 7.2). The highest rates in Figure 6.2 were encountered at abandoned wells that intersected a fault (Crystal Spring) and a caldera (Latera Caldera) and these rates were induced by anthropogenic activity. In flow-rate terms these two case studies provide examples of what might be possible for abandoned

wells at CO₂ storage sites. Given the flow rates presented in Figure 7.2 and areas of leakage of up to ~500 m², volumes of CO₂ leakage could reach 15000 t/yr, which is similar to the 25000 t/yr estimated for the submarine seep at Panarea, Greece (Canamarra *et al.*, 2011). Such flow rates would be significant at CO₂ storage sites, however, for a well-managed storage facility (e.g. where reservoir pressures are maintained well below fracture gradients), they are likely to represent the upper limit of what is possible.

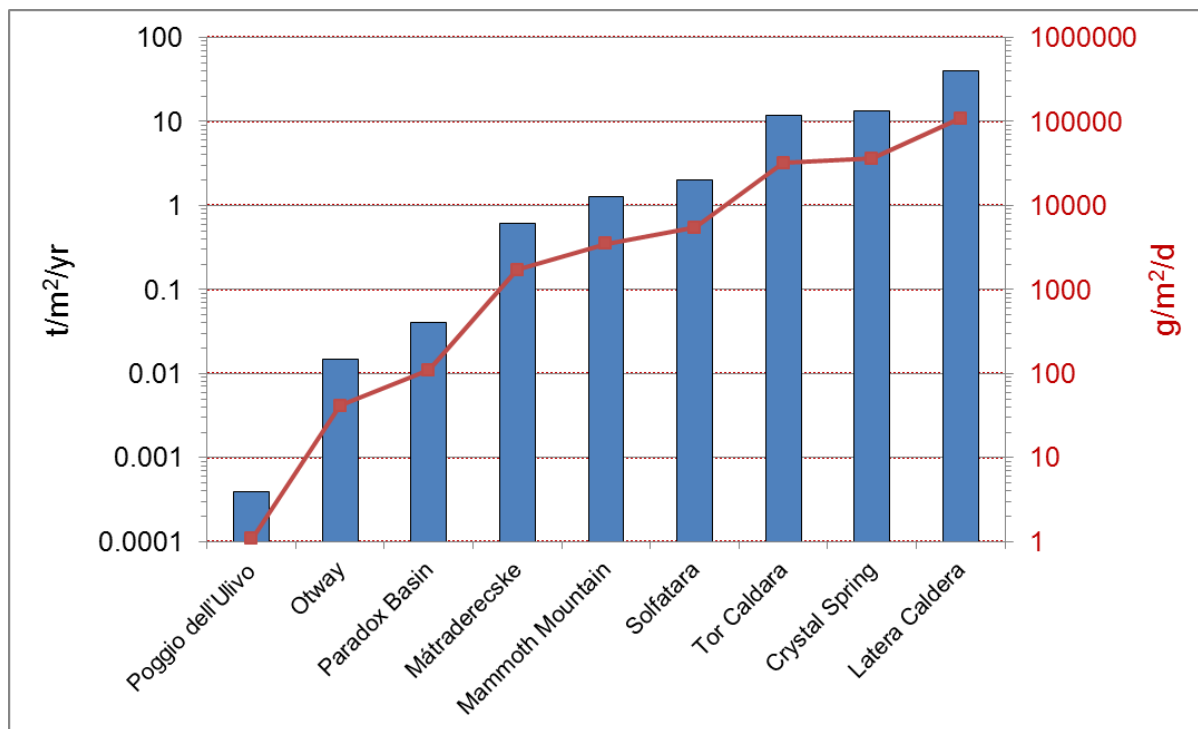


Figure 7.2 Maximum rates of CO₂ emissions from the analogue studies documented in Section 6 and Table 6.1. The rates plotted do not provide information of total volumes, or take into account temporal variations of rates, such as the spikes in rate that might occur during seismic pumping associated with proximal or distal earthquakes (e.g. Bonini, 2009; Todaka *et al.*, 2009; Han *et al.*, 2013).

CO₂ flow rates at the ground surface are closely related to migration rates in sub-surface rock formations. If CO₂ is able to escape from a target reservoir it is important to understand the potential range of migration rates for different scenarios. A compilation of gas migration rates by Brown (2000) indicates vertical velocities of 100–1000's m/yr. The majority of the flow data in the study of Brown (2000) were collected over gas storage sites or producing petroleum reservoirs and may not be representative of natural accumulations. However, rates of approximately 100–1000 m/yr agree with the large body of qualitative literature documenting changes in geochemical signatures a few years after initiation of production (e.g. Tucker and Hitzman, 1996; Schumacher *et al.*, 1997; Tedesco, 1999).. These vertical migration rates are typically <~400 m/yr and are significantly less than the rates predicted for some high pressure CO₂ storage systems. If, for example, CO₂ migration is driven by a high pressure pulse along a fault then migration rates of up to 1000 m/day might be expected (Miller *et al.*, 2004). These velocities are similar to the transport velocity of CO₂ driven by fluid over-pressures (400 m/day) (Brauer *et al.*, 2003), which reduce the effective normal stress (σ_n) acting on the fracture increasing its aperture and permeability (Revil and Cathles, 2002; Ferrill and Morris, 2003; Miller *et al.*, 2004). Collectively these data support the conclusion that an over-pressured, active CO₂-EOR or storage project may locally elevate the permeability of some faults. As a result of these increased permeabilities the geochemical expression of injected CO₂ could, in some cases, reach the ground surface or sample wells faster than most geologists intuitively expect (Klusman, 2015).

Given these rates of migration (100 m/yr to > 1 km/yr) and sufficient time (years to thousands of years) it is possible that injected CO₂ could migrate kilometres laterally. This suggestion is supported by flow simulation models which show that total lateral migration of CO₂ along faults can be of the order of 10-20 km (Jung *et al.*, 2014a). Similar lateral migration distances are often modelled in oil and gas studies, however, the rates of migration in these petroleum systems are typically millimetres to centimetres per year and require thousands to millions of years to travel large distances (e.g. >10 km). The range of estimated flow rates for petroleum and CO₂ is at least six orders of magnitude and questions remain about what flow rates will be most appropriate for faults at CO₂ storage sites. The answer to this question is likely to be site-specific and probably dependent on the volume of CO₂ injected, reservoir pressures and bedrock geology (e.g. fault, reservoir and caprock permeabilities).

Fluid flow rates vary by at least four orders of magnitude within fault systems. These variations have been documented by *in situ* flow measurements from boreholes and tunnels and by numerical modelling (e.g. Barton *et al.*, 1995; Sanderson and Zhang, 1999; Molinero *et al.*, 2002; Evans *et al.*, 2005; Tsang *et al.*, 2007; Seebeck *et al.*, 2014). These studies reached a number of conclusions about the systematics of flow rate variations within fault systems, some of which are highlighted in Figure 7.3. These conclusions are;

- Elevated fluid-flow rates (compared to unfaulted host rock) typically occur along faults,
- Flow-rate populations for faults may be approximated by a power-law relationship with a relatively small number of faults/fractures (<10%) accommodating much of the recorded flow (e.g. >50%)(Figure 3.8),
- Positive correlations have been observed between fluid flow rates, fault strike and fault size; critically stressed faults and larger more connected faults may have higher flow rates,
- The hydraulic properties of faults are similar to those of a fault-fracture network close to a percolation threshold and, predicting the location of highly permeable hydraulically conductive faults or parts of faults is likely to be challenging.

7.3 CO₂ FLOW MECHANISMS

Conceptually, CO₂ ascending from a reservoir will migrate as bubbles or continuous gas flow along faults and fracture systems until the water table is encountered, after which migration will occur via gas-phase advective or diffusive flow in the unsaturated vadose zone (Brown, 2000; Annunziatellis *et al.*, 2008; Kampman *et al.*, 2014b). CO₂ may then dissolve into groundwater and be transported laterally via groundwater flow (e.g. Kampman *et al.*, 2014b; Jung *et al.*, 2015). The vadose zone can either consist of bedrock, or of shallow sediments and soil. Depending on the thickness, porosity and permeability, water content, microbiology, and chemistry of the unsaturated vadose zone, a deep-gas signature originating from a fault may be altered. Such changes will influence our ability to locate CO₂ leakage (especially from buried faults) with any near surface monitoring technique, such as gas-geochemistry, atmospheric, biological, or remote-sensing measurements (Annunziatellis *et al.*, 2008).

Under the most favourable assumed conditions, the migration of isolated gas bubbles up fractures is too slow to account for the observed migration velocities of CO₂. At their fastest velocity, colloidal-size (radius <0.12 µm) bubbles move up fractures at <1 m/yr (Figure 7.3). This value rules out colloidal bubble migration, because the calculated seepage velocity is much slower than observed rates (for discussion refer to Brown, 2000). Single-phase gas flow in small fractures is therefore consistent with the rapid seepage velocities reported in the literature. Fractures having half widths from 0.1 to 2 µm can be responsible for buoyancy-

driven flow at rates equal to the range of reported seepage velocities (Figure 7.3) (Brown, 2000).

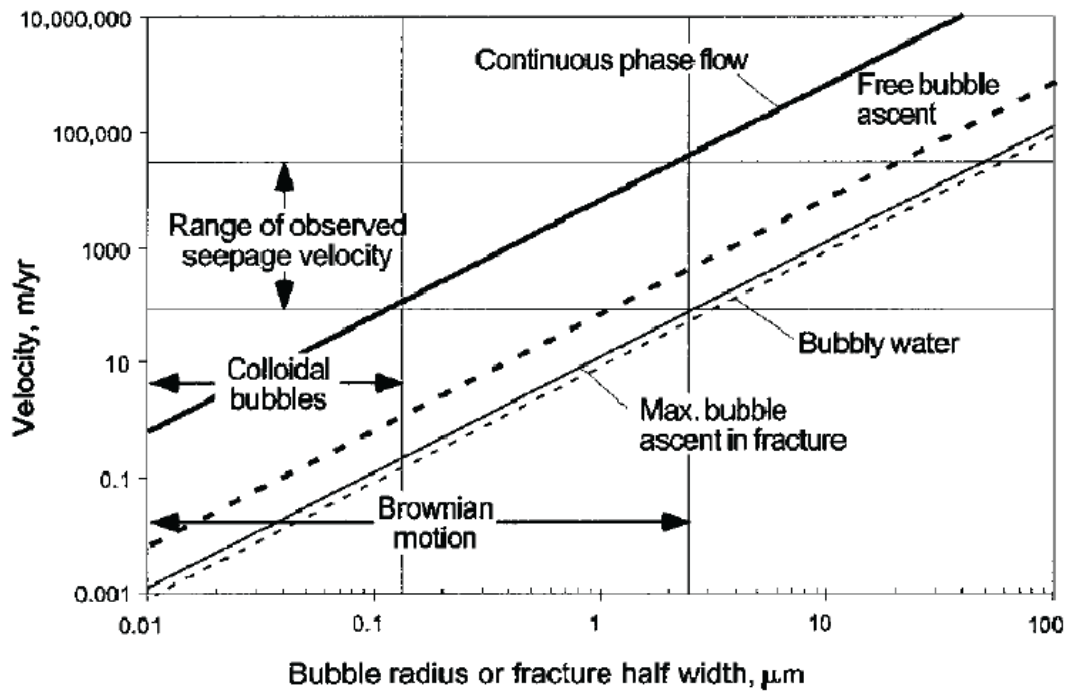


Figure 7.3 Comparison of calculated migration velocities for proposed mechanisms and observed seepage velocities (from Brown, 2000). Over the range of bubble radii where Brownian motion could occur, bubble migration is significantly less than observed seepage velocity. In contrast, gas migration as a continuous phase in fractures can easily migrate this fast at very small fracture apertures.

8.0 INDUSTRY PRACTICES FOR MEASURING AND MITIGATING UNWANTED FLUID FLOW ALONG FAULTS

Extraction and injection industries, including petroleum, geothermal and CO₂ storage, can be affected by faults which locally promote and/or retard fluid flow. The experience of the petroleum and geothermal industries, in particular, may have application at CO₂ storage sites. The techniques used to monitor, model and mitigate fluid flow were primarily designed (or utilised) for field-scale studies, and have been adapted to represent a desire to understand how these faults control fluid movement. Many of the methods for monitoring fluids provide indirect evidence for non-flow across faults and flow along faults. While mitigation measures also apply to faults as barriers and conduits, fault modelling is primarily focused on the role of faults as barriers to flow. The three processes are not independent and most sites will require a balance to be struck between monitoring, modelling and mitigation.

To mitigate many of the geomechanical risks associated with CO₂ injection a systematic geomechanical evaluation is required. Geomechanical models play a significant role in evaluating potential storage sites (e.g depleted gas fields) as CO₂ injected into reservoirs or aquifers under pressure results in changes to the *in situ* stresses (overburden as well as tectonic) (e.g. Streit and Hillis, 2004; Rutqvist, 2012; Fang and Khaksar, 2013). The geomechanical issues for CO₂ injection into depleted gas fields include: (1) drilling instability and completion optimization for any new wells, (2) the potential influence of both pressure and temperature changes induced by CO₂ injection, (3) estimation of the practical or sustainable injection pressure of the CO₂, and (4) the maximum sustainable pressure of the depleted reservoir and caprock to avoid fault reactivation or fracturing (Fang and Khaksar, 2013). Points (3) and (4) are critical in order to avoid creation of possible leakage paths for the stored CO₂. As such, a comprehensive geomechanical model should be developed at the initial stages of field appraisal. These geomechanical models should include; the mechanical properties of the reservoir and surrounding rocks (in particular the caprock), the initial (pre-injection) *in situ* stresses, the influence of the pore pressure and temperature changes on *in situ* stresses, and the criterion for wellbore failure, sand production, as well as fault reactivation (Fang and Khaksar, 2013). Parameters for these geomechanical models are normally derived from field tests, laboratory core tests, well logs, drilling, and production data. Once a geomechanical model is developed for a particular field, it can be utilized to test different parameters and scenarios associated with the geomechanical issues detailed above. For example, Fang and Khaksar (2013) describe a case study from a depleted gas field in the North Sea that highlights field specific constraints for well geometry, reservoir pressure and fault stability.

This brief summary included is unlikely to be complete, in part because industry practices are rarely published in sufficient detail to be of value. This lack of publication is understandable given the desire of companies to maximise economic benefits and maintain competitive advantage. A consequence, however, is that much evidence for industry practices is anecdotal and its inclusion in this report would likely not stand the rigors of peer review. Therefore, the publications reviewed in this section were in large part produced by industry consultants or academics with many fewer articles from industry practitioners.

8.1 FAULT AND FLUID FLOW CHARACTERISATION

8.1.1 Seismic reflection techniques

The geometries and locations of faults relative to potential reservoir/caprocks systems is a first-order variable required for understanding faults and their impact on fluid flow. Interpretation of conventional seismic reflection lines, time slices and coherence cubes are the

standard petroleum industry technique for imaging reservoirs, caprocks and associated faults. Three-dimensional (3D) seismic-reflection data with a line spacing of 12.5 m is likely to be a requirement of most CO₂ storage sites and typically permits faults with vertical displacements as small as 5–10 m to be resolved at shallow depths (e.g. <3 km). In circumstances where there are seismically-resolved faults many more sub-resolution faults are likely to be present (e.g. Yielding, 1992), while the tip regions of larger faults will also be below the resolution of the data (e.g. Meyer *et al.*, 2002). The proportion of the fault below the seismic resolution increases with decreasing maximum vertical displacement or size and also changes with lithology; the seismic resolution of faults in mudstone-dominated caprocks with low seismic reflectivity may be poorer than in adjacent reservoir strata. Despite this issue 3D seismic-reflection data represent the best available technique for determining the locations, geometries and displacement of faults in caprock at CO₂ storage sites (e.g. Zhang *et al.*, 2015). Seismic-reflection interpretation may also assist in the identification of fault bends, steps (or relays) and intersections which could be sites of relatively dense fracturing of the caprock and may locally increase its permeability (e.g. Kim *et al.*, 2004; Childs *et al.*, 2009; Eichhubl *et al.*, 2009; Dockrill and Shipton, 2010; Faulkner *et al.*, 2010).

Four dimensional (time lapse) seismic-reflection surveys have the added advantage (above 3D datasets) that they can be used for tracking the location and dimensions of injected CO₂ plumes (e.g. Chadwick *et al.*, 2009), including their relations to caprocks and mapped faults. Experience from the Sleipner CO₂ storage project suggests that CO₂ can illuminate heterogeneities, so that even very small faults (e.g. ≤5 m vertical displacement) which were previously undetectable may be visible after CO₂ injection. The results from Sleipner are consistent with data from petroleum basins where gas has been imaged. Recent developments in the analysis and interpretation of high quality 2D and 3D seismic reflection data provide a means of mapping gas chimneys and drawing conclusions about the migration of gas in both faulted and unfaulted strata (e.g. Heggland, 1997; Ligtenberg, 2005).

In addition to the explicit imaging of the largest faults, indications of the presence and orientation of small sub-seismic faulting or fracturing can be obtained from the properties of seismic waveforms. The key requirement of these techniques is to have multi-azimuthal data, which can be obtained from high-fold conventional land 3D seismic, from purpose-acquired 2D seismic (e.g. a star configuration around boreholes) and from multi-azimuth Vertical Seismic Profiles (VSP). Multi-azimuthal seismic data provide an 'integrated' measure of rock-mass properties (rather than resolving individual faults), with the fast direction of seismic waves inferred to be parallel to the strike of open fractures. More sophisticated methods employing seismic shear-wave 'splitting' or 'birefringence' could also provide important information on the strike, density and apertures of fractures which are too small to be resolved individually in seismic-reflection lines (e.g. Maultzsch *et al.*, 2003). As with conventional seismic-reflection data time-lapse datasets enable changes in the seismic properties to be tracked, providing insights into changing-rock mass parameters and fluid flow, both within the reservoir, caprock and potentially along faults).

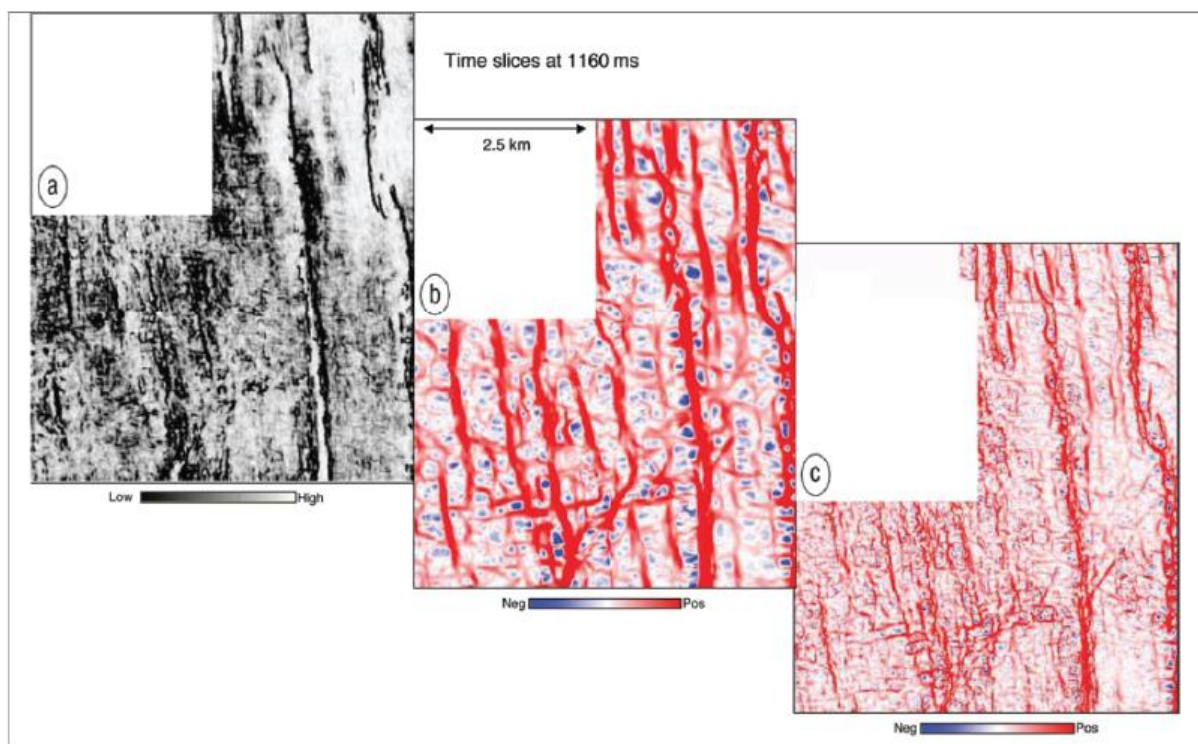


Figure 8.1 Comparison of horizon time slices for (a) coherence, (b) long wavelength most-positive curvature, and (c) short wavelength most-positive curvature volumes from a 3D seismic reflection survey in Alberta (from Chopra and Marfurt, 2007).

In recent years curvature analysis has been applied to processing seismic-reflection volumes for the purpose of imaging fractures that would otherwise be unresolved (e.g. Al-Dossary and Marfurt, 2006; Chopra and Marfurt, 2007; Zhang *et al.*, 2015). Curvature attribute values extracted from seismic volumes enable identification of lineaments on time slices, in some cases in areas where seismic horizons cannot be tracked with confidence, and little information on fault/fractures would otherwise be available. Figure 8.1 compares the results from coherence with the most-positive long-wavelength and short-wavelength curvature analyses. Visual inspection of time slices supports the view that curvature analysis is capable of imaging both the larger faults identified in the coherence time slice and smaller fractures that are below the resolution of conventional seismic reflection images. Confidence in the technique can be further improved by comparing fracture orientations from seismic-curvature analysis with data from image logs or core data (Chopra and Marfurt, 2007).

8.1.2 Borehole Image Logs and Core

In the petroleum industry, analysis of small sub-seismic fractures is typically conducted using image logs (micro-resistivity and ultrasonic tools are primarily used to generate electrical and acoustic images, respectively) and core from wells (e.g. Cheung, 1999; Mäkel, 2007). Analysis of faults and fractures observed in core and images of borehole walls represent one-dimensional samples of the fracture population which is strongly dependent on the angle between the well inclination and the dips of the fracture sets. They are of greatest value when data are available from multiple wells, the wells are oriented at a high angle to the main fracture sets, the data completeness is high and the well data include constraints on flow rates for individual faults or systems of faults. Published examples where information are available on faults (and fractures) and their flow rates is most common in the geothermal industry. In the Soultz-sous-Forêts (France) geothermal sandstone reservoir, for example, highly fractured intervals of the sandstone correlated with inflow zones in boreholes (Baisch *et al.*, 2010). In this example the fracture zones are associated with a major fault zone, which is interpreted to

operate as a fluid-flow pathway. Therefore, borehole data could contribute to an improved understanding of: 1) fault and fracture geometries and locations (both absolute and relative to the stratigraphy), 2) fault and fracture scaling properties from seismic to borehole scales, 3) fault permeabilities and, 4) fracture aperture widths.

8.1.3 Geochemical Sampling

Fluid composition and geochemical tracers sampled from wells are widely used in the petroleum and CO₂ industries to track the migration of fluids. The methods are based on the concept that buoyant fluids and gases migrate laterally and upward from the point of generation through the sedimentary column in response to tectonics, pressure, and hydrodynamics with chemical reactions possibly occurring along the migration pathway (Abrams, 2005). The methods included in the review of Klusman (2011) are; above ground open-atmosphere techniques, measurements at the land surface–atmosphere interface, and shallow subsurface sampling and measurements (Figure 8.2). In these studies it is essential that CO₂ measured by the monitoring network can be definitively identified as being sourced from the injected plume. To this end monitoring techniques are heavily reliant on the use of tracers (either natural or introduced), which provide a chemical fingerprint of the injected fluid. In the absence of chemically distinct tracers, interpreting CO₂ concentrations (particularly in the atmosphere) can be problematic because of its relatively high atmospheric concentration, high environmental variance, multiple natural sources, and solubility/reactivity with water. These factors combine to suggest that CO₂ alone may not effectively serve as an early warning tracer or surface indicator of undesirable migration (Klusman, 2011). Klusman (2011) suggests that a variety of measurements may be necessary, tailored to the scale of each sequestration project, to detect CO₂ leakage. Detection of microseepage is relatively straightforward, based on the methods outlined in Klusman (2011), however, quantification of the retention of the injected CO₂ in the reservoir is much more difficult. At present there exists no single, all-inclusive method at the current level of technology for the accurate, reliable assessment of microseepage rates over a period of time (Klusman, 2011).

In many circumstances tracers have been used successfully, however, there are also numerous examples where tracers are not encountered at sample stations and provide little information about the migration of injected fluids (other than the fact that models for this migration are incomplete) (Klusman, 2015). In some areas faults could help explain this incomplete understanding. In the Rotokawa geothermal field (New Zealand), for example, tracer test results were characterised by relatively slow returns across the Central Field Fault (Sherburn *et al.*, 2015), suggesting that this structure represents a barrier to lateral flow. In addition geothermal activity in the form of Lake Rotokawa, several hydrothermal eruption craters and the Rotokawa Fumarole (Wallis *et al.*, 2013) overlie the fault at depth and suggest that the Central Field Fault is also a conduit for vertical fluid flow. This conclusion is supported by gas geothermometry (CO₂/Ar–H₂/Ar) and chemistry (N₂–He–Ar) data of the Rotokawa Fumarole indicating that it is sourced directly from a deep, >300 °C, liquid reservoir below the regional seal, and that the fault may act as a permeable connection between the deep reservoir and the intermediate aquifer (Hedenquist *et al.*, 1988; Winick *et al.*, 2011).

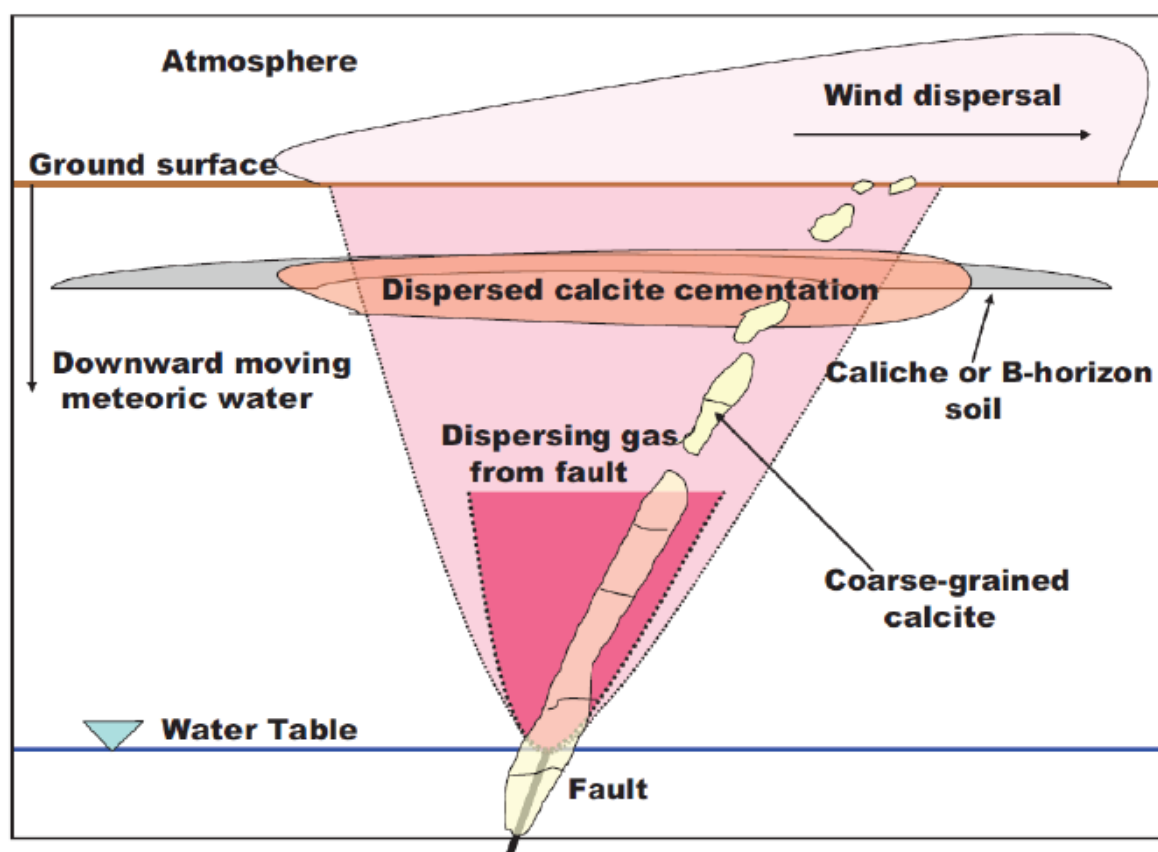


Figure 8.2 Schematic of near-surface and surface expression of fault/fracture gas seepage from depth. The oxidation of carbon-containing gases frequently produces secondary calcite and other near-surface alteration products. Gases may, or may not be transported into the atmosphere (Klusman, 2011). N.B. the fault may continue to the ground surface.

8.1.4 Microseismicity

Where site-specific earthquake monitoring programmes are implemented induced microseismicity is commonly observed at fluid injection or extraction sites. In map view microearthquakes induced by fluid injection are generally clustered or form a halo around injection wells (e.g. Figure 8.3) and are inferred to reflect rock response to changing pressure and/or temperature conditions. The spatial distribution of induced seismicity may be approximately circular or elongate with the outer margin of the zone often being irregular (Figure 8.3). In a number of cases irregular distributions of microseismicity may arise because the seismicity is locally focused along fault zones (e.g. Ake *et al.*, 2005; Sherburn *et al.*, 2015). The location of the edge of induced microseismicity is influenced by the completeness of the seismicity catalogue. Data from a number of sites suggests that the dimensions of the induced seismicity increase (both temporally at individual sites and between sites) with increasing volumes of injected or extracted fluids (IEAGHG, 2013a; Nicol *et al.*, 2013b). These data suggest that the areal extent of microseismicity is related to the size of the injected fluid plume, however, few data are available to test the model that plume and microseismicity dimensions are approximately equal (i.e. the edge of the plume is marked by the margin of the recorded microseismicity).

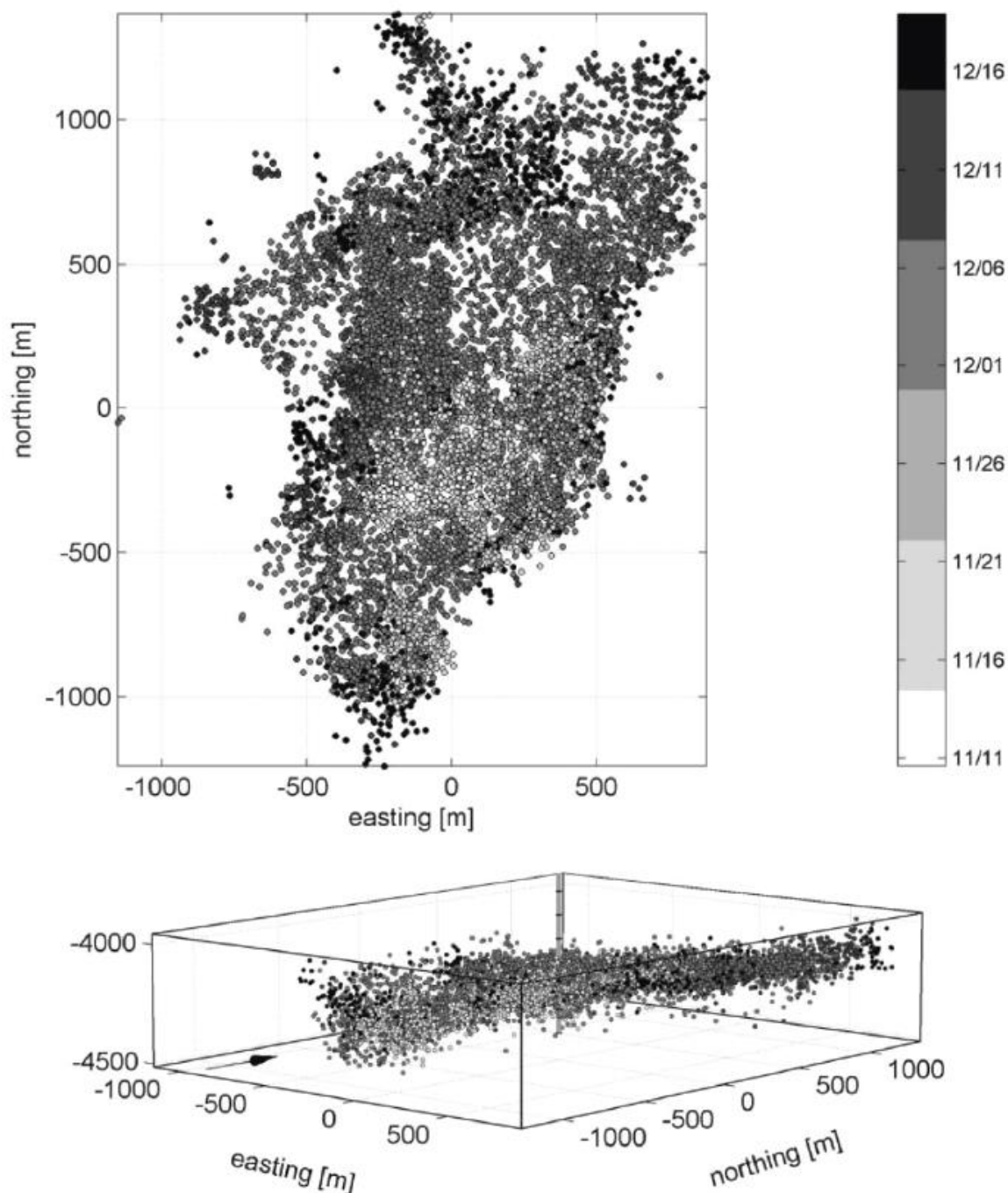


Figure 8.3 Induced seismicity epicentral locations with respect to the injection well during the first hydraulic fracture experiment at Cooper Basin, Australia. Timing of earthquakes with respect to the beginning of injection are shown in grey scale where colours get darker with time following the onset of injection (from Baisch *et al.*, 2006).

Microseismic networks are often deployed over geothermal sites where they are inferred to provide information about faulting and fluid flow. In the Coso Geothermal Field (CGF) in California (USA), for example, fluid flow appears to be controlled by a fault and fracture formed at the intersection of the Basin and Range province and the eastern California shear zone (Wu and Lees, 1999; Kaven *et al.*, 2013; Wamalwa *et al.*, 2013; Kaven *et al.*, 2014). Analysis of the microseismic-event locations reveals seismicity is constrained within two compartments of the geothermal field (referred to as the southwest field and the eastern flank), separated by an aseismic zone which is cooler than the adjacent seismic zones. Within the seismically defined compartments the events are thought to occur on pervasive, small-scale faults and fractures. Along the southern edge of the eastern flank compartment seismicity data define a prominent

SW-NE trend which is interpreted to be a large-scale fault or fracture zone. The microseismicity in this zone responds to changing fluid production and injection and is interpreted to be a permeable fault/fracture zone that facilitates fluid flow along the structure while acting as a barrier to cross-structure fluid flow.

8.2 FLUID FLOW SIMULATIONS

Fluid flow simulation studies have been employed by many industries in the last 40 years (e.g. petroleum extraction, CO₂ storage, water extraction and radioactive waste management), as a tool for improving reservoir performance during extraction/injection operations. Numerical models of fluid flow through sedimentary sequences commonly predict flow behaviour on reservoir scales (Odling *et al.*, 1999; Manzocchi *et al.*, 2010). Since the early 1990s these models have included faults which are generally considered to be barriers or baffles to lateral flow. Generally these models use empirically derived estimates of clay content of fault zones (e.g. Clay Smear Potential or Shale Gouge Ratio, see Table 4.1) as a proxy for their hydraulic properties which are permitted to vary over fault surfaces (Bentley and Barry, 1991; Fulljames *et al.*, 1997; Manzocchi *et al.*, 2010). In recent years the cross-fault permeability of faults has been expressed as a transmissibility multiplier between 1 and 0, where 1 is equivalent to an unfaulted sandstone and 0 is a fully sealing fault (Manzocchi *et al.*, 1999). In estimating these parameters an understanding of how fractures influence flow and particularly an understanding of the scale of fractures that dominate flow behaviour, are required to ensure a reliable model and therefore predictive results (Odling *et al.*, 1999; Manzocchi *et al.*, 2010). The applicability of the simulations is tested using history matching between the models and production data. Whilst the pressure history that arises from production fluid extraction yields additional insight into the permeability properties of a fault zone, those properties can only be inferred with additional information about production rates, connected pore volumes, the properties of the fluids contained within those pores (e.g. compressibility), the timing and history of all wells either producing or injecting fluid, and additional case-specific parameters. Although history-matching exercises are of great value for testing the plausibility of the models, their outputs are non-unique and a universal weakness of the models is the uncertainty of geologic input parameters. In particular, reservoir simulation problems and uncertainties can be severe for models constructed to predict reservoir performance before production wells are drilled. The use of a geocellular reservoir simulation model was introduced to help keep track of these various parameters and dependencies.

As reservoir simulations improved through evolution of raw computing power, it has become possible to treat and evaluate a full continuum of fault properties in a comprehensive reservoir simulation (Jolley *et al.*, 2007). In particular, the models include fault geometries and fault transmissibilities that reflect shale gouge properties. An important outcome of the Jolley *et al.* (2007) study is the conclusion that with the time and care invested in constructing a viable reservoir framework and the systematic application of transmissibility multipliers based on geologic principles and clay smear models, the path to achieving an acceptable history match is far more efficient. Even when reservoir simulation is used to test models of fault properties, the results are non-unique given the large number of degrees of freedom that remain in the model (i.e. multiple combinations of parameters consistent with measured data produce the same fluid pressure and rate histories). One way to further reduce the degrees of freedom in a model is with an independent data type, and Sverdrup *et al.* (2003) have shown how the application of 4D (time-lapse) seismic data are used to track the spatial movement of gas and water fluids and the corresponding pressure changes between repeat surveys. In particular, the amplitude difference map in Sverdrup *et al.* (2003; their figure 11) is an exceptional illustration of gas pooling against a fault and begs the question of whether a sandstone

connection exists at that location to support potential gas leakage across the fault, and if so, whether the gas is pooling in a small attic above the juxtaposition connection. If both of those geometric criteria are met, then cross-fault flow is restricted by fault gouge, possibly a clay smear.

To date many flow simulations focus on reservoir units and do not explicitly take account of the prospect of along-fault flow; this is a major disadvantage for modelling CO₂ storage and its migration through caprock.

8.3 FLUID FLOW MIGRATION AND REMEDIATION

Proven mitigation or remediation techniques are rare in the CO₂ geological storage field and the methods and techniques documented below are mainly adapted from other domains/industries such as petroleum industry or environmental clean-up operations (Manceau *et al.*, 2014). Corrective measures mainly stem from the past efforts in the activities of oil and gas industry such as those detailed in Benson and Hepple (2005), Perry (2005), and IEA-GHG (2007). However, the extent to which such intervention practices can be used for CO₂ geological storage in deep saline aquifers should be assessed, given the uniqueness of CO₂ geological storage, both in terms of time scale and specificity of the injected gas (Le Guenan and Rohmer, 2011). Some of these techniques have been tested and applied in several cases and under conditions that may be close to those at CO₂ geological storage sites, whereas others are niche technologies that may only be relevant to address challenges (depending on the CO₂ leakage type, location and rates, technical limitations of a given solution, environmental and cost issues) encountered in specific CO₂ storage applications (Manceau *et al.*, 2014). For migration scenarios such as caprock sealing defects including faults, fractures and high permeability areas relevant in this report, few measures can directly target the leakage pathways. In these cases, the mitigation measures are predominantly aimed at countering the forces responsible for the CO₂ migration and several fluid management options have been proposed in order to prevent or minimize CO₂ migration (Manceau *et al.*, 2014). Fluid management solutions would be employed to; (a) temporarily or permanently arrest the pressure increase or decrease the pressure in the storage aquifer, locally or globally; (b) create a pressure barrier in the overlying geological strata to prevent or minimize CO₂ leakage; (c) back-produce injected CO₂ either locally or globally; and (d) enhance non-structural trapping mechanisms (Manceau *et al.*, 2014).

8.3.1 Pressure relief in the storage formation

Natural processes of brine and rock compression, as well as dissolution of CO₂ into formation brine through density-driven convection, will naturally decrease the pressure build-up in the formation, as presented by the IEA-GHG (2010b) (Manceau *et al.*, 2014). The same study, however, notes that weak density difference between CO₂-saturated and unsaturated brine could hinder this process. Operational choices are therefore necessary for reducing the level of reservoir pressurization in case of an abnormal behaviour. Stopping the CO₂ injection may be considered as a mitigation technique if the pressure relief in the storage formation is sufficient for reducing leakage, or preventing the CO₂ plume from reaching a leakage pathway. Since this option might not be sufficient for preventing CO₂ leakage outside the storage reservoir, accelerated and enhanced strategies, such as drilling new injection wells, producing at the injection well or extracting brine at a distant location, may also be considered for application (Manceau *et al.*, 2014).

Le Guenan and Rohmer (2011), for example, evaluated means of controlling an over-pressure CO₂ storage scenario within the Paris Basin. In a case where the over-pressurization has

created a new leakage pathway through fault reactivation and/or hydraulic fracturing, for example, newly created fractures and reactivated faults may not totally close with pressure relief, particularly if they have undergone shear displacements (Section 3.5.2). This mitigation option may not be therefore sufficient for stopping a CO₂ leakage if the mobile plume reaches these areas, due to buoyancy effects and pressure gradient. This last case is an argument for considering pressure control strategies in the injection plan, and not solely as a mitigation option.

Estimation of pressurization and brine displacement over time in the case of CO₂ storage, as well as potential effects on caprock and fault integrity have been reviewed in IEAGHG (2010a). Different injection strategies are presented in IEAGHG (2010b) notably with the purpose of limiting the overpressure created by the CO₂ injection, and therefore to avoid creating leakage pathways through fault reactivation, for example (Manceau *et al.*, 2014).

When a significant irregularity (e.g. leak, upper aquifer pore pressure increase, or unexpected extension of the CO₂ plume) is detected by the operator through the monitoring system in place, shutting down the injection process or decreasing the injection rates are often effective courses of action. A monitoring well equipped with a downhole pressure gauge located in a formation above the storage reservoir could detect, for instance, pressure changes as low as 0.0007 MPa (0.007 bars) under favourable conditions (Benson *et al.*, 2006). In particular, the permeabilities and thickness of the formation, the position of the monitoring well and the natural background fluctuations are the more important parameters that determine such conditions. Alternatively, indirect monitoring methods could be used, such as seismic methods, electromagnetic methods or tilt measurements methods (used to measure the land-surface deformation). Taken separately or together, these measurements can be inverted to provide subsurface pressure changes (Le Guenan and Rohmer, 2011).

8.3.2 Hydraulic barrier

Hydraulic barriers are used as a preventive or corrective measure in pollution engineering (Manceau *et al.*, 2014). This technology consists of injecting (or producing) water to locally modify the hydrogeology and protect the drinking water against saline brine intrusion, which is one of the most widespread forms of fresh groundwater pollution in coastal areas (e.g. Parrek *et al.*, 2006). Several authors have considered adapting this method to the case of a CO₂ leakage from the storage reservoir to an overlying aquifer that is not deemed a sensitive asset. Injecting brine into the over-lying aquifer will increase the pressure just above the leak to counter-balance the CO₂ buoyancy and the storage reservoir over-pressurization that are driving this leakage (Benson and Hepple, 2005; IEAGHG, 2011). Implementing a hydraulic barrier requires the consideration of many operational and strategic issues: delays, costs and technical feasibility of re-using a former injection well or drilling a new one, levels of induced over-pressurization to avoid reactivation of existing faults and fractures widening or even creation of new ones, availability of brine, efficiency of the injection, and measure rate of response (Manceau *et al.*, 2014). Most of these issues might hinder the applicability of hydraulic barrier and restrain its design. Réveillère and Rohmer (2011) evaluate the applicability of a hydraulic barrier, both as corrective and preventive measures, and conclude that the distance from the injection well to the leakage appears as the most critical parameter. A hydraulic barrier may be efficient if applied in the immediate vicinity of the leakage plume; however, it may be an impractical solution at long distances since it requires long injection periods to be efficient (Manceau *et al.*, 2014).

8.3.3 CO₂ plume dissolution and residual trapping

8.3.3.1 *In situ enhancement of dissolution and residual trapping.*

Enhancing dissolution and residual trapping may be considered as a remediation option both for the injected CO₂ plume in the storage reservoir and/or a secondary accumulation in an overlying aquifer (Manceau *et al.*, 2014). The method relies on a brine flow over the CO₂ plume, which will enhance these two CO₂ trapping modes. The brine flow may be natural, i.e., due to groundwater flow - passive remediation - (Juanes *et al.*, 2010), but active remediation options have been also suggested for trapping small leakage plumes (Esposito and Benson, 2012) or the injected CO₂ plume (Leonenko and Keith, 2008; Nghiem *et al.*, 2009; Qi *et al.*, 2009; Manceau and Rohmer, 2011). However, the latter case requires large brine injection flow rate and induces overpressure, which raises several issues including the geomechanical integrity of the reservoir and potential brine leakages. This measure has been studied both as a design or mitigation option. Approximate analytical solutions (Juanes *et al.*, 2010; Manceau and Rohmer, 2011) or numerical models with implemented residual trapping modules (e.g. Doughty, 2007) have been proposed to estimate the efficiency of the natural or active trapping of the CO₂ plume at large scale (Manceau *et al.*, 2014).

8.3.3.2 *Ex situ CO₂ dissolution and saturated brine injection.*

As an alternative to the techniques aimed at enhancing non-structural trapping *in situ*, an option is to use surface or *ex situ* dissolution in order to store dense CO₂-saturated brine (Manceau *et al.*, 2014). Some authors have proposed the use of this extraction/CO₂-dissolution/injection process whereby the saline aquifer brine is extracted via production wells, the captured CO₂ is dissolved into the extracted brine on the surface using high pressure/temperature mixing vessels and the CO₂-laden brine is re-injected into the storing formation (e.g. Leonenko and Keith, 2008). This method is also assessed in IEA-GHG (2012) for several case studies. The technique has been proposed as a storage design by these authors, but not as a corrective measure; it may therefore be considered as a preventive measure, or as a major change of the injection strategy. Although the extraction/CO₂-dissolution/injection process appears to be an attractive solution, it may be hampered due to several reasons: (a) reservoir heterogeneities affecting the injected CO₂-laden brine movement into formation; (b) increased pressure regimes near the injectors; (c) decreased pressure regimes near the extractors; (d) the required large number of injection/production wells to enable the process and associated costs; (e) added costs required by the surface facilities; (f) need to optimize wells location; (g) possible near-well mineralization further reducing well injectivity or mineral dissolution that may threaten the reservoir integrity (Kampman *et al.*, 2014a); and (h) deployment difficulties both onshore and offshore (Manceau *et al.*, 2014).

8.3.4 Chemical or biological sealants

8.3.4.1 *Biofilms*

It is not normal industry practice to attempt to cease fluid conductivity in faults, other than where they cause losses of drilling fluid where they are intersected by wells. Curing lost circulation at the wellbore scale is common practice and there are natural and synthetic products available for this purpose. Providing a large-scale "curtain" barrier to migration is, however, not standard practice and such activities, if practised at all, are not well documented in open file literature.

Microbial biofilms have been shown to be effective at plugging pore channels and thereby forming barriers which reduce flow and mass transport through porous media (Cunningham *et al.*, 2009). Conceptually biofilm barrier technology involves the injection of nutrients (i.e. substrate, electron acceptors, trace nutrients) which stimulate growth of bacteria attached to the surface of porous media. Depending on the microbial populations present, it may be desirable to inject bacterial inocula to encourage desired phenotypic expression—such as the production of extracellular polymer substances (EPS). If EPS production can be stimulated along with cell growth, the resulting biomass will plug the free pore space of the aquifer thereby reducing porosity and hydraulic conductivity (Cunningham *et al.*, 2009).

Due to successful results of biofilm barrier technology in the shallow subsurface, the possibility of using a similar approach for CO₂ leakage mitigation is now being explored (Cunningham *et al.*, 2009). Mitchell *et al.* (2009) has examined the process of biofilm formation and associated permeability reduction in rock cores under environmental conditions representative of sites suitable for CO₂ sequestration. This study describes the use of a unique high pressure (<8.9 MPa), moderate temperature (~32 °C) flow reactor containing a 4.5 x 10⁻¹⁵ m² (46 mD) sandstone core. The flow reactor containing the sandstone core was inoculated with the biofilm forming organism *Shewanella fridgidimarina*, which was recovered from the produced water of an enhanced oil recovery operation. After 825 hours of reactor operation, electron microscopy of the rock core revealed substantial biofilm accumulation in pore channels which resulted in a two order-of-magnitude reduction (approximately 3.9 x 10⁻¹⁶ m² or 0.4 mD) in core permeability (Mitchell *et al.*, 2009). When the core was challenged with scCO₂ for a period of 71 hours the permeability was observed to increase to approximately 3.9 x 10⁻¹⁵ m² (4 mD). Mitchell *et al.* (2009) demonstrates that microbial biofilms can be grown under pressures and temperatures representative of environmental conditions in deep subsurface aquifers which can serve as reservoirs for CO₂ storage. The ability to grow biofilms and reduce permeability under these conditions suggests that it may be possible to plug preferential leakage pathways using microbial biomass in a similar manner to the biofilm barriers used in the shallow subsurface (Cunningham *et al.*, 2009).

If mitigation involves drilling into a fault or damage zone then high flow rates of CO₂ can be expected (c.f. Crystal Springs) and these could lead to well damage and increased, localised leaks. If the aim is to seal fractures by pumping in gels and additives normally used to reduce lost circulation in wells then several wells may be needed, along with large quantities of gel, depending on the size of the zone of intersection of the CO₂ plume with the fracture system; such measures may be impractical but could form a secondary mitigation measure in addition to pressure-reduction by reducing CO₂ injection, or through drilling pressure-reduction wells.

8.3.4.2 Microbially induced calcite precipitation

Biofilm communities in the subsurface are able to actively precipitate calcium carbonate minerals from the ambient Ca²⁺ and HCO₃⁻ in the subsurface water. However, by stimulating native subsurface microbial communities, or by adding specific microorganisms and growth media, we may be able to engineer the biomineralization process in beneficial ways. One feasible mechanism by which to generate calcium carbonate precipitation in the subsurface is by bacterial hydrolysis of urea, known as ureolysis (Cunningham *et al.*, 2009). Ureolysis can occur under dark subsurface conditions and increases bulk solution pH and alkalinity which, in the presence of the common cation Ca²⁺, can induce the saturation and precipitation of CaCO₃, thereby forming a barrier to flow and mass transport in porous media (Cunningham *et al.*, 2009).

Microbially induced calcite precipitation (MICP) offers an engineering option that uses the controlled biofilm growth to achieve targeted calcite precipitation (Hommel *et al.*, 2015). In subsurface applications, this process is typically associated with a reduction of porosity and, even more importantly, of permeability. As an engineering technology, it can be used to alter hydraulic flow conditions and can be applied, for example, to cut off highly permeable pathways such as fractures, faults, or behind-casing defects in boreholes within a geological formation (e.g. Phillips *et al.*, 2013).

Given the recent insight and experimental data on ureolysis and biofilm-hydraulics interactions, the model uncertainty is restricted by the currently insufficient knowledge of those processes and a lack of parameterizations which could crucially improve successful modelling of MICP (Hommel *et al.*, 2015). The difference between the experimental and modelled calcite distributions indicates that at least one relevant process for MICP is not yet implemented in sufficient detail in the conceptual model. Before a more detailed calibration of the numerical model is attempted, the conceptual understanding of all relevant processes, including the biofilm-catalyzed ureolysis, resulting calcite precipitation as well as the interplay of hydraulics and biofilm processes, has to be improved (Hommel *et al.*, 2015).

8.3.4.3 Reactive grout

The use of an aqueous solution that react chemically with CO₂ dissolved in water to produce precipitation for filling pore space and fractures in a similar manner to the MICP process detailed above has been proposed by Ito *et al.* (2014). This proposed solution would require the grout to be injected not just above the leak point but into a wide region surrounding it. Taking these conditions into account, the grout should have the following characteristics; (i) have low frictional pressure during pumping, so as to permeate over a wide region in rock, (ii) after the grout is placed, it should solidify or gel, occluding pores space and (iii) it should be safe for the environment. This concept and the solution are referred to the *in situ* reaction method and the reactive grout, respectively (Ito *et al.*, 2014). Ito *et al.* (2014) investigate the use of an aqueous solution of sodium silicate, Na₂O·3SiO₂, as the reactive grout. The solution is known to react with dissolved CO₂ and produce precipitation of amorphous silica SiO₂ (am). The silicate solution has been widely used as a civil engineering technique to enhance strength and reduce permeability of soil at a shallow depth less than tens of meters deep (Ito *et al.*, 2014).

8.3.5 CO₂ back-production

CO₂ storage is planned to be permanent. However, the back-production of stored CO₂ might be considered as a remediation measure, if the site is less suitable than anticipated (Benson and Hepple, 2005). Theoretically, all stored CO₂ in the formation can be back-produced, except the CO₂ that is stored in the form of mineral trapping. The achievable back-production ratio in real sites, however, is limited by the complex and heterogeneous nature of the geological storage, which is in addition partially known and where various phenomena occur with sometimes very large time scales (Manceau *et al.*, 2014). Partial or total back-production of the injected CO₂ has not been tested yet in CO₂ geological storage sites. Back-production of CO₂ is technically very similar to a leak in an open well, which has been the focus of many studies in the CO₂ geological storage literature using both analytical and numerical models (e.g. Humez *et al.*, 2011). It is also similar to the production of CO₂ from natural CO₂ reservoirs, or to natural gas (possibly from CO₂-rich reservoir) production. Gaseous CO₂ back-production will therefore face similar challenges to natural gas production, and will benefit from the experience of this industry (number and positioning of wells, benefits of horizontal wells, coproduction of brine, etc.) (Manceau *et al.*, 2014). A study of back-production of CO₂ after 15

years of storage in the Utsira formation (Norway) showed that 47.7% of the injected CO₂ can be produced within 7 years of production through a single horizontal well (Akervoll *et al.*, 2009). Back-production of small leakage plumes has also been studied and shows that the removal of small vertical plumes is more effective than the removal of large thin plumes of CO₂ (gravity tongues) at the top of an aquifer, however, this also induces the co-production of large quantities of brine that has to be managed (Esposito and Benson, 2012; Manceau *et al.*, 2014).

9.0 APPLICATION OF FAULT PERMEABILITY REVIEW TO CO₂ STORAGE.

Understanding fault permeability is important for effective containment of CO₂ in the sub-surface and mitigating the risk of CO₂ migration via faults to the atmosphere or into economically valuable resources. The present report reviews fault permeability and this section considers its application to CO₂ storage.

9.1 FAULT ZONE STRUCTURE AND PERMEABILITY

It is clear from the literature that faults generally exhibit extreme internal heterogeneity in structure and permeability. Recognition of this heterogeneity is the first step towards determining what impact faults may have on the effective storage of CO₂. Of particular relevance to CO₂ storage are faults cutting through low permeability strata (i.e., caprocks) that can provide pathways for fluids generated in deep, pressurized rocks to migrate into shallow levels (Miller *et al.*, 2004; Ilg *et al.*, 2012; Hermanrud *et al.*, 2014). One consequence of this variability in permeability is that CO₂ flow along faults will often be channelized. In addition, given the complexity of fault zones predicting where, and on what faults, cross- and along-fault migration of CO₂ is likely to occur will be challenging. Temporal increases in fault permeability arising from increasing pressures due to CO₂ injection may be less challenging to predict using geomechanical considerations and fault seal analysis as the capillary entry pressure of CO₂ is comparable to that of hydrocarbons under some conditions. However, it will be important to understand the different fluid–fluid and fluid–rock reactions associated with CO₂ migration. It is possible that such reactions will be accelerated within fault zones by grain crushing and an associated increase in grain surface area, although further work is required to confirm this in a CO₂ storage context.

9.2 FAULT SEAL AND GEOMECHANICAL PREDICTIONS

Fault seal and geomechanical predictions have been widely used in the CO₂ industry to determine the likelihood of cross and along-fault migration, respectively, during injection. Fault seal algorithms are routinely applied using faults interpreted in seismic reflection lines and stratigraphy from wells. Fault seal provides an indication of likelihood cross-fault flow, which has implications for reservoir CO₂ compartmentalisation and injectivity. Tests of fault seal predictions are relatively rare in the published literature for the petroleum industry and largely absent for CO₂ storage sites. Further research is required to improve the predictive power of the methodology and to determine if (and under what circumstances) low-permeability fault rock poses a substantial risk to CO₂ storage projects.

Geomechanical modelling methods are applied to predict the probability that structural permeability can, or has, developed and whether it can be maintained within the contemporary stress field during CO₂ injection (for further details see IEAGHG, 2015a). Three main geomechanical modelling methods are in common use for predicting the locations of along-fault flow: i) slip tendency, ii) fracture stability and iii) dilation tendency. Each method uses estimates of the stress tensor, fault orientation and fault coefficient of friction to determine the faults, or parts of faults, closest to failure, which are assumed to have the highest permeabilities. Multiple studies of borehole data support the use of the techniques for predicting which fractures will flow under ambient conditions, however, few publications provide independent evidence in support of the predictions at reservoir or regional scales. In addition, a number of publications suggest that non-optimally oriented fracture/faults have unpredicted high permeabilities. Further research may therefore be required to understand better the conditions in which geomechanical predictions of fluid flow along faults is likely to be

of most value for examining potential CO₂ storage sites and the permeability response of reservoirs/caprocks during injection.

9.3 CO₂ NATURAL SEEPS AND FAULT-RELATED FLOW RATES

Natural CO₂ seeps at the ground surface that are interpreted to be facilitated by faults provide information about the potential flux rates of CO₂ in the absence of increased pressures induced by injection. In most of these cases the role of faults is inferred based on elongation of the CO₂ anomalies and their parallelism to, or coincidence with, mapped faults. Analysis of natural CO₂ seeps suggests that even in well managed storage systems migration along faults is possible. Therefore, if faults are present in reservoir and/or caprocks they should be considered as potential migration pathways even where CO₂ injection is not expected to significantly increase reservoir pressures. Analyses of CO₂ seeps in the Paradox Basin support a model in which faults promote the upward flow of CO₂, with the flux rates being greatest where the highest densities of small-scale faults and fractures occur. Flow simulation modelling suggests that low-permeability fault rock may also be an important ingredient for promoting upward flow of CO₂. Independent of where and how faults influence the upward flow of CO₂, the present case studies are likely to be biased towards examples where the flux rates are high and, at best, might provide an indication of the upper-bound of potential rates at CO₂ storage sites. These high rates also indicate that self-sealing by mineral formation cannot necessarily be expected to occur in storage operations where CO₂-rich fluids migrate along faults, particularly on sub-geological timescales. Lastly, the Crystal Geyser “seep” in the Paradox Basin, which formed along an uncased abandoned petroleum exploration well drilled into a “leaky” fault (Little Grand Wash Fault), indicates that it is possible to drill into faults without inducing earthquakes or inducing fault slip. Therefore, targeting faults inferred to be locally promoting CO₂ flow could present a tool for modifying unwanted CO₂ migration and/or relieving reservoir pressures.

9.4 INDUSTRY PRACTICES FOR MITIGATING UNWANTED FLUID FLOW ALONG FAULTS

CO₂ leakage identification, intervention and remediation requires a balance of engineering efficacy, geomechanical assessment and cost-benefit analysis (Zahasky and Benson, 2014). Few measures have been outlined in the published literature to specifically combat along-fault flow at CO₂ storage sites, although techniques such as pressure relief, hydraulic barriers and chemical or biological sealants have received some attention as possible solutions. At the present time the proposed techniques have not been extensively trialled at CO₂ storage sites, and it is not known how effective they will be for remediating unwanted migration of CO₂ along faults. Injection shutoff or passive remediation is the fastest, easiest, and likely the cheapest method to quickly reduce leakage along faults from a CO₂ storage reservoir. Usually injection shutoff alone is not able to completely stop a leakage. If passive remediation is not sufficient, various hydraulic controls such as water injection or reservoir fluid production can be employed to further reduce leakage rates and trap mobile CO₂. In some cases, water injection alone may be enough to stop current and future CO₂ leakage, especially when the leak is detected early, before a large amount of CO₂ has accumulated close to a fault. Additional hydraulic controls such as reservoir fluid production and water injection below the caprock increase rates of dissolution and thus trapping of CO₂ in the storage reservoir (Zahasky and Benson, 2014).

Fluid-flow simulation studies that incorporate faults are an important tool for improving the assessment of potential risk of undesirable flow and reservoir performance during CO₂ injection operations. The outputs of the models are non-unique and can be influenced by significant uncertainty of the geologic input parameters (e.g. fault permeabilities). Geological uncertainties will probably be large for models constructed to predict reservoir performance

before data or injection wells are drilled (as is often the case in the CO₂ industry). Incorporating a range of faulting scenarios and alternative parameter values will be essential for testing the sensitivity of CO₂ migration where the input parameters carry large uncertainty.

10.0 KNOWLEDGE GAPS AND CHALLENGES FOR UNDERSTANDING CO₂ MIGRATION ALONG FAULTS

Fault permeability is an important issue in the effective development and management of storage reservoirs following injection of CO₂. Despite the large number of investigations conducted on geological faults and their hydraulic properties, it is clear from the literature review contained in this report (and from many other publications – see references in Sections 2–9) that present understanding is, in many cases, not sufficiently complete to routinely predict when and where faults are likely to influence CO₂ migration. In line with other industries (e.g. petroleum, waste water and geothermal), the CO₂ storage industry is presently reliant on numerical flow simulation and geomechanical models for predicting the potential migration of CO₂. Interpretation of these models is generally undertaken in the knowledge that the results can incorporate significant uncertainty arising from a number of factors including limited understanding of; heterogeneities in fault geometries and fault-zone permeabilities, spatial and temporal variations in stress conditions, fault rock properties, the scaling of outcrop fault properties (centimetre-metre scales) to modelling scales (e.g. >100 m), and sub-seismic faults. As a result of these knowledge gaps we would question whether flow simulation and geomechanical models contain sufficient information to adequately describe CO₂ migration in faulted reservoir and seal rocks. Estimating the permeability of faults is routinely achieved in the petroleum and water management sectors, where the effects of pressure transients introduced into the subsurface by wells producing or injecting gas, oil, or water fluids is monitored and the results interpreted in terms of aggregate permeability properties of intervening faults. However, many of these data do not reach the public domain and, as a consequence, empirical data constraining the hydraulic properties of fault zones is relatively rare. Similarly, published examples of direct measurements of *in situ* fluid flow rates within fault zones is less common than might be expected given the importance of such data for the petroleum, water (extraction and disposal), geothermal and CO₂ storage industries. These knowledge gaps and limitations in the available data, together with their implications for fault permeability and CO₂ migration, are briefly discussed in this section.

10.1 FAULT GEOMETRY, SCALING AND PERMEABILITY

In some cases the fault damage zone model, where a central low-permeability core is enclosed in a halo of fractures that may locally elevate permeability (e.g. Caine *et al.*, 1996), has useful application. However, it is widely acknowledged that the distribution of low-permeability fault rock, small-scale faults adjacent to the fault rock and displacement (or shear) within fault zones are highly heterogeneous (Wallace and Morris, 1986; Caine *et al.*, 1996; Childs *et al.*, 1996; Childs *et al.*, 2009; Faulkner *et al.*, 2010). These heterogeneities are reflected in variations of fault zone (and fault rock) thickness and the distribution of small-scale faults across individual fault zones (Childs *et al.*, 2009; Faulkner *et al.*, 2010; Faulkner *et al.*, 2011; Savage and Brodsky, 2011). Except in rare cases (e.g. Childs *et al.*, 1997 clay smear model) present understanding of variations in fault-zone architecture and permeability is limited to a two-dimensional perspective. While such two-dimensional data improve understanding of fault-zone architecture and permeability, the flow of fluids is a three-dimensional process which demands a volumetric understanding of rock permeability. Therefore, a better understanding of the three-dimensional heterogeneity of faults is required. In particular, we presently lack the three-dimensional quantitative descriptions of faults necessary to build numerical models of fault-zone permeability. In the absence of empirical flow data these models are a pre-requisite to examine the role of heterogeneous fault permeability on CO₂ migration.

In many cases fault-size distributions are fractal (e.g. Scholz and Cowie, 1990; Walsh and Watterson, 1991; Gillespie *et al.*, 1993; Bailey *et al.*, 2005). Fractal fault systems comprising seismically-resolvable faults will contain many more sub-seismic faults. Whether such sub-seismic faults are present, where they are located and what impact they might have on the migration of CO₂ are all questions that need to be addressed at individual storage sites. The locations and geometries of larger faults in CO₂ storage reservoirs are primarily determined using seismic-reflection lines, and in the case of three-dimensional seismic data, seismic attribute cubes (e.g. coherence) (e.g. Jolley *et al.*, 2007). In many fault systems small sub-resolution faults are likely to be clustered near the larger faults, however, their precise locations will be uncertain. The largest of these sub-seismic faults can be incorporated into flow simulations and in some cases are found to have a minimal impact on the lateral migration of hydrocarbons during full-field production (Manzocchi *et al.*, 2010). Further investigations are required however, to examine the influence of these small faults on both lateral and vertical, or up-sequence flow. In particular, consideration should be given to small faults (e.g. with displacements smaller than the seal thickness that pass from reservoir to caprocks and may reduce seal integrity). These small faults have proved important for injected CO₂ migration at In Salah (Rinaldi and Rutqvist, 2013) where reservoir permeabilities are relatively low (e.g. < 2 x 10⁻¹⁴ m² or 20 mD) but whether this is also the case at CO₂ storage sites dominated by higher reservoir permeabilities requires investigation. If these smaller faults prove important for reservoir compartmentalisation and caprock integrity, then developing techniques that reduce fault-detection thresholds may prove beneficial for improved understanding of fault systems and potential migration pathways.

10.2 CROSS-FAULT PERMEABILITY PREDICTION

Faults may represent barriers to lateral flow and could compartmentalise CO₂ storage containers, modify CO₂ dispersal after injection and/or reduce reservoir permeability. Cross-fault permeability prediction is based on the recognition that fault zones typically comprise low-permeability fault rock (also referred to as fault gouge or fault core) which, on timescales of days to years, has the ability to impede the lateral flow of fluids (e.g. Yielding *et al.*, 1997; Manzocchi *et al.*, 1999; Manzocchi *et al.*, 2002; Yielding, 2002; Manzocchi *et al.*, 2010; Yielding *et al.*, 2010). Prediction of cross-fault permeability is typically based on the use of clay-smear algorithms, which were largely developed for, and by, the petroleum industry over the last 30 years (see Table 4.1 and Section 4). These algorithms use measures of the thickness or proportion of shale/mudstone strata in the faulted sequence and fault displacement to estimate the clay content within the fault zone from which permeability can be inferred (e.g. Fisher and Knipe, 2001; Childs *et al.*, 2002; Jolley *et al.*, 2007). The utility of these algorithms is supported by the positive relationships between predicted clay in fault zones and across fault pressure difference, hydrocarbon column height or capillary threshold pressure (Yielding, 2002; 2012). Despite these correlations a number of questions remain around the production of low-permeability fault rock and the interpretation of the results of clay-smear analysis, and these are outlined below.

Whilst the clay-smear algorithms offer the prospect of capturing variable fault-zone clay content (and permeability), it remains uncertain whether this variability is sufficient to account for that observed at outcrop scale within fault zones. Clay smears can vary enormously in geometry and thickness and often do not adhere to the general model in which clay smears are thickest and most clay-rich proximal to the source bed. Fault-seal prediction algorithms can be used for multiple clay smear scenarios, yet few detailed studies have been published in which the output of algorithms have been tested against field examples of clay smears. Clay-smear amalgamation, whether it influences variations in the thickness of low permeability fault

rock and the extent to which it impacts on fault seal (and fault rock thickness), has also not been widely examined in the literature. Few studies have attempted to quantify these variations in fault rock thickness and their relations to source beds. Of particular importance will be to improve understanding of the spatial distribution of holes or thin points in clay smears over fault surfaces and the processes that result in the generation of these 'weak' points. The distribution and frequency of these 'holes' will influence the fault-seal capacity and is presently poorly understood.

Many studies present excellent examples of clay smear without providing quantitative data on the frequency of these smears. At present the clay-smear algorithms assume that all mudstone beds in a faulted sequence will, to some extent, be incorporated into the fault zone and contribute to a reduction in fault permeability. If this assumption is not correct and all clay beds do not produce clay smear, then the algorithms could over-predict the sealing potential of faults. Such over-estimates may not occur in circumstances where fault rock is generated by additional mechanisms to clay smear. Many studies reveal the presence of fault rock generated by cataclasis or grain-size reduction due to grain crushing during fault slip. Cataclasis is widely acknowledged to be an important process, yet it is not explicitly incorporated into the algorithms for estimating the sealing potential of fault zones. In the absence of detailed studies relating fault-rock permeability and thickness to the mechanism that produced it (e.g. cataclasis or clay smear), it remains uncertain whether the models developed to account for the production of fault rock replicate nature closely enough to routinely provide information about fault-seal potential. In particular, it is important to determine under what geological conditions and for what rock types cataclasis could be important for fault seal prediction?

As is the case for many aspects of fault permeability prediction estimates of cross-fault permeability are based on models constructed using outcrop-scale observations which are assumed to apply to fault-seal analysis at larger scales, yet the scale independence of smear has not been widely demonstrated. Similarly, few studies of clay smear on strike-slip or reverse faults have been published. In the absence of studies on strike slip and reverse faults it is generally assumed that observations for normal faults apply to all fault types.

10.3 ALONG-FAULT PERMEABILITY PREDICTION

Over the last 100 years a significant body of anecdotal evidence has been gathered to suggest that faults can locally enhance the flow of fluids (e.g. Wallace and Morris, 1986; Hooper, 1991; Shipton *et al.*, 2004; Wibberley *et al.*, 2008; Faulkner *et al.*, 2010). Despite this long history of research, few studies present empirical fluid flow data to test the models. These models take three forms; i) Qualitative fault geometry models in which flow is inferred to be localised at fault irregularities (e.g. fault bends, fault intersections, fault relays), where high densities of small-scale faults might be expected to produce wide fault zones (e.g. Cox, 1999; Sanderson and Zhang, 1999; Kim *et al.*, 2004; Wibberley *et al.*, 2008; Faulkner *et al.*, 2010. ii) Geomechanical models which use information on fault properties, fault geometry and the stress tensor to estimate which faults, or parts of fault are close to failure, and therefore where flow is most likely (e.g. Morris *et al.*, 1996; Ferrill and Morris, 2003). iii) Numerical flow simulators in which the hydraulic properties of faults and the faulted sequence are assigned a range of permeabilities (e.g. Tillner *et al.*, 2013; Jung *et al.*, 2014a; Rinaldi *et al.*, 2014). Geometric fault permeability models are not presently widely adopted by the CO₂ industry, which is partly because the model is qualitative and, given its subjectivity, cannot be easily incorporated into flow simulations. Further investigations are required to transform the geometric model into a quantitative methodology which can be objectively tested. By contrast, geomechanical and

flow simulator modelling have been widely adopted by fluid injection and extraction industries and their uncertainties are discussed below.

10.3.1 Geomechanical modelling

A number of geomechanical methods have been proposed for the prediction of along-fault flow (Section 5). The different methods use similar theory, input data and assumptions to predict the faults or parts of faults that are critically stressed (i.e. close to failure) and assumed to be sites of preferential along-fault flow. The theory underpinning the methods is widely accepted, however, the assumption that critically stressed faults are mostly likely to accommodate fluid flow requires further testing. Over the last 20 years numerous studies have been published in which temperature logs, spinner log and borehole images have been combined in support of the conclusion that the majority of hydraulically conductive faults/fractures are critically stressed (e.g. Barton *et al.*, 1995; Barton *et al.*, 1998; Evans *et al.*, 2005; Davatzes and Hickman, 2009; 2010; McNamara *et al.*, 2015). Equally a number of studies present empirical flow data which appears to contradict geomechanical modelling results and raise questions over the universal utility of the techniques (e.g. Dyke, 1995; Laubach *et al.*, 2004; Ameen *et al.*, 2012; Davidson *et al.*, 2012; Hemmings-Sykes, 2012; Sathar *et al.*, 2012; Ameen, 2014; Seebeck *et al.*, 2014; Cuss *et al.*, 2015). Therefore, the primary unknown is how effective are geomechanical techniques for predicting the locations of along-fault flow? When does the technique work and why? Those that have questioned the utility of the technique have raised concerns about whether the input data are sufficiently detailed for fluid flow prediction purposes. In particular, the following factors may influence the validity of the predictions and may require further consideration:

- Outcrop data suggests that locally fault surfaces within fault zones can vary in strike from the average value by up to 30°. In these circumstances fault geometries estimated from seismic reflection data, for example, are unlikely to capture the full range of possible slip surface orientations. In such cases it is possible some critically stressed slip surfaces will be overlooked while elsewhere parts of fault surfaces inferred to be critically stressed may be dominated by stable slip surfaces.
- Frictional properties of sediments and rocks have been studied extensively for civil engineering projects and hydrocarbon production. Despite these observations few data are generally available to constrain the mechanical properties of fault rock at individual CO₂ storage sites which can lead to simplification of the fault strength and frictional properties over the fault surface. In particular, faults within caprock could have different mechanical properties to those in reservoir rocks. Models that consider only the shear failure envelope as the stability criterion (e.g. Mohr-Coulomb failure), have limitations when applied to possible ductile deformation and slow slip (aseismic events). Insufficient information on fault properties may impact reliable geomechanical modelling and should be carefully assessed.
- In-situ stresses may vary in magnitudes and orientations over an individual fault surface or between faults. In many cases the *in situ* stress field is approximated using information from a limited number of wells and may not describe the inherent variability. This variation in stresses may be particularly pronounced across the primary faults or the main lithologic boundaries (e.g. from reservoir to caprocks), which have the potential to support pore pressure differences. Local changes in pore pressures are also likely to arise from CO₂ injection and will further complicate the stress conditions.

- Rheology of the host rock containing faults will have an impact on the rock response to CO₂ injection. In particular, soft caprocks may respond differently to increases in pressure than sandstone-dominated reservoir rocks. These rheological differences should be examined using geomechanical data to help develop geomechanical context for seal failure to provide guidance for CO₂ site selection.

10.4 FLOW SIMULATION MODELS

Fault zones are complex and can be responsible for tortuous CO₂ flow paths. Although the full extent of this fault zone complexity has not been quantified, sufficient information is presently available to begin to include some of this heterogeneity in flow models (e.g. Tenthorey *et al.*, 2014). Producing flow models that preserve these fault-zone complications is an important first step for addressing the question of whether they are necessary for models to match empirical data. If permeability fault zone heterogeneities are an important component of simulation models, then consideration should be given as to how to implement these complexities in a practical way. While fault rock thicknesses are known to vary by as much as three orders of magnitude on a fault of a given displacement, there are practically no data expressing the variability in thickness over fault surfaces or the correlation lengths of this variability. In this sense, modern structural and fault seal analysis and modelling is guiding the next generation of questions that need to be answered through more focused outcrop studies. Several studies have attempted to incorporate variable fault-zone properties in three dimensions over fault surfaces (e.g. Harris *et al.*, 2007; Manzocchi *et al.*, 2008), however, these studies have not resulted in common conclusions. More similar studies are required to examine how faults with a range of sizes and permeability structures modify flow in sequence with a range of stratigraphic architectures.

As is the case for geomechanical models, flow simulations require empirical data to test and validate the models. While the literature includes a number of well documented case studies (see review in Manzocchi *et al.*, 2010), development of the models and improvement of the modelling techniques is hampered by a paucity of well-documented flow simulation models for fluid extraction/injection industries. The true test and value of the methods is in their capacity to replicate and ultimately predict the effects of faults on fluid flow in the subsurface. Data to conduct these tests are available within petroleum companies, and although retrospective studies are sometimes conducted, the results of these studies are generally considered to provide a competitive advantage and therefore often remain confidential. Bridging knowledge gaps of fault permeability at CO₂ storage sites will benefit from a more cooperative approach to empirical data sharing and modelling than appears to have been common in the petroleum sector.

10.5 IN SITU FAULT PERMEABILITY AND FLOW RATES

The rates of fluid flow along faults can vary spatially and temporally. Flow rates and fault permeabilities are controlled by a range of factors including, fault-zone architecture and orientations, pore pressures, pressure gradients and fluid supply rates. The migration rates of CO₂ are likely to be site and fault specific and vary by at least four orders of magnitude within a given fault system. The permeability and flow rate data are invaluable for understanding the potential migration rates of injected CO₂; however, the data are relatively sparse. The limited quantity of data and, in some cases, the paucity of information on fault attributes (e.g. locations, detailed geometries, fault zone architecture, fault rock types) and/or flow rates make it difficult to draw firm conclusions about the relationships between faulting and flow rates. These limitations are potentially compounded by censoring of the flow-rate data, which results in a

bias in the observations towards flow rates at the high end of the possible range. Therefore, flow data from natural analogues are more likely to provide an indication of the maximum flow possible, rather than a measure of what might be likely.

10.6 CO₂ CONTAINMENT MANAGEMENT

Ensuring that a CO₂ plume does not extend beyond predefined limits is likely to be a key component of storage site management. Such a management programme requires predictions to be made prior to injection for the location and growth of the plume. Departures from these predictions form a basis for identifying a series of mitigation actions (e.g. introduction of water injection and/or production wells, reduction of CO₂ injection rates, and cessation of injection), that may be undertaken to arrest the undesirable spread of CO₂. Faster than expected migration of CO₂ laterally and/or vertically may arise for a number of reasons including; the presence of high permeability streaks in the stratigraphy, high permeability channels along fault zones and leakage along abandoned wells. While the availability and quality of 3D seismic reflection may mean that faults with vertical displacements as low as 4–5 m can be resolved in potential reservoirs/caprocks, it seems unlikely given our present state of knowledge that we could predict which faults (and parts of faults) will provide local conduits for CO₂ flow. In the absence of quantitative information on the permeability structure of faults in general and, a likely paucity of data on individual faults at specific storage sites, uncertainty remains about how faults should be modelled in flow simulators and the associated risks managed. In the absence of information on fault permeability it is common to adopt two end-member scenarios. These models are; i) that CO₂ flow will be elevated over the entire surface of all mapped faults or, ii) that faults are impermeable barriers to both lateral and vertical flow. Neither of these models captures the heterogeneity of flow inferred from outcrop fault studies and they may over-estimate or underestimate the importance of faulting for migration. The virtue of these end-member models is that they can place limits on what is possible in migration terms assuming that the thicknesses and permeabilities of fault zones are realistic.

Alternative approaches to running fluid flow simulations would be to avoid seismically-resolved faults or to recognise that modelling the migration of CO₂ along faults carries large uncertainties (dictated by the financial and technical constraints of a project), and to focus on monitoring the plume as closely as possible. A number of geophysical techniques including, 4D seismic reflection, down-hole pressure measurement, well tracer measurements, gravity, and induced seismicity have been successfully used to track the first-order location of injected CO₂ plumes (e.g. Chadwick *et al.*, 2009; Chadwick *et al.*, 2014; Jenkins *et al.*, 2015). However, these geophysical techniques are unlikely to have sufficiently high resolution to record the migration of CO₂ within fault zones that are highly fractured and probably less than a few 10's of metre wide. One potential technique for tracking CO₂ migration along faults is to position chemical tracer sampling stations within key fault zones. The cost of such monitoring is likely to be high and may only be initiated when undesirable migration thresholds have been reached. However, given the channelized nature of fluid flow often inferred for fault zones, it is possible that sample wells may miss injected fluids migrating along fault zones. Independent of the likely success of such wells, both the sampling strategies and what constitutes undesirable migration should be established before injection. Although the sampling strategies and what is deemed undesirable CO₂ migration is likely to vary between sites, general guidelines for managing potential migration along faults and mitigating risk may be desirable.

11.0 RECOMMENDATIONS FOR FUTURE RESEARCH

The CO₂ storage industry is reliant on numerical flow simulation and geomechanical models for establishing migration scenarios along and across faults (e.g. Tsang *et al.*, 2007; Rutqvist, 2012; Tillner *et al.*, 2013; Jeanne *et al.*, 2014; Rinaldi *et al.*, 2014). The use of such models to examine the role of faults on CO₂ migration is consistent with best practice across a range of industries including, petroleum, waste water and geothermal. The outputs from these models constrain CO₂ migration and, with the increase in computing power over the last 20 years, permit sensitivity testing of the results by modification of the fault and stratigraphic input parameters. However, as is the case with all modelling, interpretation of the results requires an understanding of the input parameter uncertainties and the ability of these parameters to describe the processes arising from CO₂ injection. The recommendations outlined below fall into three main categories; i) improved definition and quantification of fault hydraulic properties, ii) developing and sensitivity testing flow simulator models and geomechanical flow predictions, and iii) testing and validating these models using empirical fluid flow observations from fault zones.

11.1 FAULT ZONE GEOMETRIES AND PERMEABILITY

Faults are widely acknowledged to locally modify rock permeability and may enhance or retard the flow of fluids including supercritical CO₂ (e.g. Manocchi *et al.*, 1999; Odling *et al.*, 1999; Manocchi *et al.*, 2008; Wibberley *et al.*, 2008; Manocchi *et al.*, 2010). A plethora of mainly two-dimensional studies support the view that both the internal structure and hydraulic properties of fault zones vary in space and time (Childs *et al.*, 2009; Faulkner *et al.*, 2010; Nicol *et al.*, 2013a; Awdal *et al.*, 2014). These studies generally focus on rock types that form reservoirs (e.g. sandstones or interbedded sandstones and mudstone), and suggest that an individual fault may synchronously represent a barrier and conduit to flow. While algorithms based on empirical data have been developed for cross-fault permeability, few techniques are presently available for producing quantitative predictions of along-fault permeability. Future deterministic studies are required to improve estimates of the magnitudes of permeability and the spatial distributions of high and low permeability fault zone material in three dimensions over fault surfaces. Quantitative analysis and modelling of faults within siliciclastic sequences provides a basis for addressing recurring issues related to flow in faulted reservoirs and caprocks, such as near-fault reduction of CO₂ injectivity, unexpected CO₂ migration into (or through) caprock, and non-optimal drilling strategies for developing storage sites.

To improve understanding of the geometric and hydraulic properties of faults studies of fault outcrop, analogue and numerical models are required. Analogue and numerical modelling (e.g. discrete element models – DEM) provide powerful tools for describing the geometry and formation of fault zones. In particular, modelling can be used to determine the conditions under which high and low permeability rock volumes form in fault zones and have the potential to impact CO₂ migration. Outcrop and model information should be used to address the following:

- i. Determine the structure, content and permeability of fault zones within reservoirs and caprocks.
- ii. Quantify the locations and frequency of holes in low permeability fault rock.
- iii. Quantify the geometries, locations, frequencies, permeabilities and connectivity of high permeability bodies within fault zones.
- iv. Improve understanding of the processes and parameters that result in the generation of low permeability and high permeability fault-zone rock to facilitate the development of more accurate predictive fluid-flow models.

- v. Determine how stratigraphic sequence architecture influences fault development and fault permeability.
- vi. Determine whether the hydraulic properties of faults are scale-dependent, to what extent outcrop scale observations are applicable for seismic-scale faults and whether there are threshold fault sizes below which faults will have a minimal impact on reservoir pressure together with CO₂ and brine migration.

These studies should be designed to assist CO₂ storage operators to quantify fault zone permeability data and to develop CO₂ flow rate statistics from deterministically defined analogues and by performing sensitivity testing of flow modelling along faults.

11.2 FAULT STRUCTURE IN CAPROCKS

It is important to determine under what circumstances, and to what extent, faults in caprock would increase its bulk permeability and reduce the ability of potential reservoirs to store CO₂ for 1000 years or more. Core samples from these mudstone units can provide key information about their sealing capacity, however, where the seal is fractured, faulted or penetrated by disused wells, the bulk permeability of the caprock may be significantly different to that measured from core plugs. Although faults in caprocks could have important implications for seal integrity, such faults have not been widely studied and data on these faults in the literature is limited in quantity. Given the rheological differences between sandstones (reservoir) and mudstones (caprock), the permeabilities and geometries of fracture networks may change from one rock type to another. Thus, in order to produce robust flow models which include both reservoirs and caprocks, faults in mudstones should be examined under a range of geomechanical conditions. Investigations of faults in mudstones will have particular benefit for CO₂ storage where caprock integrity is paramount for effective sequestration.

To address the question of where and how faults will impact bulk permeabilities of caprocks, faulted mudrocks should be examined over a range of scales (e.g. using outcrop, drillhole core and FMI data, and seismic reflection lines). Given the low permeabilities of caprocks on the scale of individual core plugs, for example, faults will likely have a disproportionate impact on flow localisation and associated flow rates through seals. Therefore, emphasis of these studies should be placed on the quantitative analysis of structures which are pertinent to fluid flow, in particular conductive fluid flow. The impact of conductive fault systems on the bulk flow properties of otherwise low permeability rocks is dependent on a variety of parameters including, the aperture distributions and connectivity characteristics of the fault system, and the stress state of the caprock. Given the strongly non-linear links between geometrical characteristics of fracture systems and their impact on fluid flow, future studies should investigate the lithologic, kinematic (strain) and dynamic (stress) parameters that control the formation, geometries and flow properties of faults in caprocks. Collectively these data will permit identification of circumstances in which fluid flow through the caprock is most likely. They will also provide a basis for determining whether the geometries of faults at CO₂ storage sites differ between reservoir and seal rocks. In circumstances where the geometries of fault systems are independent of rock type, data from reservoirs and caprock may be used together to quantify faulting and to parameterise the geometries of faults in flow simulator models. Alternatively, in circumstances where the geometries (e.g. size distributions, intersection relationships, locations and densities) vary between reservoir and caprock these differences should be captured in flow simulator models.

11.3 FLUID FLOW MODELLING AND PREDICTION

Geomechanical modelling, flow simulation modelling (Eclipse, RMS) and reactive transport modelling (TOUGH-2 & FLAC) are important tools for predicting the migration pathways and flow rates of injected CO₂. Models that combine geological architecture of stratigraphy and faults together with dynamic changes in reservoir pressures and fluid chemistry will have particular value for CO₂ storage projects. However, to promote the use and applicability of coupled geology/stress/chemistry/flow models this modelling software should be made more widely available.

Fluid flow models are populated with a range of variables (e.g. fault permeability or transmissibility, pore pressures, stress magnitudes and orientations and fluid composition), which have varying degrees of uncertainty. Given sufficient time and resources it is usual to run a suite of models to examine the sensitivity of CO₂ migration to a range of generic properties of fault systems. The models are often restricted to reservoir or storage container strata, however, it is clear that greater emphasis on caprocks is required to provide some focus in future studies on containment rather than limiting resources on reservoir performance. Improved numerical models (i.e. with reduced uncertainties) require a greater understanding of natural faults and their permeability structure (see Sections 11.1 and 11.2). In addition, it is important to test the output of the models against empirical fluid flow or reservoir production data. History matching is widely used in reservoir production studies (e.g. Rinaldi and Rutqvist, 2013), however, given the large number of variables used in reservoir flow simulations the results of history matches are non-unique.

11.3.1 Geomechanical modelling

Testing the predictions of geomechanical modelling using *in situ* flow measurements is critical for acceptance of the technique, while sensitivity testing of the input parameters is required to understand better the uncertainties of the modelling results. Geomechanical modelling is routinely implemented at potential CO₂ storage sites prior to injection. At such sites future studies should focus on testing the geomechanical predictions of migration along faults. The first-order migration of fluids (e.g. CO₂, potable water or brine) within reservoir/caprock systems may be mapped or inferred using 4D seismic reflection analysis (e.g. Chadwick *et al.*, 2009), induced microseismicity patterns (Julian *et al.*, 2009) and/or cross-hole tracers tests. These tracer tests have been used to construct hydrology tomographic maps to identify reservoir compartmentalisation and low permeability zones (Bense *et al.*, 2013 and references therein), however, like the other monitoring techniques this method primarily provides indirect data on fault permeability and fluid flow rates. Perhaps of greater value would be tracer tests coupled with pressure, temperature, and fluid velocity (spinner log) data from wells which pass through fault zones (or parts of fault zones) that are predicted to be critically stressed. In circumstances that wells were drilled through key fault zones prior to injection they would provide key information on *in situ* fault zone properties (e.g. coefficient of friction, permeability, dimensions), fault stress conditions and flow rates prior to injection, during injection and post injection. In addition to providing data on the response of faults to injection (a key unknown in many cases) these wells could be cited so that tracer studies would provide information on injected CO₂. This type of information is required to test the conditions under which geomechanical modelling has utility.

Detailed studies show fault zones and their associated stresses to be highly heterogeneous. While it is common for geomechanical studies of faults resolved by seismic reflection data to consider uncertainties on the stress tensor and the coefficient of friction, it is rarer for these studies to consider changes in fault strike and/or dip at sub-seismic scales. These changes in

orientation which locally could be up to 30°, together with potential local variations in the stress tensor, could produce uncertainties on the geomechanical predictions. Understanding the magnitudes of these uncertainties and whether they are sufficiently large to alter the interpretations is potentially important and should form the focus of future studies.

11.4 IN SITU FAULT PERMEABILITIES AND FLOW RATES

As noted, permeability and flow rate data are invaluable for understanding the potential migration rates of injected CO₂. The value of these data will increase as more high-quality flow rate and permeability data become available from industry practitioners. Whilst both flow rate and permeability data are presented in this report, a more comprehensive compilation of such data is recommended. In addition to compiling such a dataset and making it available to the CO₂ storage industry, sharing of flow rate and permeability information will prove valuable for the CO₂ industry. In particular, studies drawing on high quality fault and flow rate information are required to improve understanding of fault attributes (e.g. locations, detailed geometries, fault zone architecture, fault rock types and stress state) and their relationships to flow rates. These data will improve knowledge on processes and help improve the predictive power of models.

11.5 RISK ASSESSMENT FOR ALONG-FAULT FLOW

Potential CO₂ storage reservoir/caprock systems that contain faults carry an unknown component of risk associated with unexpected migration or lack of migration and injectivity of CO₂ due to faults. Although it is widely accepted that faults and abandoned wells represent the greatest risks for migration of injected CO₂ beyond the pre-defined bounds of a storage container, there are few guidelines about how they should be treated in a risk assessment framework. This lack of guidelines is perhaps not surprising given that it could be argued that risks associated with faults will be site-specific. However, it could also be argued that in the early stages of site development the flow properties of faults are unlikely to be known and in these circumstances all faults represent a potential risk to injectivity and/or containment. Therefore there is some merit in using the available knowledge (and knowledge gaps) on faults to assist in the risk assessment of faults at CO₂ storage sites. These guidelines could address key questions including: i) under what circumstances and for what size faults should CO₂ plume contact with the fault be avoided, ii) what investigations are required to characterise the flow properties of faults, iii) under what geological and stress conditions are faults likely to constitute a leakage risk, iv) what monitoring of faults are necessary/useful to record along-fault migration, v) what constitutes acceptable levels of migration from the geological container and how do we record these migration rates, and vi) what course of action should be taken if migration exceeds pre-defined limits. Presently, avoidance of large faults during CO₂ injection may be a preferred policy, particularly at sites onshore and close to populated areas. However, in circumstances where faults are considered a low risk for along-fault migration operators may choose not to avoid such faults but to closely monitor the migration of the plume and stress state of the fault. The development of any set of guidelines should be coupled with clearly defined rates of acceptable flow or migration of CO₂ rich fluids together with clear definitions of what constitutes a CO₂-rich fluid. Surface CO₂ flux might not be a good indicator for assessing the possibility of fault leakage (Klusman, 2011; 2015), and the best method for determining leakage from a CO₂ reservoir is likely to be site specific.

12.0 REFERENCES

- Abrams, M. A. (2005), Significance of hydrocarbon seepage relative to petroleum generation and entrapment, *Marine and Petroleum Geology*, 22(4), 457-477.
- Ake, J., K. Mahrer, D. O'Connell, and L. Block (2005), Deep-injection and closely monitored induced seismicity at Paradox Valley, Colorado, *Bulletin of the Seismological Society of America*, 95(2), 664-683.
- Akervoll, I., E. Lindeberg, and A. Lackner (2009), Feasibility of Reproduction of Stored CO₂ from the Utsira Formation at the Sleipner Gas Field, *Greenhouse Gas Control Technologies* 9, 1(1), 2557-2564.
- Al-Dossary, S., and K. J. Marfurt (2006), 3D volumetric multispectral estimates of reflector curvature and rotation, *Geophysics*, 71(5), P41-P51.
- Allan, U. S. (1989), Model for Hydrocarbon Migration and Entrapment within Faulted Structures, *AAPG Bulletin*, 73(7), 803-811.
- Ameen, M. S. (2014), Fracture and in-situ stress patterns and impact on performance in the Khuff structural prospects, eastern offshore Saudi Arabia, *Marine and Petroleum Geology*, 50, 166-184.
- Ameen, M. S., K. MacPherson, M. I. Al-Marhoon, and Z. Rahim (2012), Diverse fracture properties and their impact on performance in conventional and tight-gas reservoirs, Saudi Arabia: The Unayzah, South Haradh case study, *AAPG Bulletin*, 96(3), 459-492.
- Annunziatellis, A., S. E. Beaubien, G. Ciotoli, and S. Lombardi (2004), A comparison of leaking and non-leaking CO₂ reservoirs as natural analogues for geological CO₂ sequestration (Sesta and Latera geothermal fields, central Italy), paper presented at 32nd International Geological Congress, International Geological Congress, Florence, Italy.
- Annunziatellis, A., S. E. Beaubien, S. Bigi, G. Ciotoli, M. Coltella, and S. Lombardi (2008), Gas migration along fault systems and through the vadose zone in the Latera caldera (central Italy): Implications for CO₂ geological storage, *International Journal of Greenhouse Gas Control*, 2(3), 353-372.
- Arts, R. J., J. L. Baradello, J. F. Girard, G. Kirby, S. Lombardi, P. Williamson, and A. Zaja (2009), Results of geophysical monitoring over a "leaking" natural analogue site in Italy, *Energy Procedia*, 1, 2269-2276.
- Astorri, F., S. E. Beaubien, G. Ciotoli, and S. Lombardi (2002), An assessment of gas emanation hazard using a geographic information system and geostatistics, *Health Phys*, 82, 358-366.
- Awdal, A., D. Healy, and G. I. Alsop (2014), Geometrical analysis of deformation band lozenges and their scaling relationships to fault lenses, *Journal of Structural Geology*, 66, 11-23.
- Aydin, A. (2000), Fractures, faults, and hydrocarbon entrapment, migration, and flow, *Marine and Petroleum Geology*, 17, 797-814.
- Aydin, A., and Y. Eyal (2002), Anatomy of a normal fault with shale smear: Implications for fault seal, *AAPG Bulletin*, 86(8), 1367-1381.
- Baer, J., and J. Rigby (1978), Geology of the Crystal geyser and environmental implications of its effluent, Grand County, Utah, *Utah Geology*, 5, 125-130.
- Bailey, W. R., J. J. Walsh, and T. Manzocchi (2005), Fault populations, strain distribution and basement fault reactivation in the East Pennines Coalfield, UK, *Journal of Structural Geology*, 27(5), 913-928.

- Baisch, S., R. Weidler, R. Voros, D. Wyborn, and L. de Graaf (2006), Induced seismicity during the stimulation of a geothermal HFR reservoir in the Cooper Basin, Australia, *Bulletin of the Seismological Society of America*, 96(6), 2242-2256.
- Baisch, S., R. Voros, E. Rotherth, H. Stang, R. Jung, and R. Schellschmidt (2010), A numerical model for fluid injection induced seismicity at Soultz-sous-Forets, *International Journal of Rock Mechanics and Mining Sciences*, 47(3), 405-413.
- Balberg, I., B. Berkowitz, and G. E. Drachler (1991), Application of a Percolation Model to Flow in Fractured Hard Rocks, *Journal of Geophysical Research-Solid Earth and Planets*, 96(B6), 10015-10021.
- Ballas, G., H. Fossen, and R. Soliva (2015), Factors controlling permeability of cataclastic deformation bands and faults in porous sandstone reservoirs, *Journal of Structural Geology*, 76, 1-21.
- Bandis, S., A. C. Lumsden, and N. Barton (1983), Fundamentals of rock joint deformation, *International Journal of Rock Mechanics and Mining Sciences & Geomechanics Abstracts*, 20(6), 249-268.
- Barr, D. (2007), Conductive faults and sealing fractures in the West Sole gas fields, southern North Sea, in *Structurally Complex Reservoirs*, edited by S. J. Jolley, D. Barr, J. J. Walsh and R. J. Knipe, pp. 431-451, Geological Society, London, Special Publications, 292.
- Barton, C., D. Moos, L. Hartley, S. Baxter, L. Foulquier, H. Holl, R. Hogarth, and A. Brisbane (2013), Geomechanically coupled simulation of flow in fractured reservoirs, paper presented at Proceedings, Thirty-Eighth Workshop on Geothermal Reservoir Engineering, Stanford Univ., Stanford, Calif.
- Barton, C. A., and M. D. Zoback (1994), Stress Perturbations Associated with Active Faults Penetrated by Boreholes - Possible Evidence for near-Complete Stress Drop and a New Technique for Stress Magnitude Measurement, *Journal of Geophysical Research-Solid Earth*, 99(B5), 9373-9390.
- Barton, C. A., M. D. Zoback, and D. Moos (1995), Fluid-Flow Along Potentially Active Faults in Crystalline Rock, *Geology*, 23(8), 683-686.
- Barton, C. A., S. H. Hickman, R. Morin, M. D. Zoback, and D. Benoit (1998), Reservoir-scale fracture permeability in the Dixie Valley, Nevada, geothermal field, paper presented at SPE/ISRM Rock Mechanics in Petroleum Engineering, Society of Petroleum Engineers.
- Bastiaens, W., F. Bernier, and X. L. Li (2007), SELFRAC: Experiments and conclusions on fracturing, self-healing and self-sealing processes in clays, *Physics and Chemistry of the Earth*, 32(8-14), 600-615.
- Batir, J. F. (2011), Stress field characterization of the Hellisheidi geothermal field and possibilities to improve injection capabilities, University of Iceland and University of Akureyri, Iceland.
- Becker, S. P., P. Eichhubl, S. E. Laubach, R. M. Reed, R. H. Lander, and R. J. Bodnar (2010), A 48 m.y. history of fracture opening, temperature, and fluid pressure: Cretaceous Travis Peak Formation, East Texas basin, *Geological Society of America Bulletin*, 122(7-8), 1081-1093.
- Bense, V. F., and M. A. Person (2006), Faults as conduit-barrier systems to fluid flow in siliciclastic sedimentary aquifers, *Water Resources Research*, 42(5).
- Bense, V. F., T. Gleeson, S. E. Loveless, O. Bour, and J. Scibek (2013), Fault zone hydrogeology, *Earth-Science Reviews*, 127, 171-192.
- Benson, S., and R. Hepple (2005), Prospects for early detection and options for remediation of leakage from CO₂ storage projects, in *Carbon Dioxide Capture for Storage in Deep Geologic Formations*, edited by D. C. Thomas and S. M. Benson, Elsevier Publishing, 2, UK.

- Benson, S. M., R. Trautz, and C. Shan (2006), Sensitivity of pressure monitoring for leak detection, paper presented at Proceedings of the Fifth Annual Conference on Carbon Capture and Sequestration, U.S. National Energy Technology Laboratory, Alexandria, Virginia, USA.
- Bentley, M. R., and J. J. Barry (1991), Representation of fault sealing in a reservoir simulation: Cormorant Block IV, UK North Sea, paper presented at 66th Annual Technical Conference & Exhibition of the Society of Petroleum Engineers, Dallas, Texas.
- Berkowitz, B., O. Bour, P. Davy, and N. Odling (2000), Scaling of fracture connectivity in geological formations, *Geophysical Research Letters*, 27(14), 2061-2064.
- Bickle, M., and N. Kampman (2013), Lessons in carbon storage from geological analogues, *Geology*, 41(4), 525-526.
- Bickle, M. J. (2009), Geological carbon storage, *Nature Geoscience*, 2(12), 815-818.
- Bigi, S., M. Battaglia, A. Alemanni, S. Lombardi, A. Campana, E. Borisova, and M. Loizzo (2013), CO₂ flow through a fractured rock volume: Insights from field data, 3D fractures representation and fluid flow modelling, *International Journal of Greenhouse Gas Control*, 18, 183-199.
- Birkholzer, J. T., C. M. Oldenburg, and Q. L. Zhou (2015), CO₂ migration and pressure evolution in deep saline aquifers, *International Journal of Greenhouse Gas Control*, 40, 203-220.
- Bissell, R. C., D. W. Vasco, M. Atbi, M. Hamdani, M. Okwelegbe, and M. H. Goldwater (2011), A Full Field Simulation of the In Salah Gas Production and CO₂ Storage Project Using a Coupled Geo-mechanical and Thermal Fluid Flow Simulator, *10th International Conference on Greenhouse Gas Control Technologies*, 4, 3290-3297.
- Blake, K. (2013), Stress analysis for boreholes on Department of Defence lands in the western United States: A study in stress heterogeneity, paper presented at 38th Workshop on Geothermal Reservoir Engineering, Stanford University, Stanford, California.
- Boles, J. R., P. Eichhubl, G. Garven, and J. Chen (2004), Evolution of a hydrocarbon migration pathway along basin-bounding faults: Evidence from fault cement, *AAPG Bulletin*, 88(7), 947-970.
- Bonini, M. (2009), Structural controls on a carbon dioxide-driven mud volcano field in the Northern Apennines (Pieve Santo Stefano, Italy): relations with pre-existing steep discontinuities and seismicity, *Journal of Structural Geology*, 31, 44-54.
- Bour, O., and P. Davy (1997), Connectivity of random fault networks following a power law fault length distribution, *Water Resources Research*, 33(7), 1567-1583.
- Bouvier, J. D., C. H. Kaarssijpesteijn, D. F. Kluesner, C. C. Onyejekwe, and R. C. Vanderpal (1989), 3-Dimensional Seismic Interpretation and Fault Sealing Investigations, Nun River Field, Nigeria, *AAPG Bulletin*, 73(11), 1397-1414.
- Brace, W. F. (1980), Permeability of Crystalline and Argillaceous Rocks, *International Journal of Rock Mechanics and Mining Sciences*, 17(5), 241-251.
- Branquet, Y., B. Laumonier, A. Cheilletz, and G. Giuliani (1999), Emeralds in the Eastern Cordillera of Colombia: Two tectonic settings for one mineralization, *Geology*, 27(7), 597-600.
- Brauer, K., H. Kampf, G. Strauch, and S. M. Weise (2003), Isotopic evidence (He-3/He-4, C-13(CO₂)) of fluid-triggered intraplate seismicity, *Journal of Geophysical Research-Solid Earth*, 108(B2).
- Bretan, P., G. Yielding, O. M. Mathiassen, and T. Thorsnes (2011), Fault-seal analysis for CO₂ storage: an example from the Troll area, Norwegian Continental Shelf, *Petroleum Geoscience*, 17(2), 181-192.

- Brown, A. (2000), Evaluation of possible gas microseepage mechanisms, *AAPG Bulletin*, 84(11), 1775-1789.
- Brown, A. (2003), Capillary effects on fault-fill sealing, *AAPG Bulletin*, 87(3), 381-395.
- Burnside, N. M., Z. K. Shipton, and R. M. Ellam (2007), Using spring deposits to track the evolution of fluid pathways through faults; Little Grand Wash Fault and Salt Wash Graben, Utah, USA, paper presented at GSA Annula Meeting, Geological Society of America, Denver, October 28-31.
- Burnside, N. M., Z. K. Shipton, B. Dockrill, and R. M. Ellam (2013), Man-made versus natural CO₂ leakage: A 400 k.y. history of an analogue for engineered geological storage of CO₂, *Geology*, 41(4), 471-474.
- Byerlee, J. (1978), Friction of Rocks, *Pure and Applied Geophysics*, 116(4-5), 615-626.
- Byerlee, J. (1993), Model for episodic flow of high-pressure water in fault zones before earthquakes, *Geology*, 21(4), 303-306.
- Caine, J. S., J. P. Evans, and C. B. Forster (1996), Fault zone architecture and permeability structure, *Geology*, 24(11), 1025-1028.
- Canamarra, G., P. Fietzek, and M. Maroto-Valer (2011), Monitoring techniques of a natural analogue for sub-seabed CO₂ leakages, *Energy Procedia*, 4, 3262-3268.
- Canet, C., R. M. Prol-Ledesma, E. Escobar-Briones, C. Mortera-Gutierrez, R. L. S. Cruz, C. Linares, E. Cienfuegos, and P. Morales-Puente (2006), Mineralogical and geochemical characterization of hydrocarbon seep sediments from the Gulf of Mexico, *Marine and Petroleum Geology*, 23(5), 605-619.
- Canet, C., R. M. Prol-Ledesma, P. R. Dando, V. Vazquez-Figueroa, E. Shumilin, E. Birosta, A. Sanchez, C. J. Robinson, A. Camprubi, and E. Tauler (2010), Discovery of massive seafloor gas seepage along the Wagner Fault, northern Gulf of California, *Sedimentary Geology*, 228(3-4), 292-303.
- Capaccioni, B., F. Tassi, O. Vaselli, D. Tadescio, and R. Poreda (2007), Submarine gas burst at Panarea Island, (southern Italy) on 3 November 2002: A magmatic versus hydrothermal episode, *Journal of Geophysical Research*, 112, B05201.
- Caramanna, G., P. Fietzek, and M. Maroto-Valer (2011), Monitoring techniques of a natural analogue for sub-seabed CO₂ leakages, *Energy Procedia*, 4, 3262-3268.
- Carruthers, D., and P. S. Ringrose (1998), Secondary oil migration: oil-rock contact volumes, flow behaviour and rates, in *Dating and Duration of Fluid Flow and Fluid-Rock Interaction*, edited by J. Parnell, pp. 205-220, Geological Society, London, Special Publication, 144.
- Cartwright, J. (2011), Diagenetically induced shear failure of fine-grained sediments and the development of polygonal fault systems, *Marine and Petroleum Geology*, 28(9), 1593-1610.
- Cartwright, J., M. Huuse, and A. Aplin (2007), Seal bypass systems, *AAPG Bulletin*, 91(8), 1141-1166.
- Cartwright, J. A., B. D. Trudgill, and C. S. Mansfield (1995), Fault Growth by Segment Linkage - an Explanation for Scatter in Maximum Displacement and Trace Length Data from the Canyonlands Grabens of Se Utah, *Journal of Structural Geology*, 17(9), 1319-1326.
- Cavailles, T., R. Soliva, P. Labaume, C. Wibberley, J. P. Sizun, C. Gout, D. Charpentier, A. Chauvet, B. Scalabrino, and M. Buatier (2013), Phyllosilicates formation in faults rocks: Implications for dormant fault-sealing potential and fault strength in the upper crust, *Geophysical Research Letters*, 40(16), 4272-4278.

- Cavarretta, G., G. Gianelli, G. Scandiffio, and F. Tecce (1985), Evolution of the Latera geothermal system II: Metamorphic hydrothermal mineral assemblages and fluid chemistry, *Journal of Volcanology and Geothermal Research*, 26, 337–364.
- Chadwick, R. A., D. J. Noy, and S. Holloway (2009), Flow processes and pressure evolution in aquifers during the injection of supercritical CO₂ as a greenhouse gas mitigation measure, *Petroleum Geoscience*, 15(1), 59-73.
- Chadwick, R. A., B. P. Marchant, and G. A. Williams (2014), CO₂ storage monitoring: leakage detection and measurement in subsurface volumes from 3D seismic data at Sleipner, *12th International Conference on Greenhouse Gas Control Technologies, Ghgt-12*, 63, 4224-4239.
- Chalbaud, C., M. Robin, and P. Egermann (2006), Interfacial tension data and correlations of brine/CO₂ systems under reservoir conditions., in *SPE Annual Technical Conference and Exhibition*, edited, pp. SPE-102918-MS, Society of Petroleum Engineers, San Antonio, Texas, USA.
- Chalbaud, C., M. Robin, J. M. Lombard, F. Martin, P. Egermann, and H. Bertin (2009), Interfacial tension measurements and wettability evaluation for geological CO₂ storage, *Advances in Water Resources*, 32(1), 98-109.
- Chang, C. D., M. D. Zoback, and A. Khaksar (2006), Empirical relations between rock strength and physical properties in sedimentary rocks, *Journal of Petroleum Science and Engineering*, 51(3-4), 223-237.
- Chen, M., T. A. Buscheck, J. L. Wagoner, Y. Sun, J. A. White, L. Chiaramonte, and R. D. Aines (2013), Analysis of fault leakage from Leroy underground natural gas storage facility, Wyoming, USA,, *Hydrogeology Journal*, 21, 1429–1445.
- Chester, F. M., and J. M. Logan (1986), Implications for Mechanical-Properties of Brittle Faults from Observations of the Punchbowl Fault Zone, California, *Pure and Applied Geophysics*, 124(1-2), 79-106.
- Cheung, P. S. (1999), Microresistivity and ultrasonic imagers: tool operations and processing principles with reference to commonly encountered image artefacts in *Borehole Imaging: Applications and Case Histories*, edited by M. Lovell, G. Williamson and P. Harvey, pp. 45-57, Geological Society, London, Special Publications,159.
- Chiaramonte, L., M. D. Zoback, J. Friedmann, and V. Stamp (2008), Seal integrity and feasibility of CO₂ sequestration in the Teapot Dome EOR pilot: geomechanical site characterization, *Environmental Geology*, 54(8), 1667-1675.
- Childs, C., J. Watterson, and J. J. Walsh (1996), A model for the structure and development of fault zones, *Journal of the Geological Society*, 153, 337-340.
- Childs, C., J. J. Walsh, and J. Watterson (1997), Complexity in fault zone structure and implications for fault seal prediction, in *Hydrocarbon Seals: Importance for Exploration and Production*, edited by P. Moller-Pederson and A. G. Koestler, pp. 61-72, Norwegian Petroleum Society (NPF) Special Publication.
- Childs, C., Ø. Sylta, S. Moriya, J. J. Walsh, and T. Manzocchi (2002), A method for including the capillary properties of faults in hydrocarbon migration models, in *Hydrocarbon Seal Quantification*, edited by A. G. Koestler and R. Hunsdale, pp. 187-201, Norwegian Petroleum Society (NPF) Special Publication,11.
- Childs, C., T. Manzocchi, J. J. Walsh, C. G. Bonson, A. Nicol, and M. P. J. Schopfer (2009), A geometric model of fault zone and fault rock thickness variations, *Journal of Structural Geology*, 31(2), 117-127.

- Childs, C., J. J. Walsh, T. Manzocchi, J. Strand, A. Nicol, M. Tomasso, M. P. J. Schopfer, and A. Aplin (2007), Definition of a fault permeability predictor from outcrop studies of a faulted turbidite sequence, Taranaki, New Zealand, in *Structurally Complex Reservoirs*, edited by S. J. Jolley, D. Barr, J. J. Walsh and R. J. Knipe, pp. 235-258, Geological Society, London, Special Publication 292.
- Chiodini, G., and F. Frondini (2001), Carbon dioxide degassing from the Albani Hills volcanic region, Central Italy, *Chemical Geology*, 177, 67–83.
- Chiodini, G., F. Frondini, C. Cardellini, D. Granieri, L. Marini, and G. Ventura (2001), CO₂ degassing and energy release at Solfatara volcano, Campi Flegrei, Italy, *Journal of Geophysical Research-Solid Earth*, 106(B8), 16213-16221.
- Chiodini, G., F. Frondini, D. M. Kerrick, J. Rogie, F. Parello, L. Peruzzi, and A. R. Zanzari (1999), Quantification of deep CO₂ fluxes from central Italy. Examples of carbon balance for regional aquifers and of soil diffuse degassing, *Chemical Geology*, 159, 205–222.
- Chopra, S., and K. J. Marfurt (2007), Volumetric curvature attributes add value to 3D seismic data interpretation, *The Leading Edge*, 26(7), 856-867.
- Cox, S. F. (1999), Deformational controls on the dynamics of fluid flow in mesothermal gold systems., in *Fractures, Fluid Flow and Mineralisation*, edited by K. McCaffrey, L. Lonergan and J. J. Wilkinson, pp. 123-140, Geological Society, London, Special Publications, 155.
- Cox, S. F. (2007), Structural and isotopic constraints on fluid flow regimes and fluid pathways during upper crustal deformation: An example from the Taemas area of the Lachlan Orogen, SE Australia, *Journal of Geophysical Research-Solid Earth*, 112(B8).
- Crider, J. G., and D. D. Pollard (1998), Fault Linkage: Three-dimensional mechanical interaction between echelon normal faults, *Journal of Geophysical Research-Solid Earth*, 103(B10), 24373-24391.
- Cunningham, A. B., R. Gerlach, L. Spangler, and A. C. Mitchell (2009), Microbially Enhanced Geologic Containment of Sequestered Supercritical CO₂, *Greenhouse Gas Control Technologies* 9, 1(1), 3245-3252.
- Cuss, R. J., J. F. Harrington, D. J. Noy, S. Sathar, and S. Norris (2015), An experimental study of the flow of gas along synthetic faults of varying orientation to the stress field: Implications for performance assessment of radioactive waste disposal, *Journal of Geophysical Research-Solid Earth*, 120(5), 3932-3945.
- Davatzes, N. C., and S. H. Hickman (2009), Fractures, stress and fluid flow prior to stimulation of well 27-15, Desert Peak, Nevada, EGS Project, paper presented at Proceedings: Thirty-Fourth Workshop on Geothermal Reservoir Engineering, Stanford University, Stanford, California, February.
- Davatzes, N. C., and S. H. Hickman (2010), Stress, fracture, and fluid-flow analysis using acoustic and electrical image logs in hot fractured granites of the Coso geothermal field, California, USA, in *Dipmeter and Borehole Image Log Technology*, edited by M. Pöppelreiter, C. García-Carballido and M. Kraaijveld, pp. 259-293, AAPG Memoir, 92.
- Davidson, J., P. Siratovich, I. C. Wallis, D. Gravley, and D. D. McNamara (2012), Quantifying the stress distribution at the Rotokawa Geothermal Field, New Zealand, paper presented at Proceedings of the New Zealand Geothermal Workshop, Auckland.
- Deichmann, N., and D. Giardini (2009), Earthquakes Induced by the Stimulation of an Enhanced Geothermal System below Basel (Switzerland), *Seismological Research Letters*, 80(5), 784-798.

- Dewhurst, D. N., and A. L. Hennig (2003), Geomechanical properties related to top seal leakage in the Carnarvon Basin, Northwest Shelf, Australia, *Petroleum Geoscience*, 9(3), 255-263.
- Dezayes, C., A. Genter, and B. Valley (2010), Structure of the low permeable naturally fractured geothermal reservoir at Soultz, *Comptes Rendus Geoscience*, 342(7-8), 517-530.
- Dieterich, J. H. (1972), Time-Dependent Friction in Rocks, *Journal of Geophysical Research*, 77(20), 3690-3697.
- Dockrill, B., and Z. K. Shipton (2010), Structural controls on leakage from a natural CO₂ geologic storage site: Central Utah, U.S.A, *Journal of Structural Geology*, 32(11), 1768-1782.
- Doughty, C. (2007), Modeling geologic storage of carbon dioxide: Comparison of non-hysteretic and hysteretic characteristic curves, *Energy Conversion and Management*, 48(6), 1768-1781.
- Doughty, P. T. (2003), Clay smear seals and fault sealing potential of an exhumed growth fault, Rio Grande rift, New Mexico, *AAPG Bulletin*, 87(3), 427-444.
- Durham, W. B. (1997), Laboratory observations of the hydraulic behavior of a permeable fracture from 3800 m depth in the KTB pilot hole, *Journal of Geophysical Research-Solid Earth*, 102(B8), 18405-18416.
- Dyke, C. (1995), How sensitive is natural fracture permeability at depth to variation in effective stress?, in *Fractured and Jointed Rock Masses*, edited by L. R. Myer, pp. 81-88, Balkema/Rotterdam.
- ECO2 (2015), Sub-seabed CO₂ Storage: Impact on Marine Ecosystems, Final publishable summary report, edited.
- Edlmann, K., S. Haszeldine, and C. I. McDermott (2013), Experimental investigation into the sealing capability of naturally fractured shale caprocks to supercritical carbon dioxide flow, *Environmental Earth Sciences*, 70(7), 3393-3409.
- Eichhubl, P., N. C. Davatzes, and S. P. Becker (2009), Structural and diagenetic control of fluid migration and cementation along the Moab fault, Utah, *AAPG Bulletin*, 93(5), 653-681.
- Eichhubl, P., P. S. D'Onfro, A. Aydin, A. Waters, and D. K. McCarty (2005), Structure, petrophysics, and diagenesis of shale entrained along a normal fault at Black Diamond Mines, California - Implications for fault seal, *AAPG Bulletin*, 89(9), 1113-1137.
- Ellsworth, W. L. (2013), Injection-Induced Earthquakes, *Science*, 341(6142), 142-+.
- Engelder, T. (1999), Transitional-tensile fracture propagation: a status report, *Journal of Structural Geology*, 21(8-9), 1049-1055.
- England, W. A., A. S. Mackenzie, D. M. Mann, and T. M. Quigley (1987), The Movement and Entrapment of Petroleum Fluids in the Subsurface, *Journal of the Geological Society*, 144, 327-347.
- Esposito, A., and S. M. Benson (2012), Evaluation and development of options for remediation of CO₂ leakage into groundwater aquifers from geologic carbon storage, *International Journal of Greenhouse Gas Control*, 7, 62-73.
- Evans, J. P., and F. M. Chester (1995), Fluid-Rock Interaction in Faults of the San-Andreas System - Inferences from San-Gabriel Fault Rock Geochemistry and Microstructures, *Journal of Geophysical Research-Solid Earth*, 100(B7), 13007-13020.
- Evans, J. P., C. B. Forster, and J. V. Goddard (1997), Permeability of fault-related rocks, and implications for hydraulic structure of fault zones, *Journal of Structural Geology*, 19(11), 1393-1404.

- Evans, K. F. (2005), Permeability creation and damage due to massive fluid injections into granite at 3.5 km at Soultz: 2. Critical stress and fracture strength, *Journal of Geophysical Research-Solid Earth*, 110(B4).
- Evans, K. F., A. Genter, and J. Sausse (2005), Permeability creation and damage due to massive fluid injections into granite at 3.5 km at Soultz: 1. Borehole observations, *Journal of Geophysical Research-Solid Earth*, 110(B4).
- Evans, K. F., A. Zappone, T. Kraft, N. Deichmann, and F. Moia (2012), A survey of the induced seismic responses to fluid injection in geothermal and CO₂ reservoirs in Europe, *Geothermics*, 41, 30-54.
- Fang, Z., and A. Khaksar (2013), Role of Geomechanics in Assessing the Feasibility of CO₂ Sequestration in Depleted Hydrocarbon Sandstone Reservoirs, *Rock Mechanics and Rock Engineering*, 46(3), 479-497.
- Faulkner, D. R. (2004), A model for the variation in permeability of clay-bearing fault gouge with depth in the brittle crust, *Geophysical Research Letters*, 31(19).
- Faulkner, D. R., and E. H. Rutter (2000), Comparisons of water and argon permeability in natural clay-bearing fault gouge under high pressure at 20 degrees C, *Journal of Geophysical Research-Solid Earth*, 105(B7), 16415-16426.
- Faulkner, D. R., A. C. Lewis, and E. H. Rutter (2003), On the internal structure and mechanics of large strike-slip fault zones: field observations of the Carboneras fault in southeastern Spain, *Tectonophysics*, 367(3-4), 235-251. Faulkner D.R., Jackson C.A.L., Lunn R.J., Schlische R.W., Shipton Z.K., Wiberley C.A.J. and Withjack M.O., 2010. A review of recent developments concerning the structure, mechanisms and fluid flow properties of fault zones. *J. Structural Geology* 32, p. 1557-1575.
- Faulkner, D. R., T. M. Mitchell, E. Jensen, and J. Cembrano (2011), Scaling of fault damage zones with displacement and the implications for fault growth processes, *Journal of Geophysical Research-Solid Earth*, 116.
- Faulkner, D. R., C. A. L. Jackson, R. J. Lunn, R. W. Schlische, Z. K. Shipton, C. A. J. Wiberley, and M. O. Withjack (2010), A review of recent developments concerning the structure, mechanics and fluid flow properties of fault zones, *Journal of Structural Geology*, 32(11), 1557-1575.
- Fenghour, A., W. A. Wakeham, and V. Vesovic (1998), The viscosity of carbon dioxide, *Journal of Physical and Chemical Reference Data*, 27(1), 31-44.
- Ferrill, D. A., and A. P. Morris (2003), Dilational normal faults, *Journal of Structural Geology*, 25(2), 183-196.
- Ferrill, D. A., and A. P. Morris (2008), Fault zone deformation controlled by carbonate mechanical stratigraphy, Balcones fault system, Texas, *AAPG Bulletin*, 92(3), 359-380.
- Ferrill, D. A., A. P. Morris, R. N. McGinnis, K. J. Smart, and W. C. Ward (2011), Fault zone deformation and displacement partitioning in mechanically layered carbonates: The Hidden Valley fault, central Texas, *AAPG Bulletin*, 95(8), 1383-1397.
- Ferrill, D. A., J. Winterle, G. Wittmeyer, D. Sims, S. Colton, A. Armstrong, and A. P. Morris (1999), Stressed rock strains groundwater at Yucca Mountain, Nevada, *Geological Society of America Today*, 9(1-8).
- Fisher, Q. J., and R. J. Knipe (1998), Fault sealing processes in siliciclastic sediments, in *Faulting, Fault Sealing and Fluid Flow in Hydrocarbon Reservoirs*, edited by G. Jones, Q. J. Fisher and R. J. Knipe, pp. 117-134, Geological Society, London, Special Publications, 147.

- Fisher, Q. J., and R. J. Knipe (2001), The permeability of faults within siliciclastic petroleum reservoirs of the North Sea and Norwegian Continental Shelf, *Marine and Petroleum Geology*, 18(10), 1063-1081.
- Fisher, Q. J., M. Casey, S. D. Harris, and R. J. Knipe (2003), Fluid-flow properties of faults in sandstone: The importance of temperature history, *Geology*, 31(11), 965-968.
- Fossen, H., and R. H. Gabrielsen (2005), *Strukturgeologi*, Fagbokforlaget, Bergen, Norway.
- Fossen, H., R. A. Schultz, Z. K. Shipton, and K. Mair (2007), Deformation bands in sandstone: a review, *Journal of the Geological Society*, 164, 755-769.
- Freeman, S. R., S. D. Harris, and R. J. Knipe (2008), Fault seal mapping – incorporating geometric and property uncertainty, in *The Future of Geological Modelling in Hydrocarbon Development*, edited by A. Robinson, P. Griffiths, S. Price, J. Hegre and A. Muggeridge, pp. 5-38, Geological Society, London, Special Publications, 309.
- Freeman, S. R., S. D. Harris, and R. J. Knipe (2010), Cross-fault sealing, baffling and fluid flow in 3D geological models: tools for analysis, visualization and interpretation, in *Reservoir Compartmentalization*, edited by S. J. Jolley, Q. J. Fisher, R. B. Ainsworth, P. J. Vrolijk and S. Delisle, pp. 257-282, Geological Society, London, Special Publications, 347.
- Frery, E., J. P. Gratier, N. Ellouz-Zimmerman, C. Loisele, J. Braun, P. Deschamps, D. Blamart, B. Hamelin, and R. Swennen (2015), Evolution of fault permeability during episodic fluid circulation: evidence for the effects of fluid-rock interactions from travertine studies (Utah-USA), *Tectonophysics*, 651, 121–137.
- Fristad, T., A. Groth, G. Yielding, and B. Freeman (1997), Quantitative fault seal prediction: A case study from Oseberg Syd, in *Hydrocarbon seals: Importance for exploration and production*, edited by P. Moeller-Pederson and A. G. Koestler, pp. 107-124, Norwegian Petroleum Society Special Publications, 7.
- Fulljames, J. R., L. J. J. Zijerveld, and R. C. M. W. Franssen (1997), Fault seal processes: systematic analysis of fault seals over geological and production time, in *Hydrocarbon Seals: Importance for Exploration and Production*, edited by P. Moller-Pederson and A. G. Koestler, pp. 51-60, Norwegian Petroleum Society (NPF) Special Publication, 7.
- Fyfe, W. S., N. J. Price, and A. B. Thompson (1978), *Fluids in the Earth's Crust*, Elsevier, Amsterdam
- Gale, J. F. W., R. M. Reed, and J. Holder (2007), Natural fractures in the Barnett Shale and their importance for hydraulic fracture treatments, *AAPG Bulletin*, 91(4), 603-622.
- Gale, J. F. W., S. E. Laubach, J. E. Olson, P. Eichhubl, and A. Fall (2014), Natural fractures in shale: A review and new observations, *AAPG Bulletin*, 98(11), 2165-2216.
- Gartrell, A., Y. H. Zhang, M. Lisk, and D. Dewhurst (2004), Fault intersections as critical hydrocarbon leakage zones: integrated field study and numerical modelling of an example from the Timor Sea, Australia, *Marine and Petroleum Geology*, 21(9), 1165-1179.
- Gay, A., M. Lopez, P. Cochonat, and G. Sermondadaz (2004), Polygonal faults-furrows system related to early stages of compaction - upper Miocene to recent sediments of the Lower Congo Basin, *Basin Research*, 16(1), 101-116.
- Gentier, S., D. Hopkins, and J. Riss (2000), Role of fracture geometry in the evolution of flow paths under stress, in *Dynamics of Fluids in Fractured Rock*, edited by B. Faybishenko, P. A. Witherspoon and S. M. Benson, pp. 169-183, American Geophysical Union, Geophysical Monograph 122, Washington, D. C.

- Giba, M., J. J. Walsh, and A. Nicol (2012), Segmentation and growth of an obliquely reactivated normal fault, *Journal of Structural Geology*, 39, 253-267.
- Gibson, R. G. (1998), Physical character and fluid-flow properties of sandstone-derived fault zones, in *Structural Geology in Reservoir Characterization*, edited by M. P. Coward, T. S. Daltaban and H. Johnson, pp. 83-97, Geological Society, London, Special Publications, 127.
- Giger, S. B., M. B. Clennell, N. B. Ciftci, C. Harbers, P. Clark, and M. Ricchetti (2013), Fault transmissibility in clastic-argillaceous sequences controlled by clay smear evolution, *AAPG Bulletin*, 97(5), 705-731.
- Gillfillan, S. M. V., et al. (2009), Solubility trapping in formation water as dominant CO₂ sink in natural gas fields, *Nature*, 458(7238), 614-618.
- Gillespie, P. A., C. B. Howard, J. J. Walsh, and J. Watterson (1993), Measurement and Characterization of Spatial Distributions of Fractures, *Tectonophysics*, 226(1-4), 113-141.
- Gouveia, F., M. Johnson, R. Leif, and S. Friedmann (2005), Aerometric Measurement and Modeling of the Mass of CO₂ Emissions from Crystal Geysers, Utah, *Report*, Lawrence Livermore National Laboratory, Livermore, CA (USA).
- Graziani, S., S. E. Beaubien, S. Bigi, and S. Lombardi (2014), Spatial and Temporal pCO₂ marine monitoring near Panarea Island (Italy) using multiple low-cost GasPro sensors, *Environmental Science and Technology*, 48, 12126–12133.
- Gross, M. R. (1995), Fracture Partitioning - Failure Mode as a Function of Lithology in the Monterey Formation of Coastal California, *Geological Society of America Bulletin*, 107(7), 779-792.
- Gross, M. R., G. Gutierrez-Alonso, T. X. Bai, M. A. Wacker, K. B. Collinsworth, and R. J. Behl (1997), Influence of mechanical stratigraphy and kinematics on fault scaling relations, *Journal of Structural Geology*, 19(2), 171-183.
- Gugliandolo, C., F. Italiano, and T. Maugeri (2006), The submarine hydrothermal system of Panarea (Southern Italy): biogeochemical processes at the thermal fluids-sea bottom interface, *Annals of Geophysics*, 49, 783–792.
- Gutierrez, M., L. E. Oino, and R. Nygard (2000), Stress-dependent permeability of a de-mineralised fracture in shale, *Marine and Petroleum Geology*, 17(8), 895-907.
- Han, W. S., M. Lu, B. J. McPherson, E. H. Keating, J. Moore, E. Park, Z. T. Watson, and N.-H. Jung (2013), Characteristics of CO₂-driven cold-water geyser, Crystal Geysers in Utah: experimental observation and mechanism analyses, *Geofluids*, 13, 283–297.
- Hancox, G. T. (1975), Completion Report on the Engineering Geology of the Moawhango Dam, *Report Engineering Geology Report 213*, New Zealand Geological Survey Department of Scientific and Industrial Research, Lower Hutt.
- Harris, S. D., A. Z. Vaszi, and R. J. Knipe (2007), Three-dimensional upscaling of fault damage zones for reservoir simulation, in *Structurally Complex Reservoirs*, edited by S. J. Jolley, D. Barr, J. J. Walsh and R. J. Knipe, pp. 353-374, Geological Society, London, Special Publication, 292.
- Heath, J. E., T. E. Lachmar, J. P. Evans, P. T. Kolesar, and A. P. Williams (2009), Hydrogeo-chemical characterization of leaking, carbon dioxide-charged fault zones in east-central Utah, with implications for geologic carbon storage, in *Carbon Sequestration and Its Role in the Global Carbon Cycle*, edited by B. J. McPherson and E. T. Sundquist, pp. 147–158, American Geophysical Union, Washington, DC.

- Hedenquist, E. K., E. Mroczek, and W. F. Giggenbach (1988), Geochemistry of the Rotokawa geothermal system: Summary of data, interpretation and appraisal for energy development, *Report Technical note 88/6*, 63 pp, Department of Scientific and Industrial Research (DSIR), Lower Hutt.
- Heggland, R. (1997), Detection of gas migration from a deep source by the use of exploration 3D seismic data, *Marine Geology*, 137(1-2), 41-47.
- Heidaryan, E., T. Hatami, M. Rahimi, and J. Moghadasi (2011), Viscosity of pure carbon dioxide at supercritical region: Measurement and correlation approach, *The Journal of Supercritical Fluids*, 56(2), 144-151.
- Hemmings-Sykes, S. (2012), The influence of faulting on hydrocarbon migration in the Kupe area, south Taranaki Basin, New Zealand, 224 pp, Victoria University of Wellington.
- Hermanrud, C., M. E. Halkjelsvik, K. Kristiansen, A. Bernal, and A. C. Strömbäck (2014), Petroleum column-height controls in the western Hammerfest Basin, Barents Sea, *Petroleum Geoscience*, 20(3), 227-240.
- Hill, D. P., and S. Prejean (2005), Magmatic unrest beneath Mammoth Mountain, California, *Journal of Volcanology and Geothermal Research*, 146, 257–283.
- Hillier, A. P. (2003), The Leman Field, Blocks 49/26, 49/27, 49/28, 53/1, 53/2, UK North Sea, *Geological Society, London, Memoir*, 20, 761-770.
- Hillis, R. R. (1998), The influence of fracture stiffness and the in situ stress field on the closure of natural fractures, *Petroleum Geoscience*, 4(1), 57-65.
- Holland, A. A. (2013), Earthquakes Triggered by Hydraulic Fracturing in South-Central Oklahoma, *Bulletin of the Seismological Society of America*, 103(3), 1784-1792.
- Hommel, J., E. Lauchnor, A. Phillips, R. Gerlach, A. B. Cunningham, R. Helmig, A. Ebigbo, and H. Class (2015), A revised model for microbially induced calcite precipitation: Improvements and new insights based on recent experiments, *Water Resources Research*, 51(5), 3695-3715.
- Hooper, E. C. D. (1991), Fluid Migration Along Growth Faults in Compacting Sediments, *Journal of Petroleum Geology*, 14(2), 161-180.
- Hull, J. (1988), Thickness Displacement Relationships for Deformation Zones, *Journal of Structural Geology*, 10(4), 431-435.
- Humez, P., P. Audigane, J. Lions, C. Chiaberge, and G. Bellenfant (2011), Modeling of CO₂ Leakage up Through an Abandoned Well from Deep Saline Aquifer to Shallow Fresh Groundwaters, *Transport in Porous Media*, 90(1), 153-181.
- Hunt, S. P., and P. J. Boulton (2005), Distinct-element stress modeling in the Penola trough, Otway Basin, South Australia, in *Evaluating fault and cap rock seals*, edited by P. Boulton and J. Kaldi, pp. 199-213, AAPG Hedberg Series.
- IEAGHG (2005), A review of natural CO₂ occurrences and releases and their relevance to CO₂ storage, *Report 2005/8*.
- IEAGHG (2007), Study of Potential Impacts of Leaks From Onshore CO₂ Storage Projects on Terrestrial Ecosystems, *Report 2007/03*.
- IEAGHG (2010a), Pressurization and brine displacement issues for deep saline formation CO₂ storage, *Report 2010/15*.
- IEAGHG (2010b), Injection strategies for CO₂ storage sites, *Report 2010/04*.
- IEAGHG (2011), Potential Impacts on Groundwater Resources of Geological Storage, *Report 2011/11*.

- IEAGHG (2012), Extraction of formation water from CO₂ storage, *Report 2012/12*.
- IEAGHG (2013a), Induced Seismicity and its Implication for CO₂ Storage Risk, *Report 2013/09*.
- IEAGHG (2013b), Summary report of the IEAGHG Modelling Network and the Risk Management Network Meeting, *Report 2013/14*.
- IEAGHG (2013c), The In Salah CO₂ storage project: Lesson Learned, in *IEAGHG Modelling Network and the Risk Management Network Meeting*, edited, Trondheim, Norway.
- IEAGHG (2015a), Criteria of Fault Geomechanical Stability during a Pressure Build-up, *Report 2015/04*.
- IEAGHG (2015b), Review of Offshore Monitoring for CCS Project, *Report 2015/02*.
- Ilg, B. R., S. Hemmings-Sykes, A. Nicol, J. Baur, M. Fohrmann, R. Funnell, and M. Milner (2012), Normal faults and gas migration in an active plate boundary, southern Taranaki Basin, offshore New Zealand, *AAPG Bulletin*, 96(9), 1733-1756.
- Illing, V. C. (1942), Geology applied to petroleum, *Proceedings of the Geologists' Association*, 96(9), 156-187.
- Ingebritsen, S. E., and C. E. Manning (2010), Permeability of the continental crust: dynamic variations inferred from seismicity and metamorphism, *Geofluids*, 10(1-2), 193-205.
- IPCC (2005), Underground geological storage, in *IPCC Special Report on Carbon Dioxide Capture and Storage*, edited by B. Metz, O. Davidson, H. C. de Coninck, M. Loos and L. A. Meyer, pp. 195-276, Cambridge University Press New York.
- Ishii, E., H. Funaki, T. Tokiwa, and K. Ota (2010), Relationship between fault growth mechanism and permeability variations with depth of siliceous mudstones in northern Hokkaido, Japan, *Journal of Structural Geology*, 32(11), 1792-1805.
- Italiano, F., R. Favara, G. Etiope, and P. Favali (2001), Submarine emissions of greenhouse gases from hydrothermal and sedimentary areas, paper presented at Water-rock Interaction 2001. Proceedings of the 10th international symposium, Swets and Zeitlinger, Lisse.
- Ito, T., T. F. Xu, H. Tanaka, Y. Taniuchi, and A. Okamoto (2014), Possibility to remedy CO₂ leakage from geological reservoir using CO₂ reactive grout, *International Journal of Greenhouse Gas Control*, 20, 310-323.
- James, W. R., L. H. Fairchild, G. P. Nakayama, S. J. Hippler, and P. J. Vrolijk (2004), Fault-seal analysis using a stochastic multifault approach, *AAPG Bulletin*, 88(7), 885-904.
- Jeanne, P., Y. Guglielmi, F. Cappa, A. P. Rinaldi, and J. Rutqvist (2014), The effects of lateral property variations on fault-zone reactivation by fluid pressurization: Application to CO₂ pressurization effects within major and undetected fault zones, *Journal of Structural Geology*, 62, 97-108.
- Jenkins, C., A. Chadwick, and S. D. Hovorka (2015), The state of the art in monitoring and verification - Ten years on, *International Journal of Greenhouse Gas Control*, 40, 312-349.
- Jennings, J. B. (1987), Capillary-Pressure Techniques - Application to Exploration and Development Geology, *AAPG Bulletin*, 71(10), 1196-1209.
- Jev, B. I., C. H. Kaarssijpesteijn, M. P. A. M. Peters, N. L. Watts, and J. T. Wilkie (1993), Akaso Field, Nigeria - Use of Integrated 3-D Seismic, Fault Slicing, Clay Smearing, and Rft Pressure Data on Fault Trapping and Dynamic Leakage, *AAPG Bulletin*, 77(8), 1389-1404.
- Jolley, S. J., H. Dijk, J. H. Lamens, Q. J. Fisher, T. Manzocchi, H. Eikmans, and Y. Huang (2007), Faulting and fault sealing in production simulation models: Brent Province, northern North Sea, *Petroleum Geoscience*, 13(4), 321-340.

- Juanes, R., C. W. MacMinn, and M. L. Szulczewski (2010), The Footprint of the CO₂ Plume during Carbon Dioxide Storage in Saline Aquifers: Storage Efficiency for Capillary Trapping at the Basin Scale, *Transport in Porous Media*, 82(1), 19-30.
- Julian, B. R., G. R. Foulger, and F. C. Monastero (2009), Seismic monitoring of EGS stimulation tests at the Coso geothermal field, California, using microearthquake locations and moment tensors, paper presented at Proceedings: Thirty-Fourth Workshop on Geothermal Reservoir Engineering, Stanford University, Stanford, California, February.
- Jung, B., G. Garven, and J. R. Boles (2014a), Effects of episodic fluid flow on hydrocarbon migration in the Newport-Inglewood Fault Zone, Southern California, *Geofluids*, 14(2), 234-250.
- Jung, N.-H., W. S. Han, K. Han, and E. Park (2015), Regional-scale advective, diffusive, and eruptive dynamics of CO₂ and brine leakage through faults and wellbores, *Journal of Geophysical Research: Solid Earth*, 120(5), 3003-3025.
- Jung, N. H., W. S. Han, Z. T. Watson, J. P. Graham, and K. Y. Kim (2014b), Fault-controlled CO₂ leakage from natural reservoirs in the Colorado Plateau, East-Central Utah, *Earth and Planetary Science Letters*, 403, 358-367.
- Kampman, N., M. Bickle, M. Wigley, and B. Dubacq (2014a), Fluid flow and CO₂-fluid-mineral interactions during CO₂-storage in sedimentary basins, *Chemical Geology*, 369, 22-50.
- Kampman, N., et al. (2014b), Drilling and sampling a natural CO₂ reservoir: Implications for fluid flow and CO₂-fluid-rock reactions during CO₂ migration through the overburden, *Chemical Geology*, 369, 51-82.
- Kaven, J. O., S. H. Hickman, and N. C. Davatzes (2013), Micro-seismicity within the Coso Geothermal Field, California, from 1996-2012, paper presented at Thirty-Eighth Workshop on Geothermal Reservoir Engineering, Stanford University, Stanford, California, February 11-13.
- Kaven, J. O., S. H. Hickman, and N. C. Davatzes (2014), Micro-seismicity and seismic moment release within the Coso Geothermal Field, California, paper presented at Thirty-Ninth Workshop on Geothermal Reservoir Engineering, Stanford University, Stanford, California, February 24-26.
- Khair, H. A., D. Cooke, and M. Hand (2015), Seismic mapping and geomechanical analyses of faults within deep hot granites, a workflow for enhanced geothermal system projects, *Geothermics*, 53, 46-56.
- Kim, Y. S., D. C. P. Peacock, and D. J. Sanderson (2004), Fault damage zones, *Journal of Structural Geology*, 26(3), 503-517.
- Kirk, K. (2011), Natural CO₂ flux literature review for the QICS project, Energy Programme, Report, 38 pp, British Geological Survey, Keyworth, Nottingham, UK.
- Kitagawa, Y., N. Koizumi, K. Notsu, and G. Igarashi (1999), Water injection experiments and discharge changes at the Nojima Fault in Awaji Island, Japan, *Geophysical Research Letters*, 26(20), 3173-3176.
- Klusman, R. W. (2011), Comparison of surface and near-surface geochemical methods for detection of gas microseepage from carbon dioxide sequestration, *International Journal of Greenhouse Gas Control*, 5(6), 1369-1392.
- Klusman, R. W. (2015), Surface geochemical measurements applied to monitoring, verification, and accounting of leakage from sequestration projects, *Interpretation*, 3(2), SM1-SM21.
- Knipe, R. J. (1997), Juxtaposition and seal diagrams to help analyze fault seals in hydrocarbon reservoirs, *AAPG Bulletin*, 81(2), 187-195.

- Knipe, R. J., S. Freeman, S. D. Harris, and R. K. Davies (2004), Structural uncertainty and scenario modeling for fault seal analysis, paper presented at Proceedings of the AAPG Annual Convention Abstracts, Dallas, Texas, April 18-21.
- Kohli, A. H., and M. D. Zoback (2013), Frictional properties of shale reservoir rocks, *Journal of Geophysical Research-Solid Earth*, 118(9), 5109-5125.
- Lander, R. H., and S. E. Laubach (2015), Insights into rates of fracture growth and sealing from a model for quartz cementation in fractured sandstones, *Geological Society of America Bulletin*, 127(3-4), 516-538.
- Laubach, S. E. (2003), Practical approaches to identifying sealed and open fractures, *AAPG Bulletin*, 87(4), 561-579.
- Laubach, S. E., J. E. Olson, and J. F. W. Gale (2004), Are open fractures necessarily aligned with maximum horizontal stress?, *Earth and Planetary Science Letters*, 222(1), 191-195.
- Laubach, S. E., P. Eichhubl, P. Hargrove, M. A. Ellis, and J. N. Hooker (2014), Fault core and damage zone fracture attributes vary along strike owing to interaction of fracture growth, quartz accumulation, and differing sandstone composition, *Journal of Structural Geology*, 68, 207-226.
- Laurent, D., et al. (2012), High-resolution architecture of a polygonal fault interval inferred from geomodel applied to 3D seismic data from the Gjallar Ridge, Voring Basin, Offshore Norway, *Marine Geology*, 332, 134-151.
- Le Guenan, T., and J. Rohmer (2011), Corrective measures based on pressure control strategies for CO₂ geological storage in deep aquifers, *International Journal of Greenhouse Gas Control*, 5(3), 571-578.
- Leclère, H., F. Cappa, D. Faulkner, O. Fabbri, P. Armitage, and O. Blake (2015), Development and maintenance of fluid overpressures in crustal fault zones by elastic compaction and implications for earthquake swarms, *Journal of Geophysical Research-Solid Earth*, 120(6), 4450-4473.
- Lee, H. S., and T. F. Cho (2002), Hydraulic characteristics of rough fractures in linear flow under normal and shear load, *Rock Mechanics and Rock Engineering*, 35(4), 299-318.
- Lehner, F., and W. Pilaar (1997), The emplacement of clay smears in syn-sedimentary normal faults: inference from field observations near Frechen, Germany, in *Hydrocarbon Seals: Importance for Exploration and Production*, edited by P. Moller-Pederson and A. G. Koestler, pp. 39-50, Norwegian Petroleum Society (NSF) Special Publication,7.
- Leonenko, Y., and D. W. Keith (2008), Reservoir engineering to accelerate the dissolution of CO₂ stored in aquifers, *Environmental Science & Technology*, 42(8), 2742-2747.
- Levens, R. L., R. E. Williams, and D. R. Ralston (1994), Hydrogeologic Role of Geologic Structures .1. The Paradigm, *Journal of Hydrology*, 156(1-4), 227-243.
- Lewicki, J. L., J. Birkholzer, and C. F. Tsang (2007), Natural and industrial analogues for leakage of CO₂ from storage reservoirs: Identification of features, events, and processes and lessons learned, *Environmental Geology*, 52(3), 457-467.
- Lewicki, J. L., M. L. Fischer, and G. E. Hilley (2008), Six-week time series of eddy covariance CO₂ flux at Mammoth Mountain, California: performance evaluation and role of meteorological forcing, *Journal of Volcanology and Geothermal Research*, 171, 178-190.
- Ligtenberg, J. H. (2005), Detection of fluid migration pathways in seismic data: implications for fault seal analysis, *Basin Research*, 17(1), 141-153.

- Lindsay, N. G., F. C. Murphy, J. J. Walsh, and J. Watterson (1993), Outcrop studies of shale smears on fault surfaces, in *The Geological Modelling of Hydrocarbon Reservoirs and Outcrop Analogues*, edited by S. S. Flint and I. D. Bryant, pp. 113-123, Special Publication of the International Association of Sedimentologists, 15.
- Lunn, R. J., J. P. Willson, Z. K. Shipton, and H. Moir (2008), Simulating brittle fault growth from linkage of preexisting structures, *Journal of Geophysical Research-Solid Earth*, 113(B7).
- Mäkel, G. H. (2007), The modelling of fractured reservoirs: constraints and potential for fracture network geometry and hydraulics analysis, in *Structurally Complex Reservoirs*, edited by S. J. Jolley, D. Barr, J. J. Walsh and R. J. Knipe, pp. 375-403, Geological Society, London, Special Publications, 292.
- Manceau, J. C., and J. Rohmer (2011), Analytical Solution Incorporating History-Dependent Processes for Quick Assessment of Capillary Trapping During CO₂ Geological Storage, *Transport in Porous Media*, 90(3), 721-740.
- Manceau, J. C., D. G. Hatzignatiou, L. de Lary, N. B. Jensen, and A. Reveillere (2014), Mitigation and remediation technologies and practices in case of undesired migration of CO₂ from a geological storage unit-Current status, *International Journal of Greenhouse Gas Control*, 22, 272-290.
- Manning, C. E., and S. E. Ingebritsen (1999), Permeability of the continental crust: Implications of geothermal data and metamorphic systems, *Reviews of Geophysics*, 37(1), 127-150.
- Manzocchi, T., C. Childs, and J. J. Walsh (2010), Faults and fault properties in hydrocarbon flow models, *Geofluids*, 10(1-2), 94-113.
- Manzocchi, T., J. J. Walsh, P. Nell, and G. Yielding (1999), Fault transmissibility multipliers for flow simulation models, *Petroleum Geoscience*, 5(1), 53-63.
- Manzocchi, T., A. E. Heath, J. J. Walsh, and C. Childs (2002), The representation of two phase fault-rock properties in flow simulation models, *Petroleum Geoscience*, 8(2), 119-132.
- Manzocchi, T., A. E. Heath, B. Palanathakumar, C. Childs, and J. J. Walsh (2008), Faults in conventional flow simulation models: a consideration of representational assumptions and geological uncertainties, *Petroleum Geoscience*, 14(1), 91-110.
- Marrett, R., and R. W. Allmendinger (1990), Kinematic Analysis of Fault-Slip Data, *Journal of Structural Geology*, 12(8), 973-986.
- Marrett, R., and S. E. Laubach (1997), Diagenetic controls on fracture permeability and sealing, *International Journal of Rock Mechanics and Mining Sciences*, 34(3/4), Paper No. 204.
- Mathieson, A., J. Midgely, I. Wright, N. Saoula, and P. Ringrose (2011), In Salah CO₂ Storage JIP: CO₂ sequestration monitoring and verification technologies applied at Krechba, Algeria, *10th International Conference on Greenhouse Gas Control Technologies*, 4, 3596-3603.
- Matthai, S. K., and G. Fischer (1996), Quantitative modeling of fault-fluid-discharge and fault-dilation-induced fluid-pressure variations in the seismogenic zone, *Geology*, 24(2), 183-186.
- Maultzsch, S., M. Chapman, E. R. Liu, and X. Y. Li (2003), Modelling frequency-dependent seismic anisotropy in fluid-saturated rock with aligned fractures: implication of fracture size estimation from anisotropic measurements, *Geophysical Prospecting*, 51(5), 381-392.
- McGinnis, D. F., M. Schmidt, T. DelSontro, S. Themann, L. Rovelli, A. Reitz, and P. Linke (2011), Discovery of a natural CO₂ seep in the German North Sea: Implications for shallow dissolved gas and seep detection, *Journal of Geophysical Research*, 116, CO3013.

- McLean, K., and D. D. McNamara (2011), Fractures interpreted from acoustic formation imaging technology: Correlation to permeability, paper presented at Proceedings, Thirty-Sixth Workshop on Geothermal Reservoir Engineering, Stanford University, Stanford, California, January.
- McNamara, D. D., C. Massiot, B. Lewis, and I. C. Wallis (2015), Heterogeneity of structure and stress in the Rotokawa Geothermal Field, New Zealand, *Journal of Geophysical Research-Solid Earth*, *120*(2), 1243-1262.
- Meyer, V., A. Nicol, C. Childs, J. J. Walsh, and J. Watterson (2002), Progressive localisation of strain during the evolution of a normal fault population, *Journal of Structural Geology*, *24*(8), 1215-1231.
- Micarelli, L., A. Benedicto, C. Invernizzi, B. Saint-Bezar, J. L. Michelot, and P. Vergely (2005), Influence of P/T conditions on the style of normal fault initiation and growth in limestones from the SE-Basin, France, *Journal of Structural Geology*, *27*(9), 1577-1598.
- Michie, E. A. H., T. J. Haines, D. Healy, J. E. Neilson, N. E. Timms, and C. A. J. Wibberley (2014), Influence of carbonate facies on fault zone architecture, *Journal of Structural Geology*, *65*, 82-99.
- Mildren, S., R. R. Hillis, P. J. Lyon, J. J. Meyer, D. N. Dewhurst, and P. J. Boulton (2005), FAST: A new technique for geomechanical assessment of the risk of reactivation-related breach of fault seals, paper presented at Evaluating fault and cap rock seals: AAPG Hedberg Series, The American Association of Petroleum Geologists.
- Miller, S. A., C. Collettini, L. Chiaraluce, M. Cocco, M. Barchi, and B. J. P. Kaus (2004), Aftershocks driven by a high-pressure CO₂ source at depth, *Nature*, *427*(6976), 724-727.
- Mitchell, A. C., A. J. Phillips, R. Hiebert, R. Gerlach, L. H. Spangler, and A. B. Cunningham (2009), Biofilm enhanced geologic sequestration of supercritical CO₂, *International Journal of Greenhouse Gas Control*, *3*(1), 90-99.
- Molinero, J., J. Samper, and R. Juanes (2002), Numerical modeling of the transient hydrogeological response produced by tunnel construction in fracture rocks, *Engineering Geology*, *64*, 369-386.
- Morretti, I. (1998), The role of faults in hydrocarbon migration, *Petroleum Geoscience*, *4*, 81-94.
- Morris, A., D. A. Ferrill, and D. B. Henderson (1996), Slip-tendency analysis and fault reactivation, *Geology*, *24*(3), 275-278.
- Morrow, C. A., D. A. Lockner, D. E. Moore, and S. Hickman (2014), Deep permeability of the San Andreas Fault from San Andreas Fault Observatory at Depth (SAFOD) core samples, *Journal of Structural Geology*, *64*, 99-114.
- Muir-Wood, R., and G. C. P. King (1993), Hydrological Signatures of Earthquake Strain, *Journal of Geophysical Research-Solid Earth*, *98*(B12), 22035-22068.
- Nadai, A. (1950), *Theory of flow and fracture of solids*, v.2, McGraw-Hill, New York.
- NASCENT (2005), Natural analogues for the geological storage of CO₂, *Report*, European Commission and the British Geological Survey.
- Neglia, S. (1979), Migration of fluids in sedimentary basins, *AAPG Bulletin*, *63*(4), 573-597.
- Nghiem, L., C. D. Yang, V. Shrivastava, B. Kohse, M. Hassam, and C. Card (2009), Risk Mitigation Through the Optimization of Residual Gas and Solubility Trapping for CO₂ Storage in Saline Aquifers, *Greenhouse Gas Control Technologies* *9*, 1(1), 3015-3022.

- Nguyen, P. T., S. F. Cox, L. B. Harris, and C. M. Powell (1998), Fault-valve behaviour in optimally oriented shear zones: an example at the Revenge gold mine, Kambalda, Western Australia, *Journal of Structural Geology*, 20(12), 1625-1640.
- Nicol, A., J. Watterson, J. J. Walsh, and C. Childs (1996), The shapes, major axis orientations and displacement patterns of fault surfaces, *Journal of Structural Geology*, 18(2-3), 235-248.
- Nicol, A., C. Childs, J. J. Walsh, and K. W. Schafer (2013a), A geometric model for the formation of deformation band clusters, *Journal of Structural Geology*, 55, 21-33.
- Nicol, A., M. Gerstenberger, C. Bromley, R. Carne, L. Chardot, S. Ellis, C. Jenkins, T. Siggins, and P. Viskovic (2013b), Induced seismicity; observations, risks and mitigation measures at CO2 storage sites, *Ghgt-11*, 37, 4749-4756.
- Noorsalehi-Garakani, S., G. J. K. Vennekate, P. Vrolijk, and J. L. Urai (2013), Clay-smear continuity and normal fault zone geometry - First results from excavated sandbox models, *Journal of Structural Geology*, 57, 58-80.
- Nygård, R., M. Gutierrez, R. K. Bratli, and K. Hoeg (2006), Brittle-ductile transition, shear failure and leakage in shales and mudrocks, *Marine and Petroleum Geology*, 23(2), 201-212.
- O'Brien, G. W., M. Lisk, I. R. Duddy, J. Hamilton, P. Woods, and R. Cowley (1999), Plate convergence, foreland development and fault reactivation: primary controls on brine migration, thermal histories and trap breach in the Timor Sea, Australia, *Marine and Petroleum Geology*, 16(6), 533-560.
- O'Connor, S. J. (2000), Hydrocarbon-water interfacial tension values at reservoir conditions: Inconsistencies in the technical literature and the impact on maximum oil and gas column height calculations, *AAPG Bulletin*, 84(10), 1537-1541.
- Obeahon, P. P., G. Ypma, and U. O. Onyeagoro (2014), Dynamic Fault Seal Breakdown Investigation -A Study of Egret Field in the North Sea, paper presented at SPE Annual Technical Conference and Exhibition, Society of Petroleum Engineers, Amsterdam, 27-29 October.
- Odling, N. E., et al. (1999), Variations in fracture system geometry and their implications for fluid flow in fractured hydrocarbon reservoirs, *Petroleum Geoscience*, 5(4), 373-384.
- Ohman, J., A. Niemi, and C. F. Tsang (2005), Probabilistic estimation of fracture transmissivity from Wellbore hydraulic data accounting for depth-dependent anisotropic rock stress, *International Journal of Rock Mechanics and Mining Sciences*, 42(5-6), 793-804.
- Olson, J. E., S. E. Laubach, and R. H. Lander (2007), Combining diagenesis and mechanics to quantify fracture aperture distributions and fracture pattern permeability, *Fractured Reservoirs*, 270, 101-116.
- Paillet, F. L., A. E. Hess, C. H. Cheng, and E. Hardin (1987), Characterization of Fracture Permeability with High-Resolution Vertical Flow Measurements during Borehole Pumping, *Ground Water*, 25(1), 28-40.
- Parrek, N., M. K. Jat, and S. K. Jain (2006), The utilization of brackish water, protecting the quality of the upper fresh layer in coastal aquifer, *Environmentalist*, 26, 237-246.
- Patton, T. L., J. M. Logan, and M. Friedman (1998), Experimentally generated normal faults in single-layer and multilayer limestone specimens at confining pressure, *Tectonophysics*, 295(1-2), 53-77.
- Peacock, D. C. P. (2002), Propagation, interaction and linkage in normal fault systems, *Earth-Science Reviews*, 58(1-2), 121-142.

- Peacock, D. C. P., and D. J. Sanderson (1991), Displacements, Segment Linkage and Relay Ramps in Normal-Fault Zones, *Journal of Structural Geology*, 13(6), 721-&.
- Peacock, D. C. P., and X. Zhang (1994), Field Examples and Numerical Modeling of Oversteps and Bends Along Normal Faults in Cross-Section, *Tectonophysics*, 234(1-2), 147-167.
- Pearce, J., I. Czernichowski-Lauriol, S. Lombardi, S. Brune, A. Nador, J. Baker, H. Pauwels, G. Hatziyannis, S. Beaubien, and E. Faber (2004), A review of natural CO₂ accumulations in Europe as analogues for geological sequestration, in *Geological Storage of Carbon Dioxide*, edited by S. J. Baines and R. H. Worden, pp. 29–41, Geological Society of London, 233, London.
- Perry, K. F. (2005), Natural gas storage industry experience and technology: potential application to CO₂ geological storage, in *Carbon Dioxide Capture for Storage in Deep Geologic Formations*, edited by D. C. Thomas and S. M. Benson, Elsevier, 2, London.
- Pettinelli, E., S. E. Beaubien, A. Zaja, A. Menghini, N. Praticelli, E. Mattei, A. Di Matteo, A. Annunziatellis, G. Ciotoli, and S. Lombardi (2010), Characterization of a CO₂ gas vent using various geophysical and geochemical methods, *Geophysics*, 75, B137–B146.
- Philip, Z. G., J. W. Jennings, J. E. Olson, S. E. Laubach, and J. Holder (2005), Modeling coupled fracture-matrix fluid flow in geomechanically simulated fracture networks, *Spe Reservoir Evaluation & Engineering*, 8(4), 300-309.
- Phillips, A. J., E. Lauchnor, J. Eldring, R. Esposito, A. C. Mitchell, R. Gerlach, A. B. Cunningham, and L. H. Spangler (2013), Potential CO₂ Leakage Reduction through Biofilm-Induced Calcium Carbonate Precipitation, *Environmental Science & Technology*, 47(1), 142-149.
- Power, W. L., T. E. Tullis, and J. D. Weeks (1988), Roughness and Wear during Brittle Faulting, *Journal of Geophysical Research-Solid Earth and Planets*, 93(B12), 15268-15278.
- Qi, R., T. C. LaForce, and M. J. Blunt (2009), Design of carbon dioxide storage in aquifers, *International Journal of Greenhouse Gas Control*, 3(2), 195-205.
- Reches, Z., and D. A. Lockner (1994), Nucleation and Growth of Faults in Brittle Rocks, *Journal of Geophysical Research-Solid Earth*, 99(B9), 18159-18173.
- Reilly, C., A. Nicol, J. J. Walsh, and K. F. Kroeger (2016), Temporal changes of fault seal and early charge of the Maui Gas-condensate field, Taranaki Basin, New Zealand, *Marine and Petroleum Geology*, 70, 237-250.
- Reveillere, A., and J. Rohmer (2011), Managing the risk of CO₂ leakage from deep saline aquifer reservoirs through the creation of a hydraulic barrier, *10th International Conference on Greenhouse Gas Control Technologies*, 4, 3187-3194.
- Revil, A., and L. M. Cathles (2002), Fluid transport by solitary waves along growing faults - A field example from the South Eugene Island Basin, Gulf of Mexico, *Earth and Planetary Science Letters*, 202(2), 321-335.
- Rice, J. R. (1992), Fault Stress States, Pore Pressure Distributions, and the Weakness of the San Andreas Fault., in *Fault Mechanics and Transport Properties of Rocks*, edited by B. Evans and T.-F. Wong, pp. 475-503, Academic Press San Diego.
- Rinaldi, A. P., and J. Rutqvist (2013), Modeling of deep fracture zone opening and transient ground surface uplift at KB-502 CO₂ injection well, In Salah, Algeria, *International Journal of Greenhouse Gas Control*, 12, 155-167.
- Rinaldi, A. P., J. Rutqvist, and F. Cappa (2014), Geomechanical effects on CO₂ leakage through fault zones during large-scale underground injection, *International Journal of Greenhouse Gas Control*, 20, 117-131.

- Rivenæs, J. C., and C. Dart (2002), Reservoir compartmentalisation by water saturated faults: is evaluation possible with today's tools?, in *Hydrocarbon Seal Quantification*, edited by A. G. Koestler and R. Hunsdale, pp. 173-186, Norwegian Petroleum Society (NPF) Special Publication, 11.
- Roche, V., C. Homberg, and M. Rocher (2012), Architecture and growth of normal fault zones in multilayer systems: A 3D field analysis in the South-Eastern Basin, France, *Journal of Structural Geology*, 37, 19-35.
- Rochelle, C. A., I. Czernichowski-Lauriol, and A. E. Milodowski (2004), The impact of chemical reactions on CO₂ storage in geological formations: a brief review, in *Geological Storage of Carbon Dioxide*, edited by S. J. Baines and R. H. Worden, pp. 87-106, Geological Society, London, Special Publications, 233.
- Rogie, J. D., D. M. Kerrick, M. L. Sorey, G. Chiodini, and D. L. Galloway (2001), Dynamics of carbon dioxide emission at Mammoth Mountain, California, *Earth and Planetary Science Letters*, 188, 535-541.
- Rowland, J. V., and S. F. Simmons (2012), Hydrologic, Magmatic, and Tectonic Controls on Hydrothermal Flow, Taupo Volcanic Zone, New Zealand: Implications for the Formation of Epithermal Vein Deposits, *Economic Geology*, 107(3), 427-457.
- Rutqvist, J. (2012), The Geomechanics of CO₂ Storage in Deep Sedimentary Formations, *Geotechnical and Geological Engineering*, 30(3), 525-551.
- Rutqvist, J., and O. Stephansson (2003), The role of hydromechanical coupling in fractured rock engineering, *Hydrogeology Journal*, 11(1), 7-40.
- Sager, W. W., I. R. MacDonald, and R. S. Hou (2004), Side-scan sonar imaging of hydrocarbon seeps on the Louisiana continental slope, *AAPG Bulletin*, 88(6), 725-746.
- Sanderson, D. J., and X. Zhang (1999), Critical stress localization of flow associated with deformation of well-fractured rock masses, with implications for mineral deposits, in *Fractures, Fluid Flow and Mineralization*, edited by K. McCaffrey, L. Lonergan and J. J. Wilkinson, pp. 69-81, Geological Society, London, Special Publications, 155.
- Sathar, S., H. J. Reeves, R. J. Cuss, and J. F. Harrington (2012), The role of stress history on the flow of fluids through fractures, *Mineralogical Magazine*, 76(8), 3165-3177.
- Savage, H. M., and E. E. Brodsky (2011), Collateral damage: Evolution with displacement of fracture distribution and secondary fault strands in fault damage zones, *Journal of Geophysical Research-Solid Earth*, 116.
- Scholz, C. H. (1987), Wear and Gouge Formation in Brittle Faulting, *Geology*, 15(6), 493-495.
- Scholz, C. H., and P. A. Cowie (1990), Determination of Total Strain from Faulting Using Slip Measurements, *Nature*, 346(6287), 837-839.
- Schöpfer, M. P. J., C. Childs, and J. J. Walsh (2006), Localisation of normal faults in multilayer sequences, *Journal of Structural Geology*, 28(5), 816-833.
- Schöpfer, M. P. J., C. Childs, and J. J. Walsh (2007), Two-dimensional distinct element modeling of the structure and growth of normal faults in multilayer sequences: 2. Impact of confining pressure and strength contrast on fault zone geometry and growth, *Journal of Geophysical Research-Solid Earth*, 112(B10).
- Schroot, B. M., and R. T. E. Schüttenhelm (2003), Expressions of shallow gas in the Netherlands North Sea, *Geologie en Mijnbouw*, 82, 91-105.

- Schumacher, D., D. C. Hitzman, J. Tucker, and B. Rountree (1997), Applying high-resolution surface geochemistry to assess reservoir compartmentalization and monitor hydrocarbon drainage, in *Applications of emerging technologies: unconventional methods in exploration for petroleum and natural gas V proceedings*, edited by R. J. Kruijenga and M. W. Downey, pp. 309-322, Methodist University Press.
- Seebeck, H., E. Tenthorey, C. Consoli, and A. Nicol (2015), Polygonal faulting and seal integrity in the Bonaparte Basin, Australia, *Marine and Petroleum Geology*, 60, 120-135.
- Seebeck, H., A. Nicol, J. J. Walsh, C. Childs, R. D. Beetham, and J. Pettinga (2014), Fluid flow in fault zones from an active rift, *Journal of Structural Geology*, 62, 52-64.
- Segall, P., and D. D. Pollard (1980), Mechanics of Discontinuous Faults, *Journal of Geophysical Research*, 85(Nb8), 4337-4350.
- Sherburn, S., S. M. Sewell, S. Bourguignon, W. Cumming, S. Bannister, C. Bardsley, J. Winick, J. Quinao, and I. C. Wallis (2015), Microseismicity at Rotokawa geothermal field, New Zealand, 2008-2012, *Geothermics*, 54, 23-34.
- Shi, J. Q., C. Sinayuc, S. Durucan, and A. Korre (2012), Assessment of carbon dioxide plume behaviour within the storage reservoir and the lower caprock around the KB-502 injection well at In Salah, *International Journal of Greenhouse Gas Control*, 7, 115-126.
- Shipton, Z. K., and P. A. Cowie (2001), Damage zone and slip-surface evolution over mu m to km scales in high-porosity Navajo sandstone, Utah, *Journal of Structural Geology*, 23(12), 1825-1844.
- Shipton, Z. K., A. M. Soden, J. D. Kirkpatrick, A. M. Bright, and R. J. Lunn (2006), How thick is a fault? Fault displacement-thickness scaling revisited, *Earthquakes: Radiated Energy and the Physics of Faulting*, 170, 193-198.
- Shipton, Z. K., J. P. Evans, D. Kirschner, P. T. Kolesar, A. P. Williams, and J. Heath (2004), Analysis of CO₂ leakage through 'low-permeability' faults from natural reservoirs in the Colorado Plateau, east-central Utah, in *Geological Storage of Carbon Dioxide*, edited by S. J. Baines and R. H. Worden, pp. 43-58, Geological Society, London, Special Publications, 233, London.
- Shipton, Z. K., J. P. Evans, B. Dockrill, J. Heath, A. Williams, D. Kirchner, and P. T. Kolesar (2005), Natural leaking CO₂-charged system as analogs for failed geologic storage reservoirs, in *Carbon Dioxide Capture for Storage in Deep Geologic Formations*, edited by D. C. Thomas and S. M. Benson, pp. 699-712, Elsevier New York.
- Sibson, R. H. (1981a), Controls on Low-Stress Hydro-Fracture Dilatancy in Thrust, Wrench and Normal-Fault Terrains, *Nature*, 289(5799), 665-667.
- Sibson, R. H. (1981b), Low-Stress Hydro-Fracture Dilatancy in Thrust, Wrench and Normal-Fault Terrains, *Journal of Structural Geology*, 3(2), 193-193.
- Sibson, R. H. (1989), Earthquake Faulting as a Structural Process, *Journal of Structural Geology*, 11(1-2), 1-14.
- Sibson, R. H. (1990), Conditions for fault-valve behaviour, in *Deformation Mechanisms, Rheology and Tectonics*, edited by R. J. Knipe, pp. 15-28, Geological Society, London, Special Publications, 54.
- Sibson, R. H. (1994), Crustal stress, faulting and fluid flow, in *Geofluids: Origin, Migration and Evolution of Fluids in Sedimentary Basins*, edited by J. Parnell, pp. 69-84, Geological Society, London, Special Publications, 78.
- Sibson, R. H. (1996), Structural permeability of fluid-driven fault-fracture meshes, *Journal of Structural Geology*, 18(8), 1031-1042.

- Sibson, R. H. (1998), Brittle failure mode plots for compressional and extensional tectonic regimes, *Journal of Structural Geology*, 20(5), 655-660.
- Sleep, N. H., and M. L. Blanpied (1992), Creep, Compaction and the Weak Rheology of Major Faults, *Nature*, 359(6397), 687-692.
- Soden, A. M., and Z. K. Shipton (2013), Dilational fault zone architecture in a welded ignimbrite: The importance of mechanical stratigraphy, *Journal of Structural Geology*, 51, 156-166.
- Soliva, R., and A. Benedicto (2005), Geometry, scaling relations and spacing of vertically restricted normal faults, *Journal of Structural Geology*, 27(2), 317-325.
- Sperrevik, S., P. A. Gillespie, Q. J. Fisher, T. Halvorsen, and R. J. Knipe (2002), Empirical estimation of fault rock properties, in *Hydrocarbon Seal Quantification*, edited by A. G. Koestler and R. Hunsdale, pp. 109-126, Norwegian Petroleum Society (NPF) Special Publication, 11.
- Stauffer, D. (1987), *Introduction to Percolation Theory*, Taylor and Francis Ltd, London.
- Streit, J. E., and R. R. Hillis (2004), Estimating fault stability and sustainable fluid pressures for underground storage of CO₂ in porous rock, *Energy*, 29(9-10), 1445-1456.
- Streit, J. E., and M. N. Watson (2005), Estimating rates of potential CO₂ loss from geological storage sites for risk and uncertainty analysis, paper presented at 7th International conference on Greenhouse Gas Control Technologies (GHGT-7), Elsevier, Vancouver.
- Streit, J. E., and N. M. Watson (2007), Final risk assessment report for the FutureGen project environmental impact statement. October 2007 revision, *Report*, US Department of Energy, <http://energy.gov/sites/prod/files/EIS-0394-FEIS-RiskAssessment-2007.pdf>.
- Sverdrup, E., J. Helgesen, and J. Vold (2003), Sealing properties of faults and their influence on water-alternating-gas injection efficiency in the Snorre field, northern North Sea, *AAPG Bulletin*, 87(9), 1437-1458.
- Tadokoro, K., M. Ando, and K. Nishigami (2000), Induced earthquakes accompanying the water injection experiment at the Nojima fault zone, Japan: Seismicity and its migration, *Journal of Geophysical Research-Solid Earth*, 105(B3), 6089-6104.
- Talwani, P., L. Chen, and K. Gahalaut (2007), Seismogenic permeability, $k(S)$, *Journal of Geophysical Research-Solid Earth*, 112(B7).
- Tanikawa, W., M. Sakaguchi, T. Hirono, W. Lin, W. Soh, and S. R. Song (2009), Transport properties and dynamic processes in a fault zone from samples recovered from TCDP Hole B of the Taiwan Chelungpu Fault Drilling Project, *Geochemistry Geophysics Geosystems*, 10.
- Tedesco, S. A. (1999), Anomaly shifts indicate rapid surface seep rates, *Oil & Gas Journal*, 97(13), 69-72.
- Tenthorey, E., S. F. Cox, and H. F. Todd (2003), Evolution of strength recovery and permeability during fluid-rock reaction in experimental fault zones, *Earth and Planetary Science Letters*, 206(1-2), 161-172.
- Tenthorey, E., T. Dance, Y. Cinar, J. Ennis-King, and J. Strand (2014), Fault modelling and geomechanical integrity associated with the CO₂CRC Otway 2C injection experiment, *International Journal of Greenhouse Gas Control*, 30, 72-85.
- Tewksbury, B. J., J. P. Hogan, S. A. Kattenhorn, C. J. Mehrtens, and E. A. Tarabees (2014), Polygonal faults in chalk: Insights from extensive exposures of the Khoman Formation, Western Desert, Egypt, *Geology*, 42(6), 479-482.

- Tillner, E., T. Kempka, B. Nakaten, and M. Kuhn (2013), Brine migration through fault zones: 3D numerical simulations for a prospective CO₂ storage site in Northeast Germany, *International Journal of Greenhouse Gas Control*, 19, 689-703.
- Todaka, N., S. Nakanishi, T. Xu, and K. Pruess (2009), Hydrogeochemical Modeling for Natural Analogue Study of CO₂ Leakage due to Matsushiro Earthquake Swarm, *Energy Procedia*, 1, 2413-2420.
- Townend, J., and M. D. Zoback (2000), How faulting keeps the crust strong, *Geology*, 28(5), 399-402.
- Tsang, C. F., and I. Neretnieks (1998), Flow channeling in heterogeneous fractured rocks, *Reviews of Geophysics*, 36(2), 275-298.
- Tsang, C. F., J. Rutqvist, and K. B. Min (2007), Fractured rock hydromechanics: from borehole testing to solute transport and CO₂ storage, *Rock Physics and Geomechanics in the Study of Reservoirs and Repositories*, 284, 15-34.
- Tucker, J., and D. Hitzman (1996), Long term and seasonal trends in the response of hydrocarbon-utilizing microbes to light hydrocarbon gases in shallow soils, in *Hydrocarbon migration and its near-surface expression*, edited by D. Schumacher and M. A. Abrams, pp. 353-357, AAPG Memior,66.
- van der Zee, W., and J. L. Urai (2005), Processes of normal fault evolution in a siliciclastic sequence: a case study from Miri, Sarawak, Malaysia, *Journal of Structural Geology*, 27(12), 2281-2300.
- Van Hulst, F. F. N. (2010), Geological factors effecting compartmentalization of Rotliegend gas fields in the Netherlands, in *Reservoir Compartmentalization*, edited by S. J. Jolley, Q. J. Fisher, R. B. Ainsworth, P. J. Vrolijk and S. Delisle, pp. 301-315, Geological Society, London, Special Publications,347.
- Vass, A., D. Koehn, R. Toussaint, I. Ghani, and S. Piazzolo (2014), The importance of fracture-healing on the deformation of fluid-filled layered systems, *Journal of Structural Geology*, 67, 94-106.
- Vilarrasa, V., J. Carrera, and S. Olivella (2013), Hydromechanical characterization of CO₂ injection sites, *International Journal of Greenhouse Gas Control*, 19, 665-677.
- Voltattorni, N., A. Sciarra, G. Caramanna, D. Cinti, L. Pizzino, and F. Quattrocchi (2009), Gas geochemistry of natural analogues for the studies of geological CO₂ sequestration, *Applied Geochemistry*, 24, 1339–1346.
- Vrolijk, P. J., R. Skelly, S. E. Bradley, A. C. Ostridge, N. MacCallum, and J. Wood (2012), Methods to Evaluate and Predict the Effects of Extreme Reservoir Compartmentalization, BNA Reservoir, Canada, in *3rd EAGE International Conference on Fault and Top Seals* edited, Montpellier, France
- Wade, A. (1913), The natural history of petroleum, *Proceedings of the Geologists' Association*, 24(1), 1-13.
- Wallace, R. E., and H. T. Morris (1986), Characteristics of faults and shear zones in deep mines, *Pure & Applied Geophysics*, 124(1/2), 105-125.
- Wallis, I. C., C. J. Bardsley, T. S. Powel, J. V. Rowland, and J. M. O'Brien (2013), A structural model for the Rotokawa geothermal field, New Zealand, paper presented at 35th New Zealand Geothermal Workshop 2013, Rotorua.
- Walsh, J., J. Watterson, and G. Yielding (1991), The Importance of Small-Scale Faulting in Regional Extension, *Nature*, 351(6325), 391-393.

- Walsh, J. J., and J. Watterson (1991), Geometric and kinematic coherence and scale effects in normal fault systems, in *The Geometry of Normal Faults*, edited by A. M. Roberts, G. Yielding and B. Freeman, pp. 193-203, Geological Society, London, Special Publication, 56.
- Walsh, J. J., W. R. Bailey, C. Childs, A. Nicol, and C. G. Bonson (2003), Formation of segmented normal faults: a 3-D perspective, *Journal of Structural Geology*, 25(8), 1251-1262.
- Wamalwa, A. M., K. L. Mickus, L. F. Serpa, and D. I. Doser (2013), A joint geophysical analysis of the Coso geothermal field, south-eastern California, *Physics of the Earth and Planetary Interiors*, 214, 25-34.
- Wang, J. S. Y., T. N. Narasimhan, and C. H. Scholz (1988), Aperture Correlation of a Fractal Fracture, *Journal of Geophysical Research-Solid Earth and Planets*, 93(B3), 2216-2224.
- Watson, M. N., C. J. Boreham, and P. R. Tingate (2004), Carbon dioxide and carbonate cements in the Otway basin: implications for geological storage of carbon dioxide, *APPEA Journal*, 44(Part 1), 703-720.
- Watson, Z. T., W. S. Han, E. H. Keating, N.-H. Jung, and M. Lu (2014), Eruption dynamics of CO₂-driven cold-water geysers: Crystal, Tenmile geysers in Utah and Chimayó geyser in New Mexico, *Earth and Planetary Science Letters*, 408, 272-284.
- Watterson, J., J. J. Walsh, P. A. Gillespie, and S. Easton (1996), Scaling systematics of fault sizes on a large-scale range fault map, *Journal of Structural Geology*, 18(2-3), 199-214.
- Watts, N. L. (1987), Theoretical Aspects of Cap-Rock and Fault Seals for Single-Phase and 2-Phase Hydrocarbon Columns, *Marine and Petroleum Geology*, 4(4), 274-307.
- Wei, Z. Q., P. Egger, and F. Descoedres (1995), Permeability Predictions for Jointed Rock Masses, *International Journal of Rock Mechanics and Mining Sciences & Geomechanics Abstracts*, 32(3), 251-261.
- Wibberley, C. A. J., and T. Shimamoto (2003), Internal structure and permeability of major strike-slip fault zones: the Median Tectonic Line in Mie Prefecture, Southwest Japan, *Journal of Structural Geology*, 25(1), 59-78.
- Wibberley, C. A. J., G. Yielding, and G. Di Toro (2008), Recent advances in the understanding of fault zone internal structure: a review, in *The Internal Structure of Fault Zones: Implications for Mechanical and Fluid Flow Properties*, edited by C. A. J. Wibberley, W. Kurtz, J. Imber, R. E. Holdsworth and C. Collettini, pp. 5-33, Geological Society, London, Special Publications, 299.
- Wilkins, S. J., and M. R. Gross (2002), Normal fault growth in layered rocks at Split Mountain, Utah: influence of mechanical stratigraphy on dip linkage, fault restriction and fault scaling, *Journal of Structural Geology*, 24(9), 1413-1429.
- William Carey, J., Z. Lei, E. Rougier, H. Mori, and H. Viswanathan (2015), Fracture-permeability behavior of shale, *Journal of Unconventional Oil and Gas Resources*, 11, 27-43.
- Wilson, J. E., J. S. Chester, and F. M. Chester (2003), Microfracture analysis of fault growth and wear processes, Punchbowl Fault, San Andreas System, California, *Journal of Structural Geology*, 25(11), 1855-1873.
- Winick, J., T. Powell, and E. Mroczek (2011), The natural-state geochemistry of the Rotokawa reservoir, paper presented at New Zealand Geothermal Workshop 2011 Auckland.
- Wiprut, D., and M. D. Zoback (2000), Fault reactivation and fluid flow along a previously dormant normal fault in the northern North Sea, *Geology*, 28(7), 595-598.

- Wiprut, D., and M. D. Zoback (2002), Fault reactivation, leakage potential, and hydrocarbon column heights in the northern North Sea, in *Hydrocarbon Seal Quantification*, edited by A. G. Koestler and R. Hunsdale, pp. 203-219, Norwegian Petroleum Society Special Publications, 11.
- Wu, H. T., and J. M. Lees (1999), Three-dimensional P and S wave velocity structures of the Coso Geothermal Area, California, from microseismic travel time data, *Journal of Geophysical Research-Solid Earth*, 104(B6), 13217-13233.
- Xue, L., et al. (2013), Continuous Permeability Measurements Record Healing Inside the Wenchuan Earthquake Fault Zone, *Science*, 340(6140), 1555-1559.
- Yielding, G. (1992), The prediction of small-scale faulting in reservoirs, *First Break*, 10, 449-460.
- Yielding, G. (2002), Shale Gouge Ratio — calibration by geohistory, in *Hydrocarbon Seal Quantification*, edited by A. G. Koestler and R. Hunsdale, pp. 1-15, Norwegian Petroleum Society (NSF) Special Publications, 11.
- Yielding, G. (2012), Using probabilistic shale smear modelling to relate SGR predictions of column height to fault-zone heterogeneity, *Petroleum Geoscience*, 18(1), 33-42.
- Yielding, G., B. Freeman, and D. T. Needham (1997), Quantitative fault seal prediction, *AAPG Bulletin*, 81(6), 897-917.
- Yielding, G., P. Bretan, and B. Freeman (2010), Fault seal calibration: a brief review, in *Reservoir Compartmentalization*, edited by S. J. Jolley, Q. J. Fisher, R. B. Ainsworth, P. J. Vrolijk and S. Delisle, pp. 243-255, Geological Society, London, Special Publications, 347.
- Zahasky, C., and S. M. Benson (2014), Evaluation of the effectiveness of injection termination and hydraulic controls for leakage containment, paper presented at 12th International Conference on Greenhouse Gas Control Technologies, GHGT 2014, Elsevier Ltd.
- Zhang, C. L. (2011), Experimental evidence for self-sealing of fractures in claystone, *Physics and Chemistry of the Earth*, 36(17-18), 1972-1980.
- Zhang, C. L. (2013), Sealing of fractures in claystone, *Journal of Rock Mechanics and Geotechnical Engineering*, 5(3), 214-220.
- Zhang, C. L., and T. Rothfuchs (2008), Damage and sealing of clay rocks detected by measurements of gas permeability, *Physics and Chemistry of the Earth*, 33, S363-S373.
- Zhang, R., D. Vasco, T. M. Daley, and W. Harbet (2015), Characterization of a fracture zone using seismic attributes at the In Salah CO₂ storage project, *Interpretation*, 3(2), SM37-SM46.
- Zhang, X., and D. J. Sanderson (1996a), Effects of stress on the two-dimensional permeability tensor of natural fracture networks, *Geophysical Journal International*, 125(3), 912-924.
- Zhang, X., and D. J. Sanderson (1996b), Numerical modelling of the effects of fault slip on fluid flow around extensional faults, *Journal of Structural Geology*, 18(1), 109-119.
- Zhang, X., and D. J. Sanderson (1998), Numerical study of critical behaviour of deformation and permeability of fractured rock masses, *Marine and Petroleum Geology*, 15(6), 535-548.
- Zhang, X., and D. J. Sanderson (2001), Evaluation of instability in fractured rock masses using numerical analysis methods: Effects of fracture geometry and loading direction, *Journal of Geophysical Research-Solid Earth*, 106(B11), 26671-26687.

- Zhang, Y., P. M. Schaub, C. Zhao, A. Ord, and B. E. Hobbs (2008), Fault-related dilation, permeability enhancement, fluid flow and mineral precipitation patterns: numerical models, in *The Internal Structure of Fault Zones: Implications for Mechanical and Fluid-Flow Properties*, edited by C. A. J. Wibberley, W. Kurtz, J. Imber, R. E. Holdsworth and C. Collettini, pp. 239-255, Geological Society, London, Special Publications, 299.
- Zhou, X., and T. J. Burbey (2014), Fluid effect on hydraulic fracture propagation behavior: a comparison between water and supercritical CO₂-like fluid, *Geofluids*, 14(2), 174-188.
- Zoback, M. D. (2010), *Reservoir geomechanics*, Cambridge University Press.